THE UNIVERSITY
of EDINBURGH

Investigating the role of segment 3 in H9N2 avian influenza virus pathogenicity

Anabel Lucy Clements

THE UNIVERSITY *of* EDINBURGH

Submitted for the degree of Doctor of Philosophy

The University of Edinburgh

August 2018

Declaration

I declare that this thesis was composed by myself and the work contained within is my own, with the exception or where it is explicitly stated in the text, and that the work has not be submitted for any other degree or professional qualification.

Signed: ……..... Date: ……..

Anabel Clements

Acknowledgements

Firstly, I would like to thank my supervisors; Prof. Paul Digard, Prof. Munir Iqbal and Dr Holly Shelton for giving me the opportunity to undertake my PhD. I thank them for their guidance and support during my time at the Roslin Institute and the Pirbright Institute. It has been a pleasure to work alongside you and without your help I would have been unable to complete my PhD.

I am very grateful to all members of the 'Digard Lab' and those at the Roslin Institute would helped me complete my PhD. I would like to thank Dr Saira Hussain for her initial encouragement and training in teaching me invaluable skills and lessons which set me up for the next four years. Drs Nikki Smith, Helen wise, Liliane Chung and Lita Murphy, thank you all for your scientific discussions and advice along the way.

I extend my thanks to other students and friends from the Roslin Institute; Seema, Matt, Carina, Rute and Tom M for your friendship, 'Friday Bar Fun' and making my time in Edinburgh the most enjoyable. Finally, thank you to my best friend, Becca. If I gained one thing from being in Edinburgh it was you, you will truly be a friend for life. Thanks for the coffee breaks, gin and laughs!

I would also like to thank members of the Pirbright Institute. I would like to thank Jean-Remy Sadeyen for your incredible knowledge and guidance. You are invaluable to the Avian Influenza laboratory and your organisation, support and assistance in particular with animal studies was greatly appreciated. Thanks to Drs Pengxiang Chang, Sushant Bhat and Dagmara Baily for your help, guidance and advice throughout my studies. Further thanks go to the animal services staff for help completing animal studies and for caring for all the birds. To other past and present members of the Avian Influenza and Influenza Labs thank you for your friendship and discussion.

Particular thanks to Tom P, Joe and Josh for making me feel welcome when I started and to Tom P for proof reading much of my thesis. Final thanks have to go Phoebe, Sarah, Tom W, Kate, Ross, Michael, Helena and Erica for listening to my complaints at tea and for keeping me sane with plenty of coffee. I wish you all the best of luck for your future.

I would also like to thank my family for all of your unwavering support, love and belief that I can do this! In particular to my husband, Simon, for putting up with me when I was stressed, for letting me go to Edinburgh for 6 months and not being "too" annoyed when it ended up being 2 years! At least the proposal worked and I came back eventually. Thank you for everything, you are my rock.

Finally, thanks to the University of Edinburgh and The Pirbright Institute for funding my PhD and supporting me throughout the process.

Table of contents

List of figures and tables

Chapter 1: Introduction to influenza A virus

Chapter 2: Investigating the effect of segment 3 on H9N2 AIV fitness *in vitro*

Chapter 3: How do PA mutations modulate H9N2 virus pathobiology within avian models *in vivo*?

Chapter 4: Investigating the contribution of PA-X to H9N2 AIV fitness *in vitro*

Chapter 5: How does mutating H9N2 PA-X alter AIV pathobiology *in vivo*?

Chapter 7: Materials and Methods

Lay summary

H9N2 avian influenza viruses (AIV) are widespread in poultry populations worldwide, causing large economic losses. Influenza viruses have an RNA genome which is split into 8 sections called segments. Different strains of virus can swap segments to produce new strains in a process known as reassortment. Within H9N2 AIVs, the exchange of gene segments has led to an increased pathogenicity of the virus in poultry but the reasons behind this remain undetermined. Previous experiments have shown that segment 3 may be important. This segment produces multiple proteins including PA, a subunit of the viral RNA polymerase, and the PA-X virulence factor. It is important to understand the factors responsible for enhancing pathogenicity in order to improve control measures and identify risk factors. This study uses H9N2 AIV as a model to understand how evolutionary molecular changes in segment 3 (PA gene) modulate virus virulence in birds.

To investigate the molecular basis of this, reciprocal alterations were made to the PA genes of two pre- and post- reassortment H9N2 AIV strains, A/guineafowl/Hong Kong/WF10/99 (WF10) and A/chicken/Pakistan/UDL-01/08 (UDL-01) respectively. One method used to determine the fitness of a virus is to see how it can spread within cell sheets to create holes termed plaques. A single change next to the PA endonuclease active site (K26E) was identified to have the largest effect on viral phenotypes; by swapping the size of the plaque the virus makes within MDCK cells as well as the amount of viral output after infection. This change also reduced overall pathogenicity in infected chickens by

reducing viral replication in the birds. These experiments identified the E26K change as a pathogenicity determining residue.

The E26K mutation lies within the protein domain common to PA and PA-X. PA-X has roles in host cell protein synthesis shut off, which is a mechanism viruses use to avoid the host immune response. When the shut off activity of the WF10 and UDL-01 PA-Xs were assessed, there was a marked difference. WF10 PA-X was unable to control host cell protein synthesis whereas UDL-01 PA-X had highly active host cell shut off ability. This activity could be switched with the introduction of the E26K PA mutation.

Further functions of the H9N2 PA-Xs were then investigated. Removal of PA-X expression from UDL-01 led to the production of smaller plaques and reduced viral replication. Removal of PA-X from WF10 had no viral fitness implications. When chickens were infected with the UDL-01 strain either with or without PA-X expression, loss of PA-X reduced viral shedding at earlier times post infection.

Overall, these studies show that a single amino acid change within the PA gene of H9N2 avian influenza viruses is able to reduce replication and pathogenicity of these viruses in poultry via impacting upon ability of the virus to control host cell protein synthesis. These results can potentially be exploited to attenuate the viruses for use as a live virus vaccine to improve control measures.

Abstract

H9N2 avian influenza viruses (AIV) are widespread in poultry populations worldwide, causing large economic losses. Reassortment events with other co-circulating AIV strains has led to an increased pathogenicity of H9N2 in poultry. However, the molecular basis of this increased pathogenicity remains largely undetermined, although previous experiments have implicated exchange of segment 3; encoding the PA subunit of the viral RNA polymerase and the PA-X virulence factor. It is important to understand the factors responsible for enhancing pathogenicity in order to improve control measures and identify risk factors. This study uses H9N2 AIV as a model to understand how evolutionary molecular changes in segment 3 (PA gene) modulate virus virulence in birds.

To investigate the molecular basis of this, site directed mutagenesis was used to introduce reciprocal alterations to the PA genes of two pre- and post-reassortant H9N2 AIV strains: A/guineafowl/Hong Kong/WF10/99 (WF10) and A/chicken/Pakistan/UDL-01/08 (UDL-01) respectively. A single polymorphism adjacent to the PA endonuclease active site (K26E) was identified as having the largest impact on viral phenotype. This change did not significantly affect the transcriptional activity of the viral polymerase. However, when the mutation was introduced into viruses, the replication phenotypes (assessed via plaque size and viral titre) were switched between the WF10 and UDL-01 strains. During *in vivo* pathogenicity studies within the UDL-01 virus, the introduction of the E26K change altered viral replication as well as reducing overall pathogenicity in directly inoculated and contact chickens but without affecting transmission. In

contact birds, the mutant virus was less able to disseminate beyond the respiratory tract to the visceral organs. Thus overall, the E26K change altered viral replication *in vitro* and *in vivo*, identifying it as a pathogenicity-determining residue.

The E26K mutation lies within the protein domain common to PA and PA-X. PA-X has roles in host cell protein synthesis shut off and when the shut off activity of the WF10 and UDL-01 PA-Xs were assessed, there was a marked difference in their activity. WF10 PA-X was unable to control host cell protein synthesis whereas UDL-01 PA-X had highly active host cell shut off ability. This activity could be switched with the introduction of the E26K PA mutation. Further functions of the H9N2 PA-Xs were then investigated. Polymerase transcriptional activity was also similar between the virus strains. However, removal of PA-X expression from UDL-01 led to a reduced plaque phenotype and viral replication. Removal of PA-X from WF10 had no viral fitness implications. When both the E26K change was made and PA-X expression was removed from UDL-01 segment 3, viral replication and plaque diameter was reduced, the reciprocal effect was observed with the introduction of both mutations into WF10. During *in vivo* pathogenicity studies with the UDL-01 strain with or without PA-X expression, loss of PA-X reduced viral shedding at earlier times post infection.

Overall, these studies show that a single amino acid change within the PA gene of H9N2 avian influenza viruses is able to reduce replication and pathogenicity of these viruses in poultry via impacting upon ability of the virus to control host cell protein synthesis.

Abbreviations

AIV	Avian influenza virus
AUC	Area under the curve
β-gal	β-galactosidase
CPE	Cytopathic effect
cRNA	complementary ribonucleic acid
DAPI	4', 6-diamidino-2-phenylindole
DI	Defective interfering
DNA	Deoxyribonucleic acid
EID_{50}	Egg infectious dose 50
FS	Frameshift
GDP	Guanosine diphosphate
GFP	Green florescent protein
GTP	Guanosine triphosphate
G3BP	ras GTPase-activating protein-binding protein
HA	Hemagglutinin
HPAIV	High pathogenicity avian influenza virus
h.p.i	Hours post infection
IAV	Influenza A virus
IVPI	Intravenous pathogenicity index
IVT	*In vitro* translation
LD_{50}	Lethal dose 50
LPAIV	Low pathogenicity avian influenza virus
MOI	Multiplicity of infection
mRNA	messenger ribonucleic acid
M1	Matrix protein 1
M2	M2 proton channel
NA	Neuraminidase
NEP	Nuclear export protein

NGS	Next generation sequencing
NLS	Nuclear localisation signal
NP	Nucleoprotein
NPC	Nuclear pore complex
NS	Non-structural protein
ORF	Open reading frame
PA	Polymerase acidic protein
PB1	Polymerase basic protein 1
PB2	Polymerase basic protein 2
PCR	Polymerase chain reaction
PFU	Plaque forming unit
PTC	Premature termination codon
qRT-PCR	quantitative reverse transcription polymerase chain reaction
RG	Reverse genetics
RNA	Ribonucleic acid
RNP	Ribonucleoprotein
RT-PCR	Reverse-transcription polymerase chain reaction
SA	Sodium arsenite
SDS-PAGE	Sodium dodecyl sulphate polyacrylamide gel electrophoresis
SG	Stress granule
SPF	Specific pathogen free
TIA-1	T-cell intracellular antigen 1
UDL-01	A/chicken/Pakistan/UDL-01/2008
UTR	Untranslated region
vRNA	viral ribonucleic acid
VTM	Viral transport media
WF10	A/guineafowl/Hong Kong/WF10/1999
WT	Wild-type

Chapter 1: Introduction to influenza A virus

1.1: Influenza viruses

Influenza viruses are members of the *Orthomyxoviridae* family (McGeoch et al., 1976). There are 4 described genera within influenza viruses, *Influenzavirus* A, B, C and D (Rota et al., 1990; Francis et al., 1950; Hause et al., 2014). However, this thesis will only concentrate on influenza A viruses (IAV). IAV are enveloped RNA viruses with a genome consisting of eight negative sense, single stranded segments (McGeoch et al., 1976). The natural reservoir of IAV is thought to be wild aquatic birds of the *Anseriformes* and *Charadriiformes* orders. IAV are subtyped according to the presence of two surface antigens; Hemagglutinin (HA) and Neuraminidase (NA). To date, 16 HA and 9 NA subtypes have been identified to circulate within the aquatic bird reservoir, with each virus containing a combination of HA and NA such as H1N1 or H7N9 (reviewed by Webster et al., 1992). However, in recent years two further HA/NA combinations have been identified in bats (H17N10 and H18N11) which have not yet been found in other species (Tong et al., 2012; Tong et al., 2013).

Several pandemics have resulted from IAV infection in humans in the past century due to the introduction of novel HA subtypes into the population (Yoon et al., 2014). The most severe pandemic recorded was the 1918 H1N1 Spanish Flu. This resulted in between 50 and 100 million deaths worldwide (Taubenberger et al., 2012; Johnson et al., 2002) with many deaths due to severe complications related to secondary bacterial pneumonia (Taubenberger and Morens, 2006; Morens et al., 2008). More recent pandemics including the 1957

Asian Flu (H2N2), 1968 Hong Kong Flu (H3N2) and 2009 Swine Flu (H1N1) have had lower mortality rates but still show the potential of IAV to periodically cross over into human populations. Once an animal strain of IAV has caused a pandemic within the human population, a baseline of protective immunity against the virus develops, so the virus then causes seasonal epidemics which peak during the winter period (Taubenberger and Kash, 2010). Seasonal influenza infections are usually transmitted by airborne droplets and fomites, usually leading to mild respiratory infection. Currently, only H1, H2 and H3 subtypes have been known to persist in human populations, although other strains such as H5, H7 and H9 have sporadically crossed over (Schrauwen and Fouchier, 2014).

1.2: The influenza virus genome

IAV have a segmented, negative sense RNA genome of around 13.4 Kb in size. Each segment encodes at least one protein; with the genome encoding 10 core proteins and several accessory proteins (Figure 1.1). Each segment has one main open reading frame (ORF) which allows for the faithful translation of a protein product; Polymerase Basic protein 2: PB2 (segment 1), Polymerase Basic protein 1: PB1 (segment 2), Polymerase Acidic protein: PA (segment 3), Hemagglutinin: HA (segment 4), Nucleoprotein: NP (segment 5), Neuraminidase: NA (segment 6), Matrix protein: M1 (segment 7) and Non-Structural protein 1: NS1 (segment 8). However, other mechanisms are adopted by IAV to increase the coding capacity of the genome including alternative splicing, frameshifting and alternative translation initiation events (Table 1.1).

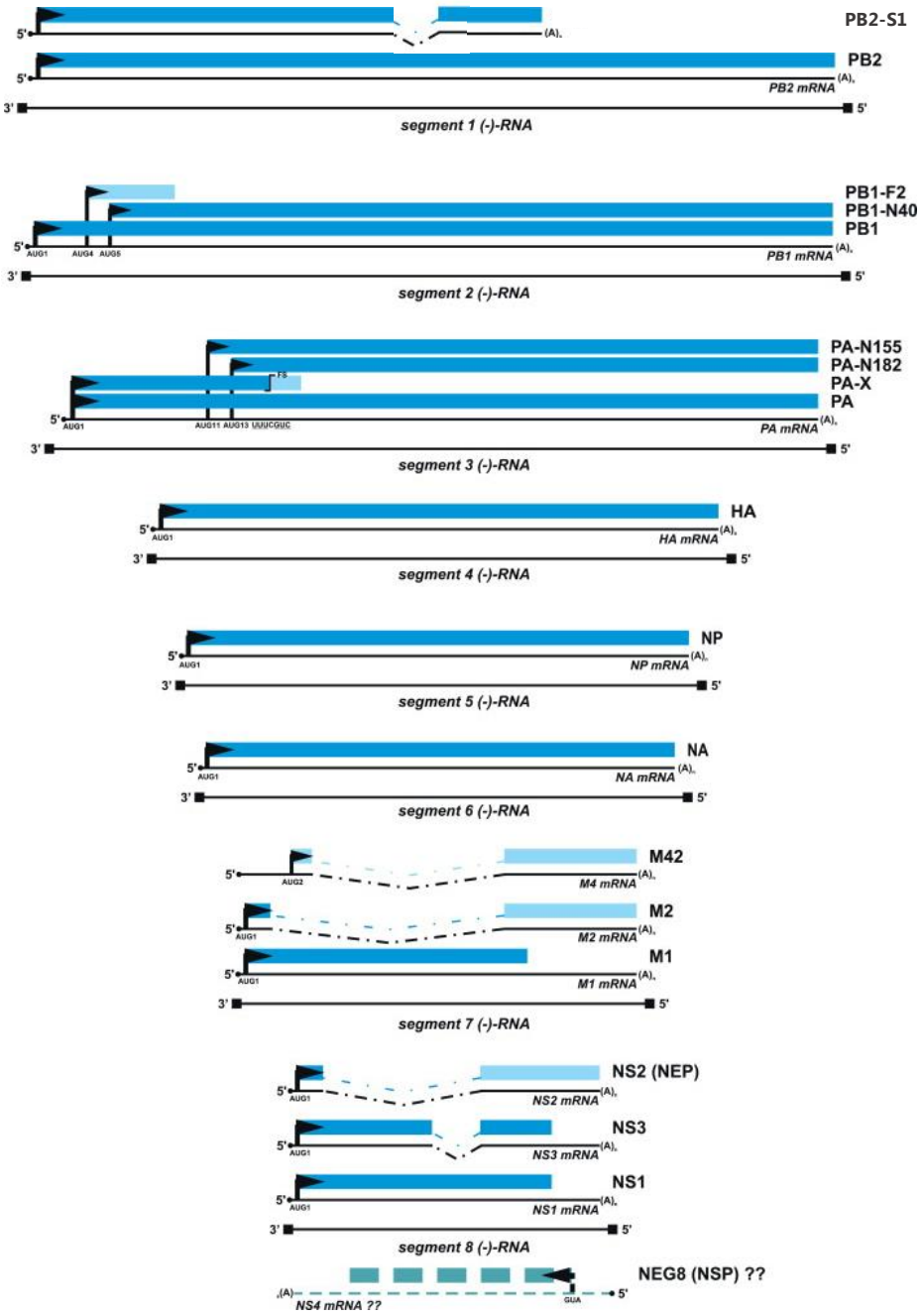

Figure 1.1: Schematic of the influenza A virus genome. The IAV genome consists of 8 segments of ssRNA which encode for a range of proteins shown within this diagram. The RNA genome segments are indicated by the square ended black lines, mRNAs are shown as black lines with the 5' cap structures depicted as black circles and the polyA tails as $(A)_n$. Spliced regions are represented by dotted lines. Black arrows indicate initiation sites of protein synthesis. Proteins are shown as blue rectangles with the alternative ORFs depicted in different shades. FS indicates the conserved frameshift site. The hypothetical NEG8 mRNA and resulting protein are also shown as a dotted line at the base of the schematic. Figure adapted from Vasin et al., 2014.

Table 1.1: Gene products encoded by IAV

Segment	Protein	Expression mechanism	Function(s)	Reference
1	**PB2**	Faithful translation	Binds capped host non-coding RNAs within trimeric polymerase to prime viral mRNA transcription	Blaas et al., 1982
	PB2-S2	Spliced mRNA	Inhibitor of RIG-I signalling	Yamayoshi et al., 2016
2	**PB1**	Faithful translation	Contains catalytic site for RNA dependant RNA polymerase	Braam et al., 1983
	PB1-N40	Alternate AUG site	Unknown	Wise et al., 2012
	PB1-F2	Alternate AUG site	Reduces IFN induction and roles in viral virulence	Chen et al., 2001
3	**PA**	Faithful translation	Cleaves host mRNAs during cap-snatching via endonuclease activity to prime viral mRNA transcription	Dias et al., 2009
	PA-X	Ribosomal frameshifting	Host cell shut off	Jagger et al., 2012
	PA-N182	Alternate AUG site	Unknown	Muramoto et al., 2013
	PA-N155	Alternate AUG site	Unknown	Muramoto et al., 2013
4	**HA**	Faithful translation	Attachment to cell surface via receptor binding, fusion of endosomal membranes and budding	Johnson et al., 1964; Connor et al., 1994; Skehel and Wiley, 2000
5	**NP**	Faithful translation	Coats viral genome, required for polymerase activity	Baudin et al., 1994; Huang et al., 1990; Ortega et al., 2000
6	**NA**	Faithful translation	Virus release from cell surface, membrane scission during budding	Hirst et al., 1941; Kobasa et al., 1999; Palese et al., 1974
7	**M1**	Faithful translation	Roles in virion structure, associated with recruitment of vRNPs during viral budding	Gomez-Puertas et al., 2000
	M2	Spliced mRNA	Forms a proton channel within endosomal membranes, required for virion budding	Lamb and Choppin, 1981; Pinto et al., 1992
	M42	Spliced mRNA	Modified version of M2	Shih et al., 1995
8	**NS1**	Faithful translation	Interferon antagonist	Hale et al., 2008
	NEP	Spliced mRNA	Nuclear export of vRNPs, regulates switch between viral transcription and translation	Inglis et al., 1980; O'Neill et al., 1998; Paterson and Fodor, 2012;
	NS3	Spliced mRNA	Unknown	Selman et al., 2012
	NEG8	Unknown	Protein expression not detected	Clifford et al., 2009

Genomic viral RNA segments (vRNA) are encapsidated in multiple copies of the nucleoprotein (NP). Influenza viruses encode a heterotrimeric RNA dependant RNA polymerase (PB2, PB1 and PA) which is responsible for the transcription of viral mRNA and also for replication of the viral genome (Fodor, 2013) (Figure 1.2A, B). One copy of each subunit of the polymerase complex is bound to the promoter region of the vRNA which leads to the formation of viral ribonucleoproteins (vRNP), the minimal unit required for transcription and replication (Huang et al., 1990). Each genome segment is flanked by conserved sequences at each end which have some complementarity, termed untranslated regions (UTRs). The polymerase sits on the panhandle structure formed via this terminal complementarity and the vRNPs take on the form of a helical filament, seen in Figure 1.2B (Hsu et al., 1987; Baudin et al., 1994; Klumpp et al., 1997; Compans et al., 1972).

1.3: Influenza virion structure

IAV particles are pleomorphic in shape producing filamentous or spherical morphologies (Mosley and Wyckoff, 1946). Lab adapted strains tend to have more spherical phenotypes, with particles of 100nm in diameter whereas clinical isolates tend to adopt filamentous phenotypes of up to 20μm in length and 100nm in diameter (Mosley and Wycoff, 1946; Harris et al., 2006; Cox et al., 1980). M1 plays a vital role in virion structure and is important for overall morphology (Roberts et al., 1998; Bourmakina and Garcia-Sastre, 2003; Elleman and Barclay, 2004). However, the function of IAV particle morphology remains unclear (Dadonaite et al., 2016).

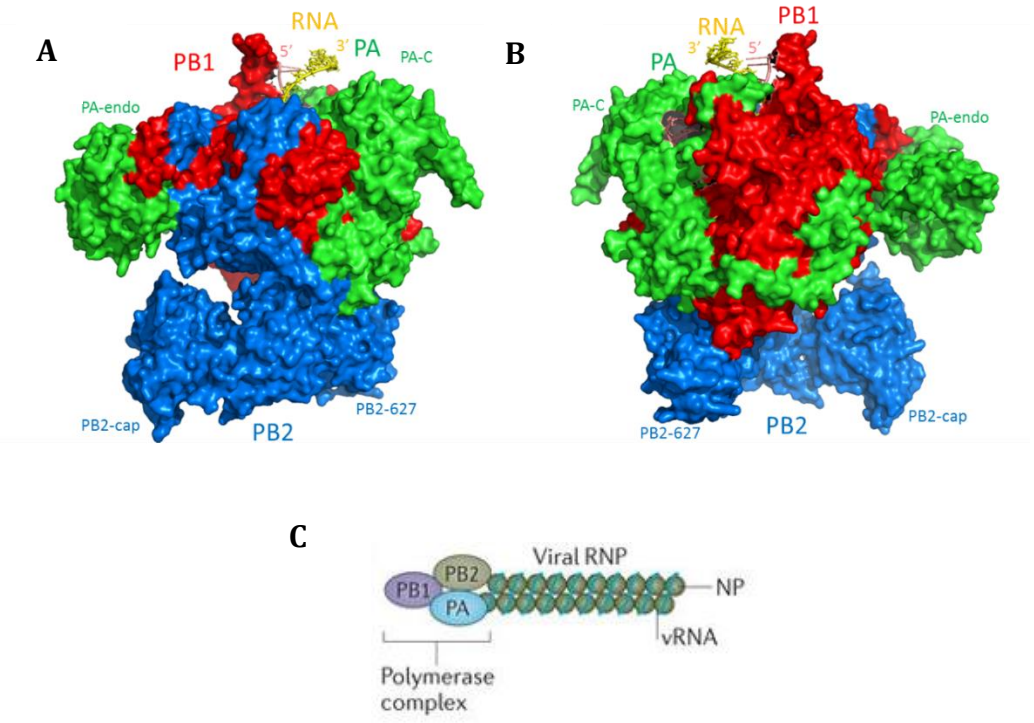

Figure 1.2: Diagrams of the structure of the polymerase heterotrimer and vRNP organisation. Structure of the polymerase heterotrimer (A) front and (B) back. PB2 shown in blue, PB1 shown in red, PA in green, 3' vRNA in yellow and 5' vRNA in pink. Polymerase structure adapted from Reich et al., 2014 PDB = 4WSB, provided by Tom Peacock. (C) vRNP structure cartoon with the polymerase complex depicted at the panhandle terminus and NP encapsidating the vRNA. Taken from Shi et al., 2014.

A schematic of a spherical IAV particle is shown in Figure 1.3. IAV are enveloped viruses whose membrane is derived from the host phospholipid bi-layer. Three transmembrane proteins are present: HA, NA and the M2 proton channel (Laver and Valentine, 1969; Zebedee and Lamb, 1988). HA and NA are surface glycoproteins which protrude from the virion, acting as antigenic determinants, usually present in a ratio of 4:1 (Webster et al., 1968). The M1 protein is the most abundant protein in the virion and forms a 'shell' underlying the viral envelope, giving the virus structure (Richardson and Akkina, 1991; Hutchinson et al., 2014). The 8 vRNPs are packaged into the space inside the virion along with NS1, NEP and other cellular factors which vary depending on the originating host species (Hutchinson et al., 2014; Shaw et al., 2008). M1 interacts with the lipid bilayer and the vRNPs (Ruigrok et al., 2000, Noton et al., 2007; Noton et al., 2009). A 7+1 'core-bundle' arrangement has been suggested for the structure of vRNPs within the virion with the presence of one central segment surrounded by the other 7 was detected via transmission electron microscopy (Noda et al., 2012).

1.4: Virus life cycle

Unlike most other non-retroviral RNA viruses, IAV completes RNA synthesis within the host nucleus, allowing easier access to host mRNA transcription and processing machinery. This may also reduce the likelihood of activating host cytoplasmic sensors for vRNA and thereby triggering an innate immune response. A schematic of the IAV lifecycle is shown in Figure 1.4.

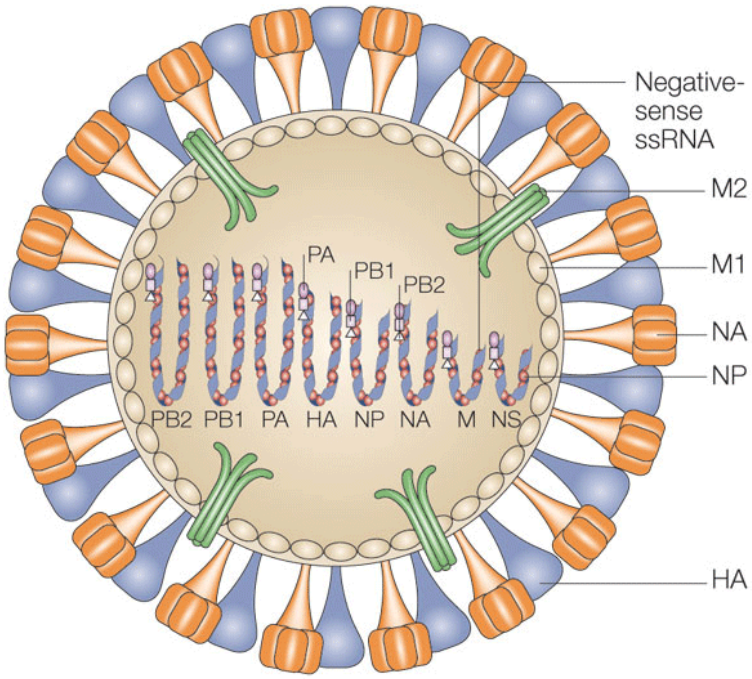

Figure 1.3: Schematic of IAV spherical virion structure. IAV have two surface glycoproteins, HA and NA, which are embedded in the host derived lipid bilayer envelope of the virion along with the M2 proton channel. Oligomers of viral M1 protein provide the structural shell of the virion. The ssRNA of the genome is split into 8 segments each encapsidated with multiple copies of NP. The trimeric polymerase sits on the panhandle at the termini of the vRNA which forms a vRNP. Figure taken from Horimoto and Kawaoka, 2005.

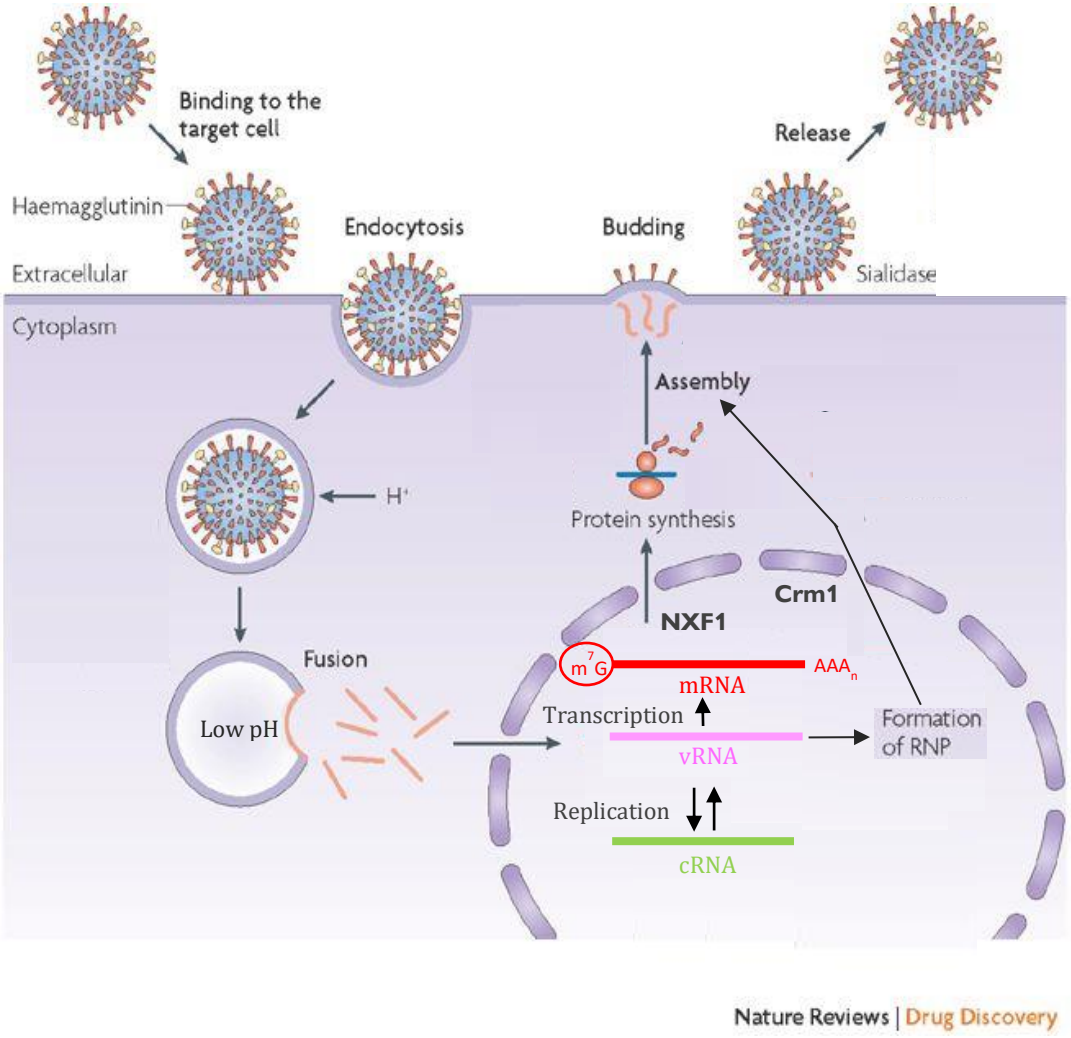

Figure 1.4: Schematic of the IAV lifecycle. IAVs enter the host cell via attachment of HA to sialic acid on the cell surface followed by endocytosis. As the endosome acidifies, membrane fusion is triggered, mediated by HA, which allows for release of vRNPs into the cytoplasm. vRNPs enter the nucleus using importins and genome replication and transcription take place. Newly synthesised copies of the genome and translated viral proteins assemble to form progeny vRNPs which are exported from the nucleus via Crm1 mediated export and trafficked to the cell surface. Virus assembly and budding takes places and infectious particles are released from the cell. Figure adapted from von Itzstein (2007).

1.4.1: Virus entry

IAV infection starts with binding of virus to the host cell surface, a processes mediated via the influenza HA protein attaching to N-acetylneuraminic (sialic) acids covalently linked to oligosaccharides on glycoproteins or glycolipids, via its receptor binding site (Johnson et al., 1964). Avian- and human-IAVs have been shown to preferentially recognise different terminal sialic acid linkages; with avian influenza viruses (AIVs) recognising sialic acids attached to galactose in α-2,3 linkage, and human IAVs recognising sialic acids attached to galactose in α-2,6 linkage (Connor et al., 1994). This receptor binding preference correlates to the abundance of cellular receptors in sites of replication within the host. Human upper respiratory tracts have an abundance of α-2, 6 linked sialic acids whereas the avian enteric and respiratory tracts have an abundance of α-2, 3 linked sialic acids (Matrosovich et al., 2004).

Upon binding, virions are internalised via methods dependent on virion morphology. Spherical virions are internalised via clathrin-mediated endocytosis (Eierhoff et al., 2010), whereas filamentous virions enter via macropinocytosis (Rossman et al., 2012). To enter the cell cytoplasm, the virus must fuse its membrane with that of the endosome to allow release of vRNPs, a process mediated by HA (Jardetzky and Lamb, 2004). HA contains a fusion peptide, which is a hydrophobic stretch of amino acids at the N-terminus of the HA2 subunit. On the virion at neutral pH, HA is present in a state whereby the fusion peptide is hidden at the base of the molecule (Chen et al., 1998a+b). As the endosome containing the virion acidifies, cleaved HA (in multiple trimers) undergoes a

conformational change at between pH 5-6, enabling the fusion peptide to insert into the endosomal membrane (Huang et al., 1981; Maeda et al., 1980; White et al., 1981). This is followed by further protein re-folding to bring the fusion protein into close proximity with the HA C-terminal transmembrane domain, bringing the endosomal and viral envelope membranes together (Sauter et al., 1989; Bizebard et al., 1995; Skehel et al., 1982). The energy released from this conformational change permits the fusion of the two membranes. Simultaneously within the endosome, the M2 proton channel is activated allowing H+ ions to be transferred into the virion interior. This allows for dissociation of M1 from the vRNPs, enabling them to enter into the host cytoplasm and complete virus entry (Bui et al., 1996; Ciampor et al., 1992)

1.4.2: Nuclear import of vRNPs and transcription and replication machinery

Transport of vRNPs from the endosome to the nuclear membrane is rapid, although the exact mechanism is undetermined. vRNPs must enter the nucleus for vRNA synthesis to occur. Due to the large size of the vRNPs, an active transport mechanism is required, as any molecules larger than 2.6nm cannot pass passively through the nuclear pore complexes (NPC) (Eibauer et al., 2015). Several influenza proteins have been identified to contain nuclear localisation signals (NLSs) including all three of the polymerase components and NP (O'Neill et al., 1995). NLSs consist of a series of basic residues forming a single cluster or bipartite motif (Cingolani et al., 2002) and allow for the transport of the vRNPs into the nucleus by mediating binding to host importins in the cytoplasm. Binding of importins to Ran-GTP releases vRNPs into the cell nucleus. Once within the

nucleus the viral polymerase can carry out a primary round of transcription and the viral mRNAs can be exported into the cytoplasm for translation via host machinery.

Viral RNP components that have been translated within the cytoplasm are required to be imported back into the nucleus to further aid in transcription and replication of the genome, a process mediated by NLSs. PB2 contains two NLS regions (residues 449-495 and a bipartite NLS within the C-terminal domain) allowing import of PB2 via the classical pathway (Tarendeau et al., 2007). A PB1 and PA heterodimer is required for efficient nuclear import of these proteins via a non-classical pathway interacting with RanBP5, however, the full import mechanism remains undetermined (Fodor and Smith, 2004; Deng et al., 2006; Hutchinson et al., 2010). NP contains an unconventional NLS in the N-terminal 13 residues (Wang et al., 1997) allowing it to utilise the classical import pathway via interaction with various isoforms of importin-α (O'Neill et al., 1995; Gabriel et al., 2008). These processes allow for all of the required components to be present within the nucleus for further RNA synthesis to be completed.

1.4.3: Transcription and replication of the IAV genome

The hetero-trimeric viral RNA-dependent RNA polymerase, consisting of PB2, PB1 and PA subunits, is responsible for the transcription and replication of the vRNA genome segments (Arranz et al., 2012; Coloma et al., 2009; Moeller et al., 2012). All eight vRNPs serve as separate transcription units. Synthesis of viral mRNA is initiated via a *cis*-acting viral RNA polymerase which is part of the vRNP structure bound to the 5' and 3' UTRs (Fodor et al., 1994; Tiley et al., 1994; Luytjes

et al., 1989). Viral mRNA synthesis is dependent on cellular RNA polymerase II activity, as this allows for access to a pool of host pre-mRNAs (Engelhardt et al., 2005). Transcription is primed via a 'cap-snatching' mechanism, involving the cleavage of 10-13 nucleotide RNA fragments from host precursor mRNAs (particularly small non-coding RNAs) containing 5' 7-methylguanosine caps which act as primers for viral transcription (Plotch et al., 1981; Gu et al., 2015). The influenza PB2 subunit is involved in binding to the 5'cap of the host pre-mRNAs (Blaas et al., 1982) and the endonuclease within the PA subunit is responsible for mRNA cleavage. These caps are used for viral mRNA initiation within the polymerase active site (Hara et al., 2006; Yuan et al., 2009; Dias et al., 2009). The PB1 subunit contains the main catalytic site for the RNA dependant RNA polymerase, allowing for RNA elongation in the 3' to 5' direction (Braam et al., 1983). Transcription is terminated at a sequence of 5-7 U residues which leads to stuttering of the polymerase and the addition of a poly (A) tail (Robertson et al., 1981; Moeller et al., 2012; Poon et al., 1998; Te Velthuis et al., 2016). Therefore, the nascent viral mRNAs contain both a 5' 7-methylguansine cap and a 3'poly (A) tail and resemble mature host mRNAs.

Once viral mRNAs have been transcribed they are processed similarly to host mature mRNAs and can take advantage of host splicing machinery to increase coding capacity (Amorim et al., 2007; Read and Digard, 2010; Bier et al., 2011; York and Fodor, 2013). Viral mRNAs from segment 7 and 8 are spliced within nuclear speckles in a NS1-dependent manner (Robb and Fodor, 2012; Mor et al., 2016). Viral mRNAs are exported from the nucleus via interaction with numerous host proteins including the cap binding complex (CBC) and the

transcription export complex (TREX) and the nuclear export factor 1 (NXF1) pathway for export via the NPC is utilised. Once in the cytoplasm host translation machinery is accessed for protein expression (Wang et al., 2008; Hao et al., 2008; Read and Digard, 2010; Bier et al., 2011).

Replication of the viral RNA genome consists of two stages: i) synthesis of a positive sense copy of vRNA termed complementary RNA (cRNA) using vRNA as a template and ii) synthesis of vRNA using the cRNA as a template. Replication does not require a primer for initiation leading to the presence of a 5' triphosphate moiety within both the cRNA and vRNA (Hay et al., 1982). However, the precise mechanism of initiation is not fully understood. Vreede et al. (2008), suggested that the polymerase binds to GTP, followed by phosphodiester bond formation with ATP directed by template position 1, which gives rise to the pppApG dinucleotide needed for elongation via the polymerase. Newly generated RNAs synthesised during replication are encapsidated by free NP and polymerase subunits within the nucleus to form vRNPs which are exported from the nucleus prior to viral assembly (Shapiro et al., 1987; Tchatalbachev et al., 2001). The mechanisms by which the viral polymerase is able to switch from transcription of viral mRNAs to replication of the viral genome are unclear. It has been suggested that accumulation of NEP is involved in this regulation while others have suggested small vRNAs (22-27 nucleotides in length) play a role (Robb et al., 2009; Perez et al., 2010).

1.4.4: Nuclear export and trafficking of vRNPs

vRNPs are exported from the nucleus via the chromosome region maintenance 1 (Crm1) pathway (Elton et al., 2001; Watanabe et al., 2001; Neumann et al., 2000). The viral protein NEP mediates this nuclear export by direct interaction with Crm1 through the presence of nuclear export signals (NES) and binding to the M1 protein, which is then believed to bind NP on the vRNP (O'Neill et al., 1998; Akarsu et al., 2003; Wakefield and Brownlee, 1989; reviewed by Paterson and Fodor, 2012). However, interactions between NEP and the polymerase have also been more recently identified (Manz et al., 2012). Prior to export, vRNPs have been shown to be tethered to chromatin, which is thought to improve efficiency of binding to Ran-GTP via association with Rcc-1 (Chase et al., 2011). Crm1 is activated for nuclear export by binding to Ran-GTP, and crosses the NPC via interaction with nucleoporins. This allows for nuclear vRNPs to be transported across the NPC into the cytoplasm where they can be assembled into virions. Once transported into the cytoplasm the vRNPs are dissociated from Crm1 via conversion of Ran-GTP to Ran-GDP via Ran-GAP (Eisfeld et al., 2015).

Once within the cytoplasm, vRNPs need to be trafficked towards the cellular membrane for virus assembly and budding. vRNPs accumulate at the perinuclear cytoplasm in regions containing the microtubule organising centre (MTOC), where they interact with Y-box binding protein-1 (YB-1) allowing association with microtubules (Kawaguchi et al., 2012; Amorim et al., 2011; Momose et al., 2007). Transport through the cell requires interaction of the vRNPs with recycling endosomes through Rab11's interaction with PB2 which

mediates vesicular transport via microtubules to the apical plasma membrane (Momose et al., 2007; Amorim et al., 2011; Eisfeld et al., 2011; Bruce et al., 2012).

1.4.5: Virus assembly and budding

For an influenza particle to be infectious all eight gene segments must be packaged into the virion and studies have shown this occurs through segment-specific packaging mechanisms (reviewed in Hutchinson et al., 2010). Virions do not typically package more than eight segments and each segment usually only occurs once per virion. This is known to be mediated by the presence of RNA packaging signals at the termini of each segment (Inagaki et al., 2012; Chou et al., 2012; Duhaut and McCauley, 1996; Fujii et al., 2003; Gog et al., 2007). At the point of packaging, complexes of eight parallel and closely packed vRNPs can be observed by electron tomography. These segments appear to be of distinctive lengths and only a small number of segment orders are observed. The RNP complexes are specifically packaged in a 7+1 arrangement where one central RNP is surrounded by the seven others (Noda et al., 2018; Nakatsu et al., 2016; Noda et al., 2006; Harris et al., 2006; Noda et al., 2012; Fournier et al., 2012). These interactions appear to be hierarchical, with certain segments (1 and 7) being shown to have importance in co-ordinating the interactions of the RNPs. The mechanism of how influenza viruses make use of these packaging signals is still debated although there is increasing evidence to suggest that RNA-RNA interactions may be important for the selective packaging of vRNPs (Gerber et al., 2014).

Virion assembly and budding takes place at lipid raft domains within the plasma membrane of infected cells. These are regions rich in cholesterol and sphingolipids (Brown and London, 1998). IAV HA and NA are intrinsically linked with these regions whereas M2 is excluded (Chen et al., 2007; Leser and Lamb, 2005; Rossman et al., 2010; Takeda et al., 2003). The concentration of HA within lipid raft domains allows for initiation of virus budding although the exact mechanism is unknown. However within virus-like particle (VLP) studies, HA alone appears to possess the ability to alter membrane curvature leading to initiation of budding (Chen et al., 2007). Other studies have shown that co-expression of HA, NA, M2 and M1 enhances VLP release, suggesting all four components are required for the most efficient budding process (Chen et al., 2007; Lai et al., 2010). M1 mediates recruitment of the viral proteins necessary to complete budding by crosslinking the cytoplasmic tails of HA and NA to facilitate their incorporation into the budding virion (Gomez- Puertas et al., 2000; Ruigrok et al., 2000; reviewed by Schmitt and Lamb, 2005). Within the virion M1 interacts with both the plasma membrane and NP (within the vRNPs) (Bui et al., 1996; Noton et al., 2007; Zhang and Lamb, 1996). M1 polymerises at the sites of viral budding which can lead to the elongation of the budding virion and therefore production of a filamentous virus. Membrane bound M1 can also mediate additional alterations in membrane curvature, further progressing the budding process (Chen et al., 2007). M2 appears to stabilise the site of budding and aid with proper virion assembly before budding occurs. It also alters the membrane curvature to provide the final force required to mediate membrane scission (Rossman et al., 2010). Some host factors such as G-protein, F1Fo-ATP activity

and Rab11 are also required for virus budding (Gorai et al., 2012; reviewed by Ludwig et al., 1999; Bruce et al., 2010). Following membrane scission, the virion may still be attached to the cellular membrane via interaction of HA with sialic acid moieties. NA can then cleave the sialic acid, allowing the virion to be released (Palese et al., 1974).

1.5: Influenza A virus evolution

There are two main mechanisms by which IAVs can evolve:

i) Antigenic drift:

The error rate within the IAV RNA polymerase is high due to a lack of proof-reading ability which leads to the gradual addition of mutations within the genome. Drake et al. (1993) estimated that every time the IAV polymerase replicates its genome around one error is made. Antigenic drift describes the introduction of mutations into viral surface glycoproteins which can result in alterations to antigenic regions leading to immune escape from neutralising antibodies (reviewed by Scholtissek, 1995). Antigenic drift can occur under the selection pressure of the natural immune response or from vaccines. Lauring and Andino (2010), described the theory that a viral 'quasi-species' exists during each round of infection where a swarm of viruses, inherently linked via mutation, are produced. The highest frequency mutations within the population depends on the ability of individual members of the virus population to survive within the environment they find themselves in. Many of the mutants created during antigenic drift will be detrimental to viral fitness and will not persist.

ii) Antigenic shift:

Antigenic shift refers to the introduction of a new IAV subtype into the human population, either via direct introduction or as a result of reassortment (Schrauwen et al., 2014). This latter event occurs when two or more viruses infect the same cell, allowing for the exchange of gene segments between the viruses, potentially leading to the emergence of a new viral subtype to which the population may have no prior immunogenicity. If the combination of segments is advantageous to viral fitness and the virus can successfully replicate, a 'reassortant' strain can emerge. This has occurred numerous times within the human population, for example, in 1957 when the H2N2 subtype replaced the H1N1 subtype. The appearance of this novel H2N2 strain was the result of natural reassortment between the prevailing human H1N1 strain and an avian H2N2 virus which donated its HA, NA and PB1 genes (Scholtissek et al., 1978).

1.6: Avian influenza viruses (AIVs)

It is believed that all IAV originate in aquatic birds such as ducks and sea birds as the majority of HA and NA subtype combinations have been isolated from them (Fouchier et al., 2005; Webster et al., 1992; Alexander., 2000). Within the natural host species IAV replicates within the gastrointestinal tract and are usually asymptomatic (Webster et al., 1992). AIVs are spread via the faecal-oral route and can remain infectious for weeks within lake water, facilitating efficient spread within the aquatic bird reservoir (Webster et al., 1978). IAV also have lower rates of nucleotide substitution within their natural reservoirs compared to those viruses which infect humans and poultry (Webster et al., 1992). AIVs can

cause infection within domestic poultry, with numerous subtypes jumping from the natural aquatic bird reservoir, including H5Nx, H6N1, H7Nx and H9N2 subtypes. Within poultry species such as chickens, clinical disease signs can be severe, and mortality can result from infection, leading to large economic losses for the poultry industry (Swayne and Pantin-Jackwood, 2006).

IAV are often categorised based on the severity of the disease they cause within a galliform host (Capua and Alexander, 2004). Low pathogenicity avian influenza viruses (LPAIV), generally cause little morbidity; characterised by mild respiratory signs, depression and egg production problems in layers (reviewed by Yoon et al., 2014). However, co-infections or other environmental factors have been shown to exacerbate disease signs and lead to high mortality rates in the field (Kishida et al., 2004; Pan et al., 2012; Seifi et al., 2010). Within poultry, LPAIV are mainly restricted to replication within the respiratory and gastrointestinal tracts and transmit via the faecal-oral route, although some airborne transmission has been observed (Claes et al., 2013; Pantin-Jackwood et al., 2013; Zhou et al., 2016; Lv et al., 2015).

On the other hand, high pathogenicity avian influenza viruses (HPAIV) can cause up to 100% mortality in chicken flocks within several days, transmitting via a combination of airborne and faecal-oral routes (Shortridge et al., 1998; Pu et al., 2015; Spekreijse et al., 2011; Zhou et al., 2016). At the current time, HPAIVs have only been regularly derived from viruses of H5 and H7 subtypes and are defined as having an intravenous pathogenicity index (IVPI) of 1.2 or above in 6-week old chickens. Within these studies chickens are inoculated intravenously

with a high viral dose and monitored for clinical disease over a period of 10 days. A score of 0 indicate no birds died whereas a score of 3 indicates all birds died within 24 hours of infection (OIE, 2017). HPAIVs replicate systemically within the galliform host as they can utilise endogenous subtilisin-like proteases, such as furin to cleave HA0, due to the presence of a poly-basic cleavage site (PBCS) (e.g. PQ**R**E**RRRKKR**/GLF) within HA (Vey et al., 1992; Wood et al., 1993; Senne et al., 1996). The acquisition of a PBCS in HPAIV has been proposed to be the result of the error prone polymerase, where polymerase slippage would result in accidental repetition of nucleotides (Perdue et al., 1997). Monne et al. (2014), showed that HPAIVs emerged from low-pathogenic precursor viruses in the absence of reassortment. However, the presence of a PBCS does not automatically determine viral pathogenicity. For example, a H4N2 AIV isolated from quail in the USA had a naturally occurring PBCS, but this virus had an IPVI of 0 retaining a LPAIV phenotype (Wong et al., 2014). Conversely, an H10 AIV isolated from ducks in Singapore had an IVPI indicative of a HPAIV despite not having a PBSC (Wood et al., 1996). This indicates that other viral factors play a role in overall determination of pathogenicity. Some well characterised markers of pathogenicity include NA stalk deletions which increase AIV pathogenicity (Matsuoka et al., 2009; Sun et al., 2013b), polymerase polymorphisms (Suzuki et al., 2014), the presence or absence of accessory proteins such as PB1-F2 and PA-X (James et al., 2016; Gao et al., 2015c) and polymorphisms in NS1 (Kong et al., 2015; Ayllon et al., 2014).

1.6.1: Host species determinants in IAV

It is important to understand the factors responsible for the ability of AIVs to infect and become transmissible within mammals to be able to better implement control measures, therefore a large body of work has been completed to identify factors responsible for this host switch.

One of the main determinants is the ability of the HA to bind to α-2, 3 (generally avian) or α-2, 6 (generally mammalian) linked sialic acid on the cell surface (Connor et al., 1994). Multiple HA residues have been deemed important for enabling viruses to switch receptor binding preference, including mutations within the 220-loop and 190-helix. However, many studies have shown that an amino acid change from Q to L at position 226 (H3 numbering) within HA is sufficient to alter receptor binding preference from avian- to human-like, enabling viruses to transmit between ferrets. This has been seen within H2, H3, H5, H7 and H9 AIVs (Rogers et al., 1983; Wan et al., 2007; Imai et al., 2012; Schrawen et al., 2016; Matrosovich et al., 2000). Other residues including G228S have also been shown to influence receptor binding preference of H2, H3, H5 and H7 viruses (Schrawen et al., 2016; Gambaryan et al., 1997; Teng et al., 2016).

Another determinant of host range is the pH stability of cleaved HA. AIVs, along with swine influenza viruses, have a higher pH of fusion than that of human viruses. Human HAs usually fuse at a pH of 5.4-5.6 where avian and swine HAs fuse at a pH of 5.6-6.0 (Galloway et al., 2013; Russier et al., 2016; Costello et al., 2015). This alteration in fusion pH can be seen when AIVs are experimentally passaged in ferrets (Linster et al., 2014; Herfst et al., 2014). It has been

hypothesised that the different fusion pHs allow for airborne transmission within humans (and ferrets) and persistence of viruses on fomites rather than in waterborne systems as with AIVs (Krenn et al., 2011). On the other hand, the mammalian respiratory tract is also mildly acidic and the lower pH of fusion may aid with stability in this environment (Washington et al., 2000). A high pH of fusion has been shown to increase pathogenicity in avian species but reduce pathogenicity in mammals (Reed et al., 2010; Zaraket et al., 2013).

The avian viral polymerase has been demonstrated to be a limiting factor in transmission and viral fitness within mammalian hosts, with avian polymerase complexes often displaying inefficient replicative abilities within mammalian cells. The most extensively characterised change to counteract this restriction is a lysine to glutamic acid substitution at position 627 of PB2 (Subbarao et al., 1993; Chen et al., 2006). It has been hypothesised that this substitution facilitates adaptation to physiological constraints of the species such as differences in body temperature (Hatta et al., 2007; Massin et al., 2001). Long et al. (2016), characterised the role of PB2 E627K as being involved in interactions with the host protein ANP32A, which varies in structure between avian and mammalian hosts. The presence of 627E mediates interaction with the avian but not human variant of the protein. However, the molecular mechanism behind ANP32A's interaction with PB2 remains unclear. Several other polymerase adaptive mutations have been identified, including PB2 D701N, which can partially compensate for AIV PB2 627E in mammalian cells by increasing binding to importin-α isotypes (Steel et al., 2009; Tarendeau et al., 2007 and Gabriel et al.,

2008). Several mutations in PA have also been investigated to impact upon host adaptation (see section 1.8.1.1 for details).

Adaptive mutations within NP have been described which alter replication of AIVs in mammalian cells including N319K which affects NP interactions with host importin-α isoforms (Gabriel et al., 2005; 2007; 2008 and 2011). Other NP mutations can overcome the restriction of AIVs by human MxA (Manz et al., 2013a). Finally, within H5N1 AIVs, particularly those which lack the PB2 E627K mutation, mutations within NEP (M16I, Y41C and E75G) have been shown to enhance viral RNA synthesis by avian polymerases in human cells (Manz et al., 2012).

1.6.2: Zoonotic potential of AIVs

Several of the human influenza pandemics over the last century were derived from viruses of avian origin. This includes the 1968 Hong Kong flu, which was the result of reassortment between the seasonal H2N2 strain and an avian H3Nx strain which donated its HA and PB1 segments (Kawaoka et al., 1989). There is also some evidence to suggest the 1918 H1N1 pandemic was of avian origin (Taubenberger et al., 2012).

As well as their pandemic potential and infection in poultry, AIVs have led to sporadic zoonotic infection in humans. HPAIV H5N1 first caused an outbreak in humans in Hong Kong in 1997, after direct transmission from poultry, causing fatality in 6 out of 18 cases (Yuen et al., 1998). Since this outbreak, HPAIV H5N1 spread to poultry populations in Asia, Europe and Africa, causing severe disease outbreaks. This has corresponded with increased cases within humans; as of July

2018, there have been 860 confirmed human cases of H5N1 with 454 deaths; a case fatality rate of 53%. Most of the human cases have been within Egypt, Indonesia and Vietnam (WHO, 2018a). The majority of human H5N1 infections have been the result of direct transmission from poultry in areas such as live bird markets and there is little evidence of human-human transmission. In 2013, a new AIV zoonotic incursion occurred in China with a novel reassortant H7N9 virus. This LPAIV causes little disease signs in poultry, however, in humans it leads to severe and often fatal respiratory disease (Kalthoff et al., 2014). As of July 2018, there have been 1625 laboratory confirmed cases resulting in 623 deaths; a case fatality rate of 38% (WHO, 2018b). Again human-human transmission is limited but, studies have shown transmission can occur via direct contact within ferret models (Zhang et al., 2013). Several mammalian adaptation markers have been identified within these H7N9 strains, including HA 226L and PB2 627K changes (Zhang et al., 2014a; Watanabe et al., 2014). In 2017, a H7N9 virus was isolated from a human infection which contained the HPAIV signature PBCS (Yang et al., 2017). Other viral subtypes including H5N6, H6N1, H7N2, H7N3, H7N7, H9N2, H10N7 and H10N8 have also caused a limited number of human infections (see Table 1.2 for details). All of these data suggest that it is important to fully understand the potential of AIVs to cause zoonotic infections to prevent further pandemics.

Table 1.2: Total human infections with different AIV subtypes. Data collected from WHO, July 2018.

Influenza subtype	Cases total	Deaths total	Case fatality rate	Years	Countries	Reference
H5N1	860	454	53%	1997-present	Egypt, Indonesia, Vietnam	Yuen et al., 1998
H7N9	1625	623	38%	2013-present	China	Kalthoff et al., 2014
H9N2	39	1	3%	1999-present	China, Egypt, Bangladesh	Peiris et al., 1999
H5N6	19	6	43%	2014-present	China	Shen et al., 2016
H10N8	2	2	100%	2014	China	Chen et al., 2014
H6N1	1	0	0%	2013	Taiwan	Shi et al., 2013
H7N3	2	0	0%	2012	Mexico	CDC., 2012
H10N7	2	0	0%	2010	Australia	Arzey et al., 2012
H7N2	1	0	0%	2004	USA	CDC., 2004
H7N7	78	1	1%	2003	Netherlands	Fouchier et al., 2004
H7N4	1	0	0%	2017	China	Tong et al., 2018

1.6.3: Avian influenza virus control

Once an HPAIV outbreak has been confirmed within a poultry flock, the preferred method of control is quarantine and 'stamping out'. This involves culling all birds in an infected farm as well as those within a 10km perimeter. Movement restrictions are also placed upon birds and their products to prevent further spread to other surrounding farms (OIE, 2017). However, in many countries AIV has become enzootic and therefore it is not practical to cull the entire poultry populations, so vaccination has become the main method for control (Swayne, 2012). For example, vaccination has been used against H5N2 viruses in Mexico, H7N3 in Pakistan and H5N1 in China (Capua and Alexander, 2004). Vaccination has been shown to protect against clinical signs and mortality, reduce shedding and increase resistance to infection. However, viral replication is not always fully ablated, allowing the viruses to spread without the presence of clinical signs (Capua and Marangon, 2004). Currently, the majority of vaccines used within the field are inactivated vaccines; where viruses are grown in eggs and then inactivated using formalin (Swayne, 2012; Rahn et al., 2015). However, in recent years, research has been focused on developing recombinant vectored vaccines for AIV, using either avian herpesviruses, Newcastle disease virus or fowlpox virus backbones expressing the IAV HA (Rahn et al., 2015). A combination of monitoring systems, strict biosecurity and depopulation is suggested as the best method for control of AIVs (Capua and Alexander, 2004).

1.7: H9N2 AIVs

H9N2 AIVs have become endemic in poultry populations throughout much of Asia and North Africa. H9N2 are LPAIV which do not usually induce obvious clinical signs in chickens, with birds typically only showing signs including depression and ruffled feathers (Sun et al., 2010). Despite this, infection with H9N2 has led to cases with high morbidity, mortality and reduced egg production in layers (Bano et al., 2003; Kishida et al., 2004), although this is usually linked with secondary co-infections, poor housing or nutrition. In one case, an H9N2 AIV was isolated that caused lethal infection in chickens, where 8 out of 10 6-week old SPF chickens died after infection (Zhang et al., 2014b).

1.7.1: Epidemiology, ecology and evolution

As stated above, throughout much of Asia, the Middle East and North Africa, H9N2 AIVs have become endemic in poultry populations and although the virus has not yet crossed into poultry flocks in Europe, recent incursions into Morocco and Turkey in 2016 suggest that the threat is increasing (Figure 1.5). H9N2 AIVs can be grouped phylogenetically via their HA gene which splits them into two main branches; Eurasian and America. The American branch of H9N2 are mainly responsible for historical infections in turkey farms (Homme et al., 1970). Within the Eurasian branch, there are 3 distinct lineages of virus. These are named after the prototypic virus in each group: A/chicken/Beijing/1/94-like (BJ/94-like), A/quail/Hong Kong/G1/97-like (G1-like) and A/duck/Hong Kong/ Y439/97 (Y439-like). The G1 lineage is the most widespread in the regions between Southern China and Morocco. It can be further split into two sub-

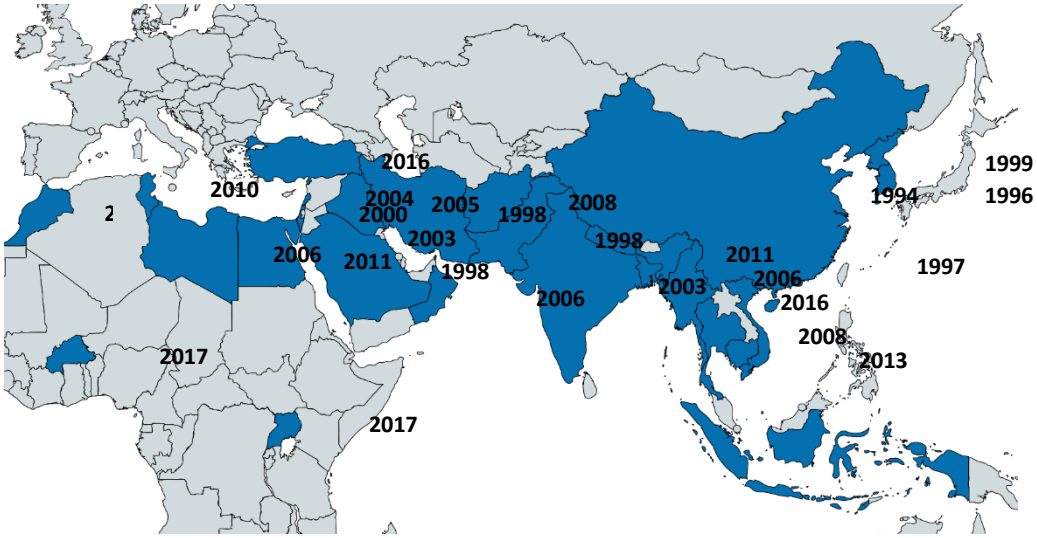

Figure 1.5: Enzootic spread of H9N2 viruses in poultry in Asia, Middle East and North Africa. H9N2 enzootic countries represented in blue. Dates show the first isolation in chickens within the given country. Map made using mapchart.net

lineages based on geographical location: G1-Western (Bangladesh to Morocco) and G1-Eastern (South China, Vietnam and Hong Kong). The BJ/94 lineage mainly affects poultry in China but is also found in Vietnam and Cambodia. The Y439 lineage is mainly isolated in wild birds throughout Eurasia and occasionally causes disease in poultry. In addition, a BJ/94 sub-lineage (A/chicken/Shanghai/F/98 – F/98-like), has persisted in poultry in Eastern China since 1998 (Lu et al., 2005, Zhang et al., 2009 and Zhang et al., 2008). However, since 2010 a novel genotype (G57 or genotype S) has become predominant in vaccinated poultry flocks in China and Vietnam (Gu et al., 2014; Liu et al., 2016). This genotype has been shown to have greater infectivity and is the predominant strain to donate internal gene segments to highly zoonotic AIVs (Pu et al., 2015; Gao et al., 2013).

H9N2 infections occur throughout the year within poultry flocks and are frequently isolated from live bird markets in apparently healthy chickens, ducks and other poultry species (Xu et al., 2007b). Between 2008 and 2010, 2.6% of birds tested in live bird markets in Shanghai were positive for H9N2 AIV (Wang et al., 2014). These viruses are transmitted between birds via air droplet, dust, feed or water (Liu, 2012).

1.7.2: Pathogenicity in different hosts

The first outbreak of H9N2 in China was characterised by a mortality rate of 10-40% in broiler birds and reduced laying rates by 14-17% (Chen et al., 1994; Zhang et al., 1994). However, when introduced into SPF chickens, no mortality was observed. Since this time, H9N2 AIVs have been shown to display an

enhanced clinical presentation within poultry as well as increased transmission (Gao et al., 2016; Iqbal et al., 2013; Zhong et al., 2014; Seiler et al., 2018). Along with chickens, H9N2 AIVs have also become established in other poultry species such as quail, guinea fowl, partridge and pheasants (Zhou et al., 2016; Xu et al., 2007a). Quail have been shown to be more susceptible to H9N2 infection than other species; they also possess more 'human-like' receptors than chickens suggesting they could play a role in the zoonotic potential of H9N2 AIVs (Perez et al., 2003; Wan and Perez, 2006; Costa et al., 2012).

There have also been several isolations of H9N2 in swine, mainly in China. Mammalian adaptation markers including full length NA stalks and a high affinity for binding human-like α-2,6 sialic acids via an HA Q226L mutation have been identified in some of these viruses (Xu et al., 2004; Cong et al., 2007; Cong et al., 2008; Yu et al., 2008). H9N2 infection in swine is of particular interest because of the propensity for pigs to be 'mixing vessels' for infection between mammalian and avian influenza viruses due to the presence of both human- and avian- like receptors in their respiratory tracts (Ito et al., 1998). Pigs with H9N2 AIV infection display symptoms such as high fever, coughing and tearing (Xu et al., 2004). However, in experimental infections, H9N2 AIV show little replicative ability and limited transmission between pigs, although this was viral strain-dependent (Obadan et al., 2015; Wang et al., 2016a). The lack of transmission between pigs suggests outbreaks are the result of repeated reintroduction from avian species.

Within canine and equine hosts there have been a handful of isolations of H9N2 AIVs. In China, BJ/94-like H9N2 AIVs were identified in dogs displaying classical signs of influenza infection (Sun et al., 2013a) and several studies have shown seroconversion in stray dogs present at live poultry markets in China to H9N2 (Zhou et al., 2015; Su et al., 2014). There has been a single case of H9N2 equine influenza, which was again a BJ/94 lineage virus from China (He, 2012).

Within ferret models, H9N2 AIVs have been shown to replicate efficiently although to a lesser extent than a human H3N2 virus. Direct transmission between experimental animals occurred with 2 strains of H9N2, deemed to be the result of the mammalian adaptation marker HA Q226L (Wan et al., 2008; Gao et al., 2016). In addition, several of the G57 genotype H9N2 AIVs have been shown, within ferret models, to transmit via respiratory droplet (Li et al., 2014; Yuan et al., 2015). The ability of H9N2 AIV to replicate and acquire mammalian adaptive mutations increases their zoonotic and pandemic potential. H9N2 AIVs have caused sporadic infections in humans. The first recorded case was two children displaying cold and flu-like symptoms, from Hong Kong in 1997 (Peiris et al., 1999). In humans, H9N2 infections are generally mild and only one death has been reported; in a patient with underlying health conditions (WHO report, 2016). H9N2 is most often reported as the result of screening for zoonotic H5N1 and H7N9 infections in China, Egypt and Bangladesh (Zhou et al., 2016; Monne et al., 2013; ICDDRB, 2011). Therefore, due to the mild clinical presentation of human disease it is likely that many cases go unreported. Studies looking at seropostivity to H9N2 in poultry exposed groups show that 1.7% - 6.5% of individuals display α-H9 antibodies (Wang et al., 2009; Pawar et al., 2012; Ma et

al., 2018). Many of the cases of H9N2 can be attributed to prior contact with poultry and there is no evidence of human-human transmission (Uyeki et al., 2002). However, Matrosovich et al. (2001) reported that Asian poultry H9N2 viruses show increased binding to human-like receptors and Chrzastek et al. (2018) showed a heterogeneity in Q and L at HA226. Overall, this suggests that although H9N2 infections are usually mild or asymptomatic and do not transmit further that the initial zoonotic event, further adaptation could lead to viruses becoming a true pandemic threat.

1.7.3: Reassortment

H9N2 AIVs, have been recognised as viruses which readily donate and receive gene segments from many other viral subtypes, including highly pathogenic and zoonotic strains. In experimental studies, a high frequency of reassortment (40-64%) was seen during co-infection of H4N6 and H9N2 IAVs in chickens (Li et al., 2018). This is particularly notable with the donation of the 6 internal gene cassette of G57-like H9N2 AIVs to viruses such as human infecting H7N9, H10N8 and H5N6 shown to have a high propensity to cause death within humans (Shen et al., 2015; Zhang, 2016; Lam et al., 2013; Kageyama et al., 2013). The donation of H9N2 internal genes has been linked back as far back as the HPAIV H5N1 outbreak in Hong Kong in 1997, where retrospective analysis showed that all internal genes were derived from co-circulating G1-like H9N2 AIVs (Guan et al., 1999). Live poultry markets are suggested as places where the H9N2 AIVs can mix and reassort with H7 and H5 subtype strains, with co-

circulation often being reported (Yu et al., 2014; Su et al., 2015; Wu et al., 2015; Naguib et al., 2015; Horwood et al., 2018).

H9N2 AIVs have also donated their internal genes to novel genotypes of virus emerging in poultry populations. For example, a H5N2 AIV isolated from apparently healthy chickens in China was found to contain 7 gene segments (minus HA) derived from H9N2 (Wang et al., 2016b; Zhao et al., 2012). Another example comes from the identification of an H5N1 virus where four of the internal genes (PB2, PB1, PA and M) were of H9N2 origin (Gu et al., 2010). The emergence of a novel H7N7 AIV in chickens in China has also been shown to be the result of reassortment with H9N2 viruses and the donation of the internal gene cassette (Lam et al., 2013).

On the other hand, H9N2 viruses readily accept internal genes from other IAV subtypes. For example, the currently circulating H9N2 lineage in Pakistan and Bangladesh is known to have received several internal genes from HPAIV H7N3 and H5N1 viruses (Iqbal et al., 2009; Parvin et al., 2014). The viruses circulating in Bangladesh contain the NS, NP, M, PA and PB1 genes from H7N3 originating in Pakistan (Shanmuganatham et al., 2014). These reassortant viruses have an enhanced replication and transmission in both quail and chickens compared to the predecessor strains (Seiler et al., 2018). In China, there have also been multiple reports of H9N2 viruses isolated with internal genes derived from HPAIV H5N1 strains including the entire internal gene cassette (Guan et al., 2000) or different combinations of genes such as PB1 alone (Dong et al., 2011b) or PB2, PA and NP (Choi et al., 2004).

These reassortment events have enabled H9N2 AIVs to drastically change since they were first isolated in poultry and all their internal genes clustered with the G1-lineage (Cameron et al., 2000). The reassortant viruses have been shown to have increased fitness and to cause more severe clinical signs within chickens and wild terrestrial species such as quails and sparrows (Iqbal et al., 2013; Aamir et al., 2007; Guo et al., 2000; Zhang et al., 2014b). In experimental infections, some H9N2 AIVs, isolated from 2000-2002, were able to replicate in mice and lead to a 5-20% weight loss compared to the pre-2000 strains which were unable to replicate (Li et al., 2005). Deng et al. (2010) also showed that a H9N2 AIV from 2008 led to up to 60% mortality in mice caused by severe respiratory distress. These factors demonstrate the importance of furthering our understanding of the molecular factors responsible for the increased pathogenicity of H9N2 AIVs in both avian and mammalian hosts.

1.7.4: H9N2 segment 3

In Pakistan, H9N2 AIV segment 3 has been shown to be derived from HPAIV H7N3 viruses, which H9N2 acquired, along with the PB2, PB1 and NS gene segments, during its spread throughout the country (Iqbal et al., 2009). A similar pattern has also been seen in Bangladeshi H9N2 AIVs, where reassortment again with HPAIV H7N3 has resulted in novel viral genotypes emerging. The currently circulating H9N2 viruses possess the PA gene plus PB1, NP, M and NS derived from these highly pathogenic strains (Shanmuganatham et al., 2014). These reassortant strains, in both cases have been demonstrated to have increased replication and transmission in poultry compared to the parental G1-like viruses

(Seiler et al., 2018; Iqbal et al., 2013). Sealy et al., (2019), recently showed that theses internal gene reassortment events including the PA gene have remained prominent within the Pakistani H9N2 virus population, cementing their importance for viral fitness.

1.7.5: Vaccines

Many countries which have enzootic H9N2 infection have adopted vaccination as a control method, including China (Zhang et al., 2008), Morocco (El Houadfi et al., 2016), Pakistan (Naeem et al., 2006), Iran (Bahari et al., 2015) and Egypt (Kilany et al., 2016). The majority of vaccines are traditional inactivated vaccines which, unlike the human seasonal vaccine, are not regularly updated. This has led to H9N2 continuing to infect and cause disease in poultry flocks in many areas (Zhang et al., 2008).

1.8: The PA segment of IAV

The role of the PA segment (segment 3) in determining H9N2 AIV viral fitness and pathogenicity forms the basis of this thesis. Accordingly, this section gives a further introduction to the proteins encoded by segment 3 and their functions.

1.8.1: PA

The influenza Polymerase Acidic (PA) protein is translated from segment 3 of the viral genome (Braam et al., 1983; Fodor., 2013). PA is 716 amino acids in length and consists of two protein domains: a 25 kDa N-terminal domain and a 55 kDa C-terminal domain (Hara et al., 2006; Guu et al., 2008). The domains are

connected via a 60 amino acid linker domain, which allows for conformational flexibility of the protein (Guu et al., 2008), see Figure 1.6 for details.

The N-terminal domain of PA - PA_N (residues 1-197) contains the major functional region of the protein, the endonuclease domain, and has pleiotropic effects. Crystal structures of the PA_N domain show that it contains five mixed β-strands which form a twisted plane surrounded by seven α-helices. It contains a strongly negative charged cavity, which houses a metal binding site, with a similar structure to other endonucleases. Several residues have been identified which are important for the enzyme's catalytic activity including H41, E80, P107, D108, E119 and K134, as these residues coordinate the magnesium metal ion found in the active site (Yuan et al., 2009; Dias et al., 2009). The endonuclease activity allows PA to cleave host mRNAs 10-15 nucleotides downstream of the 5'cap during the 'cap snatching' process of viral mRNA synthesis. The short host mRNAs are then used as primers for the initiation of transcription via the PB1 polymerase segment. A number of important residues have been identified which can affect the catalytic ability of the PA endonuclease which are summarised in Table 1.3. There is also limited data to suggest the PA_N domain plays a role in regulating cRNA/vRNA synthesis as when PA T157 is present an increased cRNA synthesis is observed (Huarte et al., 2003) and has vRNA/ cRNA promotor binding ability with PA more involved in cRNA promotor binding suggesting possible functions in the cRNA/vRNA production switch by the polymerase (Hara et al., 2006; Maier et al., 2008). Kashiwagi et al., (2009), showed that H5N1 PA has an increased RNA polymerase activity due to enhanced cRNA promotor binding.

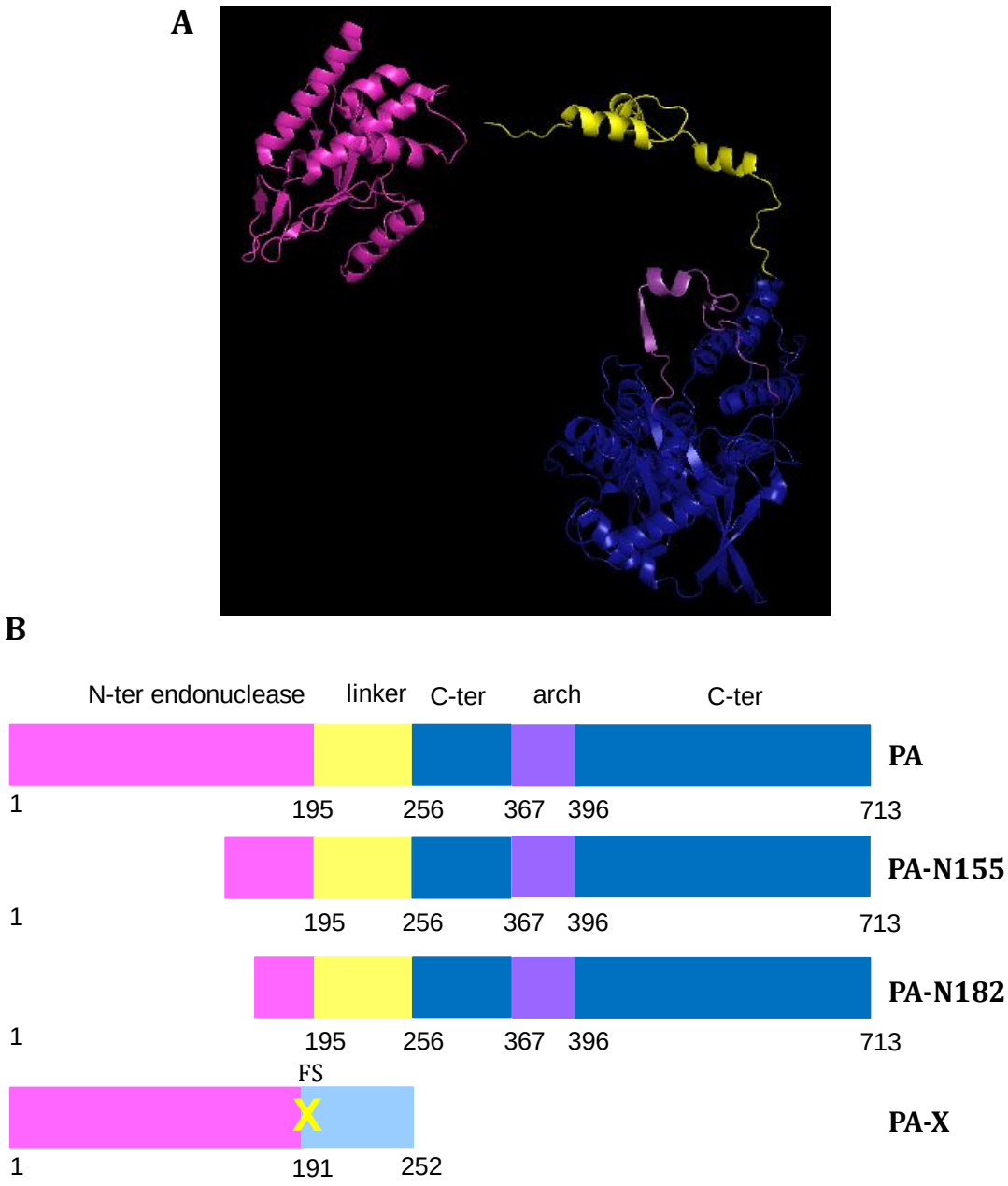

Figure 1.6: Influenza segment 3 structure. (A) Pymol software was used to map the structural domains onto the crystal structure of the influenza PA protein (PDB ID: 4WSB). PA endonuclease- pink, linker- yellow, C-terminus- blue, arch- purple. (B)Schematic to show the codon positions of the breaks between regions and the domains present in the PA accessory proteins. Colour scheme as above, X-ORF – pale blue.

The PA C-terminal domain- PA_C (residues 256- 713), is involved in the binding of PA to PB1 (Gonzalez et al., 1996). The two polymerase components directly interact and form a stable complex which allows for binding to vRNA promotors. The PA_C domain consists of 13 α-helices, one short 3_{10} helix, 9 β-strands and several loops/turns split into two domains (He et al., 2008; Obayashi et al., 2008). The binding of PB1 and PA is between the PA_C residues 668 and 692 and $PB1_N$ residues 1-12 (Perez and Donis, 2001), specific resides summarised in Table 1.3. This interaction is essential for viral replication and polymerase activity, shown by the introduction of mutations into specific residues in PB1 (Ghanem et al., 2007) and could pose an interesting target for the development of novel antivirals, as the interacting residues are highly conserved across not only IAV but also influenza B and C strains (Liu et al., 2009; Watanabe et al., 2017; Muratore et al., 2012). During the late stages of influenza virus infection, several studies have shown PA to be important for packaging and assembly of the viral genome. Regan et al. (2006), showed that introduction of G507A and R508A into the PA gene disrupts the assembly of infectious virions.

The PA_C domain has also been shown to interact with host proteins. In a screen of PA interactions using liquid chromatography-tandem mass spectrometry, Bradel-Tretheway (2011) putatively identified interactions with over 300 cellular proteins of which ~20% were mitochondrial proteins. One interaction that has been well validated is with the host protein human homologue chicken CLE (hCLE) (Huarte et al., 2001). This interaction is involved with the active reconstitution of vRNPs and positively modulates RNA polymerase II activity (Perez-Gonzalez et al., 2006). Kawaguchi et al. (2007), also

Table 1.3: Mutations affecting endonuclease activity and PB1 binding of the PA gene segment

Amino acid position	Function	Reference
H41	Endonuclease active site	Yuan et al., 2009
E80	Endonuclease active site	Yuan et al., 2009
K102A	Decreases viral transcription and replication. Decreases cap and vRNA promotor binding activity	Hara et al., 2006
D108	Endonuclease active site ; D108A-selectively inhibits transcription	Yuan et al., 2009; Hara et al., 2006
E119	Endonuclease active site	Yuan et al., 2009
K134	Endonuclease active site	Yuan et al., 2009
T157A	Decreases proteolytic activity and synthesis of cRNA	Perales et al., 2000
T162A	Decreases protease activity and RNP replication, delays nuclear import of PA	Huarte et al., 2003
K328	PB1 binding site	He et al., 2008
H501A	Decreases transcriptional activity of the polymerase	Fodor et al., 2002
G507A, R508A	Disrupt virion assembly	Regan et al., 2006
R566	PB1 binding site	He et al., 2008
K574	PB1 binding site	He et al., 2008
K539	PB1 binding site	He et al., 2008

identified an interaction of PA with the minichromosome maintenance complex (MCM), a DNA replicative helicase, which was proposed to stabilise viral replication elongation complexes and stimulate virus replication.

1.8.1.1: Influenza PA, host adaptation and virulence

There is considerable research to suggest that PA is important for AIVs to adapt to replication within mammalian hosts, although a sequence alignment between several avian and mammalian PA genes (Figure 1.7) suggests there are no conserved markers for host adaptation, at least within this limited number of strains. However, several amino acid changes have been implicated with increasing viral replication and pathogenicity in mice including K356R and E684G within H9N2 and V44I, V127A, C241Y, A343T and I573V within H5N1 (Xu et al., 2016a; Lee et al., 2018; Yamaji et al.,2015). Conversely, several PA codon alterations can also attenuate AIVs within mammalian hosts including R185K within H5N1 and P103H and S659L within H7N7 (Fan et al., 2014; Zhao et al., 2016). P190S and Q400P alterations in H7N3 PA decreased viral virulence in mice due to a corresponding reduction in inflammation after infection (DesRochers et al., 2016). When the recently described H5N6 AIVs, which can cause severe disease and death in humans, were passaged in mice to determine any markers of mammalian adaptation an amino acid substitution within the PA gene (A343T) was identified which mildly increase polymerase activity in mammalian cells and contributed to increased viral virulence within mice (Peng et al., 2018). Several residues within H7N9 PA have also been identified to increase polymerase activity within human cells and increase viral virulence in a

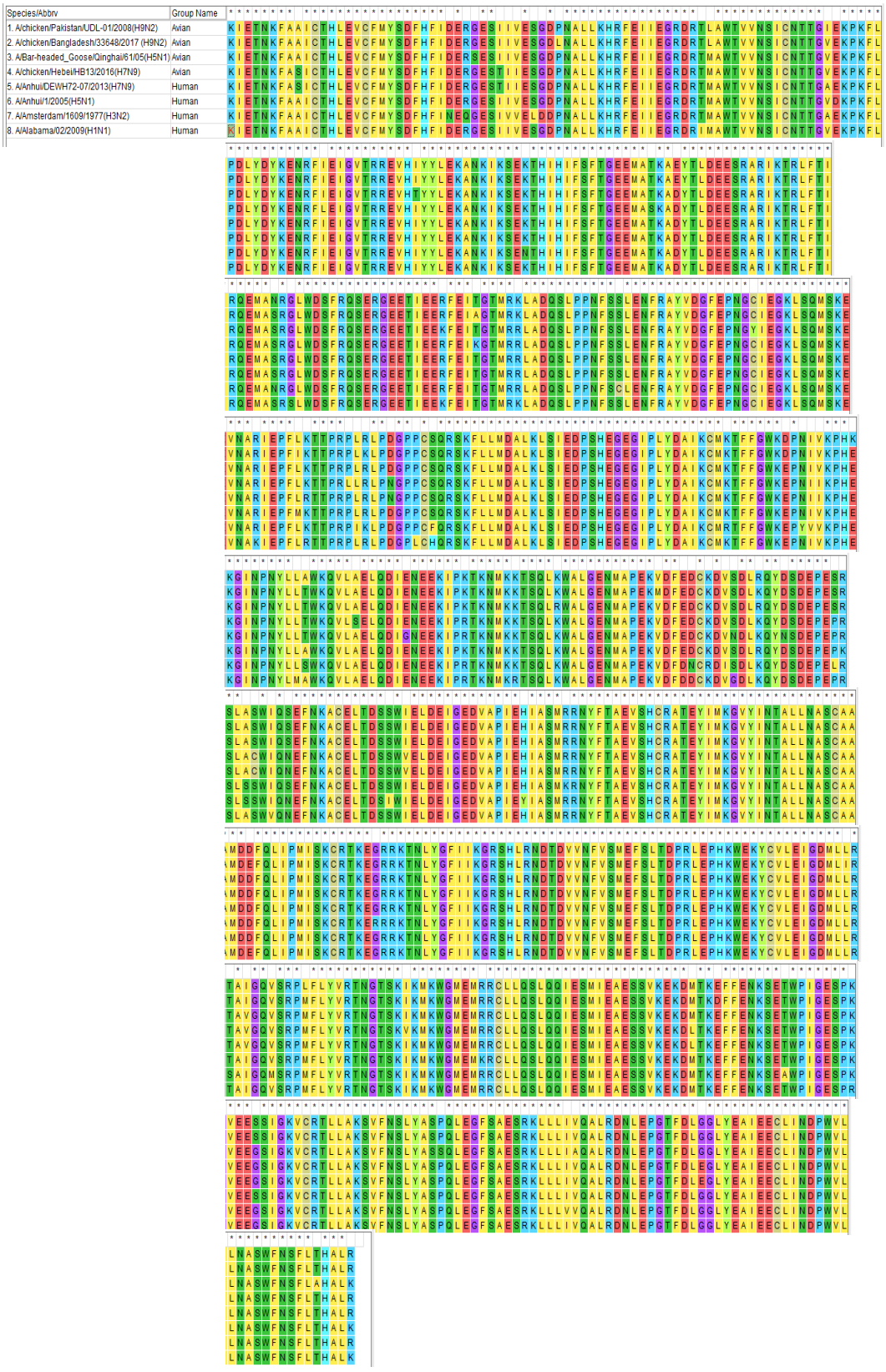

Figure 1.7: Sequence alignment of avian and mammalian PA genes. Randomly selected avian and mammalian PA protein sequences were downloaded from the NCBI database and aligned using MEGA 7.0 CLUSTAL multiple alignment software.

mouse model (Yamayoshi et al., 2014).

Within 2009 pH1N1, numerous studies have been completed to passage the virus in mice to determine key residues for adaptation. Several markers within PA have been identified such as F35L (Seyer et al., 2012), A36T (Zhu et al., 2012), L259P (Ilyushina et al., 2010), M21I, and S616P (Sakabe et al., 2011). In addition to forcing adaptation of viruses to the mammalian host, several natural polymorphisms have been identified within PA which can contribute to altered viral replication and virulence in a mammalian host. For example, PA K142E is associated with high polymerase activity and replication within several human viruses and when introduced into an H5N1 background these viruses displayed increased replication and virulence within a mouse model as well as enhance polymerase activity in mammalian cells (Kim et al., 2010; Manz et al., 2013b). These studies all show that several residues within the PA gene can govern the pathogenicity and adaptation of IAV to mammalian hosts.

Along with amino acid substitutions in PA influencing host adaptation, exchange of the entire gene has been shown to affect IAV adaptation in mammalian hosts (Mehle et al., 2012; Chen et al., 2008; Hara et al., 2013). Of particular note, is the successive passage of the PA and PB2 genes from the pandemic 1918 H1N1 through to the 1957 H2N2 strain and then to the 1968 H3N2 virus, suggesting that these two gene segments are important for the maintenance of these viruses within the human host (Wright et al., 2007).

PA has also been shown to be a virulence determinant within the natural host in several scenarios. Studies have attributed the PA gene to the increased

pathogenicity of H5N1 AIVs in mallard ducks. For example, Hu et al. (2013a + b), demonstrated that the PA and HA genes of H5N1 AIVs contribute to high pathogenicity of the virus in mallard ducks and mice via the enhancement of the innate immune response and detection of virus within the brain. Song et al. (2011) also demonstrated that S224P and N383D mutations within PA of H5N1 AIV contribute to the enhanced pathogenicity in mallard ducks due to increased viral replication, polymerase activity and delayed nuclear accumulation of PA and PB1. Kajihara et al. (2013), also identified the PA gene to be a contributing factor in the high virulence of a H5N1 strain in domestic ducks. Current data suggests that adaptive mutations within PA may enhance the ability of IAV to disseminate throughout the birds to organs such as the brain and therefore contribute to enhanced lethality (Bingham et al., 2009; Kishida et al., 2005; Londt et al., 2008).

1.8.2: PA-X

IAV segment 3 encodes several accessory gene products, including PA-X. PA-X is a +1 frameshift product of segment 3 which is accessed via a highly conserved frameshift site (FS). The resulting protein is a 29 kDa fusion protein consisting of the N-terminal 191 amino acids of PA and a (usually) 41 or 61 amino acid X-ORF which is viral strain-dependent (Jagger et al., 2012). The shorter 41 amino acid X-ORF is most notably present within 2009 pH1N1 viruses as well as other swine viruses, equine H7N7, canine H3N8 and H3N2 as well as the bat influenza virus strains. However, the remaining 75% of sequences possess the 61 codon X-ORF (Shi et al., 2012).

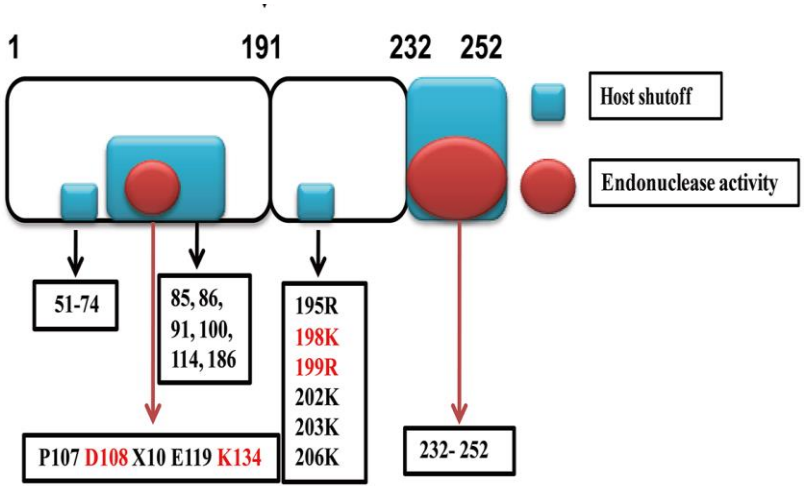

Figure 1.8: Schematic for active domains of the influenza PA-X protein. Locations of amino acid residues previously identified to affect host cell shut off activity or endonuclease activity highlighted in the above diagram. Regions identified to affect host cell shut off in blue, regions identified to affect endonuclease activity seen in red. Figure adapted from Hu et al., (2018).

The production of PA-X is the result of +1 ribosomal frameshifting at a highly conserved UCC UUU CGU C site. The conservation of amino acids at this site is highly unusual as both serine (UCC) and arginine (CGU) can be encoded by any of 5 other codons, CGU is also one of the least used codons within both mammalian and avian genomes. Frameshifting to the +1 ORF is promoted due the presence of a slow-to-decode amino acid within the A site of the ribosome. This results in the ribosome pausing at this site and, in this case, slippage into the +1 frame can occur when the UUU codon is positioned in the ribosomal P site and the rare CGU codon in the A site. Frameshifting is further promoted as both UUU and UUC are translated via a single phenylalanine tRNA (GAA) which has a higher affinity for UUC than UUU, so therefore favours P-site re-pairing within the +1 frame (Yewdell and Ince, 2012; Firth et al., 2012). The efficiency of frameshifting into the +1 X-ORF is approximately 1.3% (Jagger et al., 2012). PA-X has been shown to localise equally within both the nucleus and the cytoplasm of cells (Hayashi et al., 2016).

PA has been previously proposed to be a protease that degrades both viral and host proteins (Sanz-Ezquerro et al., 1996; Perales et al., 2000). However, Jagger et al. (2012) showed that this function is the result of the accessory protein PA-X, acting on mRNA instead of the protein products themselves. It was described that PA-X is involved in modulation of the host immune response during viral infection via selective degradation of host mRNAs, abolishing their translation and reducing expression of cellular proteins; a process termed host cell shut off. This process allows for viruses to inhibit expression of many cellular genes to dampen the antiviral response and also direct the ribosome towards the

translation of viral mRNAs (Weber and Haller, 2007). PA-Xs derived from multiple IAV subtypes have been shown to induce host cell shut off including equine and canine H3N8 viruses (Feng et al., 2016), H1N1 and pH1N1 (Khaperskyy et al., 2016; Hayashi et al., 2015; Gao et al., 2015b; Lee et al., 2017; Gong et al., 2017), H5N1 (Hu et al., 2015; Gao et al., 2015b; Hu et al., 2016), H9N2 (Gao et al., 2015c) and swine H1N2 (Xu et al., 2016b; Xu et al., 2017). Khaperskyy et al. (2016) reported that PA-X is able to selectively degrade host RNA polymerase II transcribed RNAs within the nucleus, including non-coding RNAs in a way that is independent of mRNA translation. Complete degradation of these PA-X cleaved host mRNAs is also dependent on the host 5'-3' exonuclease Xrn1. The N-terminal 15 amino acids within the C-terminus of PA-X (amino acids 192-206), particularly six basic amino acids within this area (195R, 198K, 199R, 202K, 203K and 206K), have been shown to be important for the host shut off activity of PA-X (Desmet et al., 2013; Oishi et al., 2015). Hayashi et al. (2016) took this further and identified 195K, 198K and 199R to be the most important residues in determining the host cell shut off activity of PA-X. Oishi et al. (2018), also identified a further 22 amino acids distributed throughout the protein, which are important for PA-X shut off activity via alteration of the subcellular localisation of PA-X (from nuclear to cytoplasmic) within mammalian cells. To identify host proteins that PA-X may interact with to exert its host shut off functions, Li et al. (2016), performed affinity purification and mass spectrometry looking at interactions between H5N1 PA-X and cellular proteins within chicken (DF-1) cells. Within this screen, 56 host proteins were shown to interact with H5N1 PA-X. Many of the identified proteins had previously been described as pro- or

antiviral host factors. Several protein groups which have specific biological functions were identified to interact with PA-X. This included proteins involved in i) protein transport between the Golgi complex and endoplasm such as archain 1 and ARF1, ii) ribosomal protein complexes such as RPLPO and RPS20, iii) ATP hydrolysis including myosin light chain 1 and 2. Therefore, PA-X-binding proteins were apparently enriched in mitochondria and lipid transport, nucleosome assembly and RNA processing factors. However, many of these polymorphisms are common contaminants in "pull down" interaction assays (Mellacheruyu et al., 2013) and more work still needs to be completed to fully understand the mechanism of action of PA-X.

PA-X has also been shown to be a virulence determinant in several IAV strains, although (as with so many aspects of the virus biology) this appears to be strain- and host-dependent. For example, within pH1N1 2009 virus the expression of PA-X enhances viral replication and pathogenicity in mice, which corresponded with a reduced host innate immune response. At early time points post-infection, mice lungs showed an increased viral load and histopathology score when PA-X was present (Lee et al., 2017). However, Gao et al. (2015b) showed that mice infected with pH1N1 2009 virus containing PA-X had a reduced mortality compared to viruses which lacked PA-X, with these viruses displaying a reduced pathology and viral titre in the mouse lung. Both studies used Balb/c mice; however, the strain of pH1N1 was different between the studies which potentially could have had an impact on the study outcome. Within pH1N1 1918 IAVs, the virus which contained PA-X showed reduced weight loss and increased survival compared to a virus with PA-X removed (Jagger et al., 2012). The kinetics

and magnitude of the host immune response within the lungs of infected animals was altered with the presence or absence of PA-X in particular genes related to inflammation, apoptosis and cell differentiation and tissue remodelling. When PA-X was removed, many genes were more highly induced compared to the WT virus, including genes involved in CCR5 signalling in macrophages and T cells, IL-15 signalling, CD28 signalling and IFN-γ signalling (Jagger et al., 2012). Within classical swine H1N1 viruses, PA-X has been shown to inhibit viral replication and decrease virulence in a mouse model (Gao et al., 2015b) similarly to that seen for pH1N1 by Jagger et al. (2012). However, within swine H1N2 IAV expression of the PA-X protein enhances viral replication and transmissibility within pigs by delaying the proinflammatory response within the lungs (Xu et al., 2017).

Again, with AIVs, the presence of PA-X has been shown to have differential effects on pathogenicity depending on the viral strain in question. Within H9N2 LPAIV, PA-X has been shown to be a pro-virulence factor. Presence of PA-X induced a 33.3% mortality rate and corresponding 15% weight loss in infected mice compared to no mortality or significant weight loss in mice when PA-X was removed from the virus. The mice infected with virus containing PA-X showed enhanced vascular congestion and higher viral titres within the lungs than those from mice infected with virus lacking PA-X. Cytokine and chemokine protein levels (including IL-6, IL-1β, CCL3, IFN-γ and TNF-α) were consistently higher in lungs of mice infected with virus expressing PA-X at both 3 and 5 days post-infection. Collectively these data demonstrated that within H9N2 AIVs PA-X leads to an increased pathogenicity and up-regulation of cytokines within a mouse model (Gao et al., 2015c). However, within H5N1 HPAIVs, PA-X has been shown

to reduce viral virulence in mice, chickens and ducks acting to inhibit viral replication and dampen the host immune response (Gao et al., 2015b; Hu et al., 2015; Hu et al., 2016). Within the chicken lung, PA-X globally blunts the immune response, particularly by downregulating genes associated with inflammation and cell death. A global downregulation of the cytokine response in multiple organs of chickens and ducks was also observed (Hu et al., 2015).

The effect of possessing a 41 or 61 amino acid X-ORF within PA-X has also been investigated. Gao et al. (2015a) showed that pH1N1, H5N1 and H9N2 viruses which expressed PA-X with a 61 amino acid X-ORF were more virulent, showing increased replication in mouse lungs and causing an increased inflammatory response compared to the same viruses with the shorter X-ORF. When a comparison of swine H1N2 IAVs with a 41 or 61 amino acid X-ORF was conducted, the viruses containing the truncated PA-X showed increased viral replication, transmissibility and replication in pigs (Xu et al., 2016b), implicating the truncated PA-X as an adaptation marker for pigs and perhaps explaining the preponderance of truncated PA-Xs within swine influenza viruses (Shi et al., 2012). A separate study has also shown that the 41 amino acid truncated PA-X has reduced nuclease activity compared to full length PA-X (Bavagnoli et al., 2015), although the link between this finding and pathogenicity was not determined. Overall, these studies all show that PA-X is a virulence factor within IAV, but the outcome of infection when PA-X is removed from viruses appears to be strain-dependent.

1.8.3: Other gene products of PA

IAV segment 3 also encodes two further accessory proteins termed PA-N155 and PA-N182. These two PA encoded proteins are not especially well characterised within the current literature. They are translated from the 11th and 13th in-frame AUG respectively producing N-terminally truncated versions of PA (Muramoto et al., 2013). These AUG codons are highly conserved, suggesting that expression of these proteins is universal across IAVs (Gong et al., 2014). When the AUG codon are removed from a H1N1 virus replication is slowed and pathogenicity in mice is reduced (Muramoto et al., 2013). In order to further characterise the function of these proteins, Wang et al. (2018) investigated the host interactome of H5N1 derived PA-N155 and PA-N182. A total of 491 (PA-N155) and 302 (PA-N182) interacting proteins were identified; proteins involved in RNA processing, viral processing and protein transport, and signalling pathways of the proteasome, ribosome and aminoacyl-tRNA biosynthesis were enriched.

1.9: Host cell shut off

When a virus infects a cell, it can induce an antiviral host response; many viruses have evolved mechanisms to avoid, overcome and counteract this response. One such strategy is the general inhibition of host gene expression in a process referred to as host cell shut off (Aranda and Maude, 1998). Many viruses encode proteins which cause host cell shut off to occur; this includes poliovirus proteases (2A^{pro} and 3C^{pro}), which cleave essential host translation initiation factors to allow for viral internal ribosome entry site (IRES)-mediated initiation

of translation (Ventoso et al., 1998; Kuyumcu-Martinez et al., 2002). Herpesviruses also encode an endonuclease which destroys host mRNAs to ensure cap-dependent translation of viral mRNAs (Elgadi et al., 1999). Within IAVs both the accessory protein, PA-X, (described in section 1.8.2) and the protein NS1 play a role in host cell shut off (Jagger et al., 2012; Nemeroff et al., 1998).

The host shut off function of IAVs begins before PA-X is produced, coinciding with the transcription of viral mRNAs. It has been shown that two mechanisms are targeting nascent host transcripts at this stage. First, the cap-snatching ability of the polymerase destroys host pre-mRNAs to supply capped primers for viral transcription. The second mechanism is via the viral NS1 protein. NS1 acts via binding and inhibiting cellular cleavage and polyadenylation factor 30 (CPSF30). CPSF30 is essential for the 3' end processing and subsequent nuclear export of host transcripts and NS1 blocks this process (Nemeroff et al., 1998). Therefore, these two processes act together to remove competition with the host transcripts for nuclear export and translation factors. Then as the infection progresses, the host cell shut off function moves to focus within the cytoplasm rather than the nucleus to make the translation of viral proteins a priority for the host protein synthesis machinery. NS1 again acts at this stage to ensure efficient translation of viral gene products by first blocking PKR-mediated sensing of viral dsRNA and arresting translation (Lu et al., 1995; Tan et al., 1998) and secondly, supporting assembly of translation initiation complexes on the 5'-UTRs of viral mRNAs (reviewed in Yanguez and Nieto, 2011). Also, at this stage PA-X can, after its gradual accumulation during infection, act to degrade host RNA polymerase II transcribed transcripts (Khaperskyy et al., 2016). Therefore, there may be an

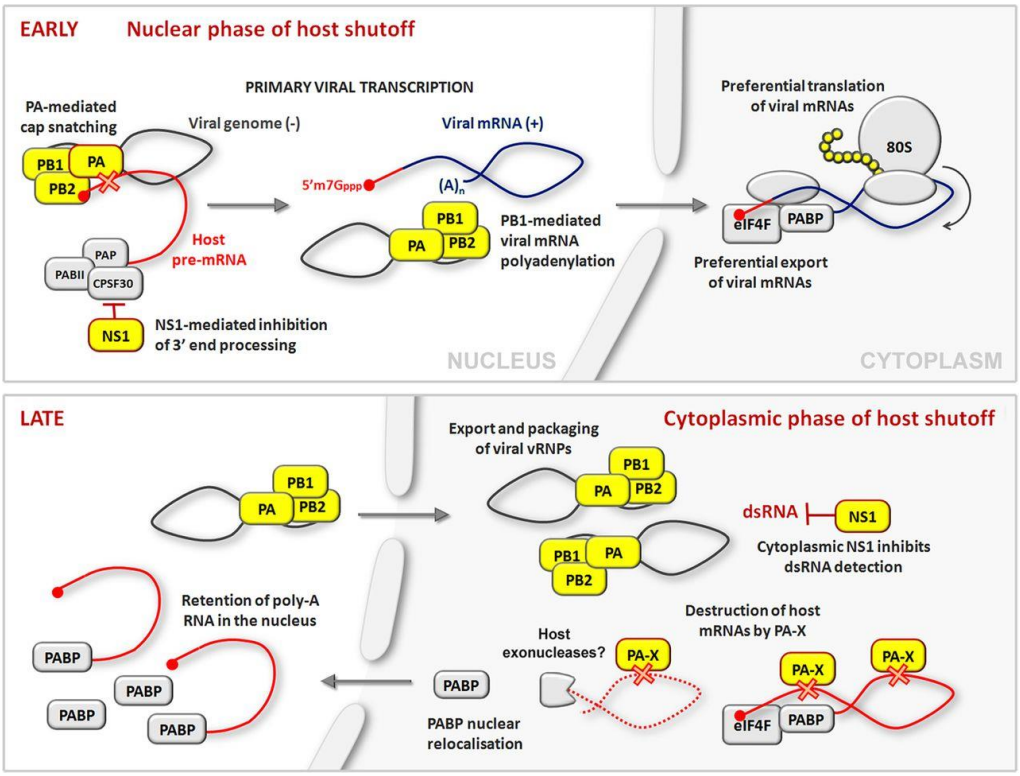

Figure 1.9: **Schematic for a temporal model of IAV induced host cell shut off**. IAV host cell shut off acts in two phases. The early phase begins in the nucleus with NS1 mediated inhibition of 3'end processing and the use of host mRNA for viral transcription. The late phase acts within the cytoplasm where PA-X degrades host mRNAs and NS1 inhibits detection of viral dsRNA. Figure taken from Khaperskyy and McCormick, 2015.

interplay between IAV NS1 and PA-X proteins to ensure sufficient host cell shut off at both early and late stages of infection (Figure 1.9).

1.10: Chicken innate immune response

The avian innate immune response plays a key role in the defence against viral infections via the recognition of pathogen associated molecular patterns (PAMPS) by pattern recognition receptors (PRRs). Activation of PRRs can lead to the induction of the interferon response and the production of cytokines which can then activate immune cells such as macrophages, dendritic cells and natural killer cells. This process should lead to the control and eradication of virus from the host (reviewed by Dzananovic et al., 2018). The signalling pathway for the avian innate immune response is summarised in Figure 1.10.

The avian innate immune system differs in its viral sensing than the mammalian system. Sensing of both double and single stranded RNA is carried out by MDA-5 rather than RIG-I, as chickens do not possess RIG-I (Karpala et al., 2011; Hayashi et al., 2014). Additionally, chickens possess LGP2, which has been shown to bind double stranded RNA, although its role in PAMP detection is uncharacterised (Uchikawa et al., 2016). Another difference comes further downstream of the activation pathway where chickens do not possess IRF-3 and IRF-9 with only IRF-7 and -10 being identified within the chicken genome (Santhakumar et al., 2017).

Many cytokines and chemokines are produced when the immune response is activated which have wide ranging functions in the maintenance of an antiviral state within the cell. The functions of key cytokines are summarised in Table 1.4.

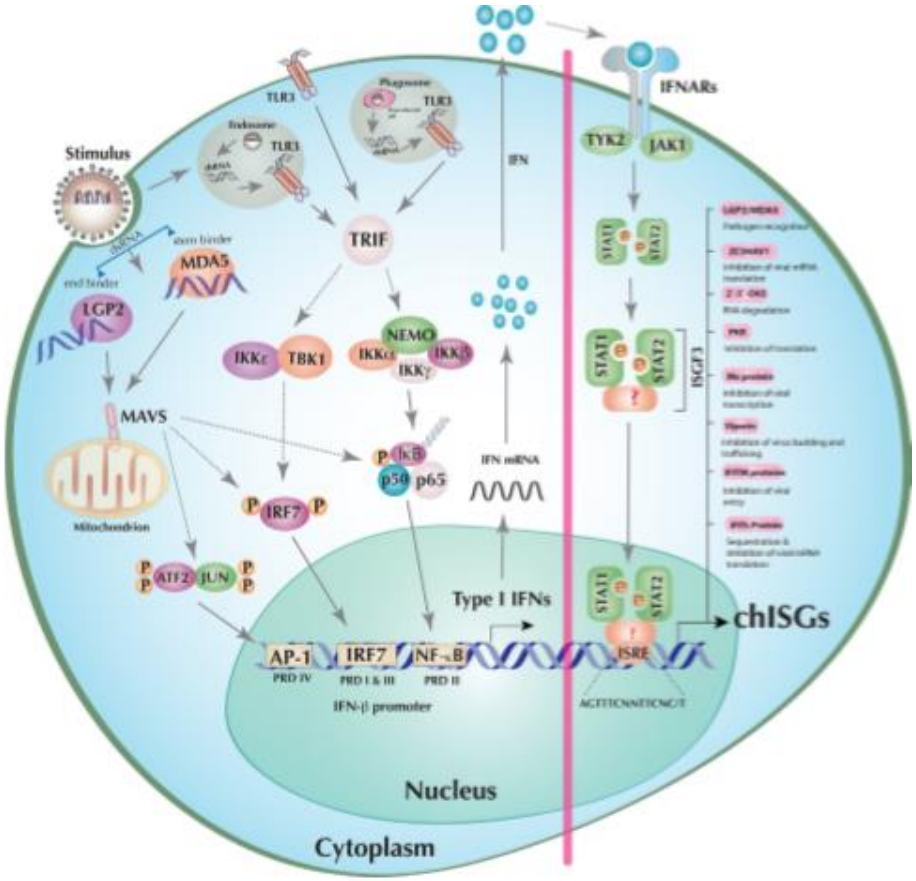

Figure 1.10: Schematic representation of the chicken interferon induction and signalling pathways. dsRNA is recognised by either MDA-5, LGP2 or TLR-3 initiating downstream signalling via MAVS or TRIF proteins. Downstream transcription factors such as IRF-7, NF-κB and AP-1 are activated which allows for their translocation to the nucleus and the stimulation of the transcription of IFNs. These transcribed IFNs can act in an autocrine or paracrine fashion and activate the JAK-STAT pathway to initiate the transcription of interferon stimulated genes (ISGs) which allow for the establishment of an antiviral state within the cell. Abbreviations used in the figure and are not described in the main text are as follows: IκB kinase (IKK) epsilon (IKKε), alpha (IKKα), beta (IKKβ), and gamma (IKKγ); NF-κB essential modulator (NEMO); TANK-binding kinase 1 (TBK1); inhibitors of NF-κB (IκB), NF-κB subunits p50 and p65; activating transcription factor 2 (ATF2); tyrosine kinase 2 (TYK2); Janus kinase 1 (JAK1); signal transducer and activator of transcription 1 (STAT1), and STAT2. "P" represents the phosphorylation state of the protein, and dotted lines indicate the involvement of multiple intermediary steps. Figure taken from Santhakumar et al. (2017).

Table 1.4: Summary of cytokine functions

Cytokine	Function	Reference
Type 1 interferons	Produced by leukocytes (IFN-α) and fibroblasts (IFN-β) Antiviral by induction of ISGs Stimulate macrophages and Natural killer cells	Platanias., 2005
IFN-γ	Produced by NK and T cells Regulates the maturation and differentiation of immune cells Activates Th1 cells and macrophages	Schroder et al., 2003
IL-1β	Produced by macrophages Mediates inflammation Involved in cell proliferation, differentiation and apoptosis	Dinarello., 2011
IL-4	Stimulates B- and T-cell proliferation Involved in differentiation of Th2 cells Reduces Th1 cells, macrophages, IFN-γ and IL-12 production.	Ul_Haq et al., 2016
IL-6	Produced by macrophages Proinflammatory cytokine via activation of the NF-κB pathway	Heinrich et al., 2003
IL-18	Produced by macrophages Proinflammatory cytokine Induces NK cells and T cells to produce IFN-γ	Dinarello., 1999; Lebel-Binay et al., 2000
TGF-β4	Induces Treg and Th17 cell- proinflammatory responses Blocks B cell proliferation Stimulates monocytes	Li and Flavell., 2008
CXCLi2	Involved in chemotaxis of lymphocytes	Barker et al., 1993

1.11: Aims

Evidence suggests H9N2 AIVs have become more pathogenic within the field and the molecular basis behind this is not understood. If the molecular mechanism behind this increased pathogenicity can be understood, there may be implications for development of more effective control mechanisms or improvements to vaccine design or assisting in disease surveillance. It would also increase our understanding of the fundamental biology of pathogenicity within AIVs. Previous unpublished work by the Iqbal lab has identified segment 3 to be important for this change in H9N2 virulence; therefore the effect of segment 3 from two H9N2 strains was investigated: A/guineafowl/Hong Kong/WF10/99 (WF10) a representative early isolate and A/chicken/Pakistan/UDL-01/08 (UDL-01) a representative novel reassortant strain possessing HA, NA and NP genes of a previously enzootic G1/97 like H9N2 virus and the PB2, PB1, PA and NP genes derived from HPAIV H7N3 virus.

The aims of this thesis were:

Aim 1: Understand the molecular basis of fitness differences between H9N2 AIV strains *in vitro*, identifying any specific polymorphisms within segment 3 which contribute to this effect.

Aim 2: Characterise any specific polymorphisms which altered viral fitness *in vitro* within a chicken model of infection. Determining the effect of any polymorphisms on viral replication, transmission, pathogenicity and immune response *in vivo*.

Aim 3: Investigate if any identified segment 3 polymorphisms alter the host cell shut off function of the accessory protein PA-X. Characterise H9N2 PA-X from the two different strains and assess the protein function *in vitro*.

Aim 4: Characterise the function of H9N2 AIV PA-X within a chicken model of infection. Determining the protein's contribution to viral replication, transmission, pathogenicity and immune response *in vivo*.

Chapter 2: Investigating the effect of segment 3 on H9N2 AIV fitness *in vitro*

2.1: Introduction

Influenza viruses have been shown to swap gene segments between two or more strains via a process known as reassortment. Reassortment occurs when different influenza viruses co-infect a single cell and viral gene segments are exchanged leading to the generation of progeny virions with new combinations of viral genes (reviewed by Steel and Lowen, 2014; Scholtissek et al., 1978; Burnet et al., 1949). This can result in viruses with increased (Sun et al., 2011) or reduced viral fitness (Villa and Lassig, 2017).

H9N2 AIVs have been shown to undergo extensive reassortment events (Dong et al., 2011a). Several viruses have emerged in recent years which contain the internal gene cassette derived from H9N2 AIVs. This includes a novel avian-origin H7N9 virus which has caused human infections in China; this virus contains HA and NA of duck origin and the internal gene cassette derived from an enzootic H9N2 (Lam et al., 2013; Liu et al., 2013). Guan et al. (1999) also reported the presence of H9N2 internal genes within human H5N1 isolates. Conversely, novel genotypes of H9N2 AIV have emerged in poultry populations due to co-circulation and reassortment with HPAIVs; where the NS gene segments were derived from H7N3 and H5N1 and the polymerase genes (PB1, PB2 and PA) derived from an Indian/Middle East lineage H9N2 AIV (Iqbal et al., 2009). These reassortant viruses have gained fitness such that the earlier ancestral G1/97 H9N2 strains previously prevalent in this region have been completely replaced

by these reassortant viruses and they have now become established within poultry in many regions of the Indian subcontinent and Middle East. They have been shown to perpetuate in poultry populations and wild terrestrial birds such as house sparrows (Iqbal et al., 2013).

These novel reassortant H9N2 AIVs have been observed to cause increased clinical disease signs in poultry in the field compared to the predecessor H9N2 viruses causing disease in the late 1990s (Guo et al., 2000; Iqbal et al., 2013; Seiler et al., 2018; personal communication M. Iqbal). However, the molecular basis for the increased pathogenicity of H9N2 AIVs has not been established. Previous unpublished data from the Iqbal lab implicates segment 3, which encodes the PA protein, in enhancing fitness of H9N2 AIVs. Gene segments were exchanged between A/guinea fowl/Hong Kong/WF10/1999 *(*WF10, a virus representing those that circulated in the late 1990s; G1 lineage) and A/chicken/Pakistan/UDL-01/2008 (UDL-01, representative of a novel reassortant H9N2 with HA, NA and NP gene of previously enzootic G1/ 97- like H9N2 virus and PB2, PB1 and PA and NS gene segments derived from HPAIV H7N3) using reverse genetics. It was noted that exchange of either segment 3 (PA gene) or segment 8 (NS gene) lead to the reciprocal alteration of plaque phenotypes between the two H9N2 virus strains. WF10 WT gives small, hazy plaques in MDCK cells whereas UDL-01 produces larger, clear plaques. Therefore, this thesis aims to further dissect the molecular mechanism of how the PA gene potentially modulates the virus phenotype (increase plaque size), pathotype (virulence) and fitness of H9N2 virus. The aims of research within this chapter were to: i) identify molecular motifs in segment 3 which were important for

enhancing viral fitness and, ii) if so, defining the functional consequences of these polymorphisms *in vitro.*

2.2 Results

2.2.1: Effect of H9N2 segment 3 exchange between two AIV strains on viral fitness *in vitro*

In order to first assess the effects of exchanging segment 3 between a progenitor H9N2 AIV strain (WF10) and a reassortant H9N2 AIV strain (UDL-01), reverse genetics (RG) was used to rescue pairs of WF10- and UDL-01-based viruses with wildtype (WT) or reciprocally swapped segment 3s. 293T cells were transfected with the UDL-01 or WF10 reverse genetics plasmid system in order to rescue RG WT viruses. The segment 3 plasmids were then swapped between RG-WF10 and RG-UDL-01 and viruses with alternate segment 3s rescued. A negative control sample was included within each rescue; this lacked the PA plasmid, so was therefore unable to generate infectious virus. 24 hours post-transfection, 293T cells were co-cultured with MDCK cells and left for up to 96 hours (until cytopathic effect (CPE) was observed). This was deemed the passage zero (P0) stock. Passage one (P1) virus stocks were generated by inoculation of 10-day old fertilised hens' eggs with diluted P0 co-culture supernatants; allantoic fluid was harvested 48 hours post-inoculation and clarified before aliquoting and storage at -80°C. P1 viral stocks were titrated via plaque assays.

All viruses rescued readily and replicated to titres of at least 10^6 pfu/ml, with the negative control rescues (missing segment 3) producing no detectable

virus within the limits of detection (2.5 pfu/ml; data not shown). To validate the identity and genetic integrity of the recombinant viruses, RNA was extracted from allantoic fluid and segment 3- and 7- specific RT-PCRs were performed. DNA sequencing was used to confirm the PA gene and backbone (by sequencing M segment) were correct in each of the viruses made and no mutations had been introduced during rescue (data not shown).

Viral plaque phenotype was used as an initial method to screen for viral fitness differences, as WF10 WT and UDL-01 WT viruses exhibit drastically different plaque phenotypes (Figure 2.1). Viral plaque phenotype has been previously shown to be a good marker for attenuation and fitness differences between viruses (Simpson and Hirst, 1961; Hale et al., 2006). Accordingly, viral plaques in MDCK cells after 72 hours were immunofluorescently stained with anti-NP to visualise virus spread. As expected from previous work in the laboratory, WT UDL-01 virus formed larger plaques than the progenitor virus WT WF10 (Figure 2.1A). When the plaque size was quantified using ImageJ software, this difference was significant, with the average UDL-01 WT plaque diameter being 1.5 mm compared to 0.5 mm for WF10 WT (Figure 2.1B). However, the reassortant viruses with swapped segment 3s showed the opposite plaque phenotypes, UDL-01 carrying WF10 PA produced small plaques, whereas, WF10 carrying UDL-01 PA produced large plaques (Figure 2.1A). Measurement of plaque diameters confirmed a statistically significant reciprocal change (Figure 2.1B), supporting previous unpublished work from the Iqbal laboratory suggesting segment 3 modulates *in vitro* replicative phenotypes of WF10 and UDL-01 viruses.

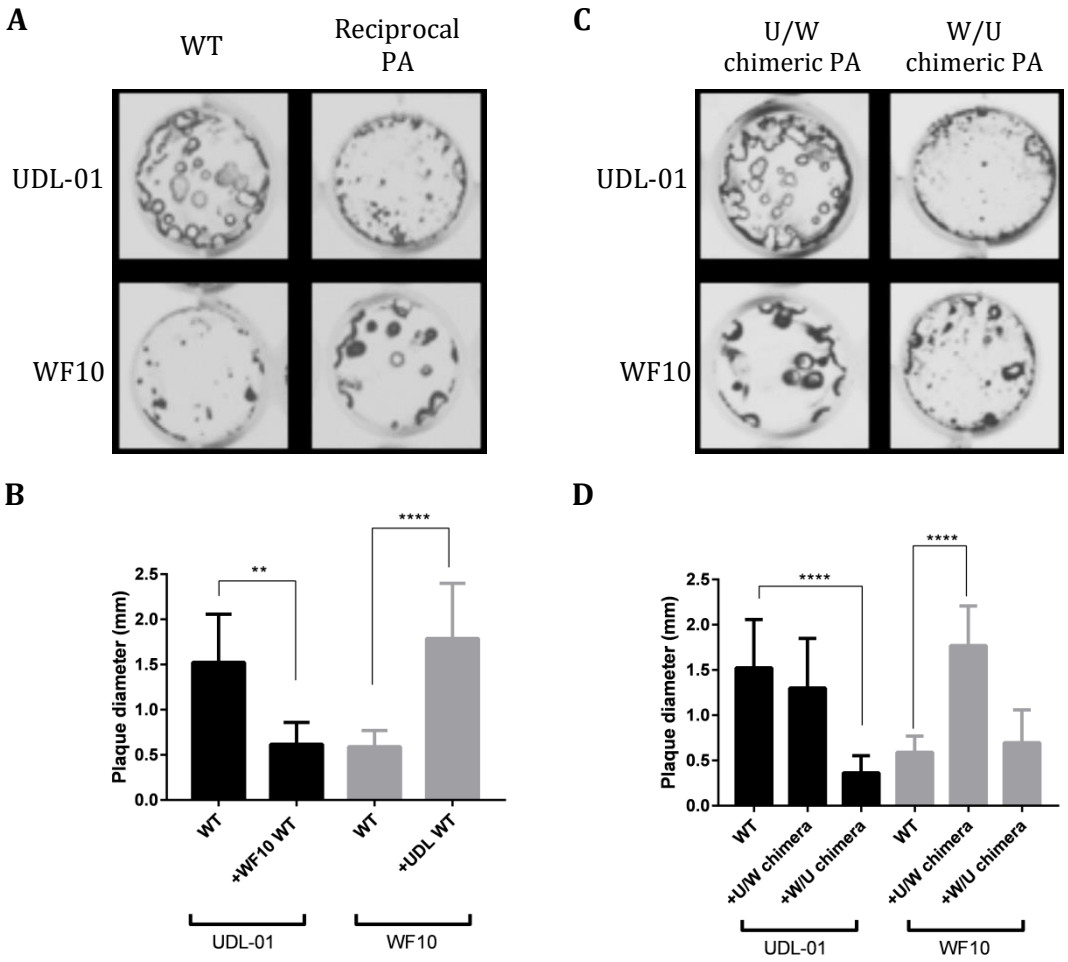

Figure 2.1: Impact of segment 3 exchange on H9N2 AIV plaque phenotypes. The indicated viruses were titrated in MDCK cells via plaque assay under a 0.6% agarose overlay and 72 h.p.i., fixed and stained for NP using immunofluorescence. (A) and (C) show representative images of plaque sizes of UDL-01 and WF10 RG viruses. (B) and (D) show diameter of 20 plaques/ virus measured using Image J analysis software. The graphs represent the average plaque diameter +/- SD. (B) Mann-Whitney Test or (D) Kruskal-Wallis with Dunn's multiple comparison test was used to determine the statistical differences between the plaque sizes. **** P value <0.0001, **= 0.0016.

To identify which region of segment 3 was responsible for this alteration in viral plaque phenotype, two chimeric segment 3s were produced using the Gibson Assembly (New England Biolabs) cloning procedure (kindly provided by Tom Peacock). These consisted of the N- terminal 1101 nucleotides from PA of one strain and the C-terminal 1047 nucleotides of the other. These segments, denoted U/W or W/U, depending on which virus had donated the N/C-terminal halves of the resulting PA polypeptides, were introduced into the backbone of both the progenitor WF10 and reassortant UDL-01 H9N2 AIVs using reverse genetics. All four viruses rescued readily and grew to titres of at least 10^6 pfu/ml (data not shown). When the plaque sizes were visualised by immunostaining, both UDL-01 and WF10 viruses containing the PA gene U/W chimera produced large plaques while viruses with the PA gene W/U chimera gave mostly small plaques with the occasional large one (Figure 2.1C). Quantification showed that on average, the small plaque size conferred by the PA gene W/U chimera within UDL-01 and the reciprocal large plaque phenotype resulting from inserting the PA gene U/W chimera into WF10 were significantly different from the parental viruses (Figure 2.1D). Thus overall, the data indicated that segment 3, particularly the PA N-terminus from the first 5'-1101 nucleotides (considering plus sense RNA), are important for the differing plaque phenotypes seen between the progenitor (WF10) and reassortant (UDL-01) strains of H9N2 AIVs.

2.2.2: Amino acid differences between WF10 and UDL-01 segment 3-encoded polypeptides

The simplest hypothesis to explain the molecular basis of the differing phenotypes conferred by the WF10 and UDL-01 H9N2 segment 3s was that one or more of the polypeptides they encode had functionally important amino acid polymorphisms. Accordingly, their sequences were examined to identify any coding differences. Using NCBI influenza gene annotation tools, the nucleotide sequence of segment 3 of WF10 (GenBank Accession number: KX859443) and UDL-01 (GenBank Accession number: CY038457) were predicted and amino acid sequences of PA and PA-X were aligned using pairwise alignment (optimal GLOBAL alignment; BioEdit). All amino acid differences within known segment 3 gene products are shown in Table 2.1. In total, there were 30 amino acids differences, these included 28 in PA (Table 2.1A) and 2 in X-ORF (Table 2.1B). The amino acid differences within PA-N155 and PA-N182 were not considered for the purpose of this study. Rather than blindly making a large mutant library, a literature search and consideration of the amino acid side chain properties was undertaken to decide which positions to focus on. Within the literature search the majority of changes had not been previously identified to affect the functional properties of IAVs. However, some polymorphisms had been highlighted by previous studies. Hu et al. (2013a) identified D101G and E237K changes within H5N1 PA as affecting viral replication, polymerase activity and virulence in ducks. DesRochers et al. (2016), also implicated PA Q400P to be important in the reduction of virulence of H7N3 compared to H7N9 AIVs in mice. This suggested that these amino acid positions could also potentially alter H9N2 AIV biology.

Furthermore the properties of the amino acid sidechains (Betts et al., 2003) that had been altered between the two strains of virus were also considered when choosing which mutations to introduce via site directed mutagenesis. Those which changed the amino acid properties significantly, for example, from non-polar to polar, or altered the charge at this position, were prioritised for mutagenesis. Together the literature search and amino acid property analysis identified 13 likely candidates within the PA gene (highlighted in green within Table 2.1). These were spread throughout the protein domains and included some within the N-terminal PA endonuclease domain and others in the C-terminal domain. Two differences within the X-ORF of PA-X were also identified (Table 2.1B).

The candidate amino acid positions were mapped onto the available crystal structure of influenza PA (Pflug et al., 2014; PDB ID-4WSB) using PyMol, to identify if any of the mutations identified during this screen could affect function due to their locations near to known active site regions shown in Figure 2.2A. Mutations identified within this screen are highlighted in cyan (endonuclease domain) or red (C-terminus). Within the endonuclease domain (pink), amino acids previously identified to alter endonuclease activity and make up the endonuclease active site are highlighted in green. These include H41, E80, D108, E119 and K134 (Yuan et al., 2009). Within the endonuclease domain one of the mutations, I118T, is located very close to the endonuclease active site. Other polymorphisms seen between WF10 and UDL-01, including A20T, E26K and I100V_D101E lie in regions surrounding the active site which could potentially interfere with endonuclease activity depending on any potential steric

hindrance caused by the amino acid alteration. One change (E237K) lies within the linker region (yellow) between the endonuclease domain and the C-terminal domain and could affect the conformational flexibility of PA. In the C- terminal domain (blue), amino acids that have been shown to alter interaction and binding of PA to PB1 are highlighted in green. This includes K328, K539, R566 and K574 (He et al., 2008). K327E lies proximal to one of the known mutations that alter PA/PB1 binding. Again, other amino acid changes could lead to conformational changes in the structure of PA and thereby alter protein function.

The locations of the identified mutations in relation to the accessory gene products of PA were depicted using the same colour scheme as within the crystal structures (green: endonuclease active site /PA-PB1 binding, cyan/red: identified mutations) (Figure 2.2B). From this it was observed that the N-terminally truncated accessory products of PA (PA-N155 and PA-N182) did not possess any of the N-terminal mutations identified within the study but would contain all the mutations identified within the linker and C-terminal domains. On the other hand, the accessory protein PA-X only contained the mutations present within the N-terminal endonuclease domain, plus the two identified within the X-ORF (R221L and Q250R).

Table 2.1A: Amino acid differences between progenitor (WF10) and reassortant (UDL-01) H9N2 segment 3s (N-terminal endonuclease, linker and C-terminus).

Amino acid position	In UDL-01 PA	In WF10 PA	Region of Segment 3	Reference
3	N	D	Endonuclease domain	
20	A	T	Endonuclease domain	
26	E	K	Endonuclease domain	
85	T	I	Endonuclease domain	
86	L	M	Endonuclease domain	
184	N	S	Endonuclease domain	
100	I	V	Endonuclease domain	
101	E	D	Endonuclease domain	Hu et al. (2013a) D101G
118	I	T	Endonuclease domain	
237	E	K	Linker	Hu et al. (2013a) E237K
316	G	D	C-terminus	
319	D	E	C-terminus	
323	V	I	C-terminus	
327	K	E	C-terminus	
352	E	D	C-terminus	
367	K	M	C-terminus	
387	V	I	C-terminus	
338	S	G	C-terminus	
394	D	Q	C-terminus	
400	S	L	C-terminus	DesRochers et al. (2016) Q400P
545	I	V	C-terminus	
553	A	S	C-terminus	
602	V	T	C-terminus	
615	K	R	C-terminus	
631	S	G	C-terminus	
651	A	S	C-terminus	
684	G	E	C-terminus	
688	E	G	C-terminus	

Table 2.1B: Amino acid differences in the PA-X ORF between progenitor (WF10) and reassortant (UDL-01) H9N2 segment 3s.

Amino acid position	In UDL-01 PA	In WF10 PA	Region of Segment 3	Reference
221	R	L	X-ORF	
250	Q	R	X-ORF	

Amino acid differences highlighted in green indicate those taken forward for further analysis. Amino acid sequences were aligned using Pairwise alignment (optimal GLOBAL alignment: BioEdit). Differences observed in both the PA gene and PA-X were noted and amino acid properties researched.

A

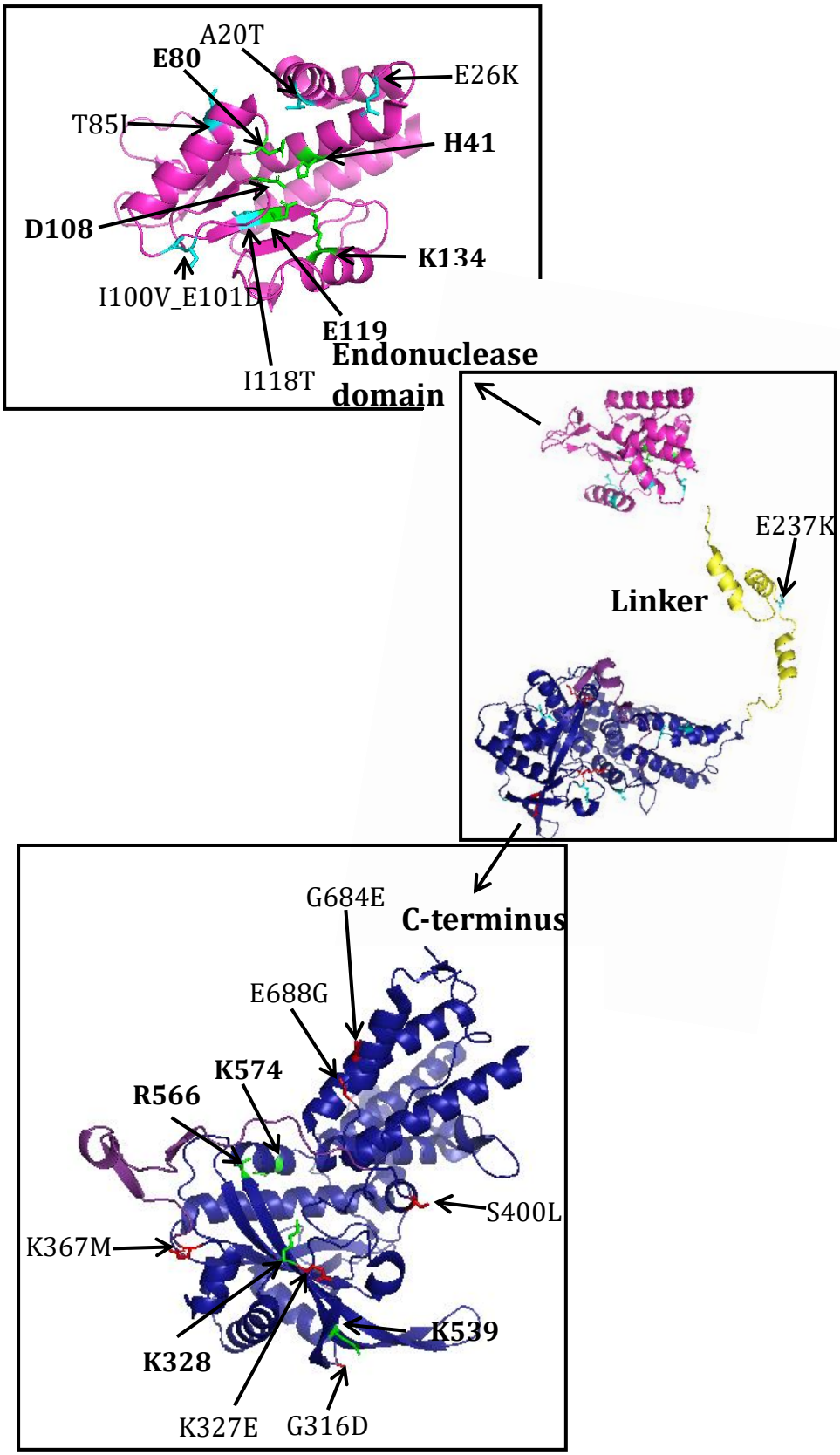
A20T
E80
E26K
T85I
H41
D108
K134
I100V_E101D
E119
I118T
Endonuclease domain
E237K
Linker
C-terminus
G684E
E688G
K574
R566
S400L
K367M
K539
K328
K327E
G316D

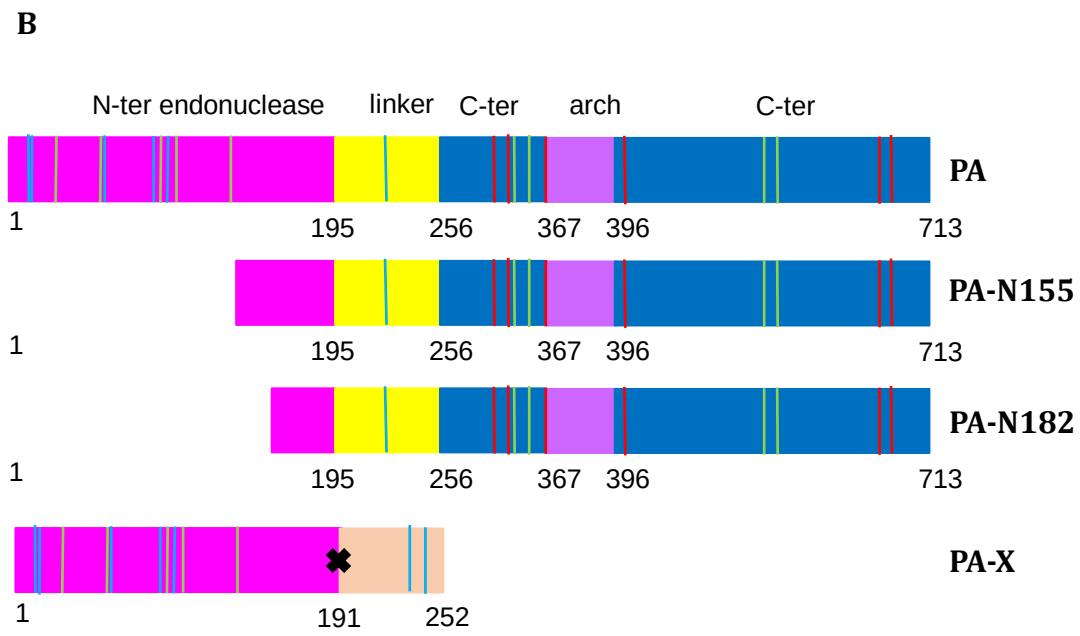

Figure 2.2: Mapping of identified mutations onto PA crystal structures. (A) PyMol software was used to map the identified PA polymorphisms onto the crystal structure of influenza PA protein (PDB ID: 4WSB). The full crystal structure in the centre with zoomed in images of the endonuclease domain and C-terminus at top and bottom respectively. PA endonuclease: pink, linker: yellow, C-terminus: blue, PA-arch: purple. The amino acids previously identified to be important for the endonuclease activity or PB1 binding of PA are highlighted in green. The mutations identified in this screen are highlighted in cyan (endonuclease domain) or red (C-terminus). (B) Schematic to identify presence of mutations within accessory gene products of PA gene (PA-N155, PA-N182 and PA-X). Colour scheme as above, X-ORF: lilac, frameshift site represented by cross.

Each of the selected mutations were introduced into both the progenitor WF10 segment 3 to make it 'UDL-01- like' and the reassortant UDL-01 segment 3 to make it 'WF10-like' using site directed mutagenesis. The presence of mutations was confirmed via sequencing of the plasmid constructs (data not shown). These plasmids were then used for further study to characterise the effect of these mutations in transcriptional activity of the polymerase, viral replication, and plaque morphology.

2.2.3: Effect of PA polymorphisms on viral gene expression

Influenza PA mutations have previously been shown to affect polymerase activity due to its position within the heterotrimeric polymerase complex. For example, Fan et al. (2014) showed that several PA mutations within H5N1 altered viral polymerase activity including D352E which increased polymerase activity 2- to 3- fold and R185K which significantly decreased polymerase activity.

Therefore, the consequences of the panel of H9N2 PA mutations identified here on the transcriptional activity of the IAV polymerase complex was assessed using a "minireplicon" or "RNP reconstitution" assay system. These assays constitute the 4 proteins of influenza RNP: the three polymerase components (PB2, PB1, and PA) and NP (abbreviated as 3PNP) that allow indirect measurement of mRNA production by the viral polymerase from a vRNA mimic (Huang et al., 1990; Foeglein et al., 2011). RNA polymerase II expression vectors containing expression cassettes of 3PNP were co-transfected into cells to produce mRNA in *trans* and thus functional protein for each viral polypeptide, which subsequently form the polymerase complex. Along with the polymerase

components a vRNA mimic reporter construct is co-transfected. This reporter plasmid contains a firefly luciferase gene in negative sense flanked by segment 8 UTRs, under the control of either a human or avian RNA polymerase I promotor. This allows for RNA to be produced by cellular RNA polymerase I which resembles vRNA to the polymerase complex and thus triggers RNP formation. This will in turn be transcribed by the IAV polymerase complex into mRNA and then translated into luciferase (Lutz et al., 2005). Therefore, luciferase output is generally proportional to the transcriptional activity of the viral polymerase complex. Some laboratories also include a renilla luciferase transfection control that the firefly luciferase values are normalised to (Hu et al., 2015; Long et al., 2016; McAuley et al., 2010). However, due to the potential for the PA mutations examined here to have variable secondary effects on host cell gene expression because of their position within the accessory gene PA-X, this control was not employed.

First, the transcriptional activity of a consistent set of viral RNPs with the PB2, PB1 and NP (2PNP) derived from PR8 but with H9N2 PAs were screened. The PR8 2PNP system was used within mammalian cells due to the presence of PB2 627E within UDL-01 and WF10. The presence of this amino acid in PB2 severely restricts the polymerase complex in mammalian cells (Long et al., 2013). 293T cells were transfected with expression plasmids for the RNP polymerase as well as a vRNA mimic reporter plasmid encoding luciferase. 48 hours post transfection cells were lysed and levels of luciferase activity quantified. A negative control lacking PA was included (2PNP), since in this case, the viral polymerase cannot form and therefore any luciferase observed would not be the

result of viral transcription. In the absence of all four RNP polypeptides, only background levels of luciferase were seen, whilst the full PR8 vRNP produced around 1000 times more luciferase activity (Figure 2.3A). When either of the two WT H9N2 segment 3s were added to the PR8 2PNP system, a similar 1000-fold increase in luciferase levels were observed compared to the 2PNP control, indicating that both WF10 and UDL-01 PAs were compatible with the other PR8 RNP components in this system.

Although the activity of an RNP containing the WT WF10 PA was relatively lower than one containing the WT UDL-01 polypeptide, this difference was not significant. Changing individual residues within the UDL-01 PA to match those found in WF10 PA had very little effect on viral gene expression. The converse changes in the WF10 protein caused slightly greater fluctuations in average activity, with the largest change seen with the introduction of the L331R mutation however, this only altered luciferase signal by 0.5 of a $\log_{10}$. Overall, within both UDL-01 and WF10 panels of vRNPs, no significant differences were seen in the transcriptional activity of the polymerase complex following the introduction of the various PA mutations.

Expression of PA and NP proteins, as well as the cellular protein tubulin- used as a protein loading control, were assessed via western blot analysis. Cells were lysed in sample buffer and proteins separated on 15% SDS-PAGE gels before transfer to nitrocellulose and western blotting with antisera specific for IAV PA, NP and tubulin. Tubulin levels were reasonably consistent across all groups, with some variances seen in some of the lanes, possibly due to transfer differences

across gels (Figure 2.3B). NP expression levels were also reasonably similar across groups with no NP observed within the cells only control as expected. Similarly, all of the PA constructs exhibited generally similar accumulation levels, with no PA expression observed in the 2PNP or cells only controls. Thus overall, none of the PA polymorphisms had major effects on the stability or ability of the polypeptides to support viral gene expression when assayed in mammalian cells in the background of a PR8 RNP.

The ability of the H9N2 segment 3 polymorphisms to affect the transcriptional activity of fully avian RNPs was then investigated. DF-1 (chicken immortalised fibroblast) cells were transfected with expression plasmids for either the UDL-01 or WF10 RNP polypeptides plus a vRNA mimic encoding luciferase under the control of an avian RNA polymerase I promotor. As above, cells were lysed and luciferase levels measured after 48 hours. Untransfected cells gave only background luciferase levels (cell only control; Figure 2.3C) while a very low level of luciferase expression was observed when only PB1, PB2 and NP were transfected (2PNP control) indicating the lack of an active polymerase complex. When all four RNP polypeptides were included within either the UDL-01 or WF10 background an approximately 100-fold increase in luciferase expression was observed compared to the 2PNP control. This was a relatively lower increase compared to that observed within the 293T cell system, likely due to differences in transfection efficiency between the cell types. Indeed, Horibe et al. (2014), described how differences in the transfection activity of cell lines can alter luciferase output. Nevertheless, the increase was enough to robustly indicate the presence of a productive viral transcriptional system. As within the

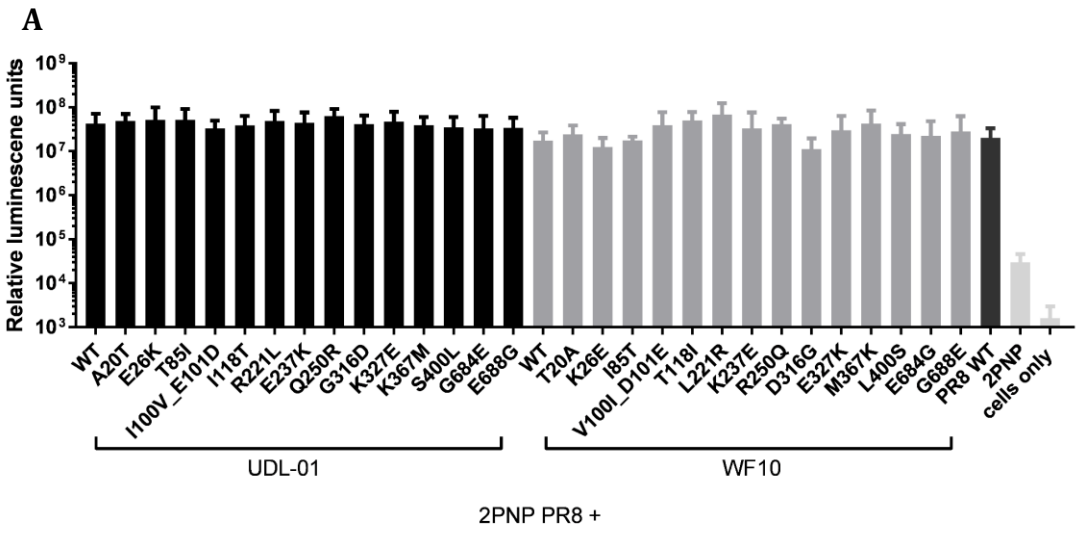
A
Relative luminescene units
10^9
10^8
10^7
10^6
10^5
10^4
10^3
WT
A20T
E26K
T85I
I100V_E101D
I118T
R221L
E237K
Q250R
G316D
K327E
K367M
S400L
G684E
E688G
WT
T20A
K26E
I85T
V100I_D101E
T118I
L221R
K237E
R250Q
D316G
E327K
M367K
L400S
E684G
G688E
PR8 WT
2PNP
cells only
UDL-01
WF10
2PNP PR8 +

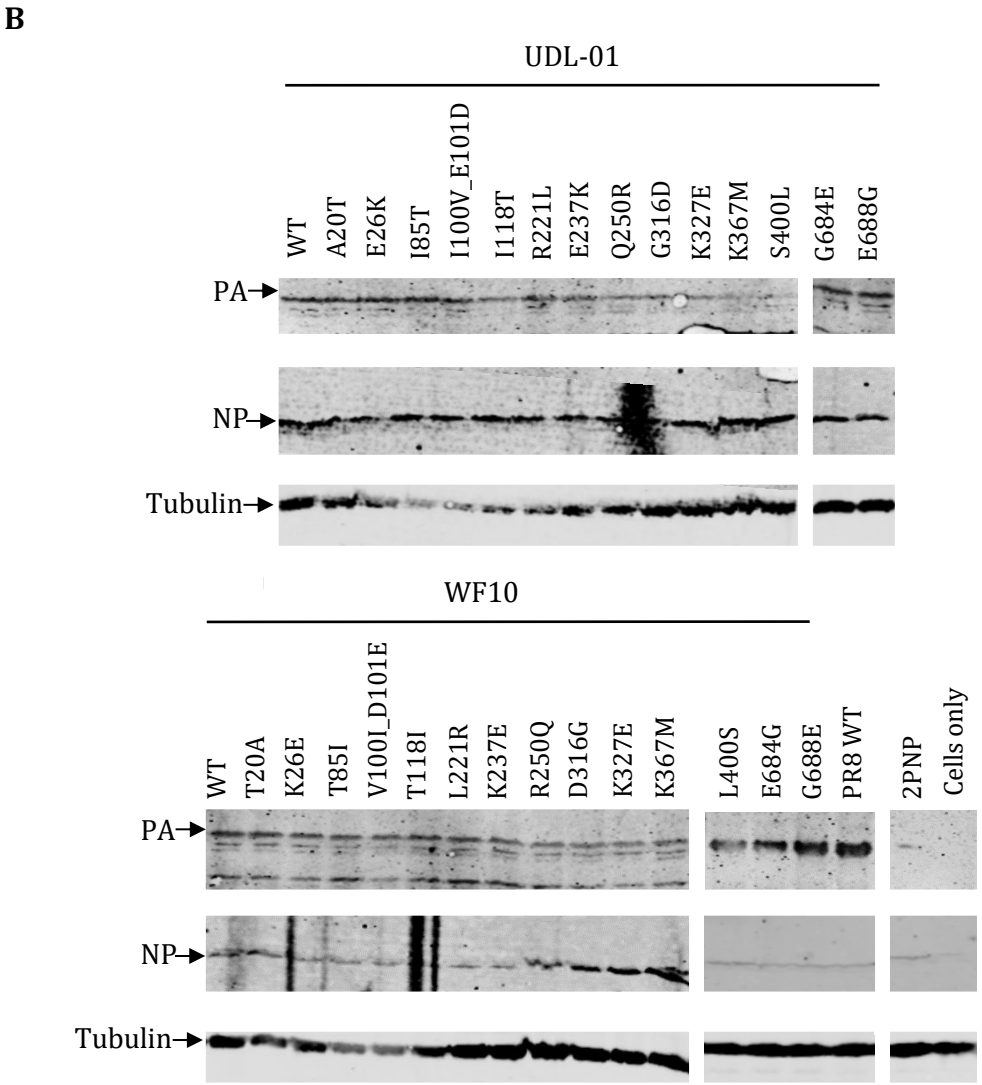
B
UDL-01
WT
A20T
E26K
I85T
I100V_E101D
I118T
R221L
E237K
Q250R
G316D
K327E
K367M
S400L
G684E
E688G
PA
NP
Tubulin
WF10
WT
T20A
K26E
T85I
V100I_D101E
T118I
L221R
K237E
R250Q
D316G
K327E
K367M
L400S
E684G
G688E
PR8 WT
2PNP
Cells only
PA
NP
Tubulin

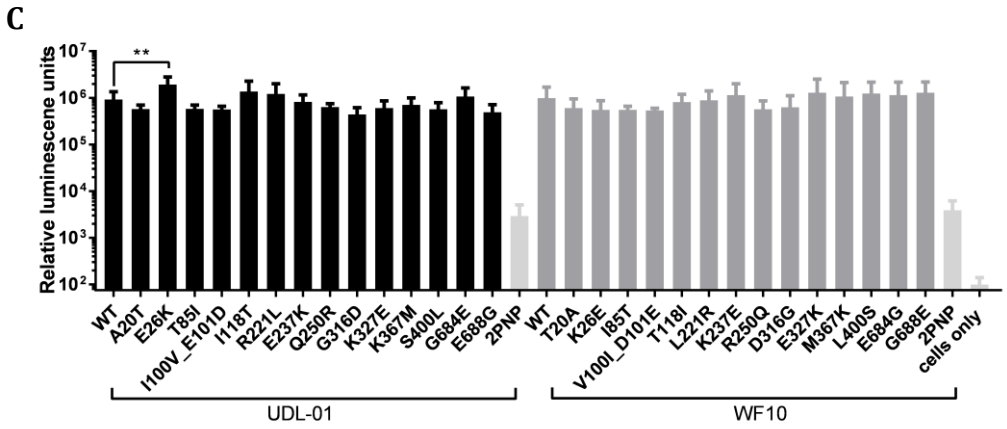

Figure 2.3: Transcriptional activity of polymerase complexes containing H9N2 segment 3 mutations. Transcriptional activity of polymerase complexes were assessed using minireplicon assays. (A) 293T cells or (C) DF-1 cells were transfected with the components of the polymerase complex (PB1, PB2, PA and NP) plus a vRNA mimic encoding luciferase under the control of (A) human or (C) avian RNA polymerase I promotors. 48 hours post transfection cells were lysed and luciferase levels measured. Data represents the mean +/- SD of 3 independent experiments. No significant differences were observed in transcriptional activity of the various polymerase complexes within 293T cells (one way ANOVA with Dunnett's multiple comparisons). DF-1 cells ** P value = 0.0056 (Kruskal-Wallis and Dunn's multiple comparisons). (B) PA and NP accumulation were analysed in comparison to tubulin levels via western blot of 293T cell lysate indicating the level of protein expression of each of the indicated proteins.

mammalian system, no significant differences were seen in DF-1 cells, between the transcriptional activities of polymerase complexes containing WT UDL-01 or WF10 PA polypeptides. However, in contrast to the mammalian system, UDL-01 E26K showed a significantly increased transcriptional activity compared to UDL-01 WT. There were no further no significant differences seen with any of the UDL-01 or the WF10 panel of PA polypeptides when comparing the activity of the relevant WT to each mutated PA within each group. In summary, these data suggest that the differences in plaque phenotype observed between WF10 (progenitor) and UDL-01 (reassortant) H9N2 AIVs was not related to the segment 3s ability to support the transcriptional ability of the polymerase.

2.2.4: Generation of H9N2 viruses with progenitor or reassortant like PAs

The panel of mutations within PA, including mutations within the endonuclease domain, linker region and C-terminal domain were built into full WF10 or UDL-01 H9N2 AIV using reverse genetics. Viruses were rescued using 293T and MDCK co-culture and were then propagated into viral stocks within 10-day old fertilised hens' eggs. After 48 hours allantoic fluid was harvested and then titrated via plaque assay under 0.6% agarose to examine plaque size at 72 hours post overlay. As described previously the full H9N2 WT viruses had contrasting plaque phenotypes, with UDL-01 WT giving clear plaques (Figure 2.4A) with an average diameter of >1.5 mm (Figure 2.4C) whereas WF10 WT gave more hazy plaques with and average plaque diameter of <0.5 mm (Figure 2.4B, C). Within the UDL-01 panel of PA mutant viruses, the only visually obvious change in plaque size was from the E26K mutant (Figure 2.4A). Quantification showed a

highly significant decrease in average plaque diameter from 1.7 mm to 0.6 mm, comparable to that of the WF10 WT virus (Figure 2.4C). No other mutations introduced into UDL-01 PA led to significantly altered plaque morphology. Within the WF10 panel of viruses, the most striking visual difference was caused by the introduction of K26E, although the D316G and L400S changes also caused some increase in plaque diameter and clarity (Figure 2.4B). Quantification showed a highly statistically significant increase of plaque diameter from 0.42 mm to 1.68 mm for K26E and smaller but also significant increases to 0.76 mm for L400S (Figure 2.4C). None of the other mutations introduced into the WF10 H9N2 AIV significantly altered plaque morphology.

The H9N2 plaque phenotype data indicated that mutation to codon 26 within both WF10 and UDL-01 viruses reciprocally altered the plaque size. These mutations restored plaque diameter to the size of the alternate WT virus i.e. E26K within a UDL-01 backbone reduced the plaque size to a similar level to WF10 WT and vice versa. Although several other mutations in the UDL-01 and WF10 PA gene altered the plaque phenotypes of the viruses, they did not change the plaque size to that of the WT viruses or act reciprocally. This suggests that the mutation at position 26 is key for defining the difference in plaque phenotype seen between the progenitor and reassortant H9N2 AIVs under study.

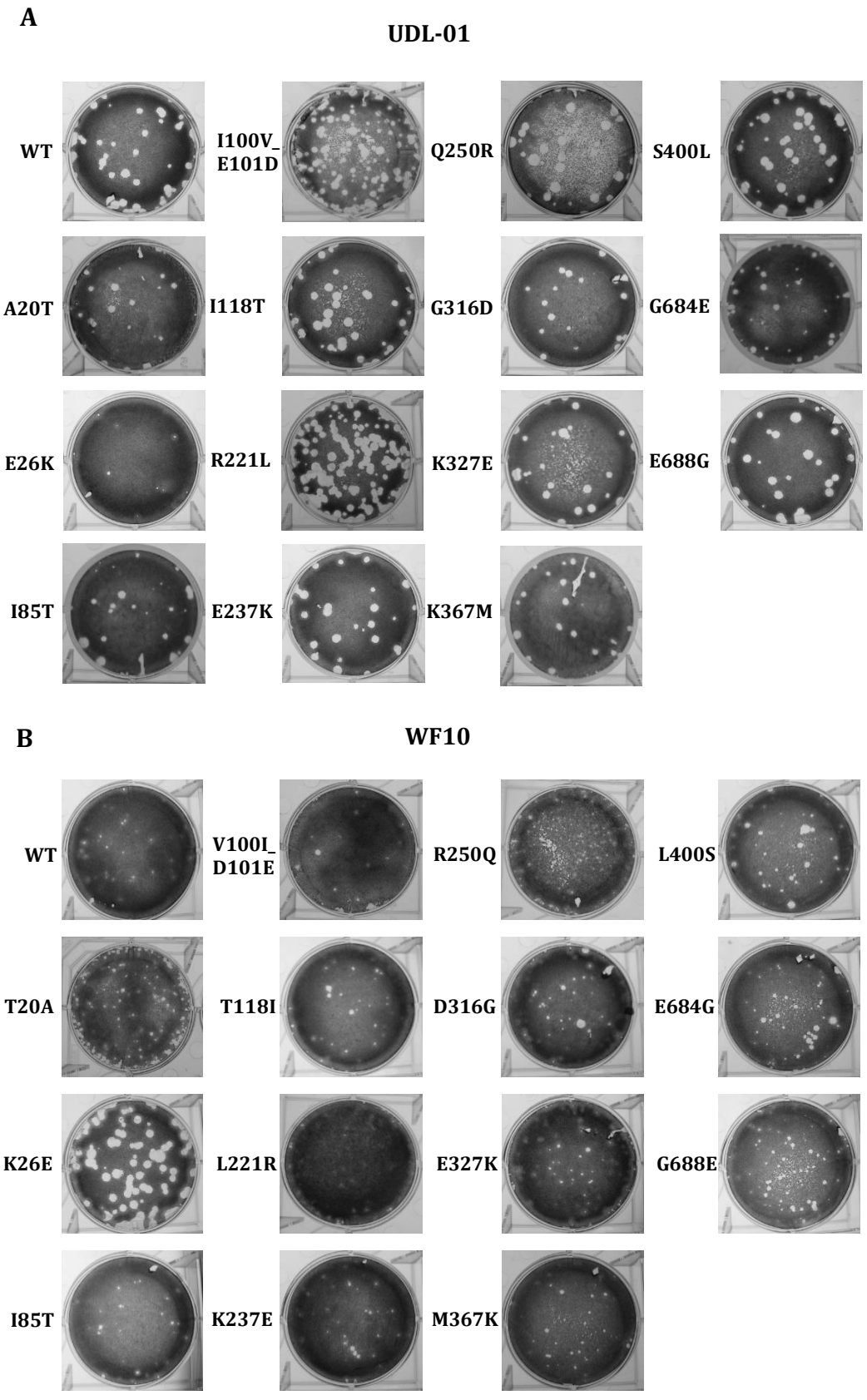
A
UDL-01
WT
I100V_
E101D
Q250R
S400L
A20T
I118T
G316D
G684E
E26K
R221L
K327E
E688G
I85T
E237K
K367M
B
WF10
WT
V100I_
D101E
R250Q
L400S
T20A
T118I
D316G
E684G
K26E
L221R
E327K
G688E
I85T
K237E
M367K

C

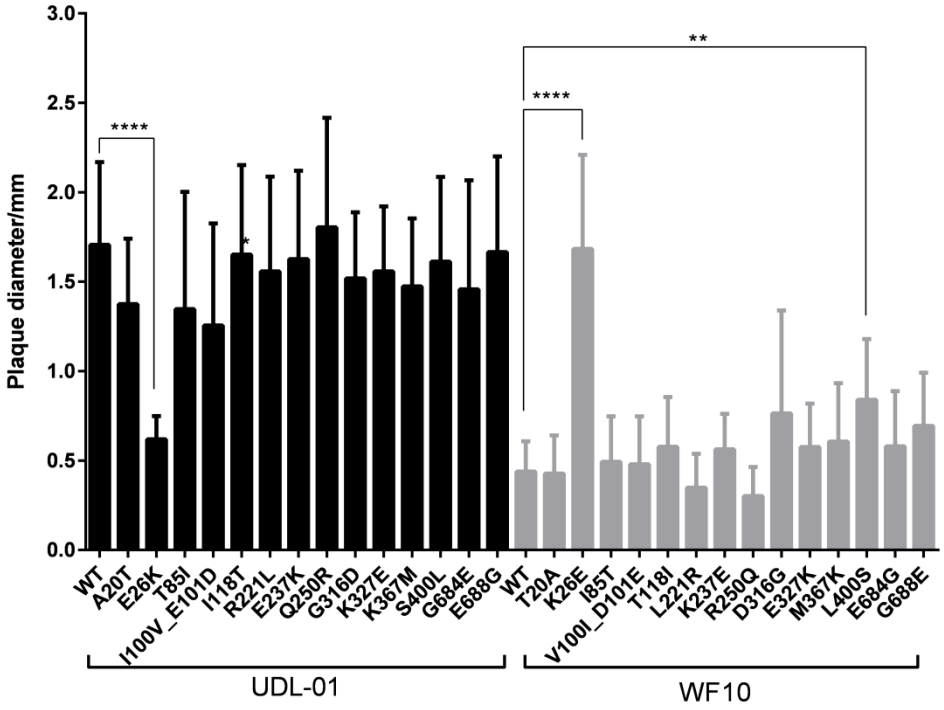

Figure 2.4: Phenotypic differences in plaque size between H9N2 AIVs containing segment 3 mutations. H9N2 AIVs with either a UDL-01 or WF10 backbone were rescued via reverse genetics. The plaque phenotypes of the rescues were assessed via plaque assay on MDCK cells under a 0.6% agarose overlay. After 72 hours cells were fixed and stained with 0.1% crystal violet solution and plaques imaged. (A) Visual representation of UDL-01 virus panel containing PA mutations to make them WF10-like. (B) Visual representation of WF10 virus panel containing PA mutations to make them UDL-01 like. (C) 20 plaque diameters per virus were measured using ImageJ analysis software and the average plaque diameter calculated. Graph represents the average +/- SD. P values= ****: <0.0001; **: <0.0039 (Kruskal-Wallis with Dunn's multiple comparisons).

2.2.5: Viral replication of H9N2 AIVs with progenitor-like or reassortant-like PAs

To examine the impact of differing plaque phenotypes on viral replication, multi-cycle virus growth was assessed. Firstly, the PA mutant viruses were screened with end-point titre experiments. MDCK cells were infected with each virus at a low multiplicity of infection (MOI) of 0.01. After 48 hours, supernatants were harvested and amount of virus was titrated via plaque assay. Experiments were repeated across 3 independent replicates and in all cases, a mock infected group was included where cells were 'infected' with serum free media rather than virus. Viral outputs from these latter controls were negative according to the limit of detection via plaque assay (2.5 pfu/ml; data not shown). When the two WT viruses were compared, UDL-01 WT showed a significantly increased viral output at 48 hours compared to WF10 WT virus (Figure 2.5). Within the UDL-01 panel of PA-altered viruses, only one mutation (E688G) significantly affected end-point virus replication at 48 hours, leading to a modest increase in titre compared to UDL-01 WT. None of the other mutations within a UDL-01 background had a significant impact on viral replication although several, including E26K, T85I, I100V_E101D, G316D, K327E and K367M slightly reduced viral output. Within the WF10 panel of viruses, no significant differences were seen in viral output of any of the mutants compared to WF10 WT. Although two mutations showed trended, but not significant, increases in viral output compared to the WT parent virus after 48 hours: K26E and D316G. These mutations increased viral output to bring replication to a similar level to UDL-01 WT. Both of these mutations also significantly increased plaque size compared to WF10 WT (Figure 2.4). Thus,

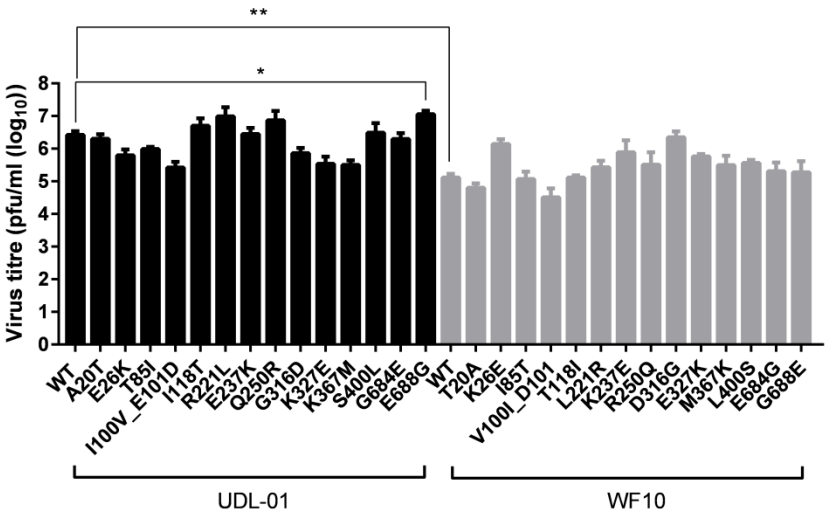

Figure 2.5: Endpoint multi-cycle replication of segment 3 mutant H9N2 AIVs in MDCK cells. MDCK cells were infected with a low MOI (0.01). After 48 hours supernatants were harvested and titrated via plaque assay. Data represents the mean +/- SD of 3 independent experiments. P values: * = <0.02; **=<0.05 (one-way ANOVA with multiple comparisons (UDL-01 panel; WT vs. mutant); Krustal-Wallis and Dunn's multiple comparisons (WF10 panel; WT vs. mutant); Unpaired T-test (WT vs WT).

consistent with the plaque size data, the novel reassortant viruses, represented here by UDL-01, displayed an enhanced replicative ability *in vitro* compared to an H9N2 progenitor, represented by WF10, which was sensitive to mutations in the PA polypeptide.

Next the replication kinetics of viruses mutated at position 26 were assessed over a time course of infection to test for any differential effect on replication the mutations may have had at earlier time points which could have been missed by only looking at end-point titres. These mutations were focussed on because they had the strongest reciprocal effect on plaque size but gave a less clear outcome in the end-point titre assays. Low MOI (0.01) infections of MDCK cells were initiated using the H9N2 WT and 26 mutant viruses, supernatant samples taken at 4, 8, 12, 24, 36, 48 and 72 hours post infection and viral output titrated via plaque assay. As before, the experiments were performed three times independently, including a mock infected group in each replicate. On each occasion the mock infected output was below the limit of detection for the plaque assay (data not shown). All four viruses showed the expected exponential rise in titre after 8 h.p.i., reaching a plateau around 48 hours (Figure 2.6A). At earlier time points there were no significant differences between WT and mutant viruses, with the UDL-01 pair continuing to show no significant difference in viral output throughout the time course. Although the UDL-01 E26K virus did appear to have a reduced output at 72 hours albeit not significant. The WF10 virus pair showed significantly different replication kinetics at 48 and 72 h.p.i., with the introduction of the K26E mutation allowing enhanced replication compared to

the parental WT virus. Thus, the identity of PA residue 26 had significant reciprocal effects on the replication of UDL-01 and WF10 viruses.

To test if the effect of PA position 26 polymorphisms held true in avian cells, viral replication was also assessed in a primary chicken kidney (CK) cells. As with MDCK cells, a low MOI was used (0.01), supernatants were harvested at 4, 8, 12, 24, 48 and 72 h.p.i. and titrated via plaque assay on MDCK cells. Three independent repeats were performed, again all with mock infected cells that showed viral levels below the limit of detection (data not shown). The viral output from CK cells varied more between experiments in comparison to MDCK cells (Figure 2.6B). Nevertheless, there were consistent differences between the replication kinetics of the viruses. Viruses with PA 26E (UDL-01 WT and WF10 K26E) reached peak titres at 24 h.p.i, while 26K-containing viruses replicated more slowly, achieving maximum titres at 48-72 h.p.i. (Figure 2.6B). The UDL-01 virus pair only showed significant differences in viral output at 24 h.p.i. At all other time points there was no significant difference in viral titre. With the WF10 pair, a significant difference in viral output was seen at 8 h.p.i. Thus, in avian cells, the PA K26E polymorphism affected the kinetics of virus growth.

Viral replication was then assessed *in ovo.* 10-day old fertilised hens' eggs (VALO breed) were infected with 100pfu of the viruses. Samples of allantoic fluid were collected from groups of 5 eggs at 4, 8, 12, 24 and 48 h.p.i. and viral titres in each egg determined via plaque assay on MDCK cells. *In ovo* (Figure 2.6C) UDL-01 WT had significantly higher titres than UDL-01 E26K mutant virus at both 12 and 24 h.p.i. However, by 48 hours replication of the mutant virus had reached

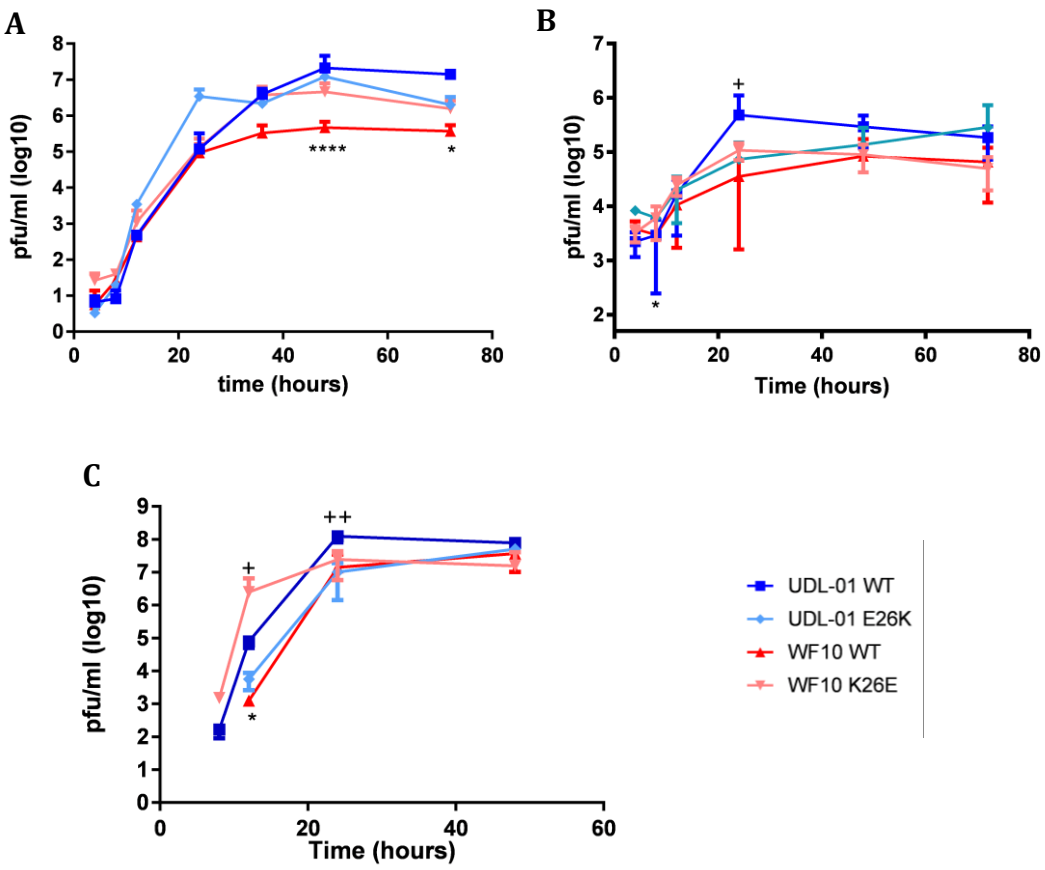

Figure 2.6: Multi-cycle replication kinetics of H9N2 AIVs with mutated PA codon 26. (A) MDCK cells and (B) CK cells were infected with the specified virus (UDL-01 WT, UDL-01 E26K, WF10 WT or WF10 K26E) at a low MOI (0.01). (C) 10-day-old fertilised hens' eggs infected with 100pfu of virus. Samples were taken at the indicated time points for titration via plaque assay. No virus was detected proior to 8 h.p.i. Data represents the average +/- SD of 3 independent experiments (cells) or 5 eggs per timepoint. Significant differences (unpaired T-tests (A; UDL-01 36 and 72 h.p.i. WF10 24, 36, 48 and 72 h.p.i., B: UDL-01 8, 12, 24 and 48 h.p.i. WF10 8, 48 and h.p.i. C: UDL-01 12 h.p.i.) or Mann-Whitney Test: (A; UDL-01 4, 8, 12, 24 and 48 h.p.i. WF10 4, 8 and 12 h.p.i. B; UDL-01 4 and 72 h.p.i. and WF10 4 , 12 and 72 h.p.i. C: UDL-01 8, 24 and 48 h.p.i. WF10 all data points) between WT and corresponding mutant at each time point depending on distribution of data) are represented via + (UDL-01 pair) and * (WF10 pair). P values: +/*= <0.035; ++/** = <0.008; **** = <0.0001. UDL-01 WT indicated by dark blue line, UDL-01 E26K indicated by the light blue line, WF10 WT virus represented by the red line and WF10 K26E represented by the pink line.

almost equal levels to the WT. Conversely, WF10 WT AIV had significantly lower viral titres at 12 h.p.i. compared to WF10 K26E mutant virus. However, after 24 hours the WT and mutant K26E WF10 viruses displayed similar titres. Thus *in ovo*, the K26E polymorphism did not affect maximum virus titres but significantly affected replication kinetics. In general, those viruses which contained an E at position 26 appeared to replicate faster with virus being detected at 8 h.p.i compared to 12 h.p.i with viruses containing a K at position 26.

Overall, from these data we can conclude that amino acid substitution at position 26 of PA within WF10 and UDL-01 H9N2 AIVs significantly altered the replication of the viruses in mammalian cell lines, in avian primary cells as well as in the *in vivo* model of embryonated hens' eggs. However, this is a cell line dependant effect and infection of different cell types alters the timings of the replication differences that are observed.

2.2.6: Stability of PA amino acid 26 mutations upon serial passage in 10-day old embryonated hens' eggs.

To assess the stability of the introduced mutations at amino acid position 26, the viruses were serially passaged in 10-day old embryonated hens' eggs. 100pfu was inoculated into the allantoic fluid of each egg and 1 egg per virus used for passaging. After each passage, virus was titrated via plaque assay and 100pfu of the virus was used to inoculate the next egg. This process was repeated until 6 passages were completed. A mock inoculated egg (PBS only) was included at each passage and this was negative for virus, to the limit of detection of the plaque assay, at each attempt (data not shown). It would have been preferable to repeat

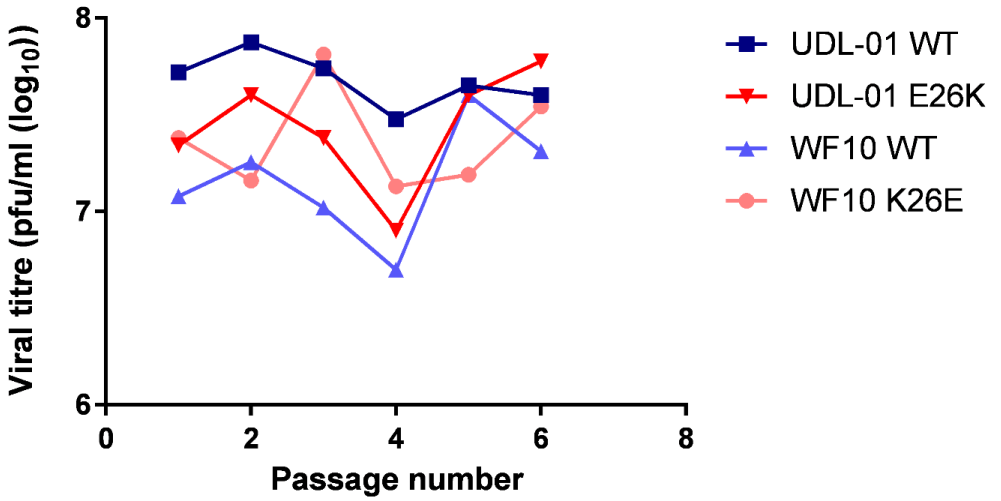

Figure 2.7: Viral titres throughout serial passage in 10-day old embryonated hens' eggs. Viruses were serially passaged 6 times at 100pfu inoculation doses. Allantoic fluid samples were collected at each passage and then titrated via plaque assay to assess viral titre. UDL-01 WT indicated by dark blue line, UDL-01 E26K indicated by the red line, WF10 WT virus represented by the light blue line and WF10 K26E represented by the pink line. N=1.

this process during independent experiments but the time constraints of the project did not allow for this. UDL-01 WT virus showed the most stable output titres across the passage period (Figure 2.7). WF10 WT and UDL-01 E26K titres decreased from passage 1 to passage 4, after which the viral titres rose. The titre of WF10 K26E was relatively stable across all passages, with some fluctuations in output being seen; for example, the increase in titre at passage 3. Statistical analyses could not be carried out because of the lack of replicate data, but overall, no virus titre varied by as much as 10-fold across the experiment.

Plaque phenotype was previously shown to be a sensitive indicator of relative fitness for the UDL-01 and WF10 viruses (Figures 2.1 and 2.4), therefore plaque phenotype may give initial clues into any alteration in viral fitness via passaging. When P1 and P6 plaque morphologies were compared, UDL-01 WT virus and WF10 K26E virus visually retained their large plaque phenotypes after 6 passages (Figure 2.8A), with quantification showing that the average plaque diameter had not significantly altered (Figure 2.8B). However, when P1 and P6 WF10 WT virus and UDL-01 K26E virus were compared the plaque phenotype had increased within the 6 passages. The plaque diameter of UDL-01 K26E significantly increased from 0.54 mm to 1.26mm, while WF10 WT plaque diameter increased significantly from 0.44 mm to 1.43 mm. This suggested that these viruses had mutated over the 6 passages to have an increased fitness *in vitro*.

As the viral plaque phenotypes had altered upon viral passaging, the molecular basis of this alteration was investigated. Viral RNA was extracted from

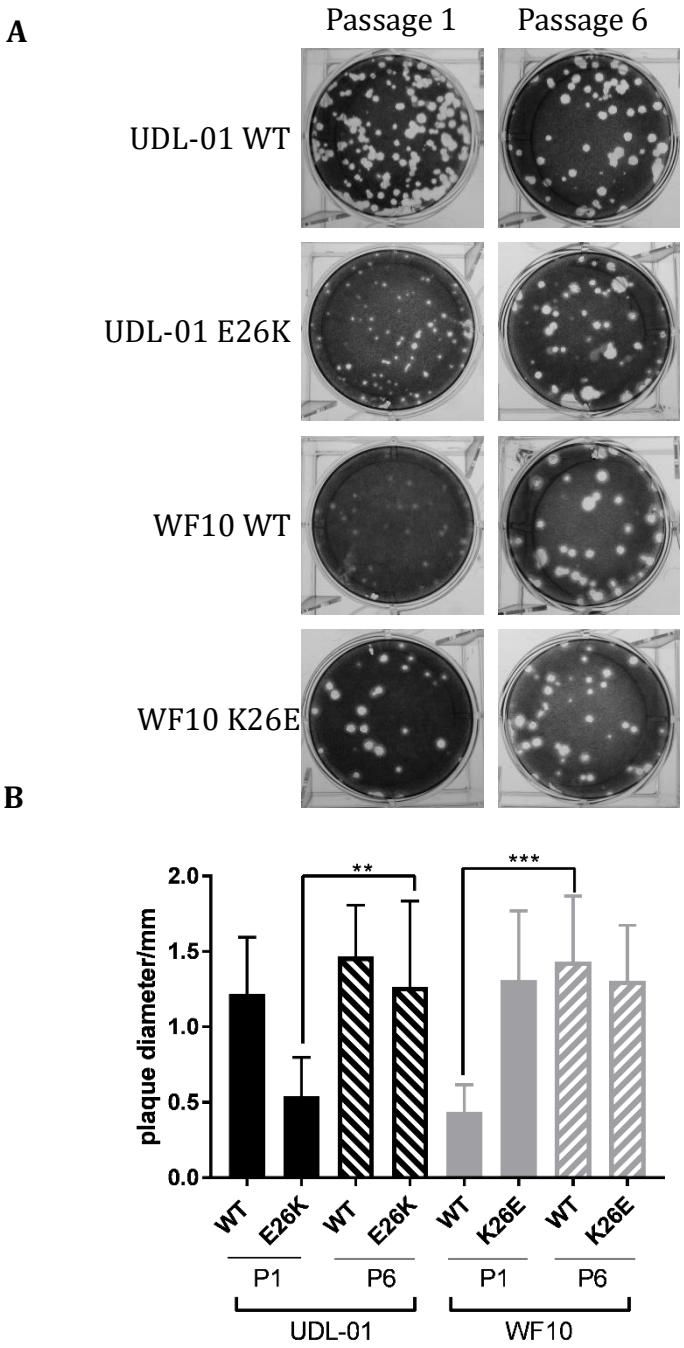

Figure 2.8: Viral plaque phenotype after serial passage in 10-day-old embryonated hens' eggs. Allantoic fluid samples from serially passaged virus were titrated via plaque assay under 0.6% agarose. 72 h.p.i. plaque assays were fixed and stained using 0.1% crystal violet solution. Images were taken and plaque diameter calculated using ImageJ analysis software. (A) Visual representation of viral plaque phenotypes comparing passage 1 virus with passage 6 virus. (B) Randomly, 20 plaque diameters per virus were measured and graphically represented as mean +/- SD. P values (unpaired T–test) comparing passage 1 (P1) to passage 6 (P6) plaque diameters; P values = **: 0.0011; ***: 0.0003.

allantoic fluid samples of passage 1 (P1) and passage 6 (P6) viruses and RT-PCR for viral segment 3 was conducted. This was sent for sequencing (Source Biosciences) to determine the codon identity at position 26 as well as to potentially identify any further compensatory mutations which may have occurred during passaging. A summary of the sequencing data is seen in Figure 1.9. After 6 passages, all four viruses had reverted to contain a Glutamic acid (E) at position 26 of PA. This correlates with the increased plaque phenotype observed with the passage 6 viruses in Figure 2.8. There were no other compensatory mutations identified within segment 3 that could have been responsible, or partially responsible for the difference in plaque phenotypes observed across 6 passages. However, the impact of mutations within other viral segments was not assessed. Overall, it appears that having a lysine (K) at position 26 of PA, as with WF10 WT and UDL-01 E26K viruses, leads to a viral fitness cost. This was soon overcome via serial passage in eggs as the 26K altered within 6 passages to replace with glutamic acid.

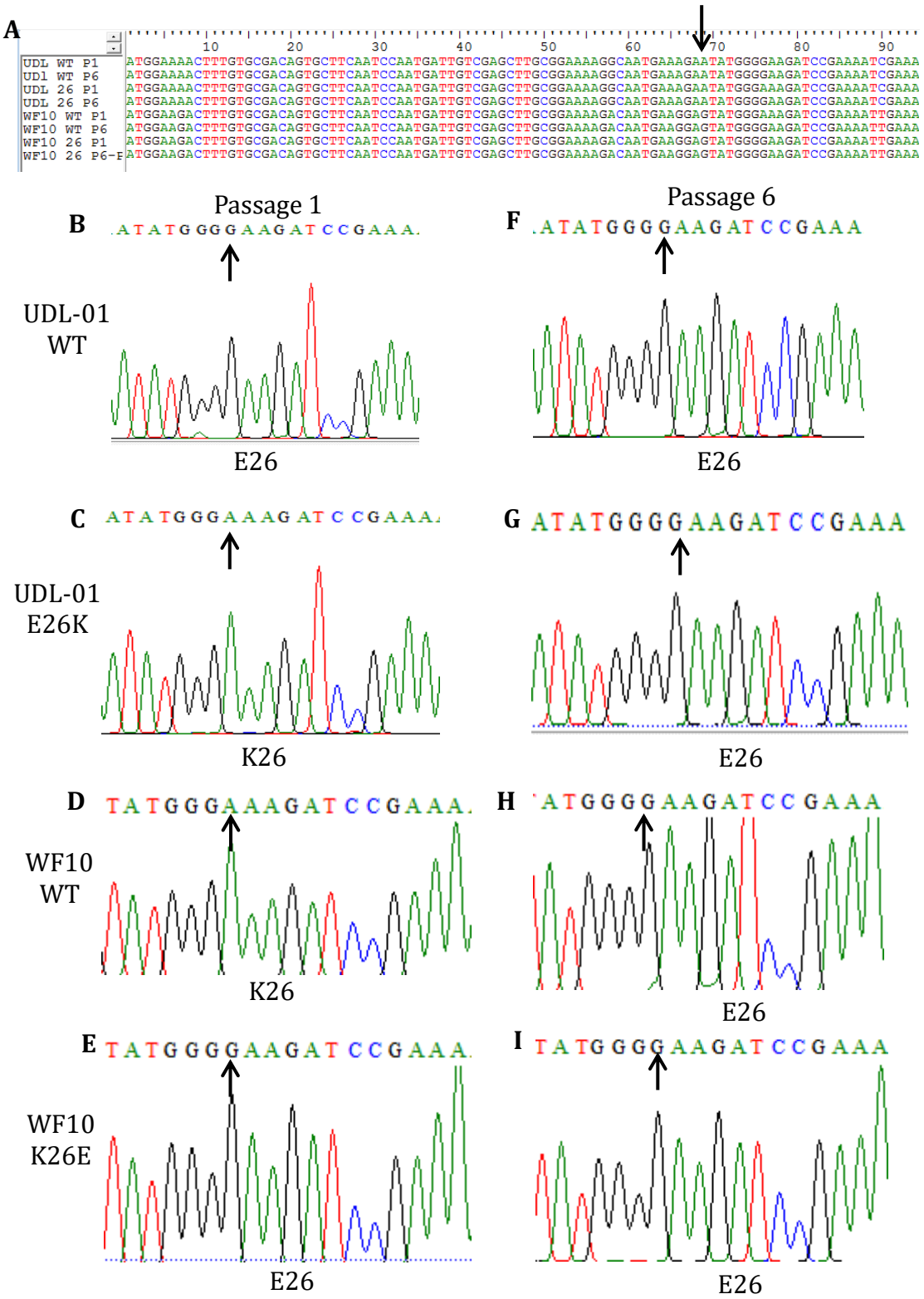

Figure 2.9: PA sequence after serial passage in 10-day old fertilised hens' eggs. Viral RNA was extracted from allantoic fluid samples of viruses passaged in 10-day old embryonated hens' eggs either once (Passage 1) or six times (Passage 6). RT-PCR specific for influenza segment 3 was completed and products sent for sequencing via GATC. (A) Sequence reads were aligned using CLUSTAL multiple alignments. (B-E) Sequence trace for Passage 1 samples with nucleotide 76 change highlighted with the black arrow. (F-I) Sequence trace for passage 6 samples with nucleotide 76 highlighted with the black arrow.

2.2.7: Prevalence of amino acid codons at PA position 26 in IAV sequences

The identification of the prevalence of amino acid codons at PA position 26 in known IAV sequences, would enable correlations to be made between the presence of an amino acid K or E at this position and viral fitness implications. To assess the natural amino acid diversity at position 26 within viral sequences available at the public database, bioinformatics analysis was carried out by Dr Samantha Lycett at the Roslin Institute. Full length sequences, with coding regions marked as complete or nearly complete, were downloaded from the NCBI influenza virus resource (23th June 2015). Files were split into 1000 base pair regions and aligned using MUSCLE (MEGA6) and then re-joined. Incomplete sequences or sequences with runs of unidentified amino acids (Ns) were excluded from the analysis (totalling 88 avian, 14 swine, 55 human and 1 canine-derived virus sequences). This left 12,248 avian, 3,082 swine, 12,148 human, 77 canine and 177 equine virus sequences for further analysis. The data were analysed by host and the consensus amino acid as well as the further 3 most common amino acids were identified for each position. The fraction of sequences with each of the amino acids was also calculated.

Within each host type E26 (Glutamic acid) was by far the most prevalent amino acid, making up 99.9% of avian, swine and human sequences; 99.1% of equine sequences and 98.7% of canine sequences (Figure 2.10). Glycine (G), Lysine (K), Aspartic Acid (D) and Glutamine (Q) made up minor proportions of the amino acids at position 26, although this did not reach more than 1.3% of sequences analysed (G26 within canine sequences). There were also a small

number of equine, swine and human IAV sequences where the amino acid at this position was not defined (X).

Table 2.3 lists the viruses which contain amino acids other than glutamic acid at position 26. Most are derived from avian species, although the numbers are small. They were isolated across a range of years from 1983 to 2011 and a number of viral subtypes (H5N8, H7N1, H9N2, H5N2, H5N1, and H3N2). Interestingly, the other H9N2 virus which has K26 was isolated in 1999 (the same year as WF10) suggesting this polymorphism could have been circulating in China at the same time as WF10 was circulating in Hong Kong. However, it appears that K26 does not persist in the field and this could be due to the reduction in viral fitness seen throughout this chapter for viruses containing PA K26. Conversely, E26 is the predominant amino acid in circulating in viral strains, consistent with the increased viral fitness seen with this mutation in the laboratory setting.

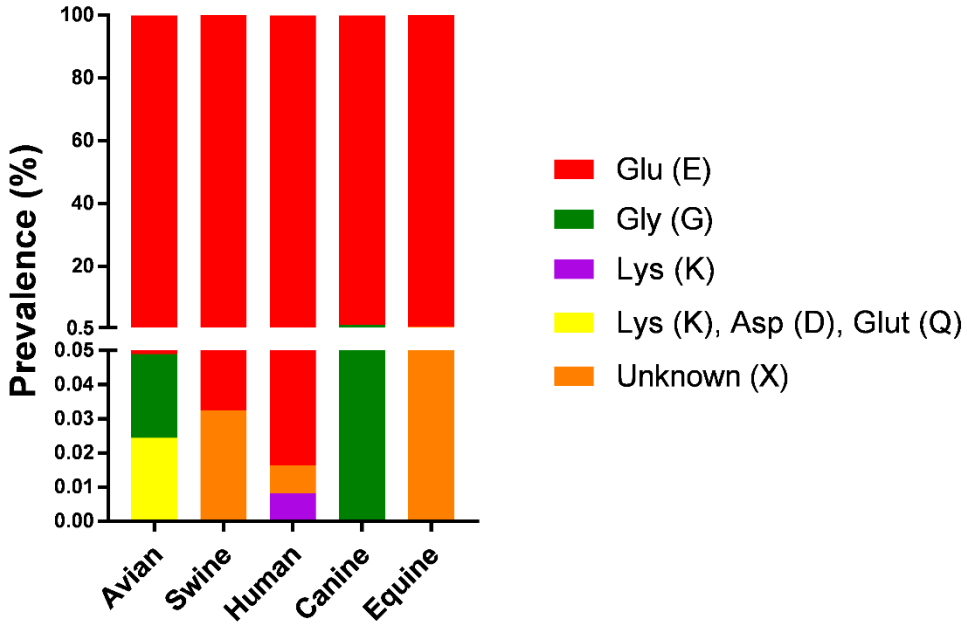

Figure 2.10: Prevalence of individual residues at amino acid 26 of PA across IAV strains from various hosts. Bioinformatics analysis of 12,248 avian, 3,082 swine, 12,148 human, 77 canine and 177 equine sequences was conducted by Dr Samantha Lycett at the Roslin Institute. Sequences were split into 1000 base pair sections, aligned using MUSCLE (MEGA 6) and then re-joined. The consensus codon at each amino acid position was identified as well as the 2nd and 3rd most frequent amino acid. The fraction of sequences containing each of the amino acids was plotted. Glutamic acid: red, Glycine: green, Lysine: purple, Lysine, Aspartic acid and Glutamine: yellow, unknown amino acid: orange.

Table 2.3: Summary of viruses which do not contain 26E within their PA gene.

Virus Name	Host species	Subtype	Amino acid at 26
A/duck/Ireland/113/1983	Avian	H5N8	Aspartic Acid (D)
A/softbill/CA/33445-158/1992	Avian	H7N1	Glycine (G)
A/chicken/Guangxi/4/1999	Avian	H9N2	Lysine (K)
A/mallard/Maryland/792/2002	Avian	H5N2	Glutamine (Q)
A/goose/Guangdong/72/2004	Avian	H5N1	Glycine (G)
A/mallard/Maryland/708/2005	Avian	H3N2	Glycine (G)
A/Vietnam/HN31388M1/2007	Human	H5N1	Lysine (K)
A/canine/Guangdong/05/2011	Canine	H3N2	Glycine (G)

Bioinformatics analysis was carried out on 12,248 avian, 3082 swine, 12,148 human, 77 canine and 177 equine PA sequences by Dr Samantha Lycett at the Roslin Institute. Those sequences which did not have the consensus E26 amino acid were identified.

2.2.8: Assessing the predicted impact of the PA E26K polymorphism on endonuclease domain structure

As the amino acid present at position 26 of PA appeared to be responsible for alteration in viral plaque phenotypes and replication, it is likely that there are alterations within the protein structure which influence viral fitness. The impact of E26, K26 and G26 (as this mutation frequently appeared within field isolates of viruses) mutations on the structure of the N-terminal domain of the PA protein were modelled using the I-TASSER server for protein structure. The I-TASSER server has been developed as an integrated platform for automated protein structure analysis. It takes the amino acid sequence of the protein of interest and generates 3-D atomic models from multiple threading alignments and iterative structural assembly situations (Roy et al., 2010). First, the secondary structural elements of the UDL-01 and WF10 WT endonuclease domains were compared (Figure 2.11A). There are two occasions when an extended or reduced α-helix was observed (highlighted in brackets); between codon 11-24 (helix 1) and between codon 126-136 (helix 2). There is the potential for the amino acid at position 26 to affect these structures due to the close localisation to helix 1 and downstream effects on helix 2. The structures of UDL-01 WT and WF10 WT PA endonuclease domains were then modelled (Figure 2.11B, C; UDL-01 WT- violet, WF10 WT- green; E26- magenta, K26 –light pink). A shorter α-helix was observed in the UDL-01 WT endonuclease domain as expected from the sequence analysis in helix 1 (Figure 2.11B-highlighted by the white arrow). The region around amino acid 26 appeared to be similar between both WT endonuclease domains. The shortened α-helix within WF10 WT between codons 126 and 136 (helix 2)

was observed within the predicted crystal structures (Figure 2.11C-highlighted with the white arrow).

When amino acid changes were introduced into the UDL-01 endonuclease domain structure and the secondary structures analysed, helix 1 appeared to alter in length depending on the amino acid present at position 26 (Figure 2.11D). E26 (WT) had the shortest helix 1, K26 had a slightly increased helix 1 and G26 had the longest helix 1 making it comparable to WF10 WT helix 1 in length. None of the mutations affected the length of helix 2 within UDL-01. The effect of 26 E, K or G was then modelled onto the predicted UDL-01 endonuclease domain structure. When the protein structures of the endonuclease domain of UDL-01 with either E26 (purple), K26 (blue) or 26G (light blue) were compared (Figure 2.11E, F), the alteration of length of helix 1 could be visualised (Figure 2.11E). No difference was seen in the length of helix 2 within the predicted crystal structure (Figure 2.11F).

When the amino acid changes were introduced into the WF10 endonuclease domain sequence and the secondary structures analysed, the amino acid present at position 26 did not alter the length of helix 1. However, introduction of 26G into WF10 PA appeared to increase the length of helix 2 (Figure 2.11G). This was mapped onto the predicted proteins structures of WF10 PA with either E26 (bright green), K26 (olive green) or G26 (dark green) changes within the endonuclease domain (Figure 2.11H and I). As with the predicted structure map, helix 1 did not appear to differ with any of the 26 mutants (Figure


Helix 1
A
UDL-01 WT
WF10 WT
Helix 2

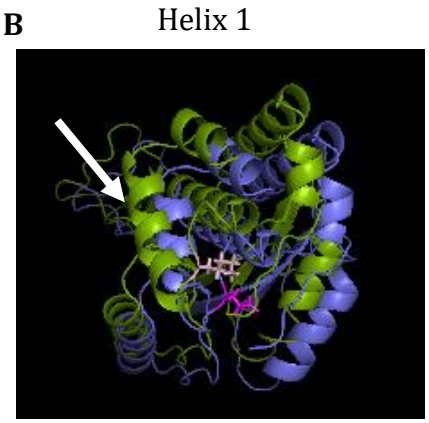
B
Helix 1

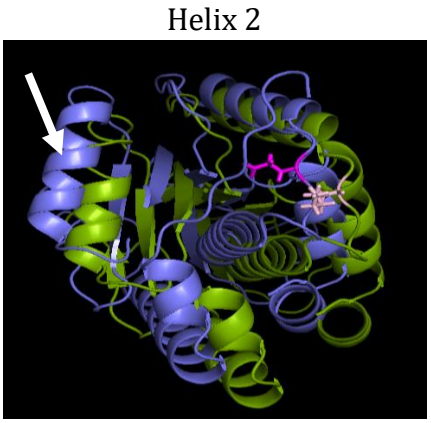
C
Helix 2

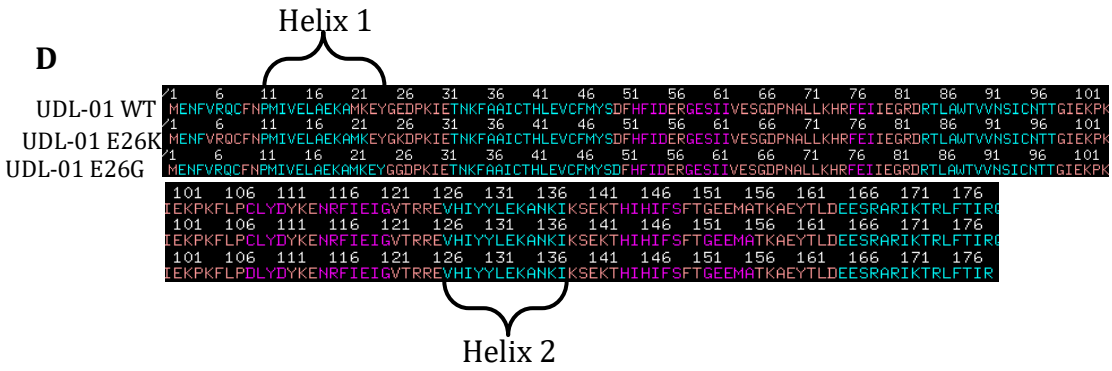
Helix 1
D
UDL-01 WT
UDL-01 E26K
UDL-01 E26G
Helix 2

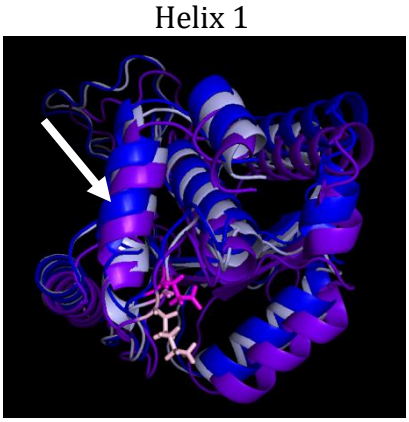
E
Helix 1

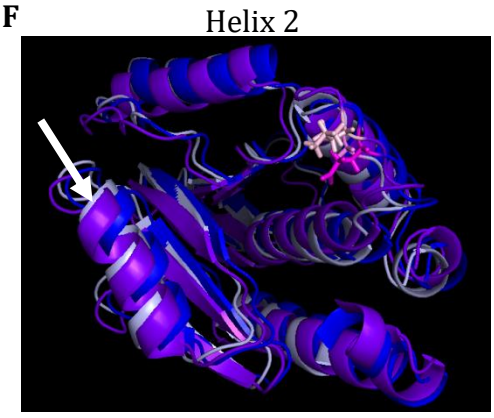
F
Helix 2

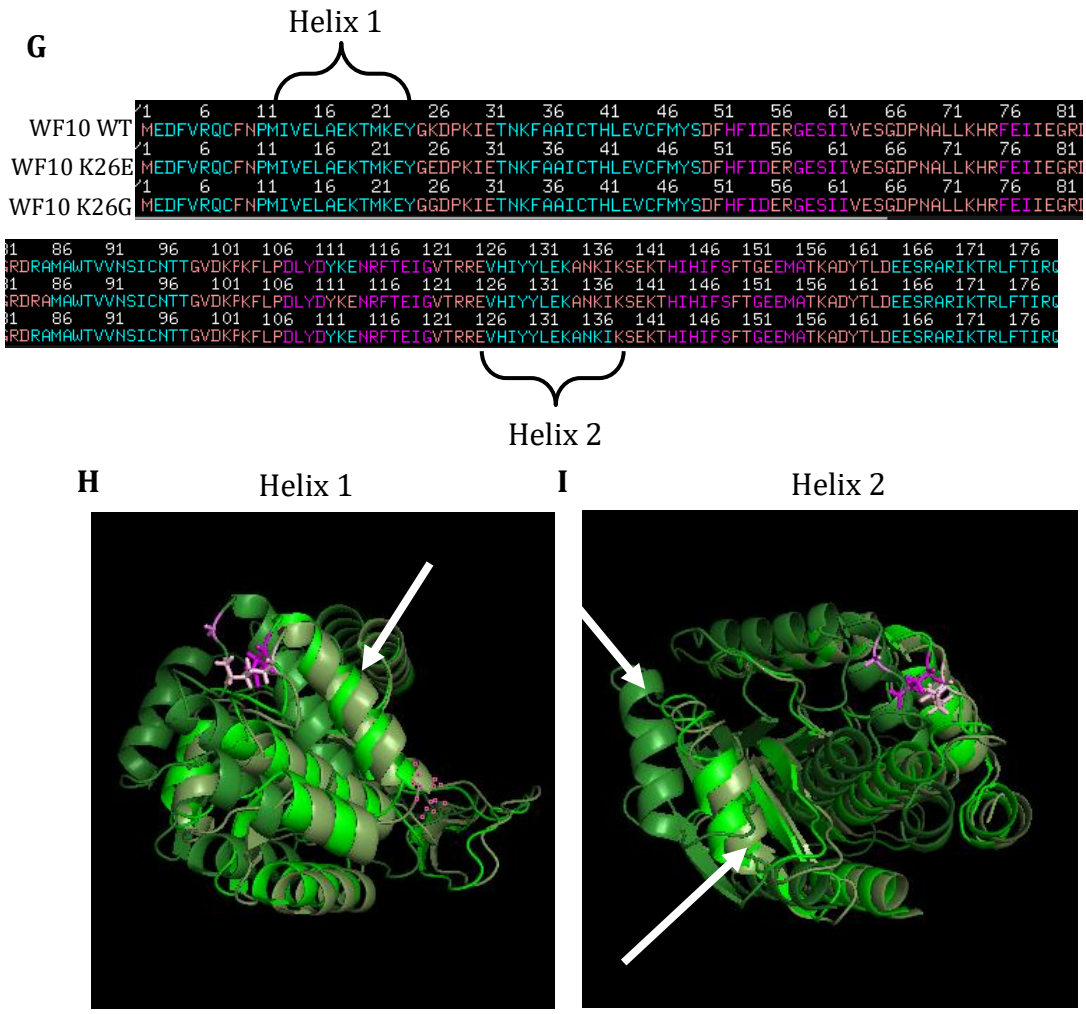

Figure 2.11: Modelling the endonuclease domain of PA with alterations to amino acid position 26. The I-TASSER server for the analysis of protein structure was used to ascertain models for the structure of the PA endonuclease domain with mutations at amino acid position 26. (A) structural markers of the endonuclease domain by sequence (B) predicted structures of UDL-01 WT (purple) and WF10 WT (olive green) endonuclease domains front. (C) predicted structures of UDL-01 WT (purple) and WF10 WT (olive green) endonuclease domains back. (D) structural markers of the endonuclease domain by (E) predicted structures of UDL-01 WT (purple), UDL-01 E26K (blue) and UDL-01 E26G (light blue) endonuclease domains front. (F) predicted structures of UDL-01 WT (purple), UDL-01 E26K (blue) and UDL-01 E26G (light blue) endonuclease domains back. (G) structural markers of the endonuclease domain by sequence (H) predicted structures of WF10 WT (olive green), WF10 K26E (bright green) and WF10 K26G (dark green)endonuclease domains front. (F) predicted structures of WF10 WT (olive green), WF10 K26E (bright green) and WF10 K26G (dark green) endonuclease domains back. Throughout structural diagrams: blue: α-helix, pink: β-sheet, peach: loop, shortened loops highlighted with brackets. White arrows indicate locations of shortened loops in predicted crystal structures.

2.11H), however, the lenghtened helix 2 can be seen within the WF10 K26G predicted structure (Figure 2.11I). There appeared to be some differences between the effect of mutations at PA position 26 between UDL-01 and WF10 endonuclease domains and the functional basis of these predicted structral alterations was not identified.

2.3: Discussion

In this chapter, the amino acid differences within the PA gene of progenitor (WF10) and novel reassortant (UDL-01) H9N2 AIVs were screened *in vitro* to investigate the molecular basis of the drastically altered plaque phenotype between the viral strains (UDL-01; large, clear plaques. WF10; small hazy plaques). A panel of PA mutations were selected (Table 2.1) and site directed mutagenesis used to alter these amino acid positions within each PA gene. Within this panel of mutants, once mapped onto the crystal structures of the endonuclease domain of PA (Figure 2.2A), several of the mutants showed promising potential due to their external locations on the structure suggesting a potential for alterations of interactions which could affect protein function. Other mutations lay next to or close to the endonuclease active site so could potentially have effects by interfering with the metal ion binding of the endonuclease. Reverse genetics was used to build a panel of viruses which differed by only a single amino acid, compared to the WT parental counterpart virus. Within this chapter the key domain for the difference in viral fitness previously observed was identified to be the N-terminal 1101 nucleotides of the PA gene (Figure 2.1).

It was observed that a single amino acid change, E26K, was able to reciprocally alter the plaque phenotypes of WF10 and UDL-01 viral strains: WF10 viruses produced a larger plaque phenotype and UDL-01 plaque formation was restricted. Although previous literature has been published on the impact of some of the introduced mutations on viral replication, pathogenicity and polymerase activity (Hu et al., 2013a; DesRochers et al., 2016), the same affect was not observed within the H9N2 AIVs tested in this study.

Although the majority of mutants had no effect on the transcriptional activity of the polymerase complex, the UDL-01 E26K mutation did show a significant increase in output compared to UDL-01 WT within DF-1 cells. This however, did not correlate with the decreased replicative ability of viruses with this mutation. Overall, the transcription rates were similar throughout the panel suggesting that vRNA production was not affected. However, further work to determine the differences in vRNA, cRNA and mRNA levels produced by each of the polymerase complexes could be completed by performing primer extension assays with the RNP complexes (Hara et al., 2006). This would allow for further insights into the mechanism of action of the mutants. The similarity in transcription levels between the RNPs with different PA mutations also suggests that PA cap snatching is not affected, as cap snatching by the PA protein is required for effective transcription of vRNA to occur (Reich et al., 2014), although this was not tested in detail. It would therefore be interesting to test the endonuclease activity and cap snatching ability of the mutant PA complexes to determine if these PA functions are altered. Another limitation of the data is the lack of a high quality antibody for the detection of the PA protein. The western

blot data presented in Figure 2.3B is of poor quality and repetition of this technique would have been preferable to gain a better quality image and to quantify levels of the PA protein to perhaps determine protein stability.

The plaque phenotypes of viruses containing each mutation showed that only a mutation at position 26 within the PA endonuclease alters plaque morphology to the same degree as when the entire segment is switched (Figure 2.4). With UDL-01 E26K displaying a small plaque phenotype and WF10 K26E displaying a large plaque phenotype. This did not necessarily correlate with replication differences within low m.o.i infections where at 48 hours post infection viruses did not have a significantly different viral outputs. However, when looking across a time course of infection, there was a general trend for viruses contain 26E to replicate faster and to higher titres than those with 26K. However, on some occasions, particularly in eggs, the peak titres were similar between groups. This suggests that having a 26E is beneficial for viral fitness in terms of replication. However, this increased titre and initial replication of the viruses with 26E could be an artefact of the larger plaque phenotype meaning it is easier to determine positive samples. To overcome this it may have been beneficial to immunostain the plaque assays or use a semi-solid overlay as this may be a more sensitive method or allow for larger plaque to form (Baer and Kehn-Hall, 2014; Juarez et al., 2013). Another possibility of the increased replication and plaque phenotype of the 26E containing viruses could be explained by the ability of these viruses to control the host IFN response. (Solorzane et al., 2005; Newby et al., 2007) has previously shown that plaque phenotype links with host immune response, with those viruses with an

enhanced ability to control the host immune response, displaying increased spread throughout cell culture and therefore cause a larger plaque phenotype. This could therefore suggest that the difference in plaque phenotype could be related to the accessory protein present in segment 3, PA-X, something which is further investigated in Chapter 4. Or it could be due to a separate and currently unknown function of segment 3 involved in the control of the host IFN response, something which could be easily investigated using *in vitro* methods such as assessing viral replication in the presence of IFN, or using reporter cell lines to assess the amount of IFN produced during infection. Unfortunately these studies were not conducted as part of this thesis but would be an interesting point to follow up.

When viruses containing mutations at position 26 were passaged in eggs, they quickly reverted (after 6 passages) to contain a glutamic acid at position 26. (Figures 2.7 and 2.8). Throughout the passaging viral titres were measured and the majority of viruses showed a decrease in viral titre until passage 4, after which titres recovered. Unfortunately this was only repeated once so statistical analysis could not be carried out and it could not be determined if this was only the result in this experiment or it occurred on multiple occasions after passaging. The increased titre after passage 4 was most pronounced in those viruses containing 26K, so it could suggest that this is the point where reversion to 26E occurred. This cannot be fully determined as sequencing analysis was not carried out at this point. In future studies it would be beneficial to sequence multiple passages across the course and to analyse plaque phenotype throughout the

experiment duration as this could elucidate the point at which the change occurred.

The reversion of K26 seen was supported by bioinformatics analysis showing that the majority of viral sequences in avian, human, canine, equine and swine hosts possessed E26 (up to 99.9%) with only a handful of sequences possessing K26 with this amino acid not circulating readily in field strains. This suggests that having PA K26 is detrimental to the polymerase somehow affecting its function or stability. Functional assays to test PA cap snatching or endonuclease activity would be useful to determine the mechanism of action and role of positon 26 in PA function. Another potential avenue to follow up is the impact of amino acid residues on PA protein or viral stability. If the PA protein has increased stability or the stability of the polymerase complex is altered by changing the amino acid at position 26 this could explain the reversion to 26E and the predominance of 26E within the virus population. The production of defective interfering particles (DIs) has previously been suggested to be involved in an unstable polymerase. Previous work has shown that increased DI production was caused by a mutation in PA (R638A), interestingly this virus also produced pin head plaques, as our mutants with 26K do (Fodor et al., 2003). This would again be an interesting topic to follow up in future studies to determine if the 26K mutation leads to an unstable polymerase and therefore the production of increased DIs.

The predicted modelling of the structures of the PA endonuclease domain (Figure 2.9), altering the amino acid present at position 26 appeared to

differentially affect predicted protein structure depending on the viral strain and could not provide conclusive evidence of a mechanism of action for the differences seen between viruses. Alteration of changes to amino acid 26 within UDL-01 altered the length of a α-helix located between codons 11-24, whereas within WF10, alterations to amino acid 26 changed the length of the α-helix between codons 126-136. There did not appear to be a correlation between plaque size and helix length. However, the exact mechanisms of action of these alterations in α-helix length on viral fitness were not further investigated. However, as both of these regions lie within the endonuclease domain it is possible that endonuclease function could be affected by the alteration of helix lengths. This is cemented as Dias et al., (2009) has shown amino acid 134 (in helix 2) is important for endonuclease function. This could be followed up further by investigating endonuclease function of PA's containing 26E vs 26K vs 26G.

The impact of K26 on influenza viruses within the field remains to be seen as very few viruses have been identified to contain this consensus codon. One of the limitations of this work is that due to the low frequency of K26 within viral sequences and reversion of K26 when passaged, the original sequence of WF10 containing K26 could have resulted from sequencing or cloning error at this position. This would suggest that potentially another factor is responsible for the differences seen between early and reassortant H9N2 AIVs. One suggestion could be the NS1 segment, which was also implicated in the earlier screen. Jackson et al. (2007), showed viruses which differ in the C-terminus of NS1 can have alterations in viral plaque phenotype and pathogenicity. This would be an interesting factor to investigate further if time and resources allowed.

Within this chapter, a single amino acid change has been identified which can alter H9N2 viral fitness within cell culture and although this mutation could be an artefact, it still gives important mechanistic insights into the role of the endonuclease domain of segment 3 in viral replication. The effect of this mutation on viral pathogenicity will be further investigated in chapter 3.

Chapter 3: How do PA mutations modulate H9N2 virus pathobiology within avian models *in vivo*?

3.1: Introduction

The results displayed within chapter 2 identified a single mutation (E26K) responsible for altering various phenotypes of viruses containing the UDL-01 and WF10 segment 3. Therefore, within this chapter, the role of this mutation was assessed *in vivo*. No previous work has identified an amino acid change at position 26 of PA as influencing influenza virus pathogenesis *in vivo*. However, several amino acid positions within PA have previously been shown to alter viral pathobiology. For example, within H9N2 AIVs, PA K356R has been shown to increase mammalian replication and pathogenicity, causing lethal infection within a mouse model (Xu et al., 2016a). Whereas in a mouse model of 2009 pandemic H1N1 challenge, a combination of PA P224S and A70V reduced the viral dose required for lethal infection of 50% of the animals (LD_{50}) by approximately 1000-fold (Sun et al., 2014). Similarly, several other studies have shown different amino acid changes within the PA genes of H5N1 (Fan et al., 2014), H7N3 (DesRochers et al., 2016), H1N1 (Llompart et al., 2014) and H7N7 (Zhao et al., 2016) viruses which can alter pathogenicity within mouse models. Thus single amino acid alterations within the PA gene of IAV can distinctly alter the viral pathogenesis in mammalian systems; therefore, based on *in vitro* results, it was predicted that the E26K mutation poses the potential to alter the pathogenicity of the H9N2 virus investigated in this study.

However, none of these previous, even those using avian-derived viruses, assessed role of PA mutations within a more natural avian model of infection. Therefore, the aims of this chapter were i) to assess the role of PA E26K change on the pathogenicity of H9N2 AIVs *in ovo*; ii) to assess the role of the PA E26K change on virus infectivity, shedding, transmission and pathogenicity *in vivo* using a chicken model of infection.

3.2: Results

3.2.1: Effect of mutations *in ovo*

In the first instance, the effect of the key mutation in the PA protein previously identified to effect virus replication and plaque phenotype (amino acid 26: Glutamic Acid or Lysine) was investigated *in ovo* in 10-day old embryos. This allowed for an insight into the differential phenotypes of wild type and mutant viruses in a less developed animal model (up to 14-day old embryos) prior to using post-hatch chickens adopting 3Rs principles.

3.2.1.1: H9N2 *in ovo* infection of embryos and gross pathological observations

The gross pathology of the 10-day old chicken embryos infected with RG H9N2 AIVs was assessed to gain insights into pathogenicity differences between viruses as the more pathogenic the virus, the more likely it would cause gross pathological signs within an infected chicken embryo. The embryos were infected with viruses containing either WT PA or PA with a substitution (K or E) at amino acid position 26. This makes the virus either progenitor (WF10)-like with PA-K26

or reassortant (UDL-01)–like with PA-E26. Groups of 6 10-day old embryonated SPF white leghorn (VALO breed) hens' eggs were infected with 100 pfu of each UDL-01 or WF10 virus, or sterile PBS for the mock group, via inoculation into allantois. The embryos were candled twice daily to check embryo viability for 48 hours; any embryos which reached humane end points (see chapter 7 for details) were discarded. 48 hours post-infection the remaining embryos were chilled, removed from the shell, washed twice in PBS and then photographed to document gross pathology. Samples of allantoic fluid were taken from each egg and viral titres assessed via plaque assay. Any embryos from virus inoculated embryonated eggs which were not positive for virus were removed from the remainder of the study. UDL-01 E26K mutant virus replicated to a significantly lower titre compared to its WT counterpart. Whereas the WF10 K26E mutant virus replicated to a higher titre than its WT counterpart virus, although this was not significant (Figure 3.1H).

Images of 4 washed embryos per virus group were selected from those that passed the criteria described above. On initial investigation, both UDL-01 WT and UDL-01 E26K mutant groups (Figure 3.1B and C) had several embryos which looked to have more severe gross pathological lesions compared to mock infected embryos (Figure 3.1A), with marked bleeding and a macerated appearance of the embryo. The WT WF10 and mutant WF10 K26E infected embryos exhibited less pronounced gross pathophysiological changes compared to mock infected embryos; none of the embryos showed clear bleeding and all remained intact (Figure 3.1D and E). The gross pathology of the embryos was then blindly scored by 3 group members.

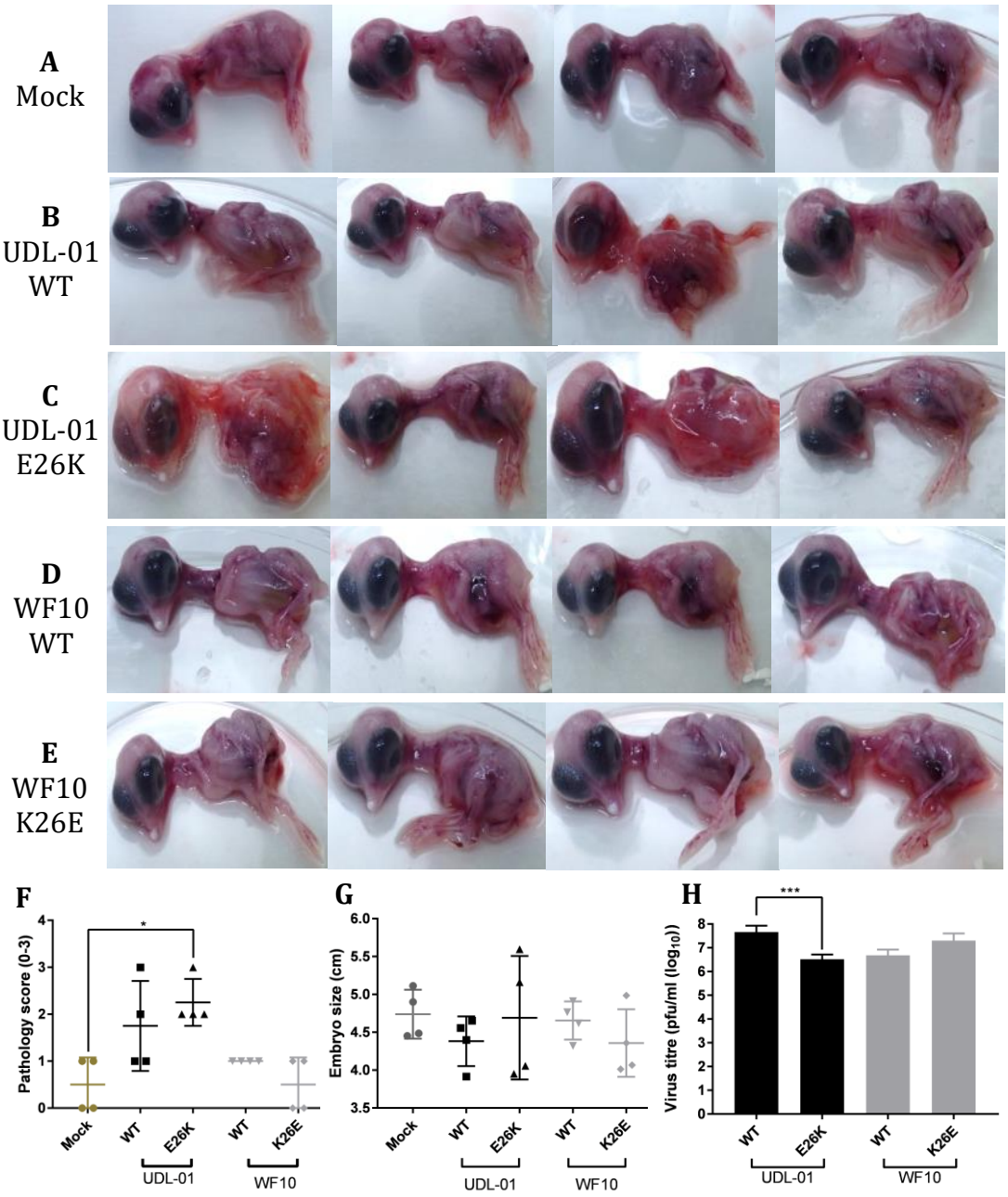

Figure 3.1: Effect of PA E26K mutation on *in ovo* replication and pathology of H9N2 AIVs. Groups of 6 10-day old VALO eggs were infected with 100 pfu of the indicated viruses. Eggs with virus-negative allantoic fluid or which displayed early embryo death were removed from the experiment. (A-E) Embryos were removed from the shell and washed twice in PBS before imaging to assess gross pathology. (F) Images were blindly scored for gross pathology by 3 independent people. Scoring was based on the following criteria: 0- no obvious bleeding, 1- subtle bleeding, 2- considerable bleeding, 3- very obvious bleeding and/or embryo not intact. Data represent the mean of 3 independent scorers, each scoring 4 embryos per group. (G) Embryo size was estimated using ImageJ analysis software by normalising to the diameter of the petri dish each embryo was imaged in. Data represents average length +/- SD. (H) Viral titres of allantoic fluid taken from positive eggs assessed via plaque assay. One-way ANOVA with multiple comparison (G), unpaired T-test (H) or Kruskal-Wallis with multiple comparisons (F); P values =*: 0.015, ***: 0.0004.

The scoring criteria were as follows: 0= no obvious bleeding, 1= subtle bleeding, 2= considerable bleeding and maceration, 3= very obvious bleeding and/or embryo not intact. There were a large range of scores within each group and not all embryos exhibited the same pathology scores (Figure 3.1F). Nevertheless, by this measure, embryos from mutant UDL-01 E26K infected eggs had significantly higher gross pathology scores compared to the mock infected group, while those from UDL-01 WT, WF10 WT and mutant WF10 K26E infected eggs were not significantly different. However, several of the UDL-01 infected embryos did display enhanced gross pathology scores compared to mock, although the range of disease presentations meant this was not significant. ImageJ analysis software was also used to estimate the length of the embryos, as a potential measure of the effects of infection on embryo growth. However, there were no significant differences in the average size of embryos compared to uninfected specimens for any of the infected groups (Figure 3.1G). Despite no significant difference being seen in gross pathology score of the embryos comparing WT UDL-01 and mutant UDL-01 E26K viruses, a significant reduction in viral titre in the allantoic fluid of eggs infected with this viral pair was seen (Figure 3.1H); this could suggest a reduced level of mutant UDL-01 E26K virus was required to cause a similar level of gross pathology as seen with WT UDL-01 virus.

3.2.1.2: Infectious dose differentials between the viruses

As no difference in gross pathology was seen between the UDL-01 and WF10 virus pairs *in ovo*, further investigation into the egg infectious dose (EID) required to cause infection in embryos was conducted. James et al. (2016) previously used EID comparisons to facilitate in characterisation of AIVs. To calculate the infectious dose required to lead to productive infection *in ovo,* 10-fold serial dilutions of each virus (10,000 pfu to 0.001 pfu) was made and used to infect 5 eggs (10-day old SPF VALO breed) per virus per dilution. A mock infected group was also included in which the eggs were inoculated with sterile PBS. Embryos were candled twice daily throughout the study period to check for embryo viability (up to 84 h.p.i.). At either the end of the study period or once an end point had been met (see chapter 7 for details), embryos were chilled. Samples of allantoic fluid were taken and "in-cell westerns" assays were performed to determine infection via staining for viral NP protein. Briefly, monolayers of MDCK cells were infected with allantoic fluid and 12 h.p.i. cells were fixed via methanol/acetone and then stained using immunofluorescence for viral NP protein. None of the 'mock-infected' eggs gave a positive signal for viral NP protein (data not shown).

The Egg Infectious Dose 50 ($EID_{50;}$ defined as the dilution of virus in which 50% of the inoculated eggs show viable infection), of each virus was then calculated via the Reed-Muench method to determine any subtle differences in infection ability of the viruses (Table 3.1). Similar EID_{50} values were calculated for WT UDL-01, mutant UDL-01 E26K and WT WF10 viruses. However, the

Table 3.1: Summary of virus dose of wild type and mutant viruses required to cause infection in 10-day old fertilised hens' eggs.

Virus	EID_{50}
UDL-01 WT	0.024
UDL-01 E26K	0.01
WF10 WT	0.032
WF10 K26E	0.0015

Five 10-day old hens' eggs were infected with 10-fold serial dilutions (10,000 to 0.001 pfu) of the indicated H9N2 AIVs. Samples of allantoic fluid were taken and screened for presence of viral NP protein. The Egg Infectious Dose 50 (EID_{50}) was calculated via the Reed- Muench method and is defined as the dose where 50% of inoculated eggs were infected.

EID_{50} of mutant WF10 K26E was approximately one log_{10} lower at 0.0015. Thus introduction of a K26E change into PA of WF10 AIV lead to a reduced EID_{50} compared to WT WF10 virus and indicating that the mutant virus is more infectious.

3.2.1.3: Embryo survival rate following infection with wild type and mutant viruses.

As the K26E mutation lowered the EID_{50} value of WF10, further investigation into embryo survival after infection at different viral doses was conducted. James et al. (2016) previously used this technique to assess viral pathogenicity *in ovo*, with viruses lacking the accessory protein PB1-F2 showing a decreased pathogenicity compared to WT. Therefore, in order to assess the pathogenicity of the H9N2 AIVs used within this study *in ovo*, 10-fold serial dilutions of each virus (10,000 pfu to 0.001 pfu) were made and used to infect 5 eggs per virus per dilution as above. Mock infected eggs inoculated with sterile PBS were included in the experiment. Embryos were candled twice daily up to 84 h.p.i. to check for embryo viability, as judged by lack of movement of the embryo and/or disruption of blood vessels within the egg. Samples of allantoic fluid for each embryo were collected to determine if the embryo death was the result of productive viral infection and "in-cell western" assays were performed as described above. All mock-infected samples were negative (data not shown). Any eggs which did not produce virus positive allantoic fluid were removed from the survival analysis: this included the 0.001 pfu group from all viruses (WT UDL-01, mutant UDL-01 E26K, WT WF10 and mutant WF10 K26E) and the 0.01 pfu group

from the WT UDL-01 virus group. None of the viruses caused any embryo death before 48 h.p.i.

An estimation of the Lethal Dose 50 (LD_{50}) was determined from survival curves of each virus although accurate LD_{50} values could not be calculated due to 100% mortality not being reached in the majority of groups. The LD_{50} estimation for UDL-01 WT virus was somewhere between 1000 and 0.1 pfu. This LD_{50} range was large as there was resurgence in mortality at lower doses. The estimated LD_{50} for UDL-01 E26K virus was between 10 and 1pfu, so fits in the middle of the UDL-01 WT range. Therefore, no firm conclusions can be drawn over the effect of E26K within the UDL-01 background using this measure. Within the WF10 pair; no death observed at the lowest dilution (0.01 pfu) within any of the infected embryos. A higher number of total embryos across the whole dilution range died throughout the study period with the mutant WF10 K26E infected embryos (52.5% of total compared to 27.5% with WF10 WT). From the survival curves (data not shown), it was observed that within WT WF10 the most mortality was seen throughout the time course with the 10,000 pfu and 1000 pfu dilutions, with little mortality seen with the other doses. However, within the mutant WF10 K26E virus a more general mortality is seen across viral dilutions throughout the time course with all viral doses leading to similar levels of mortality. Estimated LD_{50} values suggest that WF10 WT virus needs an increased viral dose compared to WF10 K26E virus to lead to 50% embryo death; with LD_{50} values of 1000-100 pfu and 0.1-0.01 pfu respectively.

Table 3.2: Summary of embryo mortality data 84 hours post infection with different H9N2 AIV.

	10000	1000	100
UDL-01 WT	80%	60%	20%
UDL-01 E26K	100%	100%	100%
WF10 WT	70%	60%	30%
WF10 K26E	60%	60%	60%

In each group 5 eggs per virus per dilution were infected and candled every 12 hours for up to 84 hours post-infection. Once an egg displayed any of the end points signs (such as lack of movement of the embryo or disruption of the blood vessels lining the shell), it was chilled and classified as dead. Allantoic fluid samples were tested for presence of viral NP in order to determine viral infection. Any eggs which did not display virus-positive allantoic fluid were removed from the study. The death rate for each dilution at 84 hours post-infection is displayed above.

Embryo mortality levels at 84 hours post infection were assessed for the highest viral dilutions at the lower dilutions more variability was seen and a lack of repeat data made this difficult to interpret (Table 3.2). Both of the WT virus strains appeared to have a dose-dependent effect on embryo mortality within 100,000 to 100 pfu, whereas within the 26 mutant viruses there was no effect on embryo mortality with the decreased infectious dose. Therefore using this measure no firm conclusions can be draw on the effect of the amino acid present at position 26 of PA on pathogenicity.

3.2.2 Effect of PA E26K change on viral fitness *in vivo*

Since the PA 26 mutation altered viral pathogenicity *in ovo* and the WT UDL-01 AIV is well characterised in recently published literature (James et al., 2016; Iqbal et al., 2013; Iqbal et al., 2013; Long et al., 2016) the WT UDL-01 and mutant UDL-01 E26K virus pair were taken forward into *in vivo* studies to investigate the effect of the E26K mutation within the chicken (G*allas gallas domesticus*), a natural host of AIVs. For this experiment, the Rhode Island Red (RIR) breed of chicken was used at three weeks of age. Groups of 20 birds housed in self-contained isolators were inoculated with 100µl of a 10^5 pfu/ml stock of each virus (WT UDL-01 or mutant UDL-01 E26K) or sterile PBS via the intranasal route. These birds are hereafter termed 'directly infected'. One day post-infection, 8 naïve 'contact' birds were introduced into the isolator alongside the directly infected birds to assess viral transmission. Before infection (day -1) and then throughout the experiment, birds were swabbed in the buccal and cloacal cavities from day 1 to day 8 as well as day 10 and day 14 post-infection to determine viral

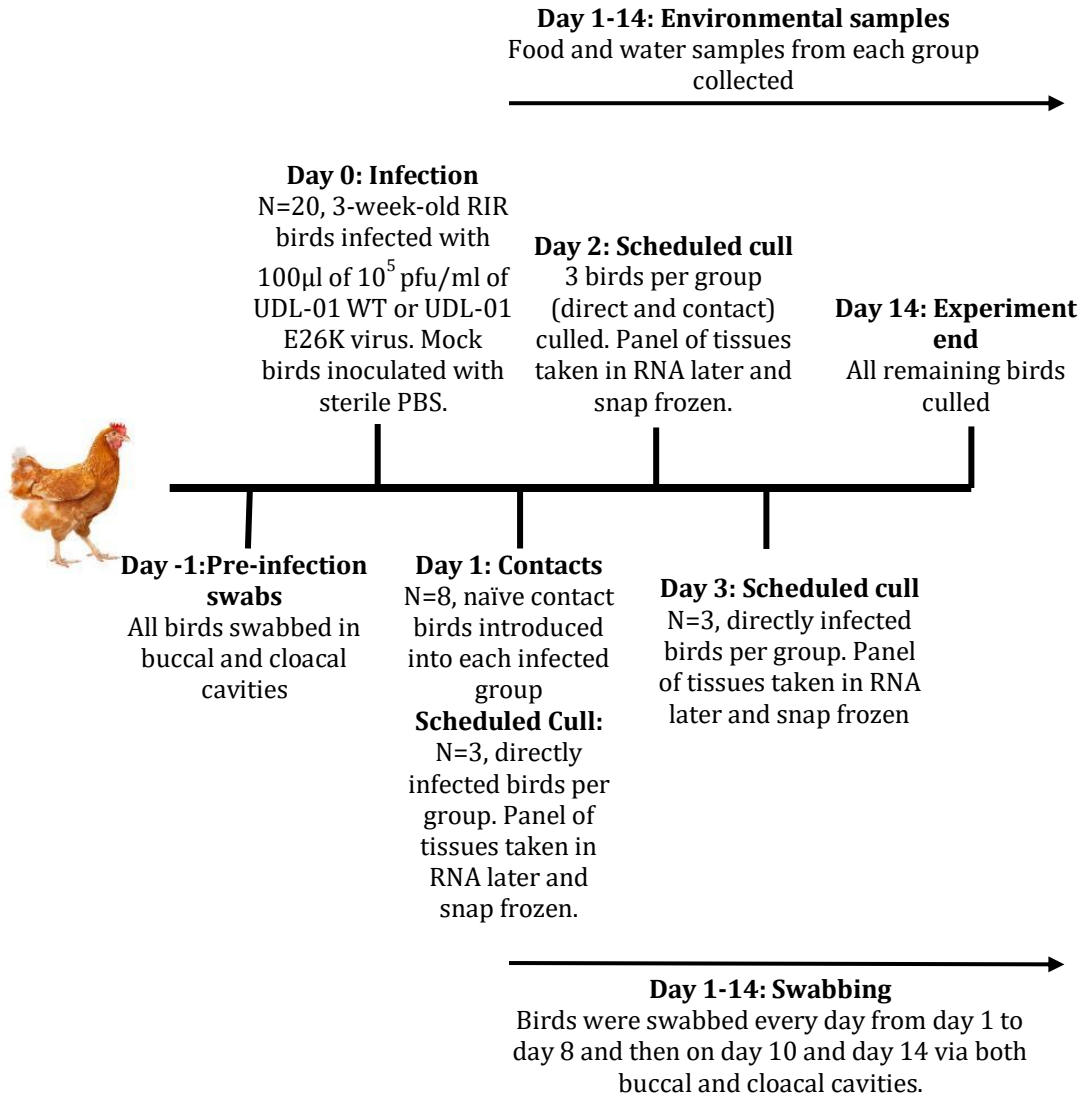

Figure 3.2: *In vivo* experimental design summary. 3-week-old RIR chicks were divided into two groups of 20 birds housed within 2 isolators and each bird was inoculated with 100µl of 10^5pfu/ml of WT UDL-01 or mutant UDL-01 E26K virus intranasally. A 3rd group was kept in a pen as mock infected group and was inoculated with sterile PBS. One day post infection, 8 naïve contact birds were introduced into each virus infected groups. Birds were swabbed daily between day 1 and 8 and then on day 10 and 14 via both the buccal and cloacal cavities. On Day 1 and 3 post-infection, 3 directly infected and mock infected birds were culled and post mortem tissues were collected. On Day 2 post-infection, 3 directly infected, contact and mock birds were culled and post-mortem tissues collected. Environmental (food and water) samples were collected throughout the study duration. Clinical signs were monitored throughout. Remaining birds were culled on day 14.

shedding (Figure 3.2). Additionally, environmental samples (taken from food and water) from each group were also collected on a daily basis throughout the experiment duration. On experimental day 2 (day 2 post-infection for directly infected and day 1 post-exposure for contact birds), 3 animals per group were culled and a panel of post-mortem tissues taken. On experimental days 1 and 3, three birds were culled from the directly infected and mock groups. Tissue sections were stored in both RNA later and snap frozen. The experiment was terminated on day 14 post initial inoculation, and all birds were humanely culled. Birds were observed twice daily by members of animal services and whilst procedures were carried out for the presence of clinical signs of infection. Mild clinical signs expected during the study included, ruffled feathers, pale comb/wattles, eye and nasal discharge, reddened eyes, snicking and depression. Additional moderate clinical signs that were expected included drooping wings, swollen heads and sporadic diarrhoea. If any signs of severe disease including laboured breathing, persistent diarrhoea, sitting alone and showing no signs to evade capture and, in the most extreme instances, paralysis and unconsciousness were observed birds were euthanised via a schedule one method.

3.2.2.1: Viral shedding analysis from infected and contact birds

To assess the ability of the H9N2 viruses, which only differ by a single amino acid within the PA gene (E26K), to replicate within the natural host, chickens infected (or mock infected) with WT UDL-01 or mutant UDL-01 E26K viruses were swabbed via both the buccal and cloacal cavities throughout a two week period. Viral titres were then determined via plaque assay. All mock

infected birds were below the limit of detection via plaque assay (2.5 pfu/ml) in both buccal and cloacal swabs (data not shown). All directly infected birds shed virus into the buccal cavity, peaking early in infection (day 1 or 2) and then declining over the next few days (Figure 3.3A). However, the UDL-01 E26K virus showed a significant reduction in the quantity of virus shed. Details of shedding on day one and two seen in Figures 3.3 B and C to show the variation in virus shed between birds. Virus was also cleared sooner when an E26K mutation was present(Figure 3.3D), by day five post infection the birds infected with UDL-01 E26K had ceased shedding whereas those infected with UDL-01 WT were mostly still shedding virus. When the area under the shedding curves (AUC) were calculated to assess the total virus shed throughout the study period, birds directly infected with WT UDL-01 virus showed a marked increased AUC compared to birds infected with the mutant UDL-01 E26K virus (215,517 versus 23,886). Therefore the mutant UDL-01 E26K virus showed a reduced total shedding throughout the study by RIR birds directly infected with virus.

The same trend was seen in contact birds introduced at day 1 post-infection (Figure 3.3E). A significant reduction in buccal shedding was seen in contact birds infected with mutant UDL-01 E26K from day 1 through to 4 post-exposure. Details of bird to bird varitations in shedding seen in Figures 3.3 F and G. However, the delayed clearance of the mutant virus was not seen in the contact bird group, with both groups of birds clearing virus by day 6 post-exposure and similar levels of virus being shed on day five post infection (Figure 3.3H). All contact birds became infected in both groups, showing that the introduction of an E26K change within UDL-01 did not drastically alter the transmissibility of the

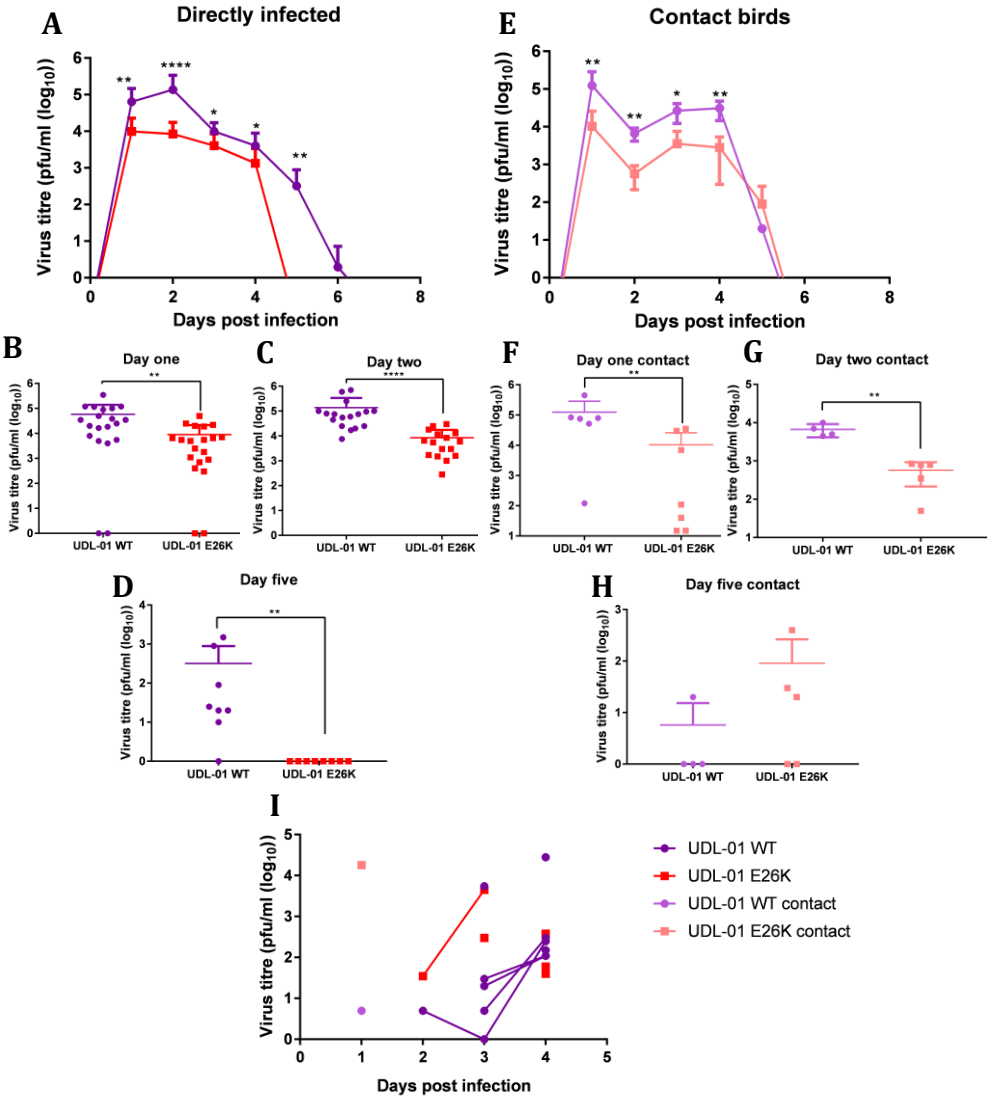

Figure 3.3: Buccal and cloacal shedding profiles of RIR birds infected with WT UDL-01 and mutant UDL-01 E26K H9N2 AIV. Groups of 20 chickens were infected with 100µl of 10^5pfu/ml stock of either WT UDL-01 or mutant UDL-01 E26K viruses (directly infected). One day post infection 8 naïve contact birds were introduced into each group (contacts). Birds were swabbed in the buccal and cloacal cavities throughout the study duration. Swabs were stored in viral transport media before being clarified and titrated via plaque assay. (A) average buccal shedding profile of directly infected birds (B,C and D) buccal shedding on separate days post infection for directly infected birds with each bird represented by a single point. (E) average buccal shedding profile of contact birds (F, G and H) buccal shedding on separate days post introduction for contact birds with each bird represented by a single point. (I) cloacal shedding detected throughout study duration. Unpaired T-test (Contact Days 2, 3, 4 and 5 (E, G, H)) or Mann-Whitney Test (all direct (A, B, C and D) + contact day 1 (F)) depending on distribution of data; P values = ****:<0.001, **: <0.0082, *:<0.033. Error bars represent +/- SD of all birds swabbed (at least 4 birds/group).

virus. When the AUC was calculated to assess the total virus shed throughout the study period, contact birds infected with WT UDL-01 virus again showed an increased AUC compared to birds infected with the mutant UDL-01 E26K virus (187,915 versus 17,367). Therefore the mutant UDL-01 E26K virus showed a reduced total shedding throughout the study by contact RIR birds infected with virus.

The profile of cloacal shedding from the birds was more sporadic (Figure 3.3I). This was expected as cloacal shedding by chickens has been reported to be more sporadic in a number of viral subtypes (H9, H7 and H5) and virus is not always shed via the cloacal route (James et al., 2016; Swayne and Beck, 2005; Van der Goot et al., 2003). In total 7 UDL-01 WT infected and 6 mutant UDL-01 E26K infected animals gave virus-positive cloacal swabs, including 1 from each of the contact groups. More birds shed virus on consecutive days within the WT UDL-01 infected group (4 birds compared to 1). However, it was difficult to draw firm conclusion as the numbers of birds shedding were too low for statistical analysis to be carried out. Overall, the shedding profiles of the infected birds suggested that WT UDL-01 viruses were more fit within the chicken host compared to mutant UDL-01 E26K virus. This supports the previously described data where mutant UDL-01 E26K virus had a reduced viral fitness *in vitro* (see chapter 2).

3.2.2.2: Stability of the E26K mutation during replication in infected chickens.

It is well established that during replication of viruses in infected animals, mutations can occur within the virus genome (Taubenberger and Kash, 2010).

Indeed, as reversion of the UDL-01 E26K mutation was seen when the mutant UDL-01 E26K virus was passaged in eggs (Table 2.2) it was important to determine if the outcome of the *in vivo* challenge experiment was potentially affected by reversion or adaptive mutations within the IAV genome, or if the E26K change remained fixed through the study. Initially, the plaque phenotypes of the viruses isolated from swab samples was examined, as this was previously identified to be a defining factor of E versus K at position 26 (Figure 2.4). If PA 26K had remained within the viral population the maintenance of a smaller plaque phenotype might be expected. Plaque titrations of the input viruses and swab samples were imaged and the diameter of 20 plaques per group measured using ImageJ analysis software, with the exception of the cloacal mutant UDL-01 E26K sample where only 6 plaques were measurable. As expected, the inoculum WT virus showed a large plaque phenotype while the E26K mutant produced small, hazy plaques (Figure 3.4A). The UDL-01 WT virus retained an obvious large plaque phenotype throughout the experiment. Conversely, the mutant UDL-01 E26K output virus appeared to have retained a small plaque phenotype in both directly infected and contact bird populations. However, when plaque diameters were measured (Figure 3.4B), both the viruses isolated from contact buccal and direct cloacal swabs showed a significantly larger plaque size than the mutant UDL-01 E26K input virus. Although the plaque size did not reach the same diameter as WT UDL-01, this was suggestive of mutations leading to increased viral fitness. Similarly, viruses recovered from cloacal swabs from birds that were directly inoculated with WT UDL-01 virus had a significantly larger plaque

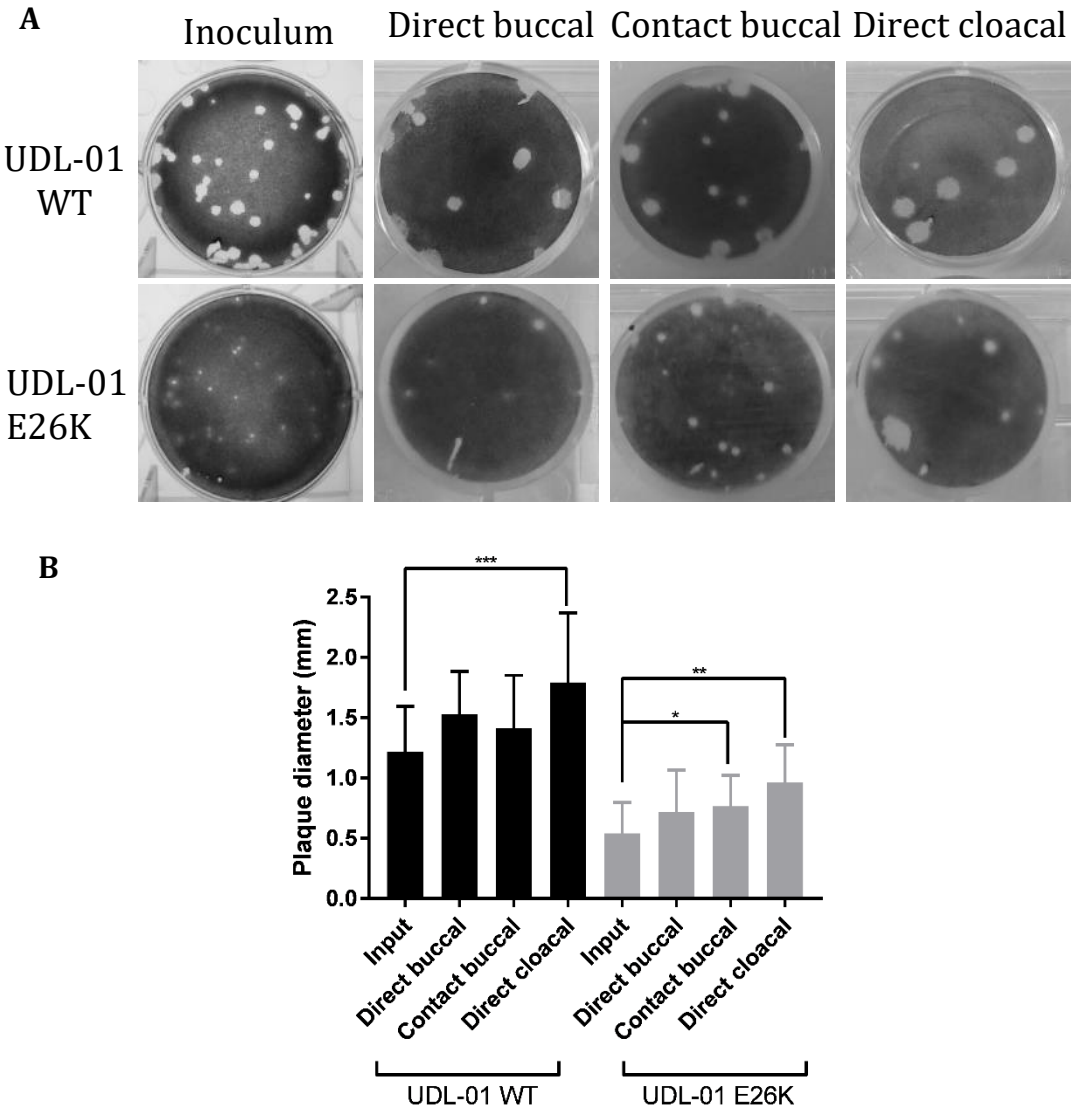

Figure 3.4: Plaque phenotypes of viruses recovered from chickens infected with WT UDL-01 or mutant UDL-01 E26K AIVs. RIR chickens were swabbed and virus plaque morphologies characterised via plaque assay under 0.6% agarose. After 72 hours cells were fixed and stained with 0.1% crystal violet solution. (A) Representative images of plaque phenotypes from viruses obtained from buccal swabs from directly inoculated and contact birds and cloacal swabs of directly inoculated birds. (B) The average diameter of 20 plaques per virus (with the exception of cloacal UDL-01 E26K where only 6 plaques were available) was measured using ImageJ analysis software. Graph represents the average +/- SD. Kruskal Wallis with Dunn's multiple comparisons, P values = *: <0.02, **: <0.0077, ***: 0.0005.

diameter compared to the inoculum virus again suggesting potential chicken-adaptive mutations within this group.

To determine if the increase in plaque diameter of the mutant UDL-01 E26K virus isolated from the infected chickens was the result of reversions at PA position 26, RNA was extracted from the swab supernatants and PCR completed to enable samples to be sent for Next Generation sequencing (NGS). The consensus sequences for each segment were analysed and time constraints of the project did not allow for additional sequence analysis of minor variants to be assessed. The input viruses all contained the desired PA mutations with WT displaying 26E and the mutant displaying 26K. Within the output virus samples, sequencing did not indicate any other compensatory mutations in the PA gene at the consensus level. All samples tested were identical to the input virus in the remainder of the viral gene segments including within the X-ORF of the accessory protein PA-X. Focussing on the codon present at amino acid 26, the WT UDL-01 samples tested from both buccal and cloacal swabs remained at 26E at consensus level. Within the mutant UDL-01 E26K samples, 26K remained in the consensus sequence within the viral population isolated from buccal swabs. However, within the cloacal swab sample tested the amino acid reverted to 26E. This could explain the increased plaque phenotype seen within the mutant UDL-01 E26K virus isolated from cloacal swabs (Figure 3.4). However, only a limited number of samples were sequenced and it is not known if other birds within the mutant UDL-01 E26K group were shedding virus which had PA 26E.

3.2.2.3: Persistence of virus within the environment

In order to assess the presence and persistence of virus within the environment of each isolator, samples of water and food were taken, as these communal areas are likely to be points of viral dissemination (James et al., 2016; Brown et al., 2007; Hinshaw et al., 1979). Samples (1 gram of food and 1 ml of water) were taken daily from each of the isolators and from the pen where mock infected birds were housed. Food samples were homogenised in 1 ml of serum-free DMEM, clarified and supernatants stored at -80°C. Water samples were clarified and stored at -80°C. Presence of virus in each sample was assessed using plaque assays. No detectable virus was found in any of the food or water samples from the mock pen or within any food samples from the infected groups (data not shown). However, virus was detected within the water samples taken from both the WT UDL-01 and mutant UDL-10 E26K infected isolators (Figure 3.5). Virus was detected up to day 7 post-infection, despite virus being cleared from birds (as assessed by detection of virus in buccal swabs) by this point (Figure 3.3). Virus was more commonly detected within water collected from the water feeder of WT UDL-01 infected birds, with positive water samples detected on days 1-3, 5 and 7 post-infection. However, within the mutant UDL-01 E26K infected isolator, virus was only detected on days 1 and 6 post-infection but the latter sample gave the highest recorded titre ($>10^4$ pfu/ml). These data were broadly consistent with the higher shedding rates of the WT UDL-01 virus potentially leading to higher levels of virus within the water systems. They also suggest that the viruses were stable in the environment for at least 24 hours after shedding.

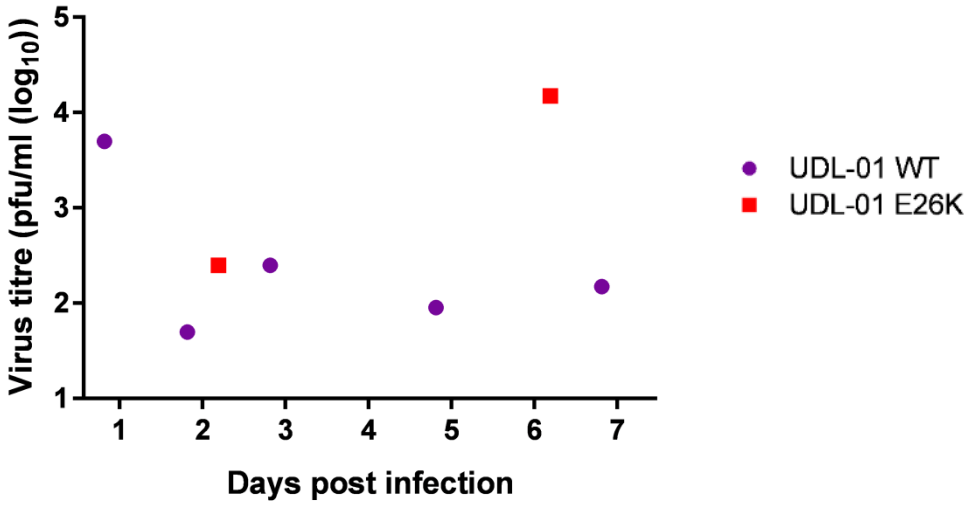

Figure 3.5: Environmental water contamination within isolators. Water samples were collected throughout the study duration and virus load determined. UDL-01 WT: purple, UDL-01 E26K: red.

3.2.2.4: Virus pathogenicity

To study the impact of the E26K mutation on viral pathogenicity, birds were monitored for clinical signs throughout the study duration and anything of note was recorded. These included diarrhoea, respiratory clinical signs (such as snicking), red eyes and swollen wattles and combs. Clinical end points were also in place to ensure that birds were not unduly suffering from the infection, including clinical signs such as difficult breathing and a lack of movement (more details in chapter 7). Any birds which reached these latter criteria were euthanised promptly via a schedule one method and then subjected to post-mortem to determine a potential cause of death.

Clinical signs throughout the study duration were mild for the most part. With the majority of birds only showing signs of mild diarrhoea with depression as expected from previous reports of H9N2 infection (Sun et al., 2010). Throughout the study duration (from days 3 to 6), 33% of birds (30% directly infected and 37.5% of contact birds) within the WT UDL-01 infected group died (either spontaneously or due to reaching end points and being culled) despite UDL-01 being classified as a LPAIV (Figure 3.6), and the survival curve profiles were significantly different from each other. This supports data showing that H9N2 AIVs have become more pathogenic in recent years (Guo et al., 2000; Iqbal et al., 2013; Zhong et al., 2014). The onset of the severe clinical signs was rapid and few observations were made prior to the point of euthanasia, the details of which can be seen in Table 3.3. Birds were either found dead (4/9) or had to be euthanised (5/9) due to severe clinical signs such as difficulty breathing. These

birds were observed to have a lack of control of their movement suggestive of a neurological impact of viral infection. When the single amino acid E26K change within the PA gene to make the UDL-01 virus WF10-like at this position, pathogenicity of the virus was clearly attenuated and all birds survived challenge (Figure 3.6).

During post-mortem examination, several birds which had been recorded before death as having difficulty breathing showed a thickening of the tracheal lining (Figure 3.7A, B). This has previously been seen in H9N2-infected birds the field in outbreaks in Pakistan (Zhang et al., 2014b; Li et al., 2005; personal communication M. Iqbal), although it was previously thought to be linked with secondary bacterial infections. Here, the presence of any potential secondary infection was not investigated and the composition of the tracheal thickening was not examined further. However, within HPAI infection, thickening of the tracheal mucosa has previously been identified to be the result of increased cellular proliferation of the epithelium (Acland et al., 1984). Several birds also had empty crops and digestive tracts, suggesting they had not been eating for a period prior to their deaths (Figure 3.7C, D). No other significant post-mortem changes were observed to elucidate the cause of death. The shedding profiles of those birds which died were not noticeably different from those which survived infection (data not shown). Tissue samples were taken for further processing to determine any differences in viral tissue dissemination between survivors and those which died.

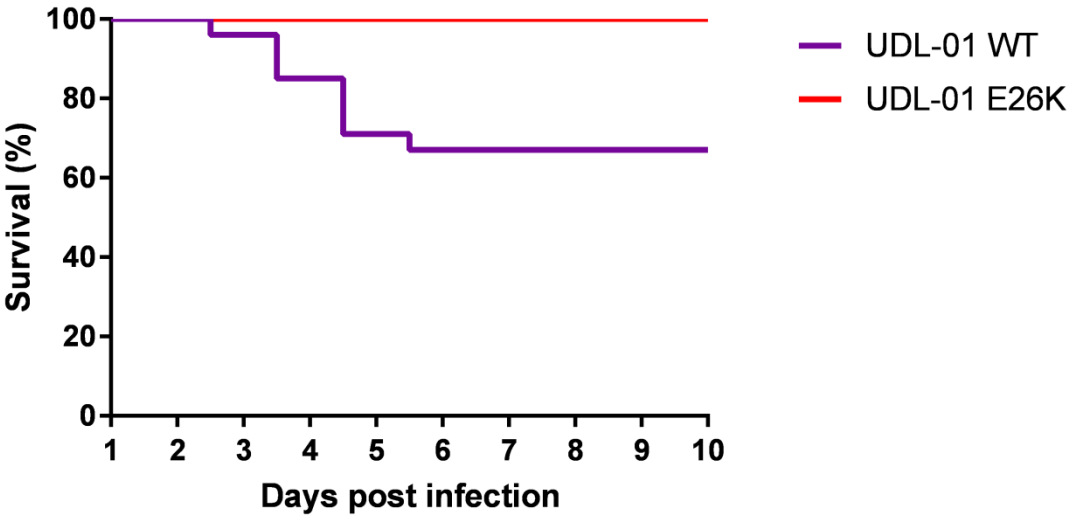

Figure 3.6 Percentage survival within H9N2 infected birds. Directly infected and contact birds infected with WT UDL-01 (purple line) and mutant UDL-01 E26K (red line) were monitored for clinical disease signs throughout the study duration. Several birds were either found dead or reached the humane end points and were culled due to ethical reasons (N=9). This graph shows the percentage mortality rate across the study duration. Survival curves significantly different P value = <0.0001 (Log rank (Mantel-Cox) test).

Table 3.3: Summary of cause of death and post-mortem observations.

Wing band	Day post-infection	End-point trigger	Group	PM observations
130	3	Found dead	UDL-01 WT direct	None
116	4	Found dead	UDL-01 WT direct	Crop and digestive track empty
112	4	Lack of control of movement	UDL-01 WT direct	None
120	4	Lack of control of movement	UDL-01 WT direct	Crop and digestive track empty
121	5	Difficulty breathing	UDL-01 WT direct	Trachea thickened
125	6	Found dead	UDL-01 WT direct	Trachea thickened
136	6	Found dead	UDL-01 WT contact	Trachea thickened
132	6	Lack of control of movement	UDL-01 WT contact	None
135	6	Difficulty breathing	UDL-01 WT contact	Crop and digestive track empty

Those WT UDL-01 infected birds which were culled due to reaching humane end points or found dead were examined via post-mortem. Prior observations are outlined plus any additional post-mortem observations.

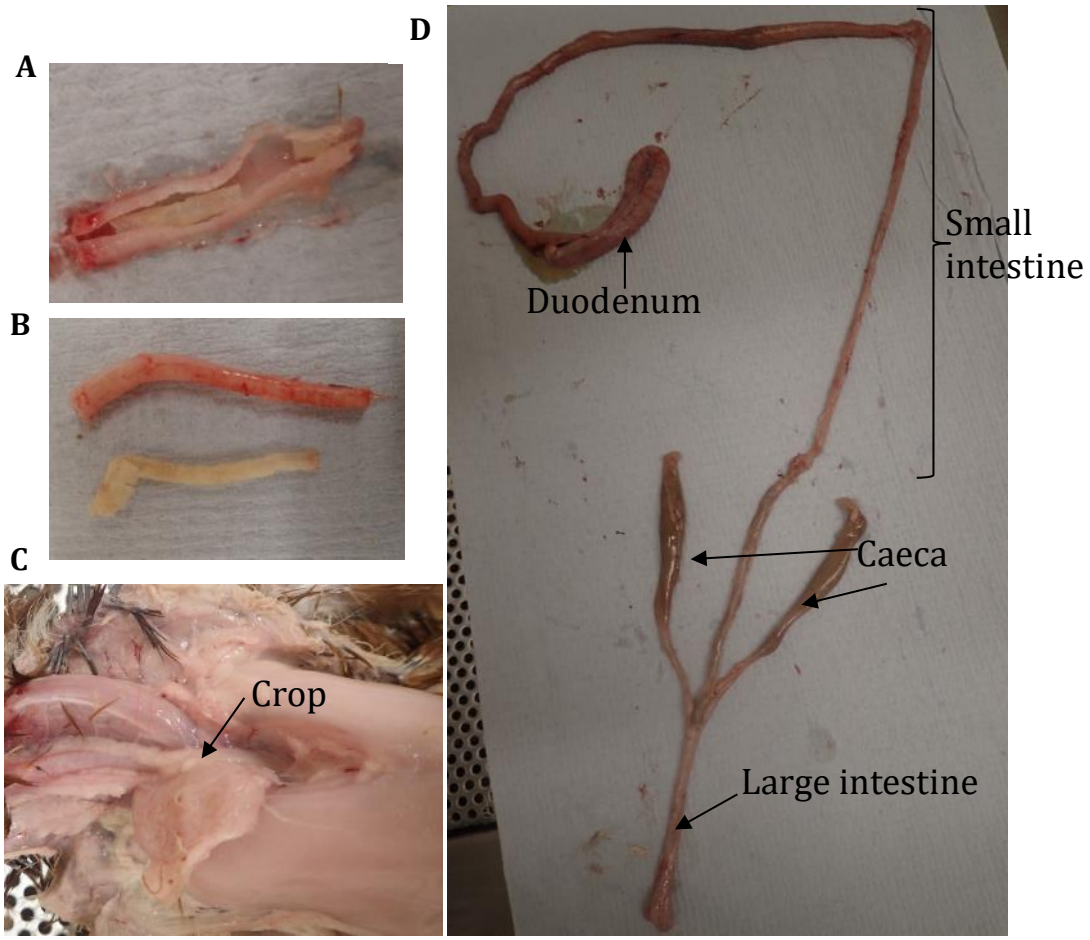

Figure 3.7: Post mortem observations. Birds which were found dead or euthanised due to reaching experimental end points (difficulty breathing, loss of control of movement) were examined via post mortem. (A) and (B) show representative images of the thickened trachea lining observed within 3 birds either *in situ* (A) or removed (B) (C) shows a representative image of a bird with an empty crop (D) shows a representative image of a largely empty digestive tract.

3.2.2.5: Viral dissemination in tissue and organs of directly inoculated birds

A panel of tissues were taken during scheduled post-mortem examination on experimental days 1 and 3 from the directly and mock infected birds and stored either in RNA later or snap frozen. This allowed for viral dissemination throughout the visceral organs to be investigated and to determine whether the more severe clinical signs and post-mortem presentations seen in the WT UDL-01 group was the result of enhanced viral dissemination within the birds.

3.2.2.5.1: Estimation of viral M gene RNA levels in the tissues from wild type and mutant virus infected birds

RNA extracted from tissue samples was used for qRT-PCR reactions to detect the viral M gene vRNA as a marker for presence of virus within tissues. This was performed alongside an M gene RNA standard which allowed for the segment copy numbers to be calculated. James et al. (2016), showed a good correlation between M gene and live virus isolation between influenza infected tissues from chickens, showing this is a robust method to measure viral presence within tissues. All the mock samples fell below the limit of detection, further confirming no infection within this group (data not shown). In directly infected animals, M gene copy number was highest in the nasal and tracheal tissues but was also readily detectable within the lung, colon, kidney, and spleen and intermittently detected in the liver (at least within UDL-01 WT infected birds). Overall, amounts were variable between days but levels were highest on day 3 post infection. Within these animals, WT UDL-01 virus was present at increased levels in a number of tissues compared to birds infected with the mutant UDL-01

E26K virus, particularly on days 1 and 3. On day 1 (Figure 3.8A) there was significantly higher copy number of segment 7 RNA (with increases of 10-to 30-fold copies being seen) within the lung, kidney, spleen and liver of the WT UDL-01 infected birds compared to mutant UDL-01 E26K infected birds. On day 3 (Figure 3.8B), UDL-01 E26K mutant virus had mainly been cleared from the visceral organs, with levels of viral RNA mostly below the limit of detection except in the nasal tissue where levels remained high (10^4 to 10^5 copies of viral M gene). The mutant UDL-01 E26K virus appeared to be being cleared from trachea whist the WT UDL-01 WT was still present at this point (10^{1-3} versus 10^5 copies of M gene). The lung, colon and kidneys also showed significantly higher levels of WT UDL-01 RNA compared to the mutant UDL-01 E26K. This suggested that while the mutant UDL-01 E26K virus was able replicate efficiently in the upper respiratory tract, it was less able to disseminate through the bird and was more rapidly cleared.

3.2.2.5.2: Detection of virus in the tissues from wild type and mutant virus infected birds

In order to determine whether the isolation of viral RNA from tissues corresponded to 'live' virus, tissues snap frozen at the time of post-mortem were processed from the birds on day 2, as this time point allowed a comparison between directly infected and contact birds. 30mg of each tissue section was homogenised in serum free DMEM, clarified and the supernatants titrated by

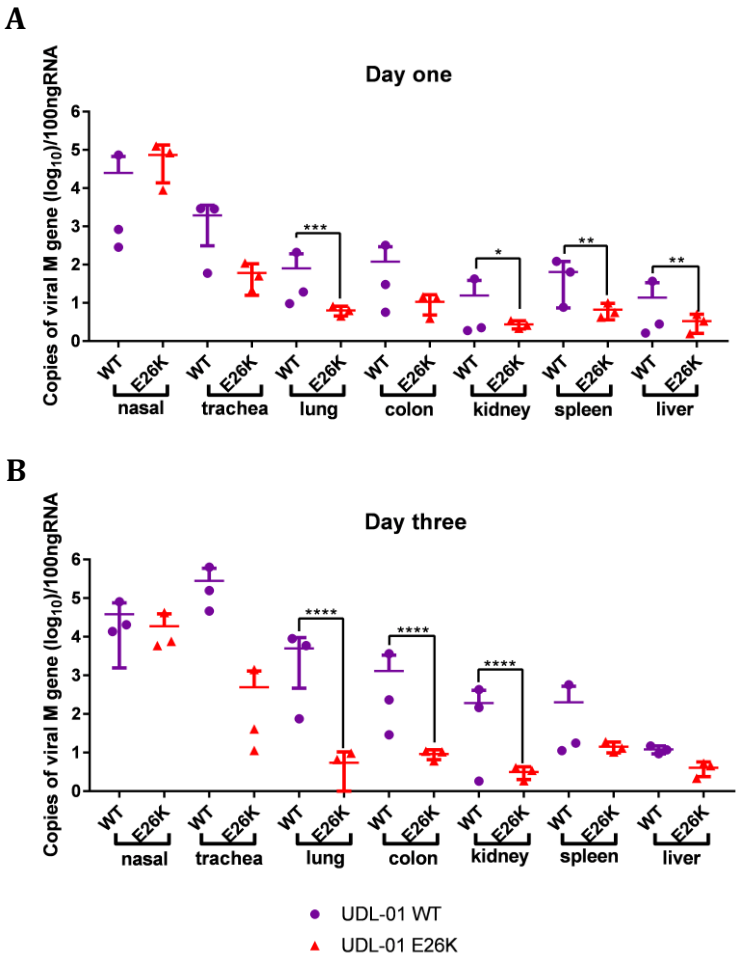

Figure 3.8: Detection of viral M gene within tissues of infected birds. On days 1 and 3 post infection 3 birds per group were culled and a panel of tissues taken and stored in RNA later. Total RNA was extracted from homogenised tissue samples and qRT-PCR for viral M gene carried out. CT values were compared to a M gene standard curve in order to determine copies of viral M gene from directly infected birds on day one post infection (A), and day 3 post infection (B). UDL-01 WT infected tissues shown in purple, UDL-01 E26K infected tissues shown in red. Each data point represents the copies of M gene from a single bird. Error bars represent average +/- SD. Unpaired T-test (Day 1- Trachea, Kidney, Spleen and Liver, Day 3- Nasal, Trachea, Colon, Kidney, Spleen) or Mann Whitney Tests (Day 1- Lung and Colon, Day 3- Lung and Liver) between UDL-01 WT and UDL-01 E26K infected birds; P values = *: <0.0147, **: <0.0057, ***: <0.0005, ****: <00001.

plaque assay. No virus was detected from any tissues collected from mock infected birds or from lung, colon, kidney, spleen and liver of infected animals (data not shown). This was in agreement with the qRT-PCR results which detected RNA at levels only marginally above the limit of detection at day 2 (data not shown). Potentially, the vRNA detected in these tissues was either derived from contamination, RNA levels were low and lost viability during storage and processing or the detected RNA was not the result of productive infection in these tissues. However, viable virus was isolated from nasal tissue (Figure 3.9A) and trachea (Figure 3.9B), albeit not from all birds in each group. Titres were higher from WT UDL-01 birds compared to the mutant UDL-01 E26K virus infected birds. Contact-infected birds in each group had relatively low levels of virus present (100-fold reductions in viral titre) in nasal and tracheal tissues compared to the directly infected birds, although this was perhaps expected as they had only been introduced to the isolator 1 day prior to culling. These data showed that WT UDL-01 virus was better able to replicate within the nasal tissue and trachea compared to the mutant UDL-01 E26K virus again supporting the buccal shedding data where lower amounts were seen with the mutant UDL-01 E26K virus.

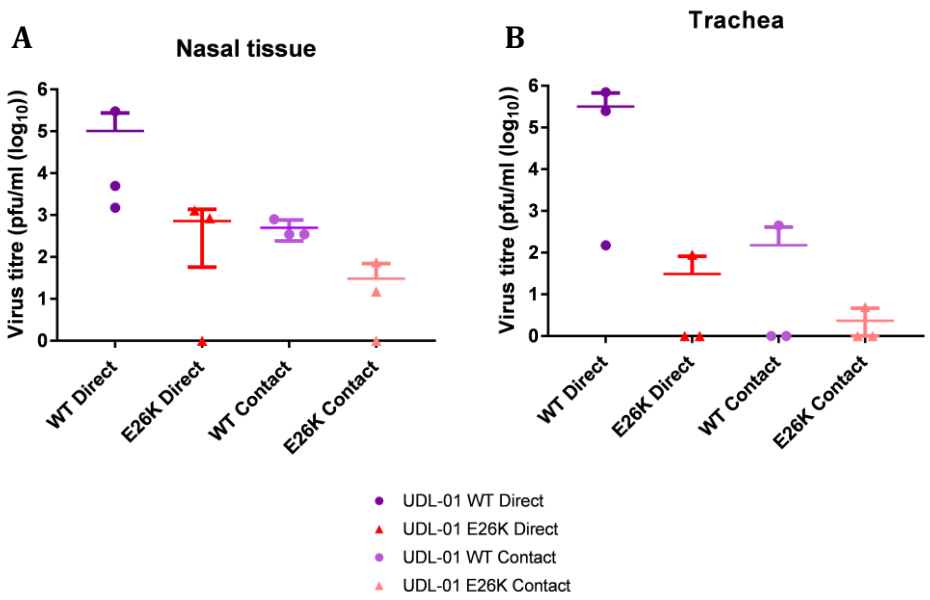

Figure 3.9: Virus titres from tissues collected from infected birds. Snap frozen tissue samples were homogenised with serum free DMEM. Supernatants were clarified and titrated via plaque assay. (A) Viral isolation from nasal tissue (B) Viral isolation from tracheal tissue. Data points represent titres from individual birds along with bars indicating the mean +/- SD. Mann-Whitney test, no significant differences. UDL-01 WT from directly infected: dark purple, UDL-01 WT from contact birds: light purple, UDL-01 E26K from directly infected: red, UDL-01 E26K from contact birds: pink.

3.2.2.5.3: Viral dissemination in birds culled due to reaching a humane end point

In order to ascertain if the birds that died during the experiment had increased levels of viral dissemination or viral presence within tissues which could have contributed to their mortality, qRT-PCR for viral M segment copy number was completed as described above. RNA was extracted from stored tissues including nasal tissue, trachea, lung, colon, liver and spleen and M gene CT values compared to an M segment standard curve in order to calculate copy number. Tissues from those birds' outlined in Table 3.3 were included in this experiment. One of the limitations of this study was that the birds taken for the scheduled culls were not taken on the same days as those which died or had to be euthanised. Therefore, for the purposes of comparison, these data were plotted against the corresponding data from day 3 already shown in Figure 3.8 where overall viral loads were at their highest. However, the levels of vRNA detected did not differ substantially from the levels found in birds from scheduled culls, with highest levels in nasal and tracheal tissues and lowest levels in liver and spleen (Figure 3.10). Generally those birds which were culled or died as a result of infection did not have differing vRNA levels within tissue compared to the WT infected birds scheduled for cull on day 3 of the experiment. However, as some of these birds were removed from the study up to day 6 of the experiment comparisons cannot be made on infection levels in the healthier birds at this point. In general those birds, culled at later time points (points coloured red, Figure 3.10), had lower levels of virus than those birds culled earlier on in the study.

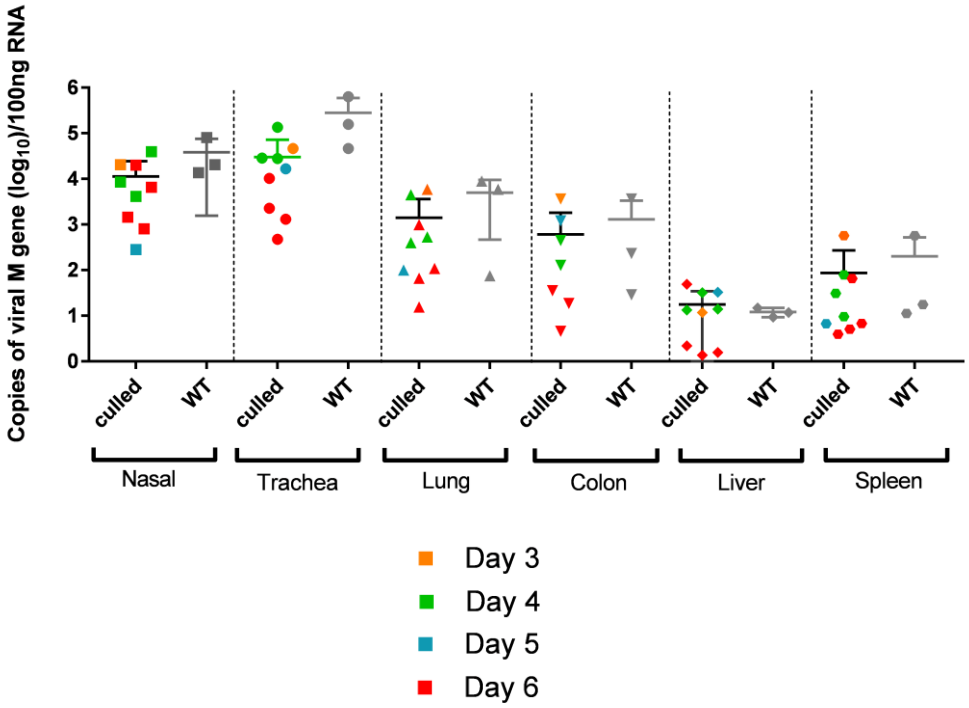

Figure 3.10: Viral RNA present in tissues from birds which reached experimental humane end points. Tissues were collected from birds which reached experimental end points or were found dead during the study duration via post-mortem examination. All birds from the UDL-01 WT group. RNA was extracted from tissues and qRT-PCR for viral M gene was conducted. The copy number of M gene was calculated via comparison of CT values to an M gene standard curve. Data plotted in comparison to previously described data from scheduled cull birds infected with UDL-01 WT virus at day 3 (Figure 3.9). Each data point represents the M gene levels in an individual animal and error bars show average +/- SD. Orange data points represent those birds culled on day 3, green those culled on day 4, blue those culled on day 5 and red those culled on day 6.

3.2.2.6: Cytokine expression in infected tissues

Next the immune responses of the chickens infected with the different viruses was assessed as mutations within the PA gene have previously been shown to affect host innate immune response. For example, Hu et al. (2013a) showed that a K237E change within PA enhanced the immune response against H5N1 AIVs in ducks. Nasal tissue from chickens culled at day 2 (as well as from 3 mock infected birds) was chosen for analysis, as all birds had high levels of vRNA and all bar one were positive for live virus at this time point. This also allowed for a transcriptomic comparison of the immune responses between the directly infected and contact birds with respect to the baseline values from uninfected animals. RNA was extracted from homogenised tissues and used to complete qRT-PCR to quantify host transcripts for a range of chicken cytokines and interferon response genes. Three reference host genes (RPLPO-1, RPL13 and 28S rRNA) were selected for normalisation and the most stable gene across the samples chosen for normalisation.

Nasal tissue of directly infected birds showed little differences in the cytokine transcript levels between UDL-01 WT and UDL-01 E26K infected birds (Figure 3.11A), this included IFN-α, IFN-β, IFN-γ, IL-18 and TGF-β4. Several cytokines had marginally increased levels in the UDL-01 WT infected birds including IFN-γ, IL-4, IL-18 and Mx although these levels did not reach significance. The only cytokine that had significantly different levels, between the WT UDL-01 and mutant UDL-01 E26K infected birds was Interleukin-6 (IL-6), a proinflammatory cytokine which promotes B cell maturation and T cell

differentiation (reviewed by Heinrich et al., 2003), with the UDL-01 WT infected birds showing higher levels of cytokine expression.

Within the nasal tissues of contact birds culled 24 hours post-exposure to the infected group (Figure 3.11B), there was again few differences in cytokine transcript levels between the infected groups. Again several cytokines showed marginally increased expression in UDL-01 WT infected birds with increases seen in IL-4 and Mx levels compared to UDL-01 E26K infected birds. As with the directly infected birds, IL-6 levels were significantly different between the UDL-01 WT and UDL-01 E26K infected birds, with the former showing increased levels.

Overall, these data showed that the both virus infections induced an immune response within the nasal tissues of the birds, with UDL-01 WT infected birds showing a marginally enhanced response compared to UDL-01 E26K infected birds. The UDL-01 WT virus induced a strong proinflammatory response with increased IL-6 induction in both directly infected and contact birds. Time and resource constraints have restricted the cytokine profiles to the nasal tissue. However, for future work, it may be beneficial map the cytokine profiles of all tissues that at least show variability of vRNA levels between the wild type and mutant viruses.

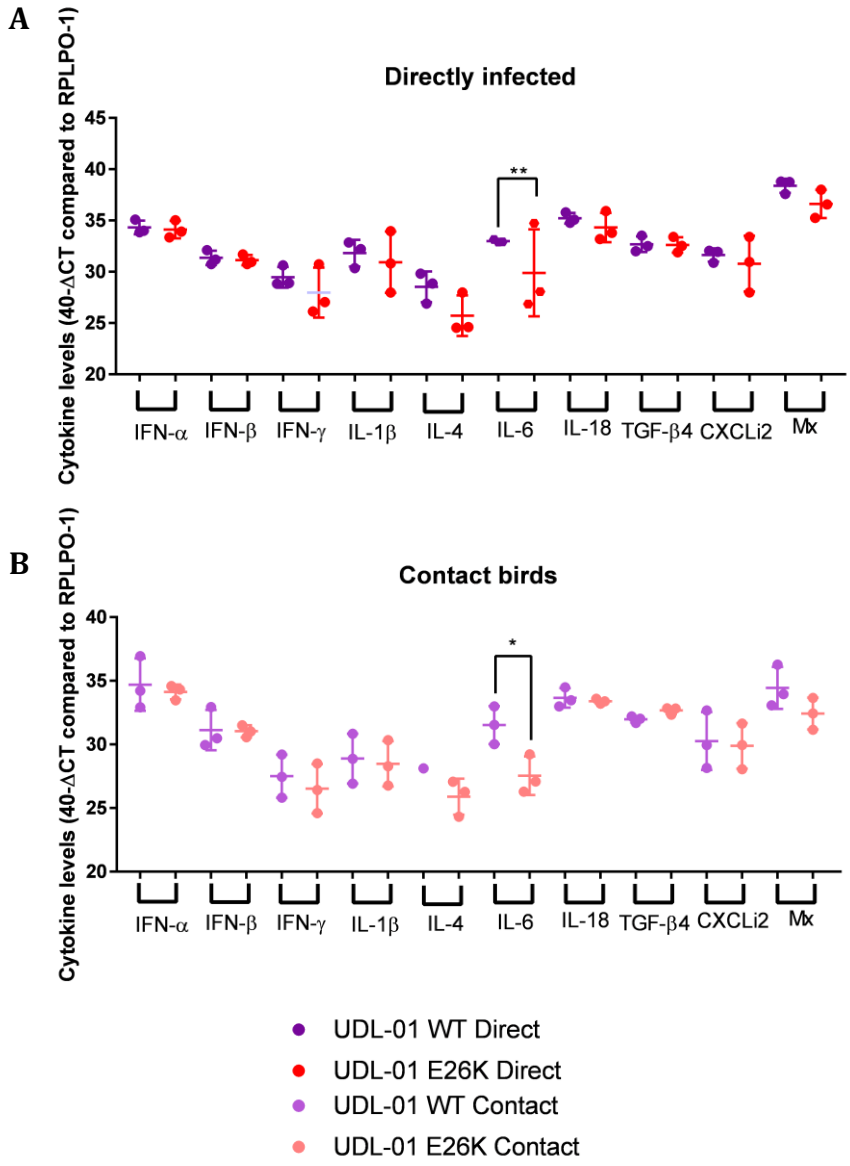

Figure 3.11: Cytokine expression compared to reference gene. RNA was extracted from nasal tissue of WT UDL-01 and mutant UDL-01 E26K infected chickens. qRT-PCR was performed for a panel of cytokines and levels compared to RPLPO-1 reference gene were calculated. Cytokine expression for each bird is represented in a single dot, with error bars displaying mean +/- SD of nasal tissue from n=3 chickens. Unpaired T-test (IFN-α, IFN-β, IFN-γ, IL-1β, IL-6, IL-18, CXCLi2, Mx and direct TGF-β4) or Mann-Whitney Test (IL-4 and contact TGF-β4) P values = **= 000021, *= 0.0316.

3.3: Discussion

In this chapter, the effect of the PA E26K mutation *in vivo* was investigated. Initially infectivity, replication and virulence of WT UDL-01, mutant UDL-01 E26K, WT WF10 and mutant WF10 K26E viruses was assessed *in ovo*, using fertilised hens' eggs as a model for studying viral pathogenicity. Within *in ovo* studies, embryos infected with either WT UDL-01 or mutant UDL-01 E26K viruses had higher gross pathology scores when compared to mock and the WT WF10 and mutant WF10 K26E virus pair. Introduction of an amino acid change at position 26 in the PA gene did not significantly alter the gross pathology score compared to WT UDL-01 virus (Figures 3.1). However, a reduced viral output was observed in the mutant UDL-01 E26K compared to WT UDL-01 infected eggs and the reciprocal alteration to viral output was seen within the WT WF10 and mutant pair (Figure 3.1H). This could suggest that a reduced quantity of virus is required to lead to the same gross pathology. The reasons behind this were not determined during this study period although one such factor could be an increased immune response caused by the UDL-01 E26K virus which could lead to increased infiltration of immune cells and enhanced gross pathology. Samples could have been taken from the embryo and qRT-PCR used to assess the cytokine levels, histopathology could have also been adopted to determine the infiltration of immune cells into the embryo to determine their contribution to gross pathology. However, reduced viral replication usually correlates with a reduced viral pathology (Xu et al., 2017; Xu et al., 2016 and Hu et al., 2013). Although enhanced immune responses have been shown to increase pathology in numerous cases (Baskin et al., 2009, Kobasa et al., 2007). Overall, the *in ovo*

method used here was not sensitive enough to determine any pathological differences between the viruses studied, although perhaps repeat experiments would enhance the sensitivity of the data collected or inclusion of addition measures such as histopathology would enhance the ability to draw conclusions from this section.

Introduction of E26K into UDL-01 PA gene did not affect the EID_{50} within eggs of the white leghorn breed (VALO). However, in the WF10 background, introduction of PA K26E reduced the EID_{50} compared to WT (Table 3.1), showing a lower viral titre was needed to cause productive infection in 10-day-old embryos. This could suggest an increased viral fitness of the WF10 K26E virus supporting *in vitro* data described in Chapter 2. Again the LD_{50} values could not further elucidate any pathogenicity differences between the virus pairs, with broad ranges of estimated LD_{50}'s observed. However, the UDL-01 E26K virus showed a lack of dose response in mortality across the three highest dilutions (Table 3.2), showing 100% mortality, higher than UDL-01 WT at these points. This high mortality could have been due to human error with artificially high levels of mortality seen with artificially high amounts of virus put into eggs based on problems with dilution, repeat experiments would enable this to be determined. Another factor that could account for the enhanced mortality of UDL-01 E26K virus at high dilutions is the transfer of contaminant RNAs, IFNs or egg artefacts, which may be increased in this stock if the virus has a reduced stability. This effect would be reduced at lower dilutions as the effect of the artefacts is diluted, however the data from the lower dilutions was inconclusive due to large variations in mortality between doses. Despite this, one of note trend seen was

that viruses which contained 26E (UDL-01 WT and WF10 K26E) appeared to have an increased mortality at lower doses than those viruses which contained 26K (WF10 WT and UDl-01 E26K). This is in contrast to the data at the higher doses and could be due to the lack of artefacts transferred at lower doses. Repeat experiments would allow for this to be confirmed.

The impact of the amino acid change at position 26 on virus fitness and pathogenesis in chickens was then investigated. In these studies, the buccal shedding of chickens infected with mutant UDL-01 E26K virus was significantly reduced throughout the shedding period compared to the WT UDL-01 infected birds (Figure 3.3). This supports data seen *in vitro* (Chapter 2), where UDL-01 E26K virus produced a smaller plaque phenotype and reduced viral replication. This suggest that the UDL-01 E26K virus has a reduced fitness *in vivo* and this position of the PA gene is important for viral replication in the chicken host, supporting the lack of PA 26K seen within bioinformatics analysis of ~27,700 sequences (Chapter 2). The UDL-01 E26K virus was also cleared from shedding faster than the UDL-01 WT virus but only within the directly infected birds. Although the contact bird population showed a reduced overall shedding throughout the study period, by day 5 the enhanced clearance of the UDL-01 E26K virus was no longer present. It is possible that those birds still infected on day 5 in the UDL-01 E26K group contained viruses which had mutations present allowing them to persist for longer periods. In fact, some reversion to 26E was seen within sequence analysis of the cloacal swab sample tested. Some reversion to 26E would be expected as this was also observed within passaging of the viruses in eggs (Chapter 2). Unfortunately, samples that were sequenced were

from Day 2 post infection so it is possible that by Day 5 an increased level of reversion would be seen.

UDL-01 WT virus appears to have an increased fitness within the chicken model of infection used within these studies, particularly in terms of virus shedding. This also correlated with the enhanced environmental deposition of UDL-01 WT compared to UDL-01 E26K (Figure 3.5). The increased environmental presence of WT UDL-01 virus could suggest that the virus is more stable in this environment and give it an advantage in transmission events (although no evidence of this was observed within this study). Further studies may evaluate a scenario in which an additional naive contact group could be included at a later period post-infection to assess if the differences seen within water samples could alter virus transmission dynamics at later time. It would also be beneficial to test the stability of each of the viruses in water systems within more controlled studies *in vitro* in order to ascertain if the mechanism of action of the 26 mutation is to contribute to the stability of the virus.

The reduction in viral replication within the buccal cavities of the UDL-01 E26K infected birds probably contributed to a reduction in severe disease and mortality (Figure 3.6). No deaths were observed in mutant virus infected birds, in contrast to a 33% mortality rate with UDL-01 WT infected animals. This increased mortality corresponded with enhanced clinical signs within the UDL-01 WT (26E) infected birds and enhanced gross pathology, such as thickened tracheal linings (Table 3.3 and Figure 3.7). The enhanced mortality rate could have potentially been due to an increased viral dissemination of WT UDL-01

compared to mutant UDL-01 E26K, where at day 3 post-infection, vRNA could be isolated not only from the respiratory tract but also from the colon, kidney and spleen tissues. Due to space constraints within the isolators, it was not possible to increase the group size and cull birds at different time points as the viral infection progresses and then regresses, so post-mortem samples were not collected beyond day 3 post-infection. In future studies, it would be interesting to analyse the tissue samples at later stages of infection, to determine if viral persistence within the host visceral organs contributes to the enhanced pathogenesis of WT UDL-01 virus compared to the mutant UDL-01 E26K AIVs. The enhanced mortality of the WT UDL-01 virus was not due to mutations within the viral genome, at least at consensus level. All of the samples sequenced showed no consensus level changes to any IAV genome segments and the inoculums confirmed isogenic mutants, only differing in the single mutation introduced within PA. This suggests that the difference in pathogenicity is either due to the E26K change within the virus or other external factors such as secondary bacterial infection not assessed within this study. Environmental factors such as hen pecking could have also contributed to the pathogenicity seen or exacerbated the outcomes. Some hen pecking was seen during the experimental duration, however, this occurred within both groups so could not be deemed an external factor in the pathogenic outcome of the infection. Viral RNA was also isolated from the brain of the birds that died during the course of the experiment (data not shown). Interestingly those with the highest detected viral M gene in the brain were also those birds which exhibited neurological symptoms (lack of control of movement) prior to euthanasia or were found dead (Table 3.3; wing

band numbers- 112, 116, 125 and 120). As this is a LPAI it was not expected that it will be able to disseminate throughout the host as LPAI should have a restricted replication within the respiratory and digestive tracts (Spickler et al., 2008; Swayne and Beck, 2005; Zepeda and Salman, 2007). Unfortunately, brain samples were not taken from those birds routinely culled, so a comparison could not be made regarding presence of vRNA within brain tissue of birds which succumbed to infection. In those tissues collected from birds culled as the result of infection (Figure 3.10, all birds from the UDL-01 WT group), there was a general decrease in the copies of the vRNA isolated the later the bird was culled. As there were no routinely culled birds collected at this later time points it was not possible to correlate whether birds which survived infection also still showed presence of vRNA within their tissues. However, studies conducted by James et al. (2016), collected tissues on day 5 following infection with the UDL-01 WT virus and virus had cleared from the lungs and spleen at this point but was still present in the upper respiratory tract and colon. This suggests that it is not unusual to be able to isolate vRNA from tissues at later time points post infection so an extended dissemination was not responsible for these birds' deaths.

An upregulation of the proinflammatory cytokine, IL-6, was also observed in both directly infected and contact chickens infected with UDL-01 WT compared to those birds infected with the mutant UDL-01 E26K virus. This could suggest the enhanced pathogenicity could be due to an increased proinflammatory response. Enhanced pro-inflammatory cytokine expression within the respiratory tissues has previously been shown to correlate to severe influenza virus infection within both human infection and animal models

(Perrone et al., 2008; Zeng et al., 2015); therefore the increased pathogenicity observed within these studies could be accounted for by the increased pro-inflammatory cytokine responses within wild type infected chicken nasal tissue. However, within these studies, only cytokine transcript levels were investigated. It would have been interesting to further investigate protein levels of cytokines and perhaps to look in more details at the infiltration of immune cells to the respiratory tract between UDL-01 WT and UDL-01 E26K viruses. In addition, time and money constraints only allowed for the cytokine profiles to be assessed from one tissue. However, it might have been beneficial to assess the cytokine profiles in another tissue with high levels of vRNA such as the trachea or to have assessed the kinetics of the cytokine response across day 1-3 post-infection. Within this study it is possible that the differences in immune modulation seen between WT and mutant viruses could just be the result of higher replication leading to higher immune responses, although this is difficult to correlate.

In order to better understand the impact of the amino acid present at position 26 it would have been useful to undertake a similar study, but in a gain-of-function, rather than loss-of-function format, with the WF10 WT and mutant pair of viruses, to ascertain if the reciprocal effect would have been observed; i.e. does WF10 carrying K26E mutation become more pathogenic than the WT WF10? However, due to the limitations in availably of our animal facility and time scales for the project this experiment was not performed.

Overall, within this chapter the effect of a single amino acid change to PA position 26 (E or K) was investigated within avian *in vivo* models. An E to K

change in PA at amino acid 26 in UDL-01 led to reduced viral replication and pathogenicity *in vivo,* correlating with a reduction in the pro-inflammatory cytokine responses and viral dissemination. It is possible that the addition of the UDL-01 E26K mutation makes the virus less stable within both the environment and within the host. This is supported by the reduced environmental deposition of the virus, the reduced shedding and the reduced dissemination observed. However, it would be beneficial to transfer these findings back into an *in vitro* setting to determine the stability of the viruses within different, controlled conditions and also to determine if the stability of the polymerase at a molecular level leads to the production of differential levels of DI's which could alter the pathogenic outcome of infection and therefore determining the mechanism of action of the mutation.

Chapter 4: Investigating the contribution of PA-X to H9N2 AIV fitness *in vitro*

4.1: Introduction

Influenza virus segment 3 also encodes several accessory proteins alongside the main PA gene, including PA-X. PA-X comprises of the N-terminal endonuclease domain of the PA protein, along with a (typically) 41 or 61 amino acid X-ORF (Jagger et al., 2012). The X-ORF is translated from the +1 frame of the PA gene which is accessed via ribosomal frameshifting. PA-X has been shown to play a role in host cell shut off (Jagger et al., 2012); the phenomenon by which viruses are able to inhibit cellular gene expression to hamper the induction of antiviral responses. This allows for translation to be shifted towards the production of viral rather than cellular proteins (reviewed by Aranda and Maule, 1998). PA-X acts in a global fashion, degrading mRNA within the cytoplasm which in turn reduces host protein synthesis (Khaperskyy and McCormick, 2015). Within H9N2 AIVs, Gao et al. (2015c) have previously shown that an active PA-X protein is present in some strains, whose removal led to a reduction in the ability of the virus to control host protein synthesis and reduced replication in A549 cells, as well as reducing virulence within a mouse model of infection.

Several amino acid polymorphisms within our H9N2 strains were identified which altered viral replication both *in vitro* (Chapter 2) and *in vivo* (Chapter 3), as well as altering viral pathogenicity in chickens (Chapter 3). Several of these amino acids lie within the N-terminal endonuclease domain common to PA and PA-X, including the key position (26) identified in chapter two.

It was therefore decided to further investigate the effect of these mutations on the main known function of PA-X; shut off of host cell protein synthesis. Consequently, the aims of this chapter were i) to identify if any of the previously identified mutations, which also lie in PA-X, are able to affect functions of PA-X, in particular host cell shut off. ii) and if so, to further investigate the role of PA-X within these H9N2 AIV strains.

4.2: Results

4.2.1: The effect of amino acid alterations in PA-X on host cell shut off activity

4.2.1.1: Rescue of PR8 7:1 H9N2 PA reassortant viruses

In order to test host cell shut off within a viral context to determine if other viral factors may interfere with the host cell shut off and to determine if plaque phenotype is affected in a similar way to previously shown data, reverse genetics was used to rescue A/Puerto Rico/8/1934 H1N1 (PR8:H1N1) reassortant viruses which contained WT and mutated segment 3s derived from either WF10 or UDL-01 H9N2 AIVs, termed PR8 7:1 UDL/WF10. Reassortant viruses were initially used as the laboratories at the Roslin Institute were not set up for use of AIVs at the time of performing this work. 293T cells were co-transfected with reverse genetics plasmids containing 7 segments (PB1, PB2, NP, HA, NA, NS, and M) derived from PR8 and the segment 3 (PA) derived from the relevant AIV. 72 hours post-transfection the resulting supernatants (P0 stocks) were clarified and used to infect MDCK cells for growth of P1 viral stocks. MDCK cells were monitored for presence of CPE for up to 72 hours, supernatants harvested and stored at -80°C

for use in subsequent experiments. Presence of the correct segment 3 with or without the desired mutation was confirmed via sequencing (data not shown). Viral plaque phenotype was then examined in MDCK cells at 48 hours post-overlay. The PR8 7:1 H9N2 PA viruses containing the WT segment 3s exhibited similar plaque phenotypes, of reasonably large, clear plaques (Figure 4.1B) which when quantified showed average plaque diameters of just over 1mm (Figure 4.1A). This was unexpected, as within the parental H9N2 AIVs, UDL-01 WT had a much larger plaque size compared to WF10 WT (Figure 2.1B) suggesting that other factors within the H9N2 backbone could affect the plaque morphology. The 7:1 reassortant UDL-01 panel of mutants showed some differences in plaque size, in particular those with A20T and T118I changes (Figure 4.1A). However, when average plaque diameters were taken, the E26K mutation showed a significantly smaller plaque size than PR8 7:1 UDL-01 WT, none of the other mutations showed significant changes compared to PR8 7:1 UDL-01 WT (Figure 4.1A). Within the WF10 panel, the K26E change within the endonuclease domain of PA was the only mutation which caused a visually obvious change in plaque size (Figure 4.1B). Quantification showed a significant increase in plaque diameter from ~1mm to 2.5mm. Two other mutations also significantly increased the plaque size of the WF10 7:1 reassortant viruses: I85T and R250Q, albeit to a smaller extent than the K26E change (Figure 4.1A).

In order to further assess the replicative abilities of the PR8 7:1 H9N2 PA viruses, low MOI (0.01) infections of MDCK cells were conducted. 48 hours post infection cell supernatants were harvested and titrated via plaque assay.

A

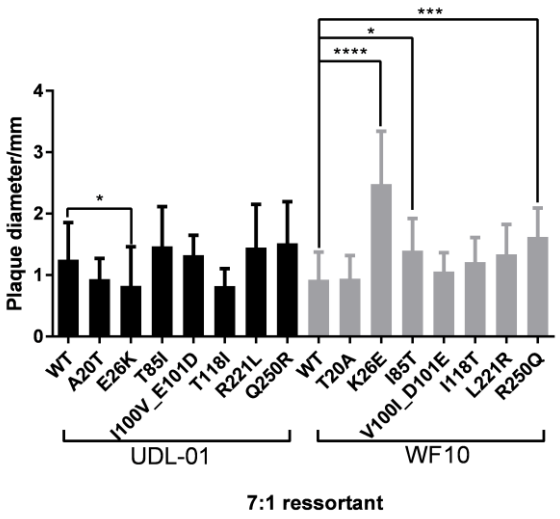
Plaque diameter/mm
4
3
2
1
0
*
***
*
****
WT
A20T
E26K
T85I
I100V_E101D
T118I
R221L
Q250R
WT
T20A
K26E
I85T
V100I_D101E
I118T
L221R
R250Q
UDL-01
WF10
7:1 ressortant

B

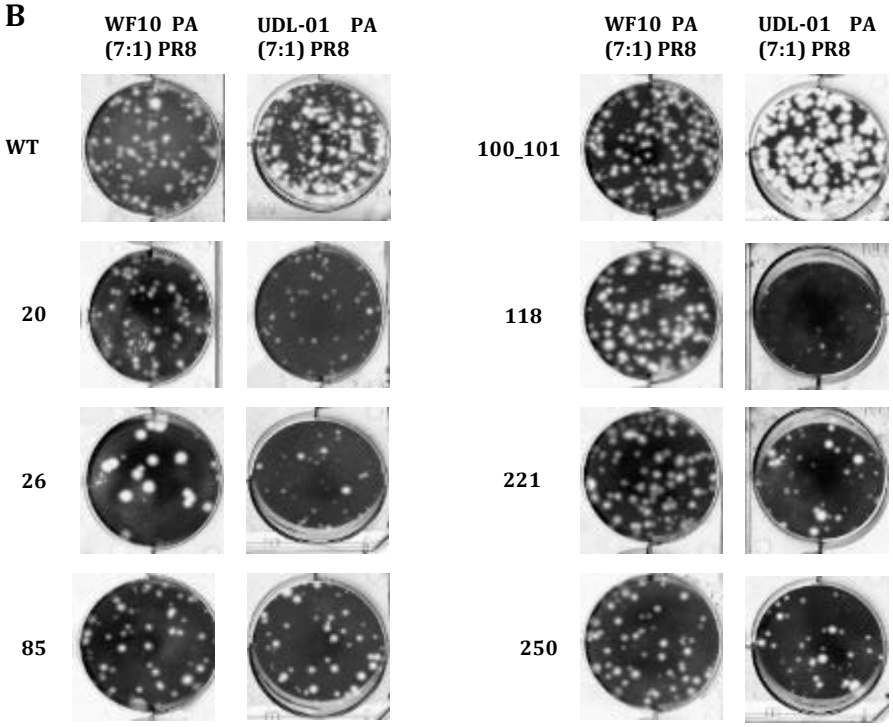
WF10 PA (7:1) PR8
UDL-01 PA (7:1) PR8
WF10 PA (7:1) PR8
UDL-01 PA (7:1) PR8
WT
20
26
85
100_101
118
221
250

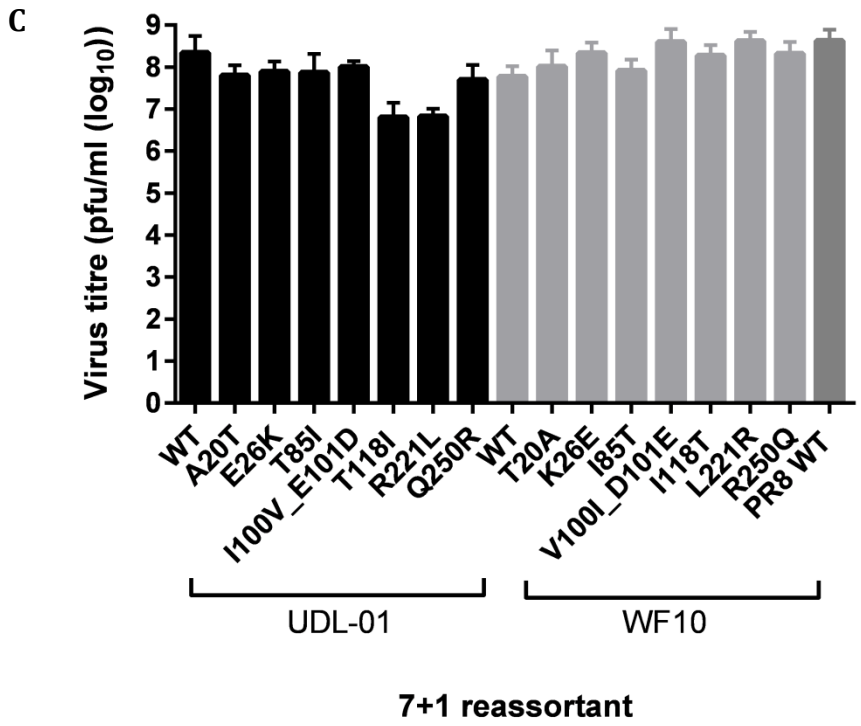

Figure 4.1: Characterisation of PR8 7:1 H9N2 PA viruses. PR8 reassortant viruses containing the indicated H9N2 segment 3s were rescued using reverse genetics and growth properties in MDCK cells examined. (A) Average +/- SD plaque diameter of 20 plaques per virus, measured using ImageJ analysis software. (B) Example of plaque phenotypes. (C) Viruses were used to infect MDCK cells at a low MOI (0.01) and 48 hours post-infection supernatants harvested and viral titres assessed via plaque assay. Mean +/- SD of three independent experiments. P values = *:0.0282, ***:0.0003, ****: <0.0001 (Kruskal- Wallis analysis with multiple comparisons).

However, in 3 independent experiments, all viruses replicated to comparable levels to the parental WT virus after 48 hours (Figure 4.1C). Thus, in the context of the PR8 background, the H9N2 segment 3 mutations had only minor effects on virus replication *in vitro*.

4.2.1.2: Reporter assays to determine host protein synthesis levels with the addition of H9N2 PAs

To test if polymorphisms within the shared domain of PA and PA-X, seen in strains of H9N2 AIVs, affect the host cell shut off activity of PA-X, a β-galactosidase (β-gal) reporter assay was used. This type of assay, in which cells are transfected with "effector" plasmids containing cDNA from segment 3 and a reported plasmid encoding β-gal under the control of a constitutive RNA pol II promoter have previously been used to characterise the ability of influenza PA-X to control host gene expression (Jagger et al., 2012). Enzymatic read out of β-gal accumulation gives a measure of host cell gene expression in the transfected cell and the ability of the polypeptides encoded by the effector plasmid to inhibit it. Transfected segment 3 will produce all four known PA-related polypeptides, but comparison of WT segments with those in which the PA-X frameshift site has been mutated suggest that the majority of the inhibition comes from PA-X (Jagger et al., 2012).

Cells of either mammalian (293T) or avian (DF-1) origin were transfected with differing segment 3 plasmids with or without mutations in PA-X (see chapter 2), along with a β-gal reporter plasmid. 48 hours post-transfection, cells were lysed and β-gal accumulation quantified by a colorimetric enzyme assay. Within

each transfection set up an empty vector control for the effector plasmid was included; to give an indication of β-gal levels in the presence of a further plasmid but in the absence of an encoded inhibitor; all data were normalised to this control. Background levels of absorbance were assessed using a "cells only" control. Within 293T cells, PR8 WT segment 3 was also included. This segment 3 has previously been shown to have low host cell shut off ability via this technique (unpublished data from Digard lab; Naffakh et al., 2001).

In 293T cells, transfection of the β-gal plasmid and empty vector resulted in enzymatic activity substantially above that seen in the cells only control (Figure 4.2A). Addition of the WT UDL-01 segment 3 significantly reduced levels of β-gal in comparison to the empty vector control indicating shut off of host gene expression. In contrast, neither WT WF10 nor PR8 segment 3s repressed β-gal accumulation. When plasmids with single codon changes, within the shared PA endonuclease domain or X-ORF, (characterised in chapter 2), were assessed, several of the alterations had no effect on the PA-X shut off ability in either UDL-01 or WF10 backgrounds compared to their parental WT segment 3s; notably the reciprocal mutations at position 20, 85, 100, 101 and 250. Two mutations had non-reciprocal effects on shut off activity. I118T, which lies within the PA endonuclease domain, removed shut off activity from UDL-01 PA-X but did not rescue repressive activity when introduced into WF10 segment 3. Similarly, L221R, which lies within the X-ORF, introduced host cell shut off activity to WF10 PA-X but did not remove it from UDL-01. However, a single amino acid change, at position 26, showed a reciprocal alteration in host cell shut off activity between

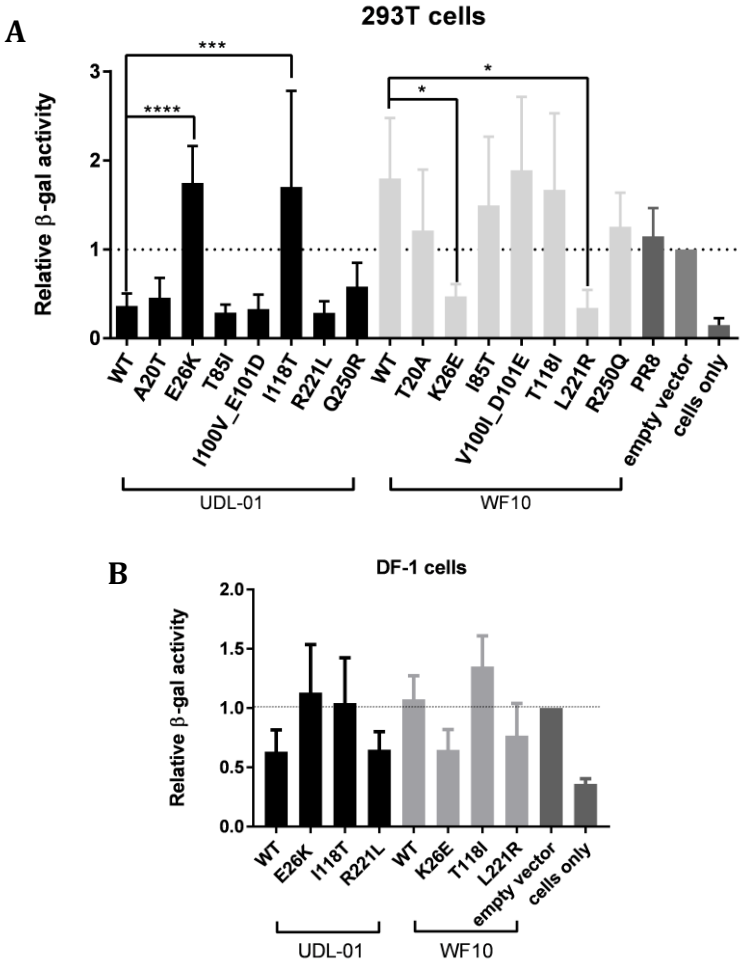

Figure 4.2: Ability of H9N2 PA-Xs to repress cellular gene expression. WT or mutant segment 3 plasmids were co-transfected into (A) 293T cells or (B) DF-1 cells with a β-gal reporter plasmid. 48 hours post-transfection cells were lysed and levels of β-gal assessed by colorimetric enzyme assay. Results were normalised to a sample where the PA plasmid was replaced with the empty vector control. Graph represents the average of 3 independent experiments +/- SD. P values: ****= <0.0001; ***= 0.0003; * = <0.003 (one-way ANOVA with multiple comparisons (all 293T and WF10 panel in DF-1) or Kruskal Wallis with multiple comparisons (UDL-01 panel in DF-1).

UDL-01 and WF10 PA-Xs. Interestingly, this change was the same one that altered plaque phenotype and pathogenicity of the UDL-01 virus (chapters 2 and 3).

Within DF-1 cells the same assay was completed, cells were transfected with the β-gal reporter plasmid and "effector" plasmids. Again, transfection of the β-gal plasmid and empty vector resulted in enzymatic activity substantially above that seen in the cells only control (Figure 4.2B). Only those key changes seen within 293T cells were carried forward to test in DF-1s and the same patterns were observed. Within UDL-01 segment 3, introduction of E26K and I118T changes removed shut off activity in a trended but non-significant manner compared to UDL-01 WT whereas introduction of R221L did not. Within WF10 segment 3, introduction of K26E and L221R led to a trended but non-significant alteration of shut off activity and T118I had no effect.

4.2.1.3: Host cell shut off activity within the context of viral infection

To assess whether the differences observed within plasmid-based shut off activity experiments transpired into differences within viral infection, first the PR8 7:1 H9N2 reassortant viruses were used in metabolic labelling experiments of infected cells. Labelling of newly synthesised cellular proteins with ^{35}S methionine has been shown on multiple occasions to be a reliable method for observation of viral host cell protein synthesis shut off (Read et al., 1993; Frolov and Schlesinger, 1994; Salvatore et al., 2002; Rowe et al., 2007; Jagger et al., 2012). Duplicate sets of CEF cells were infected at an MOI of 3 with a subset of the 7:1 viruses, selected due to the mutations effect on host cell shut off within the plasmid-based shut off assays. 7 h.p.i., cells were either pulsed with ^{35}S

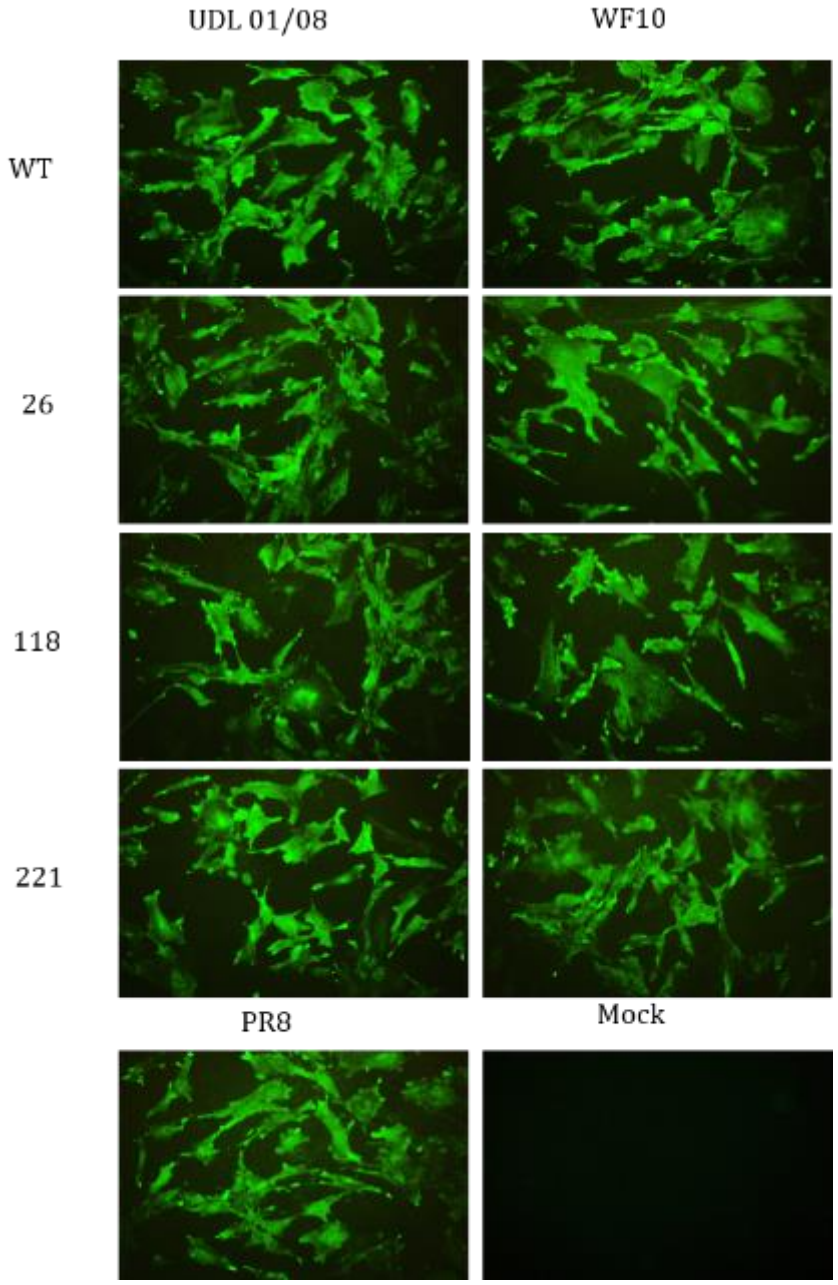

Figure 4.3: Immunofluorescent detection of NP during infection of CEF cells. CEF cells were infected (in parallel with ^{35}S methionine pulsed cells) at an MOI of 3 and 7 hours post-infection cells were fixed with 4% formaldehyde. Cells were permeabilised with 0.2% Triton-X 100 and probed for presence of viral NP. They were imaged on via an epi-fluorescent microscope.

methionine for 1 hour or fixed with formaldehyde. The latter step was to assess viral infection levels via immunostaining for NP protein, as variations in the levels of infection could lead to misleadingly high levels of measured cellular protein synthesis. Mock infected cells did not show the presence of NP and all virus infected samples showed similarly high infection levels (Figure 4.3).

The ^{35}-S methionine pulsed cells were lysed after 1 hour with protein lysis buffer and proteins separated on SDS-PAGE gels, fixed and then labelled polypeptides were detected by autoradiography (Figure 4.4A). Mock infected cell lysates allowed for constituent host cell protein synthesis levels to be assessed, showing the expected variety of polypeptide species. No viral proteins (HA0, NP and M/NS1) were observed in the mock sample but all were detected in the virally infected cell lysates. Actin levels were used as a measure of host protein synthesis; this was the most prominent band within the uninfected sample, sitting at approximately 42kDa. PR8 WT virus has been previously shown not to induce high levels of host cell shut off, because of low PA-X activity (Jagger, 2012) so was included as a point of reference. As expected, the levels of newly synthesised actin were clearly reduced in PR8 WT infected cells compared to mock, however host protein synthesis was not fully ablated. Conversely, PR8 7:1 UDL-01 WT infected cells had a further decreased actin level compared to mock infected cells suggesting that this virus was better able to shut down host cell protein synthesis levels. When an E26K change was made within UDL-01 PA, newly synthesised actin levels were increased compared to PR8 7:1 UDL-01 WT infected cells but not following the I118T and L221R changes. PR8 7:1 WF10 WT infected cells showed even less shut off of actin synthesis compared to WT PR8,

and the addition of a K26E change to lead to a visible reduction in actin synthesis compared to PR8 7:1 WF10 WT infected cells. T118I and R221L mutations appeared to have less of an effect on shut off activity, with actin levels comparable to PR8 WT or PR8 7:1 WF10 WT infected cells.

Densitometry of the actin band from the autoradiograms of three independent experiments was performed as a quantitative measure of cellular protein synthesis levels (Figure 4.4B). By this criterion, host protein synthesis was not fully ablated in PR8 WT infected cells but reduced by around 50%. The PR8 7:1 UDL-01 WT virus reduced radiolabelled actin levels to below 10% of uninfected cells whereas PR8 7:1 WF10 WT virus only reduced it by a similar level to PR8 WT virus (50% compared to mock). This was consistent with the plasmid-based assays of PA-X mediated shut off (Figure 4.1) where the same trend was observed. In both PR8 7:1 UDL-01 and WF10 viruses, when either the 118 or 221 mutations were introduced, no affect was seen on actin levels in comparison to the relevant PR8 7:1 WT virus (Figure 4.4B). This was in contrast to the plasmid-based data (Figure 4.1), indicating that other viral factors perhaps affected host cell shut off to alter this phenotype. The PR8 7:1 UDL-01 E26K virus showed a significant reduction in host shut off activity compared to the parent WT virus (Figure 4.4B). Radiolabelled actin levels increased, from ~10% to >50% of uninfected cell levels, similar to that seen with the PR8 7:1 WF10 WT reassortant. The reciprocal affect was observed with the introduction of the K26E mutation into WF10 PA, where actin synthesis was significantly reduced from ~50% of the mock value to 30%. Therefore, the change at position 26 was the only mutation that exhibited the same effect in a viral context and the PA gene

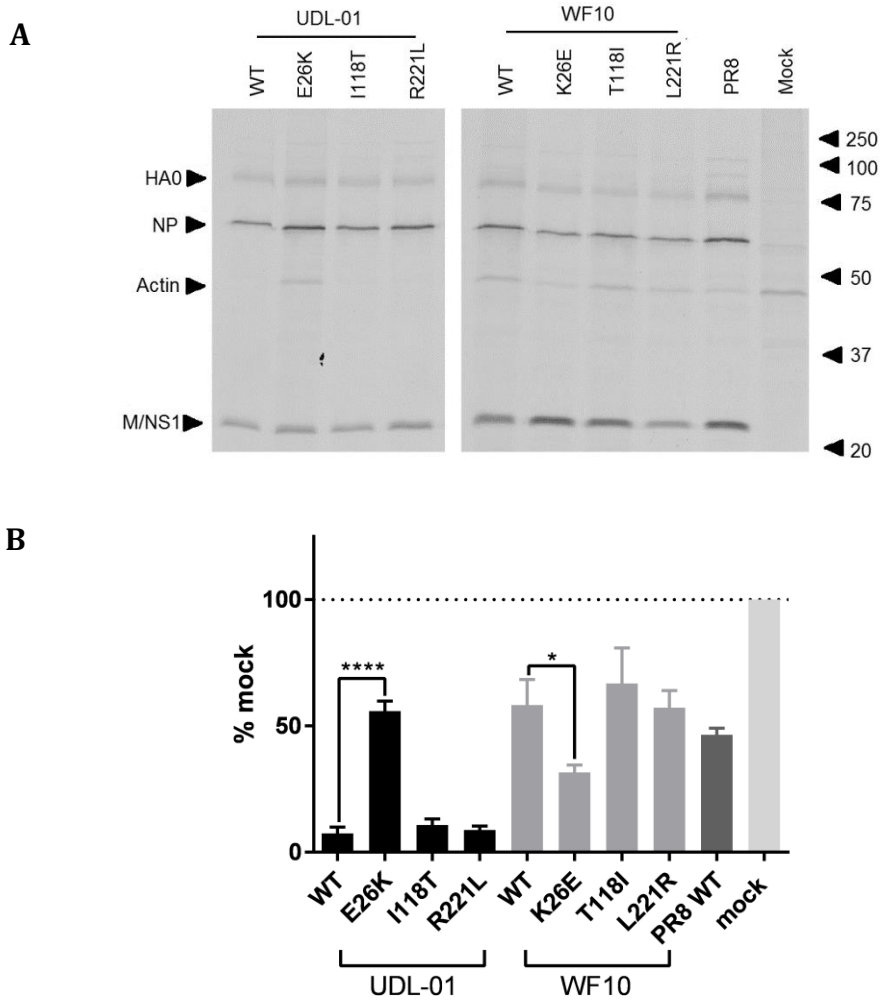

Figure 4.4 Protein synthesis levels within CEF cells infected with PR8 7:1 H9N2 PA viruses. CEF cells were infected with a high MOI (3) of virus. 7 hours post infection cells were pulsed with ^{35}S methionine for 1 hour then lysed and proteins separated by SDS-PAGE. Radiolabelled proteins were detected by autoradiography. (A) Representative SDS-PAGE gel with specific proteins and the positions of molecular mass (kDa) markers indicated. (B) Levels of radiolabelled actin were quantified by densitometry using ImageJ analysis software. Graph represents the average of 3 independent experiments +/- SD P values = *: 0.02, ****: <0.0001 (one-way ANOVA with multiple comparisons).

reporter assay further cementing the importance of position 26 in determining the shut off activity of H9N2 AIVs.

The effect of these amino acid changes on host cell shut off within full H9N2 AIVs was then tested. Since by then, work had shifted to the Pirbright Institute, a different approach was adopted, using puromycin as label rather than ^{35}-S methionine. This method has been developed as an alternative method for measuring cellular protein synthesis without using radioactive materials. Puromycin is a structural analogue of aminoacyl tRNAs and therefore can be incorporated into the newly synthesised polypeptide chain and prevents elongation of the peptide, therefore reflecting the rate of mRNA translation *in vitro.* Puromycin labelled peptides can then be visualised via western blotting (Schmidt et al., 2009). It has been used by multiple groups to study the impact of viral infection on host protein synthesis (White et al., 2011; Liao et al., 2016; Kainulainen et al., 2016) and was identified as a valid alternative technique to radiolabelling by Goodman and Hornberger (2013).

MDCK cells were infected with either WT or 26 viruses, as this mutant showed reciprocal effects on host cell shut off activity within both the plasmid-based and 7:1 reassortant virus assays, at a high MOI (5) and 7 h.p.i., cells were pulsed with puromycin for 30 minutes to allow incorporation into newly synthesised proteins. Cells were lysed and run on a 15% SDS-PAGE gel before western blotting for puromycin (Figure 4.5A). Puromycin signal was detected in all conditions except for a control sample where no puromycin was included within the pulse. Constitutive levels of cellular protein synthesis were indicated

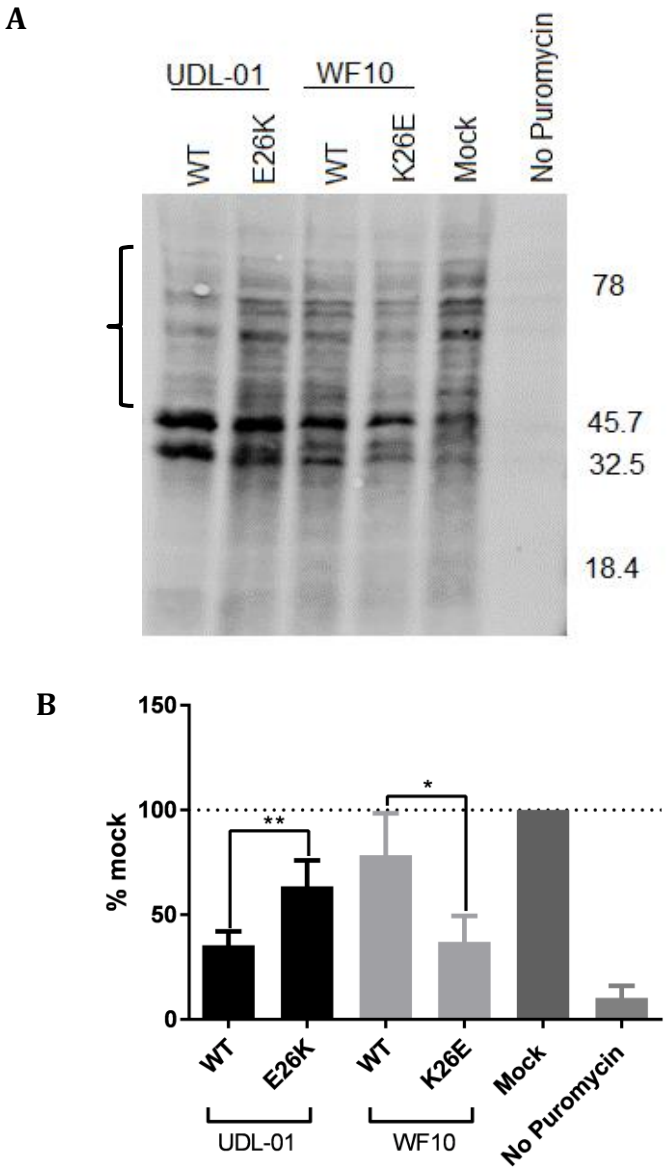

Figure 4.5: Protein synthesis levels within MDCK cells infected with H9N2 AIVs. MDCK cells were infected with a high MOI (10) of each virus. 7 hours post infection cells were pulsed with puromycin for 30 minutes. Cells were lysed, run on SDS-PAGE gels and western blotted for puromycin. (A) Representative western blot gel probed for puromycin. (B) The bracket in (A) covering the areas above 45.7kDa indicates the region quantified using ImageJ analysis software to measure the area under the curve following densitometry of this region. Data were converted to a percentage of the value seen in mock infected cells. Graph represents average +/- SD of 3 independent experiments. P values = *: 0.0124, **: 0.007(unpaired T-test).

within mock infected cell lysate. Two major polypeptide species were induced by viral infection, migrating at approximately the same positions as the 46 and 33 kDa molecular mass markers. The area of the gel above these bands (highlighted by the bracket on the figure), was quantified by densitometry to assess host protein synthesis levels within the cell, on the grounds that it was free of obviously viral-derived products. UDL-01 WT virus lead to a noticeable reduction in labelled protein levels compared to mock infected cells, which was then reversed with the introduction of the E26K mutation. The reciprocal affect was observed with the WF10 viral pair; labelling in cells infected with WT virus appeared more similar to uninfected cells while the K26E mutant reduced puromycin incorporation. Densitometry was measured using ImageJ to quantify protein synthesis within cells from 3 independent experiments and confirmed that this pattern was reproducible (Figure 4.5B). There was a significant increase in cellular protein synthesis in UDL-01 E26K infected cells compared to UDL-01 WT infected cells; 70% of mock compared to 50%. Conversely, there was a significant decrease in puromycin incorporation in WF10 K26E infected cells compared to WF10 WT infected cells. This confirmed within a full avian H9N2 virus background that codon 26 of segment 3 was important for the host shut off differences between UDL-01 and WF10 strains.

4.2.2: Production of H9N2 constructs which lack PA-X expression

As host cell protein synthesis shut off (a known function of the accessory protein PA-X (Jagger et al., 2012)) seemed to be important for the differences in pathogenicity between UDL-01 and WF10 H9N2 AIVs, it was decided to further

investigate the role of PA-X within H9N2 AIVs. In order to do this, the technique used by Jagger et al. (2012) was adopted to remove PA-X expression from segment 3 by introducing a series of synonymous (in the PA ORF) mutations within the frameshift site (Figure 4.6A). Mutation of the highly conserved UCC UUU CGU motif to AGC UUC AGA would be predicted to drastically reduce PA-X expression by removing the translational pause and frameshift-permissive sequences that prompt a low percentage of ribosomes into accessing the +1 ORF (Jagger et al., 2012, Firth et al., 2012). In addition, several premature stop codons (also synonymous in the PA ORF) were introduced into the X-ORF to determine the effect of truncating PA-X on shut off activity. These are termed PTC mutations (see Figure 4.6A and Table 4.1 for details).

The mutations were introduced into the reverse genetics constructs for UDL-01 and WF10 segment 3 and confirmed via Sanger sequencing (data not shown). *In vitro* translations (IVTs) were then completed for each of the plasmids to test if they produced the correct protein products. IVTs have been shown to be useful for looking at production of smaller protein products as seen with PB1-N40 and PA-X itself (Wise et al., 2009; Jagger et al., 2012). Coupled *in vitro* transcription-translation reactions radiolabelled with ^{35}S-methionine were carried out using the TnT rabbit reticulocyte lysate system and protein products analysed using SDS-PAGE and autoradiography (Figure 4.6B). The empty vector control did not show expression of any protein products via this method, as expected. Within the UDL-01and WF10 panel of mutants PA expression was similar across all constructs, as seen with the clear band at ~75 kDa, which was confirmed by densitometry analysis of the bands using ImageJ analysis software

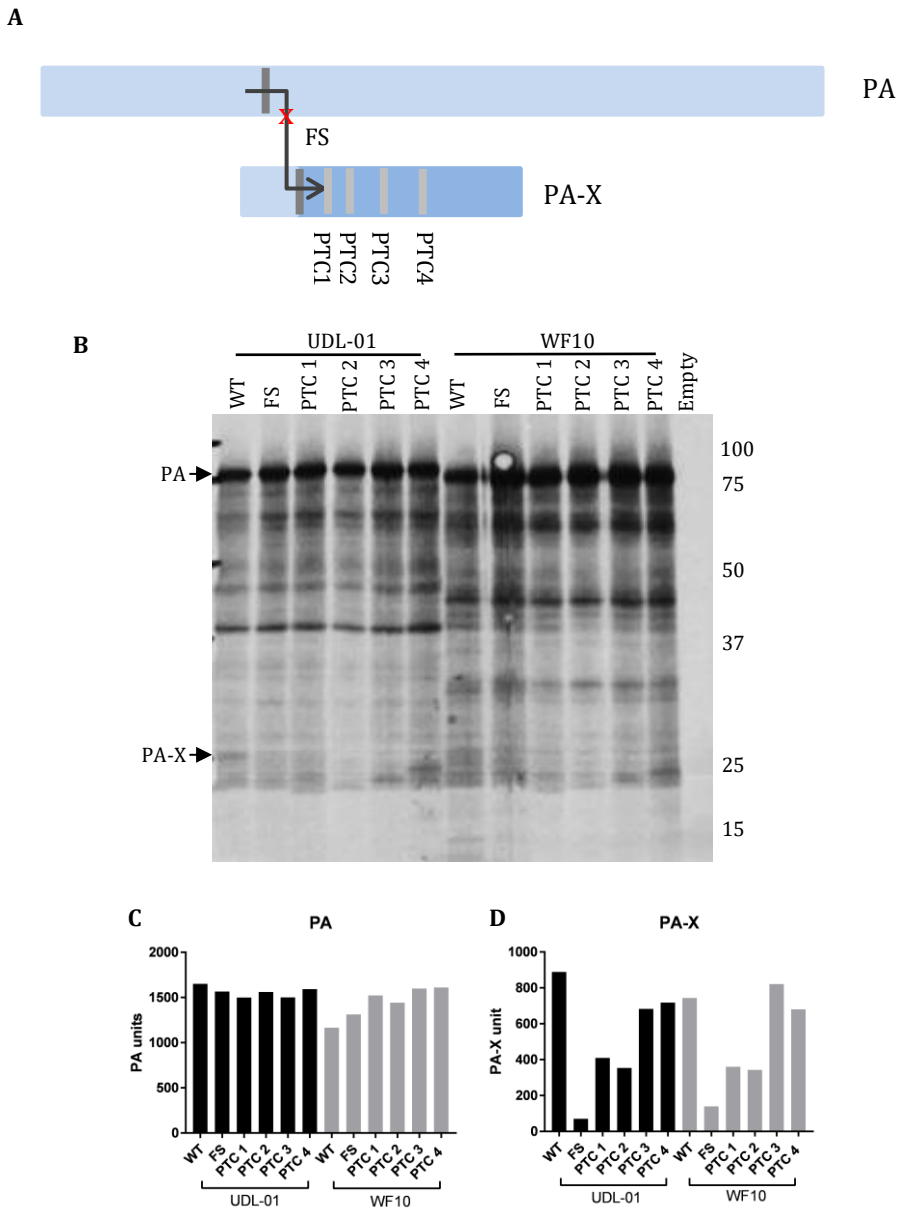

Figure 4.6: PA-X mutations made within H9N2 segment 3s. A panel of mutations were made within UDL-01 and WF10 segment 3s via site directed mutagenesis that altered PA-X expression. (A) Location of mutations within frameshift site and X-ORF. Light blue rectangle represents PA, darker blue rectangle represents X-ORF. Dark grey line represents location of the frameshift site (FS), light grey lines represents location of PTC mutations. (B) Coupled *in vitro* transcription-translation reactions radiolabelled with ^{35}S-methionine were carried out using the TnT rabbit reticulocyte lysate system and protein products analysed using SDS-PAGE and autoradiography. PA and PA-X expression are marked via black arrows. (C) quantification of the AUC of the densitometry analysis of the PA band using ImageJ analysis software. (D) quantification of the AUC of the densitometry analysis of the PA-X band using ImageJ analysis software.

Table 4.1: Summary of PA-X mutations

Mutation name	Original NT	Mutated NT	NT position(s)	Amino acid change
FS	TCC TTT CGT	AGC TTC AGA	568,569,573,574,576	
PTC1	C	A	621	I207 stop
PTC2	C, C, G	A, G, A	634,636,642	R212 stop, L214 stop
PTC3	T	A	678	L226 stop
PTC4	G	A	699	V233 stop

Site directed mutagenesis was used to mutate sites within the UDL-01 and WF10 segment 3 to alter PA-X expression. Mutations to the frameshift site (FS) were predicted to reduce PA-X expression and while premature termination codons (PTC) within the X-ORF would terminally truncate PA-X to various degrees.

(Figure 4.6C). PA levels did not vary considerably, with the highest variation observed with WF10 WT producing lower PA levels than the other plasmids. As this experiment was only conducted once it is not possible to determine if this is the result of this experiment or a more general trend. Several other unidentified protein products were also produced from the segment 3s using this method. The accessory protein PA-X was visualised within the UDL-01 WT lane by a faint band at just above 25kDa in size. Expression of this protein was drastically reduced with mutations to the frameshift site which was confirmed via quantification of the densitometry of the PA-X band (Figure 4.6D). When PA-X was C-terminally truncated, a ladder effect was observed where truncation to the X-ORF altered the protein size. Quantification of expression levels showed that although expressed to a higher level than with the introduction of the FS mutation, both the PTC 1 and PTC 2 mutation reduced expression of PA-X in UDL-01 and WF10 compared to the WT plasmid. Both the PTC 3 and PTC 4 mutations expressed similar levels of PA-X to the WT plasmids. However, again as this is only one repeat of the experiment no firm conclusions can be draw over the stability of the protein with these mutations introduced. Overall, PA expression was not altered with introduction of the PA-X mutations, whereas PA-X expression was, with protein sizes seen as expected.

4.2.2.1: Effect of PA-X expression on host cell protein synthesis shut off

As PA-X has previously been shown to contribute to IAV host cell shut off function (Jagger et al., 2012), the effect of the presence of PA-X mutations on the ability of transfected H9N2 segment 3s to repress cellular gene expression was

tested using β-gal reported assays. 293Ts were transfected with the β-gal plasmid along with various segment 3 plasmids or an empty vector control and β-gal accumulation measured by enzyme assays 48 hours later. Shut off activity is displayed as a reduction in absorbance compared to the empty vector control (Figure 4.7A). As seen previously, the WT segment 3s displayed significantly different shut off activity; UDL-01 segment 3 proficiently repressed host β-gal accumulation while WF10 segment 3 had no ability to shut off host protein synthesis. When PA-X expression was reduced from UDL-01 segment 3 by the FS mutation, shut off activity was removed, with levels of β-gal produced returning to levels similar to the empty vector control. However, when the PA-X slip site was removed from WF10, no alteration in shut off activity was observed, this was expected as the WT WF10 segment 3 showed no activity in the first place. This same trend was also seen when the assay was performed in DF-1 cells (Figure 4.7B). Truncating PA-X had little effect on shut off activity, either positively in the WF10 background, or negatively in the UDL-01 gene. Within the UDL-01 background there was a gradual re-introduction of shut off activity the less the X-ORF was truncated, although the shut off differences were not significantly different to UDL-01 WT.

4.2.2.2: Effect of PA-X on transcriptional activity of the viral polymerase complex

Influenza PA-X has previously been suggested to affect polymerase activity; for example Hu et al. (2015), showed that removal of PA-X expression enhanced the activity of the H5N1 polymerase complex. However, others have

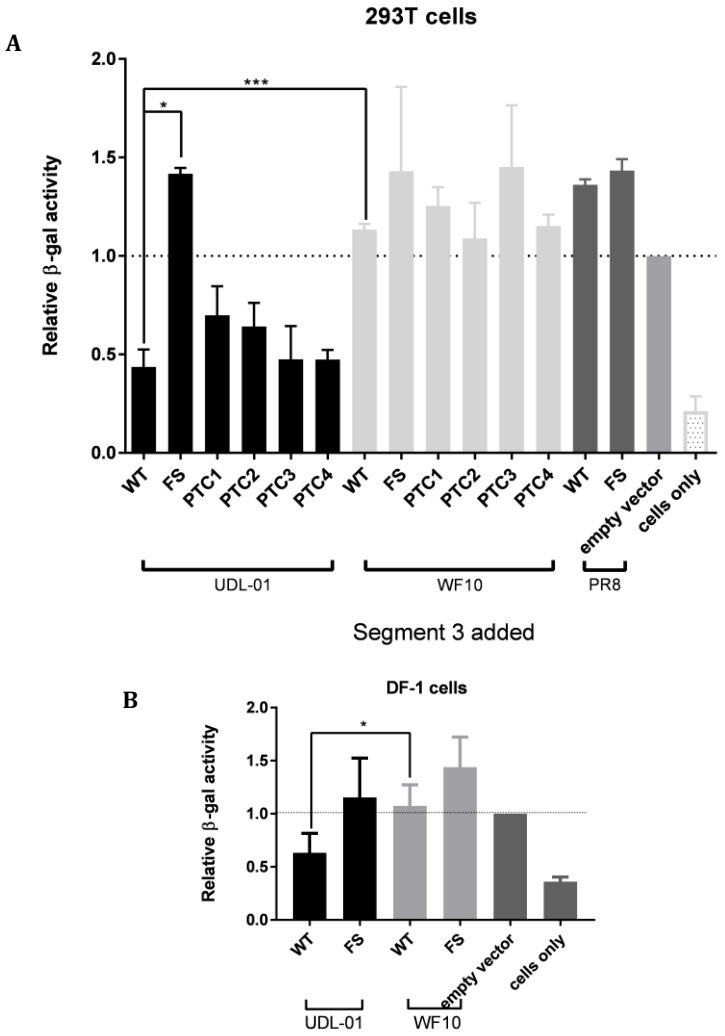

Figure 4.7: Effect of PA-X mutations on host cell shut off ability of H9N2 segment 3s. (A) 293T cells or (B) DF-1 cells were transfected with a β-gal reporter plasmid alongside the indicated segment 3 expression plasmids with or without PA-X mutations. 48 hours post-transfection cells were lysed and levels of β-gal enzymatic activity assessed by colorimetric assay. Results were normalised to an empty vector control. Graphs represent the average +/- SD of 3 independent experiments. P value: ***= 0.0002, *= <-0.05 (Kruskal Wallis with multiple comparisons (293T UDL-01 panel), one-way ANOVA within multiple comparisons (293T WF10 panel) or unpaired T –test (DF-1 cells and WT vs WT 293T)).

shown mutation of PA-X lowers activity of the pH1N1 polymerase complex (Lee et al., 2017). Therefore, these apparent effects of PA-X on polymerase activity appear to be strain dependant, consequently it was decided to investigate the effect of PA-X expression on polymerase activity within our H9N2 backgrounds.

To test if altering PA-X expression had any effect on the transcriptional activity of the IAV polymerase complex, "minireplicon" or "RNP reconstitution" assay systems were adopted. These assays indirectly measure mRNA production by the viral polymerase from a vRNA mimic (Huang et al., 1990; Foeglein et al., 2011). Plasmids encoding the RNA polymerase complex (PB2, PB1, PA), as well as NP (abbreviated as 3PNP) were co-transfected into cells to produce mRNA and thus protein for each viral polypeptide. Along with the protein components, a vRNA mimic reporter construct was co-transfected. This reporter plasmid expresses a firefly luciferase gene in negative sense flanked by segment 8 UTRs, under the control of either a human or avian RNA polymerase I promotor. This allows for RNA to be produced by cellular RNA polymerase I which resembles vRNA to the viral polymerase complex and thus triggers RNP formation. This will in turn be transcribed by the IAV polymerase complex into mRNA which is then translated into luciferase (Lutz et al., 2005). Luciferase output is assumed to be generally proportional to the transcriptional activity of the viral polymerase complex. Some laboratories also include a renilla luciferase transfection control that the firefly luciferase values are normalised to (Hu et al., 2015; Long et al., 2016; McAuley et al., 2010). However, due to the potential for the mutations

examined here to have variable secondary effects on host cell gene expression because of their position within the accessory gene PA-X, this control was not employed.

First, the transcriptional activities of a consistent set of viral RNPs with PB2, PB1 and NP derived from PR8 but with swapped PA polypeptides derived from either UDL-01 or WF10 H9N2 strains were assessed. The PR8 2PNP system was used within mammalian cells due to the presence of PB2 627E within UDL-01 and WF10. The presence of this amino acid in PB2 often severely restricts the polymerase complex in mammalian cells (Long et al., 2013). 293T cells were co-transfected with expression plasmids for RNP polypeptides as well as a vRNA mimic encoding luciferase. 48 hours later cells were lysed and luciferase activity quantified. A negative control lacking PA was included (2PNP), since the viral transcriptase cannot form in the absence of PA and therefore any luciferase observed would not be the result of viral transcription. In the absence of all four RNP polypeptides, only background levels of luciferase were seen, whilst the full PR8 RNP produced around 1000-times more luciferase activity (Figure 4.8A). When either of the two WT H9N2 segment 3s were added to the PR8 2PNP system similar 1000-fold increases in luciferase levels were observed compared to the 2PNP control, indicating that both WF10 and UDL-01 PAs were compatible with the other PR8 RNP components. There was a significant reduction in transcriptional activity after transfection of WF10 WT segment 3 compared to UDL-01 segment 3. This was not observed previously in chapter 2 (Figure 2.3). However, changing PA-X expression in either PA background had very little impact on viral gene expression, with only minor fluctuations in activity being

seen. Overall, no significant differences were seen in the transcriptional activity of the polymerase complex following mutation of PA-X. This suggests that in this system, PA-X does not affect the transcriptional activity of the polymerase.

The effect of changing PA-X expression on the transcriptional activity of a fully avian RNP was then assessed. DF-1 (chicken fibroblast) cells were transfected with expression plasmids for either UDL-01 or WF10 RNP polypeptides plus a vRNA mimic encoding luciferase under the control of an avian RNA polymerase I promotor. As above, cells were lysed and luciferase levels measured after 48 hours. Untransfected cells gave only background levels of luciferase (cells only control; Figure 4.8B) while minimal luciferase expression was observed when only PB1, PB2 and NP were transfected (2PNP control) indicating the lack of an active polymerase complex. When all four RNP polypeptides were included within either the UDL-01 or WF10 backgrounds an approximately 100-fold increase in luciferase expression was observed compared to the 2PNP control. As with the mammalian system, no significant differences were seen between the transcriptional activities of the polymerase complexes with different expression of PA-X when compared to the activity of the relevant WT. Therefore, PA-X did not affect transcriptional activity of the polymerase complex within either an avian or a mammalian adapted setting.

Expression of PA, as well as tubulin as a loading control, were analysed via western blot (Figure 4.8C). Tubulin levels were reasonably consistent across all groups, with variances seen in some samples. Similarly, all of the PA constructs exhibited generally similar accumulation levels with some fluctuations in

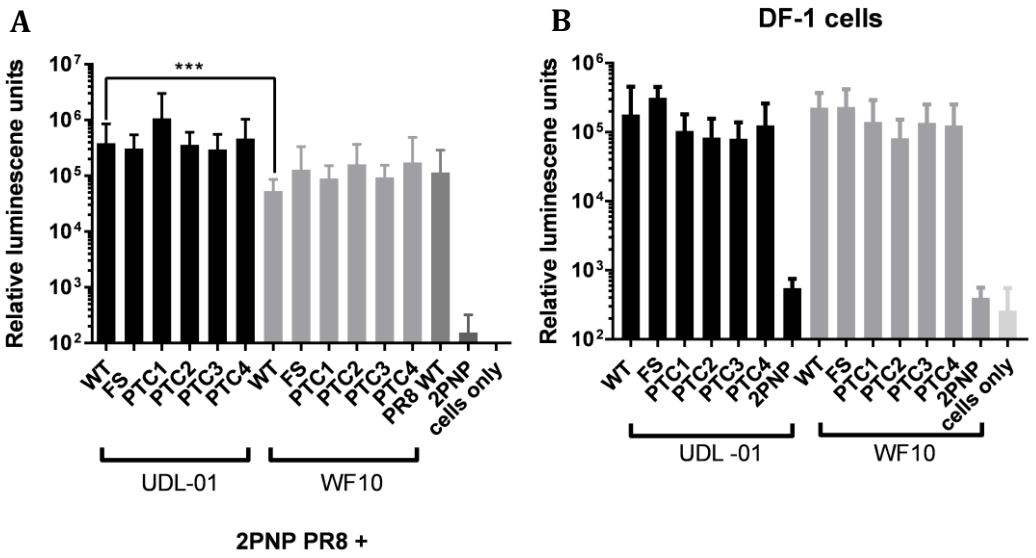

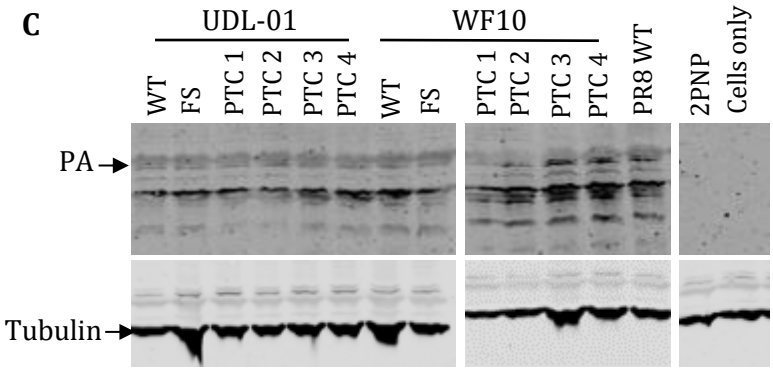

Figure 4.8: Transcriptional ability of polymerase complexes with H9N2 segment 3s with differing PA-X expression. (A) 293T cells or (B) DF-1 cells were transfected with the components of the polymerase complex (PB1, PB2, PA and NP) or as a negative control with PB1, PB2 and NP (2PNP) plus a vRNA mimic encoding luciferase. 48 hours post transfection cells were lysed and luciferase levels measured. Data are the average of 3 independent experiments +/- SD. No significant differences were seen within UDL-01 or WF10 groups (Kruskal Wallis with multiple comparisons). WT vs WT 293T cells P value - ***=0.0002 (Mann-Whitney Test) (C) PA and tubulin expression levels were determined via western blot analysis of 293T cell lysates.

accumulation observed particularly within WF10 PTC1. No PA expression was observed in the 2PNP or cells only controls. Thus overall, alteration of PA-X expression did not have any major effect on the stability of PA or the ability of polypeptides to support viral gene expression when assayed in mammalian cells in the background of a PR8 RNP.

4.2.2.3: Production of H9N2 AIVs with differential PA-X expression

To investigate the effect of PA-X expression within a viral context for example, on replication or host cell shut off, segment 3s with different PA-X expression levels were introduced into full WF10 and UDL-01 H9N2 AIVs using reverse genetics. Viruses were rescued using 293T cell and MDCK cell co-culture and then propagated into viral stocks within 10-day old fertilised hens' eggs. After 48 hours allantoic fluid was harvested and titrated via plaque assay. The presence of the desired mutations was confirmed via sequencing using segment 3- specific primers, M segment was also sequenced to confirm the correct virus backbone was present (data not shown). When the plaque morphology was examined as a first test of virus fitness, the UDL-01 panel of viruses displayed clear plaques within MDCK cells, with no obvious visual differences amongst the mutants. Within the WF10 panel of viruses, small, hazy plaques were observed within MDCK cells. However, the introduction of the PTC1 mutation produced a more distinct plaque within MDCK cells compared to the other WF10 viruses (Figure 4.9A). When the diameters of 20 plaques per virus were measured using ImageJ, a small but significant reduction in plaque diameter was observed within UDL-01 when PA-X was removed (FS) or truncated up to PTC3 (Figure 4.9B).

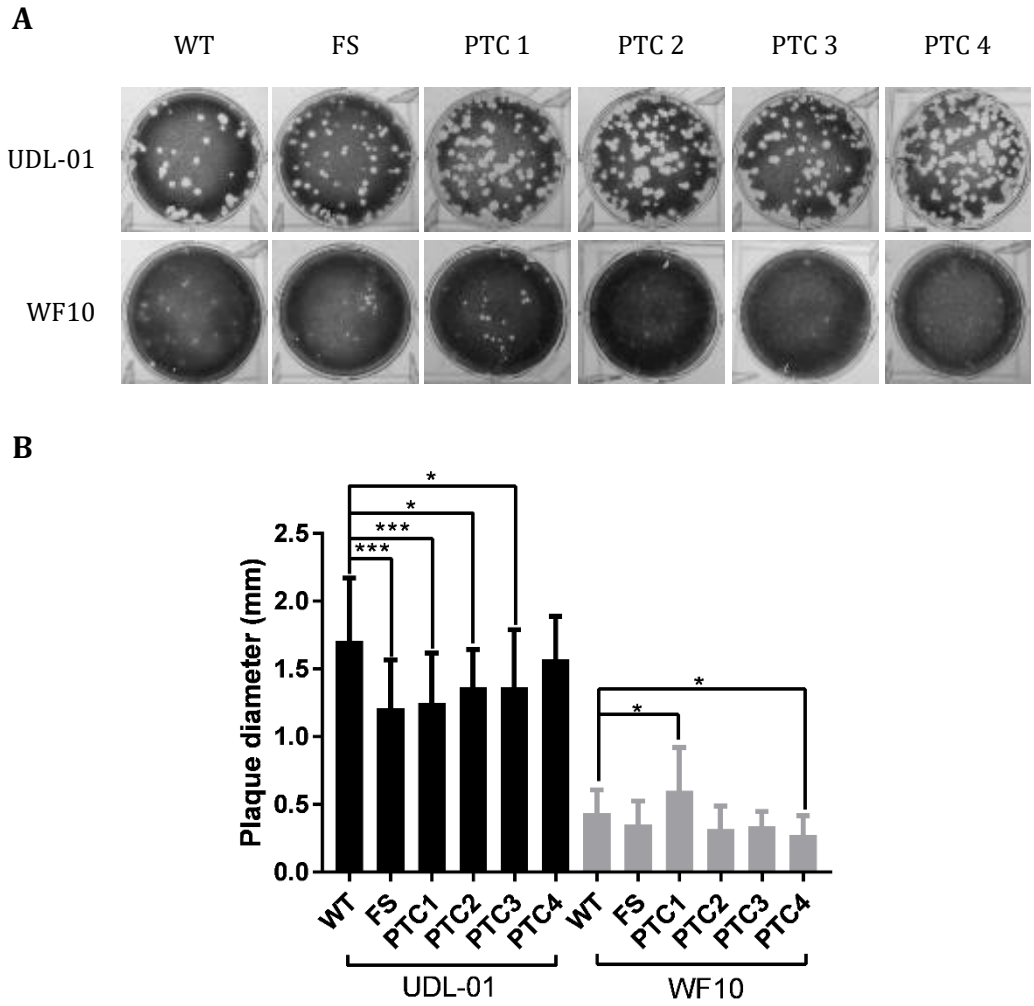

Figure 4.9: Plaque phenotypes of H9N2 AIVs with altered PA-X expression. Viruses were rescued using reverse genetics and titrated under a 0.6% agarose overlay in order to ascertain the plaque phenotype. (A) After 72 hours cells were fixed and stained with 0.1% crystal violet solution and plates imaged. (B) ImageJ analysis software was used to measure the diameter of 20 plaques per virus. Graph represents average diameter of 20 plaques +/- SD. P values: ***= <0.0009, *=<0.037 (one-way ANOVA with multiple comparisons).

Average plaque diameters decreased from 1.7mm to 1.2mm, 1.25mm, and 1.36mm respectively. There was no significant difference in plaque size with the removal of full length PA-X from WF10 PA. However, when PA-X was truncated maximally (PTC1), the average plaque diameter increased significantly from 0.44mm to 0.60mm. Truncation of PA-X with the PTC4 mutation also significantly reduced the viral plaque diameter compared to WF10 WT from 0.44mm to 0.27mm.

4.2.2.4: Replication kinetics of viruses containing differential expression of PA-X

Previous work has shown that, although non-essential, PA-X can affect viral replication. Lee et al. (2017) showed that removal of PA-X from a pH1N1 strain reduced viral replication in MDCK cells. Conversely, Hu et al. (2015) found that removal of PA-X from H5N1 virus increased replication. Closer to this study, Gao et al. (2105c) showed that within an H9N2 background, removal of PA-X had no effect on viral replication. Therefore, the effect of removal or truncation of PA-X on virus replication appears to be strain dependant so was assessed within our H9N2 strains. Following on from assessing the impact of differing plaque phenotypes multi-cycle virus growth was measured. First, the full panel of viruses were screened by completing end-point titre experiments. MDCK cells were infected with each virus at a low MOI (0.01). After 48 hours supernatants were harvested and titrated via plaque assay. Experiments were repeated across 3 independent replicates and in all cases, a mock infected group was included where cells were infected with serum free media rather than virus. Virus outputs

from these latter controls were negative within the limit of detection via plaque assay (2.5 pfu/ml; data not shown). Viral output within the UDL-01 virus panel, showed a trend towards decreased viral output with the FS, PTC1, PTC2 and PTC3 viruses with only the PTC2 mutant reaching significance (Figure 4.10). Within the WF10 panel, significant reductions in viral titre were only seen with the introduction of the PTC3 mutation, although addition of PTC2 and PTC4 showed trended decreases in viral output.

Next, the replication kinetics of viruses with or without the presence of PA-X were assessed over a time course of infection to test for any differential effects on replication at earlier time points post-infection that could have been missed by only looking at end-point titres. The FS mutations were focussed on as removal of PA-X had the strongest effect on viral plaque phenotypes in UDL-01 and also lead to a change in the host cell shut off ability of the virus. MDCK cells were infected with a low MOI (0.01) of H9N2 WT and FS viruses, supernatant samples were taken at 4, 8, 12, 24, 48 and 72 h.p.i and viral output titrated by plaque assay. As before, the experiments were performed three times independently, including a mock infected group in each replicate. On each occasion the mock infected output was below the limit of detection for the plaque assay (data not shown). All four viruses showed the expected exponential rise in titre after 8 h.p.i. reaching a plateau around 48 h.p.i (Figure 4.11A). WF10 WT and FS viruses did not exhibit any significant differences in viral replication over the time course of infection. However, UDL-01 WT virus displayed significantly higher titres at 72 h.p.i in comparison to UDL-01 FS virus at these time points. From 48 hours post infection there was a general decrease in viral output with

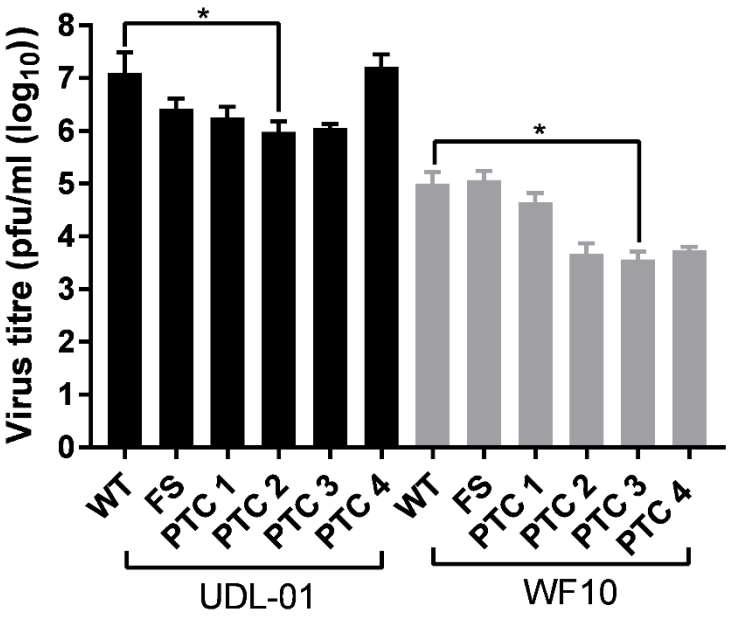

Figure 4.10: Low MOI infections of MDCK cells with H9N2 AIVs with altered expression of PA-X. MDCK cells were infected with a low MOI (0.01) of H9N2 AIVs with the indicated PA-X mutations. 48 hours post-infection cell supernatants were harvested and clarified before being titrated via plaque assay under 0.6% agarose. Graph represents the average of 3 independent experiments +/- SD. P values = *: <0.04 (Kruskal Wallis with multiple comparisons).

UDL-01 FS compared to UDL-01 WT, thus within a UDL-01 background, PA-X expression does enhance viral replication, at least within MDCK cells.

To test if the effect of removal of PA-X on viral replication held true in avian cells, viral replication kinetics were then assessed within primary chicken kidney (CK) cells. As for MDCK cells, a low MOI was used (0.01), supernatants were harvested at 4, 8, 12, 24, 48 and 72 h.p.i and titrated via plaque assay on MDCK cells. Three independent repeats were performed, again all with mock infected cells which showed viral levels below the limit of detection (data not shown). The viral output from CK cells varied more between experiments in comparison to MDCK cells, likely due to their primary nature. Nevertheless, there were consistent differences between the replication kinetics of the viruses, with both WF10 WT and FS viruses exhibiting a reduced replication compared to the UDL-01 pair (Figure 4.11B). However, in contrast to the results seen within MDCK cells there was no significant difference in viral replication of the UDL-01 pair at any time point within CK cells, indicating cell-specific effects. Therefore, as a further test, replication kinetics were assessed *in ovo*; 10-day old fertilised hens' eggs (VALO breed) were inoculated with 100 pfu of each virus. Eggs were chilled and allantoic fluid was harvested at 4, 8, 12, 24 and 48 h.p.i. Allantoic fluid samples were titrated via plaque assay to determine viral load at each point. No virus was detected prior to 8 h.p.i for all viruses or 12 h.p.i. for the WF10 pair. *In ovo,* UDL-01 WT and FS viruses nor WF10 WT and FS viruses exhibited any significant differences in viral replication throughout the course of infection (Figure 4.11C). Overall, the impact of PA-X on the replication of H9N2 AIVs was variable and replication differences appear to be host-dependent.

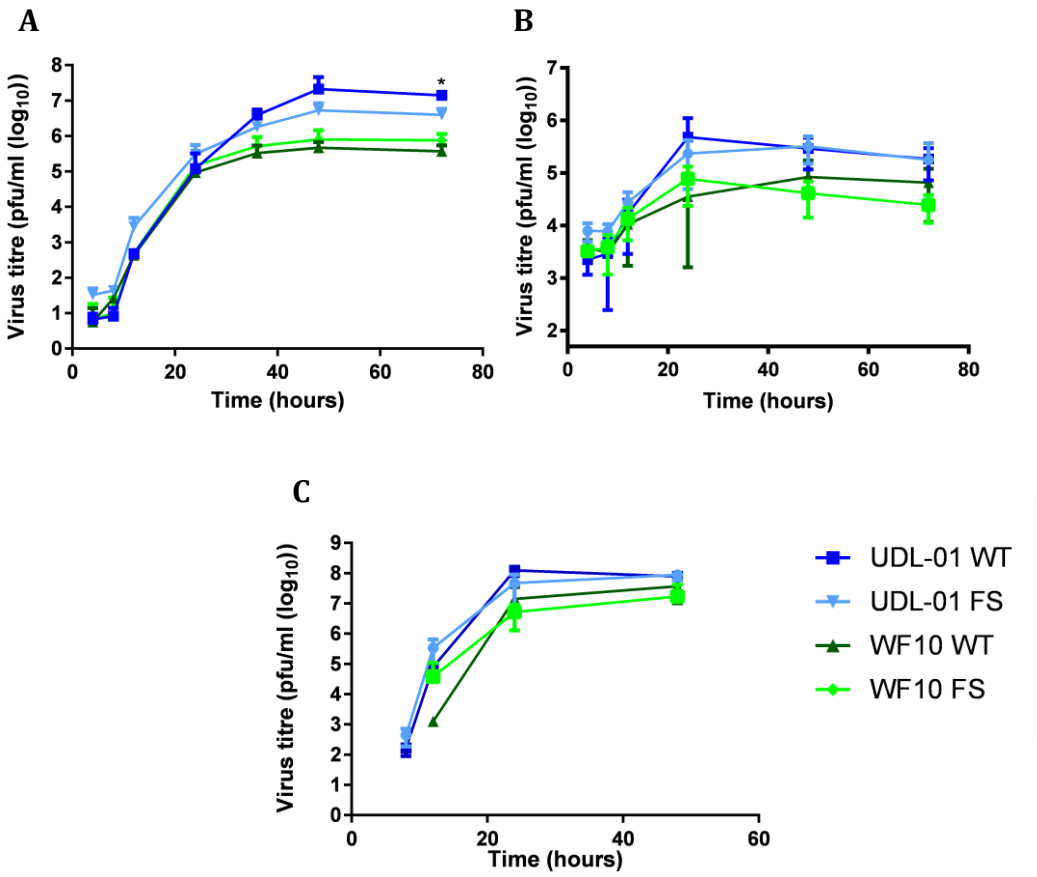

Figure 4.11: Effect of PA-X expression on replication kinetics of H9N2 AIVs with (WT) or without (FS) expression of PA-X. (A) MDCK cells or (B) CK cells were infected with a low MOI (0.01) of a H9N2 virus which expressed (WT) or did not express (FS) the accessory protein PA-X. Cell supernatants were harvested at 4, 8, 12, 24, 36, 48 and 72 h.p.i. and titrated via plaque assay in MDCK cells under 0.6% agarose. Graphs represent an average of 3 independent experiments +/- SD. (C) 10-day old fertilised hens' eggs were infected with 100 pfu of each virus. Allantoic fluid was collected at 4, 8, 12, 24 and 48 h.p.i. clarified and titrated via plaque assay. No virus was detected before 12 h.p.i in WF10 WT infected eggs. Graph represents an average of 5 eggs per virus per time point +/- SD. P values =*:0.0355, (unpaired T-test (A- UDL-01 36 and 72 h.p.i. WF10 24, 36, 48 and 72 h.p.i. B- UDL-01 4, 8, 12, 24 and 48 h.p.i. WF10 8, 12, 48 and 72 h.p.i., C- UDL-01 8, 12 and 24 h.p.i.) or Mann Whitney test (A- UDL-01 4, 8, 12, 24 and 48 h.p.i. WF10 4, 8 and 12 h.p.i., B- UDL-01 72 h.p.i. WF10 4 and 24 h.p.i, C- UDL-01 48 h.p.i. WF10 all data points)).

4.2.2.5: Effect of PA-X on host cell protein synthesis during viral infection

Previously, the host cell shut off activity of constructs with altered PA-X expression was assessed using plasmid-based assays (Figure 4.7). To determine if the effect of different PA-X expression held true within a viral context puromycin labelling of newly synthesised cellular proteins was adopted. This would allow the ability of H9N2 AIVs, with (WT) or without (FS) PA-X expression, to control host protein synthesis to be determined. MDCK cells were infected with virus at a high MOI (5), 7 h.p.i. cells were pulsed with puromycin for 30 minutes, which incorporated into protein synthesis at this point, before being lysed, separated on a 15% SDS-PAGE gel and western blotted for puromycin (Figure 4.12A). Puromycin signal was detected in all conditions except when no puromycin was included within the pulse. Constitutive levels of cellular protein synthesis were seen within mock infected cell lysate. Two proteins products were induced by viral infection: bands seen at approximately 46 and 33 kDa. The area of the blot above these bands was therefore used to assess host protein synthesis levels within the cell. UDL-01 WT virus reduced cellular protein synthesis compared to uninfected cells. This was then partially restored with the removal signal did not obviously affect host protein synthesis. To quantify protein synthesis levels, densitometry of top section of the gel (marked in brackets on the figure) was performed on 3 independent experiments (Figure 4.12B). UDL-01 WT infected cells displayed less than half the normal amount of puromycin incorporation than mock infected cells but this was significantly increased following infection with the UDL-01 FS virus, which only differs in expression of

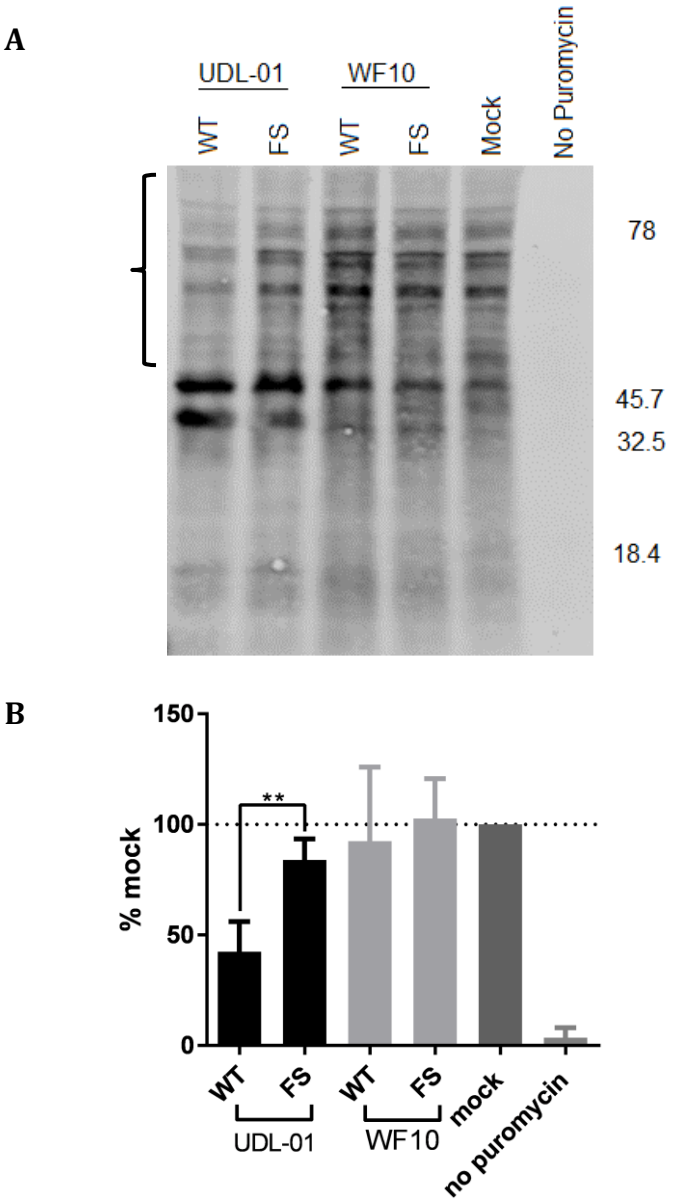

Figure 4.12: Host cell protein synthesis in MDCK cells infected with H9N2 AIVs with or without PA-X expression. MDCK cells were infected with a high MOI (5) using viruses expressing PA-X (WT) or with PA-X expression removed (FS). Seven hours post infection cells were pulsed with puromycin for 30 minutes and then lysed and samples run on SDS-PAGE gels. Membranes were probed for presence of puromycin. (A) Representative SDS-PAGE gel with the area quantified highlighted in brackets. The approximate position of molecular mass markers (kDa) is also indicated. (B) Quantification of the densitometry of the highlighted area (above 47 kDa) performed using ImageJ analysis software. Graph represents the average of 3 independent experiments +/- SD. Each data group is normalised to mock levels of protein synthesis. P value: **=0.0015 (unpaired T-test).

PA-X. However, no significant differences in the ability of WF10 WT and FS viruses to alter host protein synthesis were observed; neither virus showed any significant shut off activity above mock infected cells. These data are in agreement with the plasmid-based methods previously used, and showed that UDL-01 expresses a classically active PA-X protein; whereas, WF10 PA-X appears to possess no host protein shut off activity.

4.2.3: Investigation into the effect of introduction of both an amino acid change at position 26 and removal of PA-X

To elucidate if the change at amino acid 26 exerts its function on alteration of host cell shut off as part of PA-X or in an independent manner, constructs were produced which had both the relevant mutation at amino acid 26 (E26K: UDL-01; K26E: WF10) alongside the mutation which removes PA-X expression (FS). This also enables the investigation into the effect of the 26 mutation in the absence of PA-X.

4.2.3.1: Replication kinetics of H9N2 AIVs containing both PA position 26 and FS mutations

To test for the interplay between the FS and E26K mutations on virus replication, the double mutants were then built into full WF10 or UDL-01 H9N2 AIVs using reverse genetics. Viruses were rescued using 293T cell and MDCK cell co-culture and then propagated in eggs as before. The presence of the desired mutations was confirmed via sequencing using segment 3 specific primers and the M segment was also sequenced to confirm the correct virus backbone was present (data not shown). Plaque size was then examined as an initial indication

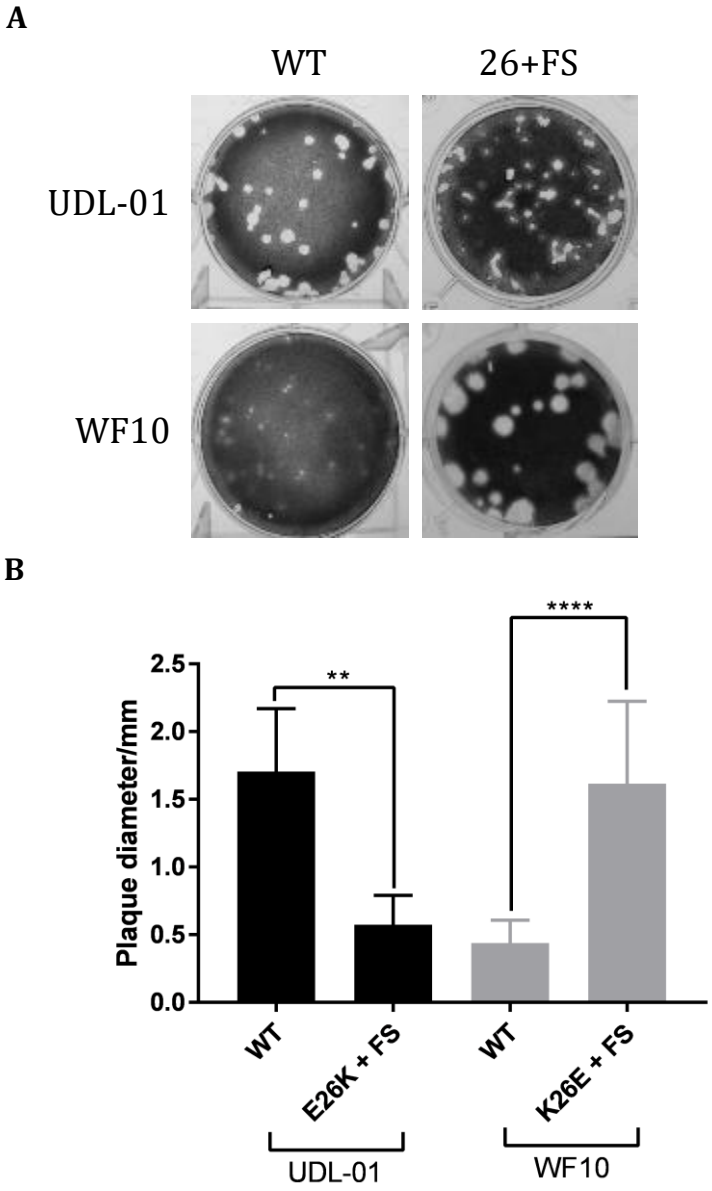

Figure 4.13 Plaque phenotypes of H9N2 AIVs with double mutations at PA codon 26 and the PA-X frameshift site. Reverse genetics was used to rescue viruses which contained both a mutation at amino acid 26 and did not express PA-X. Viral plaque phenotypes were assessed in MDCK cells under 0.6% agarose. 48 hours post infection cells were fixed and stained with 0.1% crystal violet solution and (A) plaques imaged. (B) ImageJ analysis software was used to measure the diameters of 20 plaques per virus. Graph represents average +/- SD. P values = **:0.0015, ****=<0.0001 (unpaired T-test). .

of virus replicative fitness. When both 26 and FS mutations were introduced into the H9N2 viruses, the plaque phenotype altered similarly to that previously seen with viruses only containing the 26 mutation (section 2.2.4). The E26K + FS UDL-01 virus had a reduced plaque size compared to WT but still produced clear plaques within MDCK cells (Figure 4.13A). Conversely, WF10 K26E +FS virus had a greatly increased plaque size, generating clear plaques compared to small hazy plaques produced by WF10 WT. Plaque diameters were quantified and the average diameter of UDL-01 virus plaques decreased from 1.7mm to 0.6mm with the introduction of the double mutation. The average plaque diameter of K26E + FS WF10 increased from 0.44mm to 1.6mm compared to WF10 WT, all changes were statistically significant when compared to the WT parental virus (Figure 4.13B).

Next, as a further test of virus replicative fitness, the replication kinetics of viruses containing the double mutation were assessed over a time course of infection. MDCK cells were infected with a low MOI (0.01) of H9N2 WT and double mutant 26 + FS viruses, supernatant samples were taken at varying times post infection and viral output titrated via plaque assay. As before, the experiments were performed three times independently, including a mock infected group in each replicate which gave an output below the limit of detection (data not shown). The UDL-01 E26K + FS virus did not have a significantly different replication to UDL-01 WT virus, although by 48 h.p.i viral output was reduced in a trended but not significant way (Figure 4.14). Conversely, WF10 K26E + FS virus showed higher titres at all time points with significantly higher titres at 48 h.p.i compared to WF10 WT. Therefore, the introduction of both

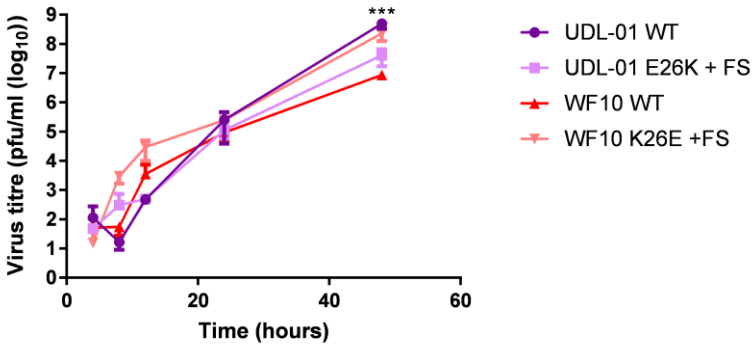

Figure 4.14: Replication kinetics of H9N2 double mutants. MDCK cells were infected with a low MOI (0.01), cell supernatants were harvested at various time points post-infection and viral titres determined via plaque assay. Graph represents the average of 3 independent experiments +/- SD. P values =, ***= 0.006 (unpaired T-test – UDL-01 4 and 24 h.p.i. WF10 8, 12, 24, 48 h.p.i. or Mann Whitney – UDL-01 8, 12 and 48 h.p.i. WF10 4 h.p.i.). *** = between WF10 WT and WF10 K26E +FS

mutations increased replication of WF10 and decreased replication of UDL-01 within MDCK cells. This was a similar pattern to that seen when only the 26 mutation was introduced (Chapter 2; Figure 2.6), so this residue is therefore an important mediator of viral fitness.

4.2.3.2: Host cell shut off ability of H9N2 PA-Xs with amino acid change at position 26 and removal of PA-X (FS)

The effect of the double mutation on the ability of PA-X to control host cell protein synthesis was tested, as previously codon 26 was seen to affect this function of PA-X. 293T cells or DF-1 cells were co-transfected with the constructs, possessing both an FS mutation to remove PA-X expression and a mutated codon 26, plus a β-gal reporter plasmid as described previously. 48 hours post transfection cells were lysed and β-gal accumulation quantified by enzyme assay. Data were normalised to an empty vector control where no host cell shut off would be expected. Background levels of absorbance were assessed using a cell only control. Within both 293T cells (Figure 4.15A) and DF-1 cells (Figure 4.15B), the same pattern of host cell shut off as seen previously for the WT and position 26 mutant genes was observed. UDL-01 WT and WF10 K26E plasmids effectively induced protein synthesis shut down compared to the empty vector control whereas WF10 WT did not have the ability to control host protein synthesis. Unusually, the UDL-01 E26K construct did show some repressive activity compared to the empty vector control which was not seen with previous experiments, although the reduced shut off was still significantly different from UDL-01 WT segment 3. When PA-X expression was removed from UDL-01

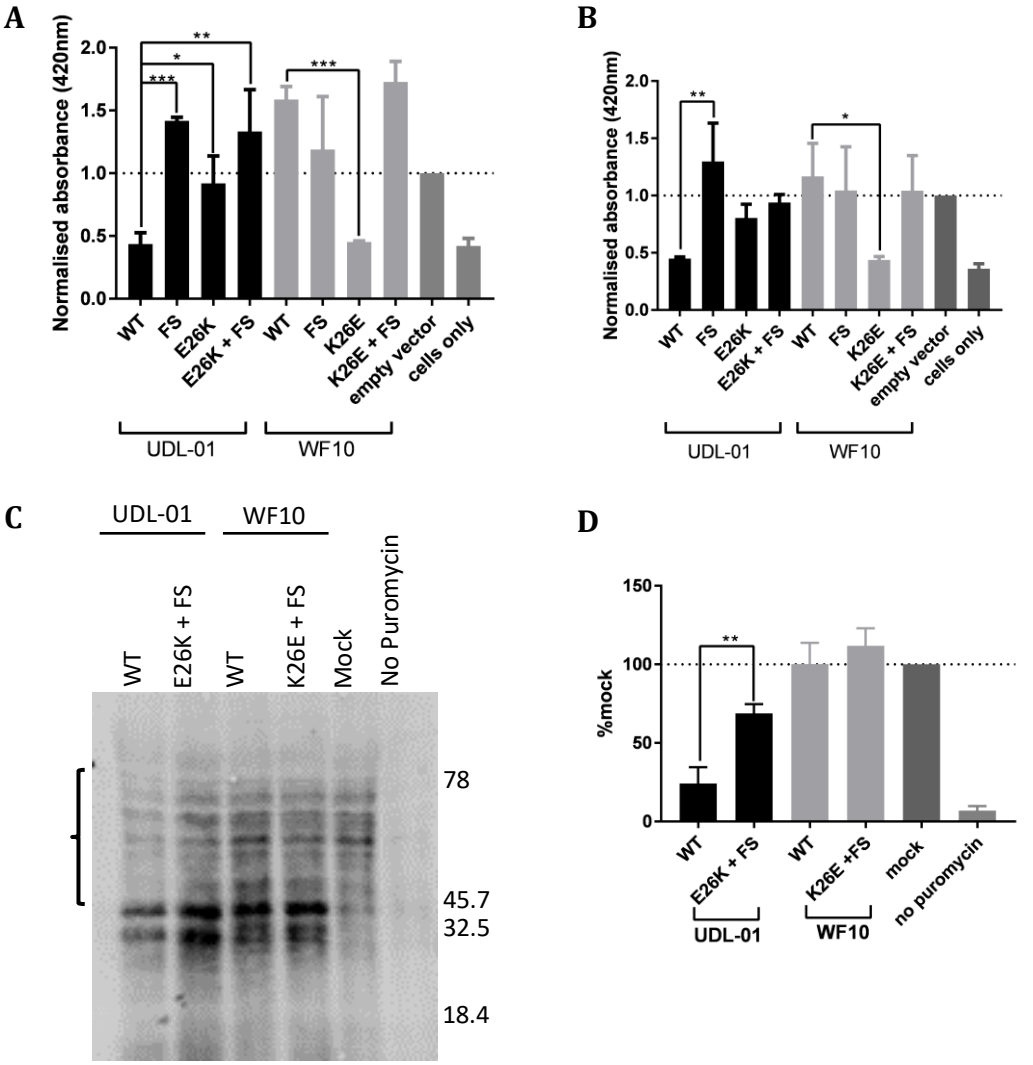

Figure 4.15: Host cell shut off ability of segment 3s containing both an amino acid change at position 26 and removal of PA-X expression. H9N2 segment 3s with differing mutations were transfected into (A) 293T cells or (B) DF-1 cells alongwith a β-galactosidase (β-gal) reporter plasmid. 48 hours post transfection cells were lysed and then levels of β-gal assessed by colorimetric enzyme assay. Results were normalised to an empty vector control where no shut off host gene expression was expected. Graph represents the average of 3 independent experiments +/- SD., P values: ***= 0.0001; **= <0.0097 * = <0.045 (one-way ANOVA – 293T all and DF-1 WF10 panel or Kruskal Wallis – DF-1 UDL-01 panel with multiple comparisons). Host cell shut off within viral infection was then assessed, MDCK cells were infected with each virus at a high MOI (5). 7 hours post infection cells were pulsed with puromycin for 30 minutes. Cells were lysed in SDS-PAGE buffer and (C) western blotted for puromycin. (D) The section highlighted in the bracket was quantified by densitometry using ImageJ analysis software. The area under the curve for each section was calculated and then compared to the mock infected sample. The Graph displays average +/- SD of 3 independent experiments. P values = **: 0.0042 (unpaired T-test).

segment 3 by the FS mutation, the ability of this plasmid to induce host cell shut off was also removed as previously observed. When both the E26K and FS mutation were introduced into UDL-01 PA-X, it was similarly unable to effectively control host cell protein synthesis. The same outcome resulted when both the K26E and FS mutation were introduced into WF10 PA-X. This construct was also unable to repress host cell gene expression acting like UDL-01 WT where shut off activity was removed after inhibition of PA-X expression. This indicated that the effect of the K26E mutation on shut off activity lies within PA- X rather than within PA.

As the double mutant constructs appeared to affect host cell shut off activity within plasmid-based assays, the ability to control host protein synthesis of viruses containing both an amino acid change at position 26 (UDL-01: E26K, WF10: K26E) plus removal of PA-X via mutation of the frameshift site (FS), was investigated using the puromycin assays described previously. MDCK cells were infected with each virus at a high MOI (5), then 7 h.p.i cells were pulsed with puromycin for 30 minutes before being lysed and western blotted for puromycylated polypeptides. As expected, the blot showed multiple bands which in samples from mock infected cells indicated the constitutive levels of cellular protein synthesis. UDL-01 WT virus showed a reduced intensity of puromycin incorporation compared to the uninfected control, but when the double mutation was introduced (E26K and FS) the ability of the virus to control host protein synthesis was removed. Within WF10 viruses neither the WT nor double mutant (K26E + FS) was able to dampen host protein synthesis compared to mock levels (Figure 4.15C). The average amount of cellular protein synthesis compared to

mock infected cells was calculated for 3 independent experiments, via densitometry of the upper region of the blot, as before. UDL-01 WT reduced cellular protein synthesis by approximately 75% compared to mock, but when both E26K and FS mutations were introduced into the virus cellular protein synthesis was only reduced by about 25% compared to mock. No significant difference was seen between WF10 WT and WF10 K26E + FS viruses (Figure 4.15D). This data supports that seen with the plasmid-based methods (Figure 4.13A and B), and suggests that with respect to shut off activity, the amino acid change at position 26 exerts its affect via its location in PA-X rather than PA.

4.3: Discussion

Within this chapter, the ability of H9N2 AIV segment 3s to induce shut off of host protein synthesis was investigated. In order to complete some experiments at the Roslin Institute the mutations previously identified in Chapter 2 which also lied within PA-X were built into 7:1 PR8 reassortant viruses as the laboratories were not set up for AIV use. Interestingly, the introduction of UDL-01 and WF10 PA's into the PR8 backbone did not alter the plaque phenotypes seen as expected, with UDL-01 PA expected to confer a larger plaque size (Figure 1.1). This suggested that the segment 3 is not the only responsible factor for the enhanced plaque phenotype, at least outside of the H9N2 background. Other viral segments that have previously been identified to alter influenza plaque size include segment 2 (Pappas et al., 2008), segment 7 (Yasuda et al., 1994), segment 8 (Solorzano et al., 2005) so this could suggest interactions of the H9N2 PA with other polymerase components could alter viral fitness within the PR8 model, or

interactions with NS1 could affect the innate immune response produced by the PR8 reassortant viruses and in turn affect cell spread. The mechanisms behind the altered plaque phenotype within the PR8 7:1 viruses with H9 segment 3's was not investigated further within this thesis although may make an interesting point to follow up. These studies did however, replicate the increased plaque size of the WF10 K26E virus and partially replicated the decreased plaque size of the UDL-01 E26K virus, cementing this mutations importance in viral replication and fitness, as seen within the previous two chapters. The replication of the viruses with any of the mutations within the PR8 7:1 background was not significantly affected within MDCK cells (Figure 4.1C). This suggests that there was not an incompatibility of the polymerase as the viruses were able to replicate as well as the PR8 WT in terms of viral output.

The main known function of PA-X, host cell shut off, was first investigated using the panel of mutations previously screened which lie in the shared domain of PA and PA-X. Initially, it was noted that a difference in host cell shut off ability was seen between progenitor (WF10) and reassortant (UDL-01) segment 3s, with WF10 WT segment 3 not being able to repress host protein synthesis and UDL-01 displaying activity (Figure 4.2). Several of the mutations screened altered the host cell shut off activity significantly, either removing it within a UDL-01 background or introducing it within a WF10 background. Within WF10 this included E26K and L221R and within UDL-01, included E26K and I118T (Figure 4.1). The E26K mutation previously identified to alter viral replication and pathogenicity reciprocally altered host cell shut off, although at this point it could not be determined if the alteration of shut off activity is the reason the virus

replication is also affected. Two other non-reciprocal mutations were also shown to alter shut off activity, as it was previously seen that WF10 and UDL-01 WT PA-X's have differing shut off activities, it is not inconceivable that the mechanism by which they act are different and therefore the mutations which alter host cell shut off could differ. Previously, others have identified different residues which can alter PA-X shut off activity based on viral strain used. For example, several H1N1 virus strains have been shown on separate occasions to have different combinations of amino acids which can alter the host cell shut off activity. In one study, residues 85, 86, 911, 100, 114 and 186 were shown to be responsible for shut off differences between two H1N1 strains (Desmet et al., 2013), whereas a separate study identified the region between amino acids 192 and 206 to be important for H1N1 shut off activity (Oishi et al., 2015). This shows that it is possible for different strains of the same viral subtype to have different amino acids which can alter PA-X shut off activity.

However, when these mutations were built into PR8 7:1 reassortant viruses no difference in shut off activity compared to WT was observed with the 221 and 118 mutations, although the importance of PA residue 26 was confirmed (Figure 4.4). The lack of change in shut off activity observed in a virus context could be due to other compensatory mechanisms within the PR8 background, perhaps these mutations affect interactions with the NS-1 protein of PR8 and this either prevents or enhances its action depending on the strain. More likely is that the plasmid based assays were not accurate, particularly the UDL-01 I118T within 293Ts has large error bars suggesting large differences between replicates. It is therefore important to use both plasmid and virus based methods

to determine which mutations actually alter host cell shut off in any future studies. Potentially the ability of the virus to control host cell protein synthesis shut off activity due to the presence of an E at position 26 is at least partly responsible for the differing pathogenicity seen between UDL-01 and WF10 viruses, although the cytokine responses seen *in vivo* (Figure 3.13), do not necessarily correlate with this. It would be expected that as the UDL-01 E26K virus does not exhibit host cell shut of *in vitro, in vivo* there would be an enhanced host response. However, the opposite of this actually occurs with UDL-01 E26K showing reduced immune responses. This could be an artefact of the reduced virus replication within the host, where less virus is produced so therefore less immune response occurs. Although nasal tissue M segment titres were largely similar between UDL-01 WT and UDl-01 E26K infected birds so this may be a true effect.

As the E26K mutation lies in PA-X and alters shut off activity the differences between UDL-01 and WF10 PA-X's were next examined. A panel of mutations were made using site directed mutagenesis to produce plasmids with altered PA-X expression; either amount or length, following the protocol described by Jagger et al. (2012). Although the expression of PA-X could be visualised using the IVT technique provided it would have perhaps been better to use α-PA-X or α-PA-N (N-terminal) antibodies to target PA-X or for completion of immunoprecipitations from the IVT product. This would give an increased accuracy to the quantification of protein expression conducted.

When this panel was screened for shut off activity UDL-01 acted as expected; when PA-X expression was removed, by mutating the frameshift site, so was the ability to control host cell gene expression. This ability was also gradually reduced by increasing truncation of the X-ORF. However, within the already inactive WF10 background, no difference in shut off activity was seen with the introduction of any of the mutations (Figure 4.7). WF10 therefore does not possess an active PA-X protein. These shut off activity differences within each strain did not transpire into differences in transcriptional activity of reconstituted RNPs with differing PA-X expression (Figure 4.8). This is in contrast to data from Gao et al. (2015c) and Hu et al. (2015), who previously found that H5N1 and pH1N1 polymerase activities were increased in systems which lack PA-X. However, Lee et al. (2017) showed that PA-X knockout within a H1N1 system decreased polymerase activity. It is known that PA-Xs from different viral strains have differing impacts on pathogenicity (discussed further in chapter 5), so the differential effects on viral transcription are not unwarranted. However, minireplicon assays rely on RNA Pol II-mediated expression of the RNP polypeptides, which will potentially be confounded by PA-X activity, as could the virally-synthesised transcript encoding the reporter gene. Therefore data from such an approach needs to be treated with some caution.

When investigating the effect of PA-X on H9N2 viral replication, it was observed that within full H9N2 AIVs, UDL-01 viruses showed a reduction in plaque diameter with all PA-X mutations other than PTC4 (Figure 4.9). This agrees with data from Khaperskyy et al. (2016), where a reduction in plaque size with PR8 without PA-X was also seen. Within the WF10 background, only PTC1

and PTC4 altered plaque size although this was not to any great extent and the complete removal of PA-X (WF10 FS) did not alter plaque size compared to WF10 WT. Supporting data from Lee et al. (2017), who found no difference in plaque size with knockout of PA-X from H1N1 viruses. The plaque alteration between UDL-01 WT and FS viruses was not as drastic as when E26K is introduced. This is the first instance which suggests that the E26K mutation's effect on virus replication and host cell shut off may occur by different mechanisms, particularly supported by the lack of alteration in plaque size between WF10 WT and FS viruses.

The minor differences in plaque phenotype observed did not transpire in differences in viral output (Figure 4.10). Only the UDL-01 PTC2 and WF10 PTC3 showed any alterations in virus replication, significantly decreasing titres compared to their respective parental WT virus. Although there was a general trend which matched the plaque size data seen previously. It would perhaps be expected that the FS mutation would have a larger effect on replication especially in UDL-01. If the virus cannot actively control the host immune response as with the UDL-01 FS virus, it would be expected that virus output would decrease as the host can more rapidly respond and control virus replication. This has been previously shown by Hayashi et al., 2015, who showed that Cal09 H1N1 virus without PA-X expression had reduced viral replication due to an increased expression of IFN-β within the cells. On the other hand, Jagger et al. (2012), only saw minor decreases in viral replication with the removal of PA-X from 1918 H1N1. It therefore, appears that the effect of PA-X on viral replication is very much strain dependant and in this case, with our H9N2 strains no difference in

viral replication was seen *in vitro* with removal of PA-X. These data suggest that perhaps the mechanism of action of the E26K mutation in host cell shut off and viral replication occurs by two different methods.

To confirm the theory that the two function observed with the E26K mutation within H9N2 viruses are in fact acting via two mechanisms a double mutation was introduced into the H9N2 PA-X's, where both the amino acid at 26 was altered and PA-X expression removed. Within these studies (Figures 4.13 to 4.15), the UDL-01 E26K +FS mutant acted like WF10 +FS, displaying a small plaque phenotype and a reduced viral replication compared to UDL-01 WT. Conversely, WF10 K26E + FS behaved like UDL-01 +FS, with increased plaque diameter and viral replication compared to WF10 WT. These experiments indicate that the two phenotypes seen with the 26 mutation, alteration of host cell shut off (this chapter) and alteration of plaque size/virus replication (chapter 2), potentially occur via two independent mechanisms. With 26 in PA-X affecting shut off and 26 in PA affecting viral replication, as when PA-X is removed but the 26 mutation remains, the viral replication differences are still observed. The mechanisms responsible for these different functions of the E26K mutation were not fully investigated within this thesis, but it could be speculated that the E26K mutation may affect the stability of the PA protein or polymerase complex and therefore alter virus replication. On the other hand, the E26K mutation may alter PA-X interaction with unknown proteins or alter PA-X localisation within the cell to change the host cell shut off ability of the proteins. As the full mechanism of action for PA-X to induce host cell shut off is not well characterised it is difficult to determine if interaction with another viral or host protein was affected. To

investigate this further, the PA-X proteins could be tagged with GFP and GFP-TRAP pull downs followed by mass spectrometry conducted to determine if any protein interactions change between the viral subtypes or with introduction of the E26K mutation. Some preliminary studies were conducted to assess the effect on subcellular localisation of PA-X, and all of the constructs tested showed the same localisation of small puncta within the cytoplasm, so the function did not seem to be linked to localisation.

Within this chapter, the impact of a single amino acid change on the host cell shut off ability of H9N2 AIV has been investigated. The role of influenza accessory protein, PA-X, in H9N2 AIV *in vitro* has also been determined. It appears that position 26 can alter viral replication and host cell shut off via two independent mechanisms although further research is needed to determine the exact mechanisms by which these effects materialise. It is also not possible to discriminate between the pathogenicity effects seen with the UDL-01 E26K virus and its impact on viral replication or host cell shut off. This will somewhat be addressed in chapter 5 where the effect of removal of PA-X from H9N2 AIV *in vivo* will be investigated further.

Chapter 5: How does mutating H9N2 PA-X alter AIV pathobiology *in vivo?*

5.1: Introduction

Chapter 4 characterised the function of H9N2 PA-X polypeptides *in vitro* and identified differences in host cell shut off ability between the UDL-01 and WF10 virus strains. Therefore, in this chapter, the role of PA-X in an *in vivo* setting was examined. Previous research has investigated the role of PA-X in pathogenicity and host immune responses mainly with a focus on mouse models. For example, Lee et al. (2017), showed that removing PA-X expression from a pH1N1 2009 virus reduced viral replication and pathogenicity in mice, which also corresponded with a reduced host immune response. In contrast, using a different strain of pH1N1 2009 virus, Gao et al. (2015b), found that mutating PA-X increased virus replication in mice with consequently higher mortality. Other studies have shown that altering PA-X expression can decrease viral replication and transmission and lead to a delayed pro-inflammatory response within the lungs of pigs infected with swine H1N2 IAV (Xu et al., 2017).

In terms of AIVs, several studies have explored the effect of PA-X, although groups still tend to use mice as the model organism rather than an avian species. Only one study has been conducted which assesses PA-X in HPAIV H5N1 viruses in both chickens and ducks where PA-X removal increased viral virulence and downregulated genes associated with inflammation and cell death (Hu et al., 2015). Conversely, within a LPAIV H9N2 background, PA-X has been shown to be

a pro-virulence factor, with viruses expressing PA-X showing an enhanced mortality in mice corresponding to an upregulation of cytokine and chemokine expression within the mouse lung (Gao et al., 2015c). All of these previous studies suggest that the effect of PA-X is very much dependent on the strain of virus and the host species in which the work is carried out.

Although one study has investigated PA-X function in an H9N2 AIV background, the *in vivo* work was carried out within a mouse model, rather than in the natural infection system of the chicken (Gao et al., 2015c). Therefore, the aim here was to assess the pathogenicity of H9N2 AIVs with different PA-X protein expression profiles and functionality in the natural host, first using fertilised hens' eggs and then using an *in vivo* infection model in White Leghorn chickens.

5.2: Results

5.2.1: Effect of removal of PA-X expression on virus infection *in ovo*

In the first instance the impact of removal of PA-X expression (via the FS mutation) from UDL-01 and WF10 viruses was assessed within 10-day old fertilised VALO (white leghorn) hens' eggs. Adopting the 3Rs principles, this would allow for insights to be gained into the effect of PA-X expression in a less sentient animal model (pre-14 day embryos) prior to using post-hatch chickens.

5.2.1.1: Embryo survival rate following infection with wild type and mutant viruses

As PA-X has previously been shown to alter viral pathogenicity in animal models (Jagger et al., 2012, Gao et al., 2015a+b; Gong et al., 2017), the pathogenicity of our H9N2 AIV strains within an embryonated egg model was first assessed. Ten-fold serial dilutions of each virus (10,000 pfu to 0.001 pfu) were made and used to infect 5 eggs per virus per dilution. Groups of 10-day old SPF white leghorn (VALO breed) hens' eggs were used as per the previous study (section 3.2.1.3). Mock infected embryos were included which were inoculated with sterile PBS. Embryos were candled twice daily up to 84 hours post-infection to check for embryo viability. If a lack of movement of the embryo and/or disruption of blood vessels was seen within the egg they were deemed to be dead. If the embryos survived until the experiment end (84 hours post-infection) they were culled via refrigeration. Samples of allantoic fluid from each egg were collected and "in-cell western" assays were performed to assay for infectious virus. Briefly, MDCK cells were infected with allantoic fluid and 12 hours later cells were fixed and stained using immunofluorescence for viral NP protein in order to determine if death was the result of productive viral infection. All mock-infected samples were negative via the screening method described above (data not shown). Any eggs which did not produce virus-positive allantoic fluid were removed from the survival analysis. This included the 0.001 pfu group from all viruses and the 0.01 pfu group from the UDL-01 WT and UDL-01 FS virus groups. The resultant survival curves only reflect eggs that were definitely infected (data not shown).

An estimation of the LD_{50} was determined from the survival curves of each virus, although accurate LD_{50} values could not be calculated due to 100% mortality not being reached in the majority of groups. With UDL-01 WT virus, the highest viral dose (10,000 pfu) leads to high levels of mortality from 48 hours onwards which is not seen with the UDL-01 FS counterpart at this dose (data not shown). However, lower doses of infection (1 pfu) appear to have increased mortality, up to 100%, in UDL-01 FS infected eggs compared to WT. The LD_{50} estimation for UDL-01 WT virus ranges from 1000 to 0.1 pfu, as a resurgence in mortality was seen at lower doses. With the UDL-01 FS virus it was difficult to estimate LD_{50} as mortality above 50% was only observed with the 1 pfu dilution and it did not occur in a dose dependant manner. However, from these data it can be estimated to be between 1 and 0.1 pfu. This falls within the LD_{50} range of UDL-01 WT so no firm conclusions can be draw over the effect of removal of PA-X expression on UDL-01 virus pathogenicity in this model. However, when % survival is plotted against viral dilution a clear difference can be seen in the trends of data (Figure 5.1), UDL-01 WT survival occurs in a dose dependant manner as seen by the ascending trend line, whereas the UDL-01 FS survival is not dose-dependent. Within the WF10 virus pair, the highest dose of virus (10,000 pfu) led to substantial amounts of mortality from around 60 hours onwards; something that was not seen with the FS counterpart (data not shown). Conversely the WF10 FS virus appeared to have an increased mortality throughout the study duration at 100 pfu compared to WF10 WT. However, 50% mortality was not reached from any dose of either virus until 84 hours post infection and no other notable differences were observed within this viral pair.

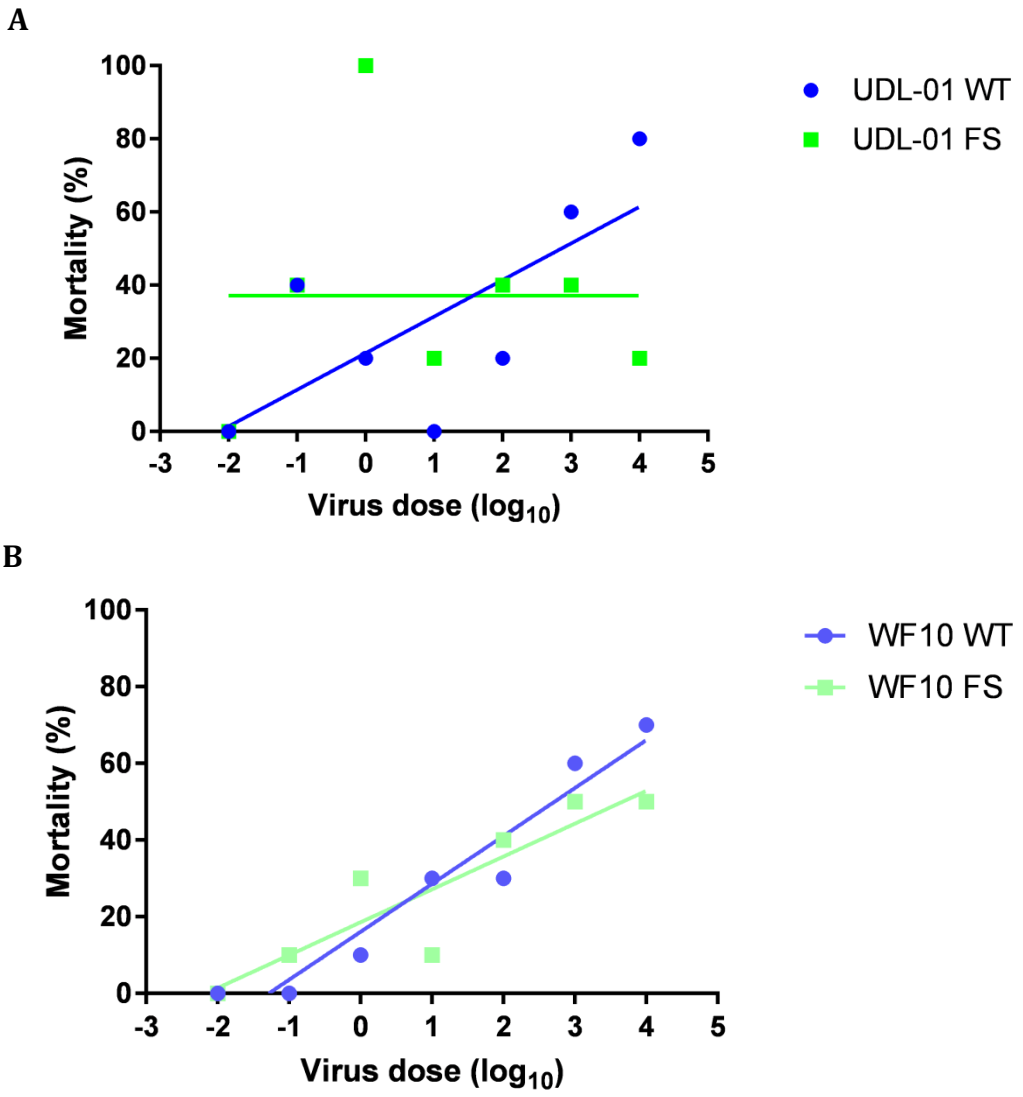

Figure 5.1: Mortality analysis versus virus dose of embryos infected with differing dilutions of H9N2 AIVs. At 84 hours post infection, total embryo mortality after infection with the indicated viruses at each viral dose was calculated. Line represents non-linear fit of data with each data point represent % mortalityl at the viral dilution.

The estimated LD_{50} value for WF10 WT virus was between 1000 and 100 pfu whereas for WF10 FS it was between 10,000 and 100 pfu. There was not a substantial difference in LD_{50} values between the WF10 virus pair. Both WF10 WT and FS have similar dose-dependent effects on survival (Figure 5.1).

The total number of embryos, across the entire dilution range, which died in each of the viral groups was similar between pairs; UDL-01 WT versus UDL-01 FS (40% and 43% respectively), WF10 WT versus WF10 FS (27.5% and 32% respectively). However, there were some differences in the overall end point mortalities amongst the virus dilutions (Table 5.1). UDL-01 FS virus had an increased mortality at 100, and 10 pfu compared to UDL-01 WT. However, at the higher viral dilutions (10,000 and 1000 pfu) lower mortality rates were observed within UDL-01 FS infected embryos. The WF10 virus pair showed generally similar end point mortality rates with some minor differences between the virus pair. Overall, these data did not clearly elucidate to pathogenicity differences amongst viruses with or without PA-X expression.

5.2.1.2: H9N2 *in ovo* infection of embryos and gross pathological observations

The gross pathology of the 10-day old chicken embryos infected with RG H9N2 AIVs was investigated to gain insights into the pathogenicity differences between viruses resulting from expression or not of the accessory protein PA-X. Six 10-day old embryonated SPF white leghorn (VALO breed) hens' eggs were infected with 100pfu of each virus, or sterile PBS for the mock group, via inoculation into the allantoic cavity. This dilution was selected as no mortality

Table 5.1: Summary of embryo mortality at 84 hours post-infection.

	10000	**1000**	**100**	**10**
UDL-01 WT	80%	60%	20%	0%
UDL-01 FS	20%	40%	40%	20%
WF10 WT	70%	60%	30%	30%
WF10 FS	50%	50%	40%	10%

Five embryos per virus per dilution were infected, eggs were candled every 12 hours for up to 84 hours post-infection. Once an egg displayed any of the experimental end points it was chilled and classified as dead. Allantoic fluid samples were tested for presence of viral NP to determine viral infection within the eggs. Any eggs which did not display virus-positive allantoic fluid were removed from the study. % mortality at 84 hours post-infection are tabulated

was seen within the survival experiment described above up to 48 hours post infection and the overall end point mortalities were generally similar. The embryos were candled twice daily to check viability for 48 hours; any embryos which died were refrigerated and removed from the study. 48 hours post-infection the remaining eggs were chilled, the embryos removed from the shell, washed twice in PBS and then photographed to document their gross pathology. Samples of allantoic fluid were taken from each egg and viral titres assessed via plaque assay. Any virus-inoculated embryonated egg which was not positive for live virus was removed from the study to ensure that any pathological differences were likely the result of viral infection. There were no significant differences in viral titres between the UDL-01 WT and UDL-01 FS or WF10 WT and WF10 FS infected eggs (Figure 5.2H). Therefore any differences seen in the gross pathology of the embryos were not obviously related to increased viral load within the eggs.

Images of 3 or 4 embryos per group were selected based on virus-positive allantoic fluid samples and removal of early dead embryos. Mock infected embryos showed little in the way of gross pathological changes, as expected (Figure 5.2A). On initial investigation, both UDL-01 WT and UDL-01 FS viruses led to several embryos displaying severe gross pathological lesions compared to mock infected embryos, with marked bleeding and a macerated appearance of the embryo (Figure 5.2 B and C). WF10 WT virus caused less pronounced changes compared to mock infected embryos; none of the virus-infected embryos showed clear haemorrhaging and all remained intact (Figure 5.2D). However several embryos within the WF10 FS group showed enhanced pathology similar to the

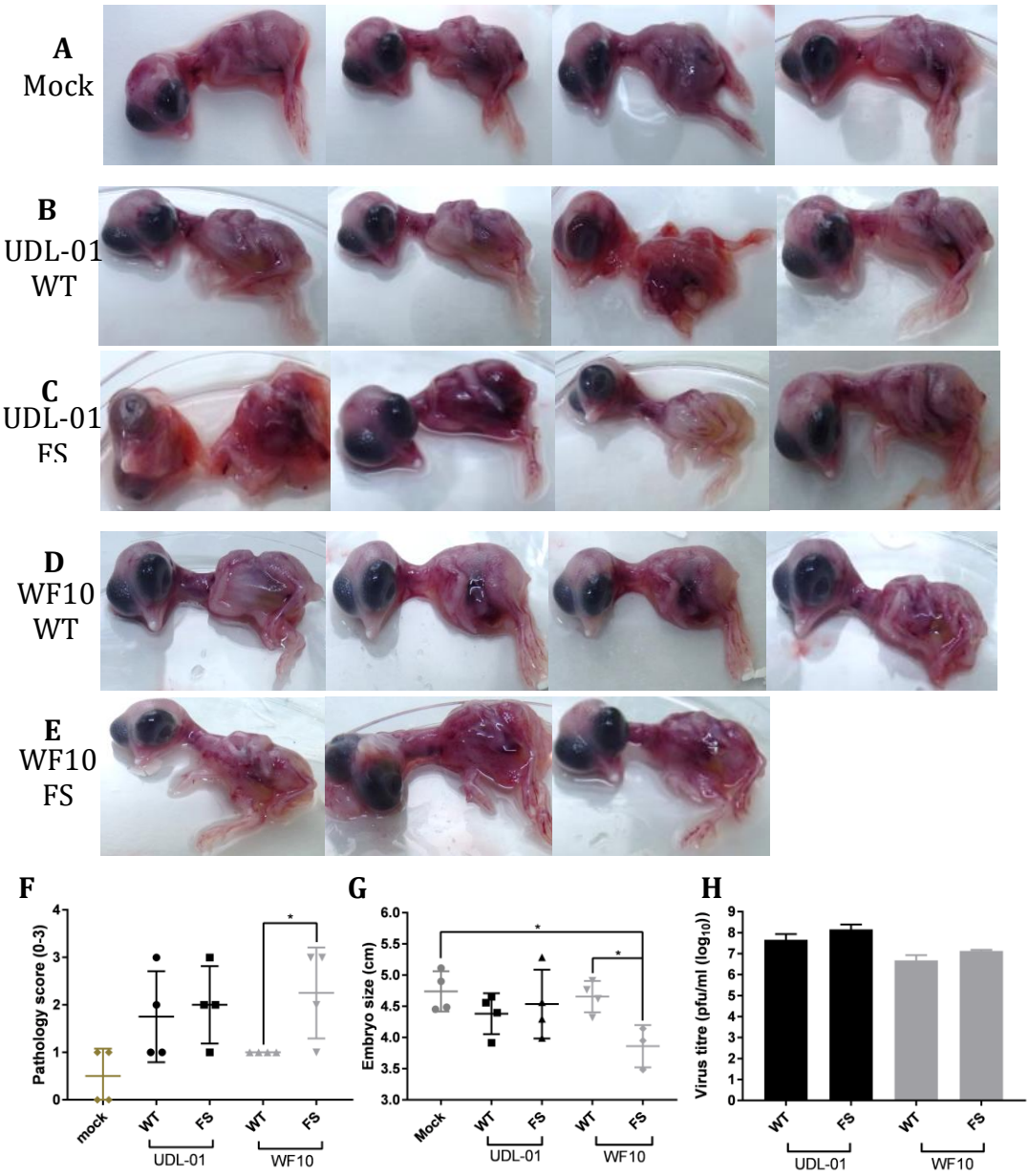

Figure 5.2: Effect of removing PA-X on *in ovo* replication and pathology of H9N2 AIVs. Groups of 6 10-day old VALO eggs were infected with 100 pfu of the indicated viruses. Eggs with virus-negative allantoic fluid or which displayed early embryo death were removed from the experiment. (A-E) Embryos were removed from the shell and washed twice in PBS before imaging to assess gross pathology. (F) Images were blindly scored for gross pathology by 3 independent people. Scoring was based on the following criteria: 0- no obvious bleeding, 1- subtle bleeding, 2- considerable bleeding, 3- very obvious bleeding and/or embryo not intact. Data represent the mean of 3 independent scorers, each scoring 4 embryos per group. (G) Embryo size was estimated using ImageJ analysis software by normalising to the diameter of the petri dish each embryo was imaged in. Data represents average length +/- SD. (H) Viral titres of allantoic fluid taken from positive eggs assessed via plaque assay. Unpaired T-test (F, H) or Kruskal-Wallis with multiple comparisons (F); P values =*: <0.033.

UDL-01 virus pair, with obvious bleeding and disruption of the embryo body (Figure 5.2E).

The gross pathology of the embryos was then blindly scored by 3 group members using the integer scale of 0-3 described in chapter 3. WF10 WT, UDL-01 WT and UDL-01 FS virus infected embryos did not have significantly different gross pathology scores than uninfected embryos. However, UDL-01 WT and UDL-01 FS did contain several embryos which scored more highly than the mock group. The range of pathology scored across the groups however, lead to this difference not being significant. On the other hand, WF10 FS infected embryos were significantly more damaged. There was also a significant difference between the scores of WF10 WT and FS embryos, with the latter group showing more pathology (Figure 5.2F). This suggested that removal of PA-X expression via mutation of the frameshift site (FS) led to enhanced pathogenesis by WF10 virus. Embryo length was also measured using ImageJ analysis software (Figure 5.2G). There were no significant differences between the sizes of UDL-01 WT, UDL-01 FS and WF10 WT infected embryos compared to mock infected animals. However, WF10 FS infected embryos were significantly smaller than mock and WF10 WT infected specimens. Therefore removal of PA-X expression from WF10 enhanced embryo pathology by two measures.

5.2.1.3: Infectious dose differentials between the viruses

To further investigate the effect PA-X expression had on H9N2 AIVs *in ovo*, experiments to assess the amount of virus required to induce infection within eggs were conducted. As before (5.2.1.1.), 10-fold serial dilutions of each virus

(10,000 pfu to 0.001 pfu) were made and used to infect 5 eggs per virus per dilution. A mock group was included which were inoculated with sterile PBS. Embryos were candled twice daily up to 84 h.p.i. to check for embryo viability. At either the end of the study period or once an end point had been met (see chapter 7 for details), embryos were chilled. Samples of allantoic fluid were taken and "in-cell westerns" were performed to assay for infectious virus as previously described (section 5.2.1.1). None of the 'mock-infected' eggs had a positive signal for viral NP protein within the "in-cell western" assays (data not shown). To determine any effects of the PA-X mutations on viral infectivity the EID_{50} of each virus was then calculated via the Reed-Muench method. Only minor differences in EID_{50} were observed between the UDL-01 and WF10 pairs, with the UDL-01 pair being slightly lower compared to the WF10 pair (0.024 vs. 0.032). However, PA-X expression did not alter the EID_{50} between the viral pairs.

5.2.2: Effect of PA-X on H9N2 viral fitness *in vivo*

Gao et al. (2015c), showed that H9N2 PA-X has a pro-virulence effect within mammalian systems of infection. However, little has been done to elucidate the effect PA-X expression has on pathogenicity of H9N2 AIVs within a natural model of infection, the chicken. When the effect of H5N1 PA-X on pathogenicity within avian models was investigated, the presence of PA-X was shown to reduce viral virulence. Therefore, within this study the effect of H9N2 PA-X within a chicken model was investigated. The UDL-01 WT and FS virus pair were taken forward within this study as the WT virus has been well characterised within previous literature (James et al., 2016; Iqbal et al., 2013; Long et al., 2016)

and this virus displays active host cell shut off activity via PA-X and some survival differences were seen after mutation of PA-X *in ovo*. For this experiment, White Leghorn (VALO breed) chickens were used at three weeks of age. Groups of 10 birds housed in self-contained isolators were inoculated with 100µl of a 10^5 pfu/ml stock of either UDL-01 WT or FS virus or sterile PBS (to provide a mock-infected group) via the intranasal route (Figure 5.3). These birds are hereafter termed 'directly infected'. One day post-infection, 8 naïve 'contact' birds were introduced into the isolator alongside the directly infected birds in order to assess viral transmission. Before infection (day -1), and then throughout the experiment, birds were swabbed in both buccal and cloacal cavities from day 1 to day 8 and as well as day 10 and 14 post-infection to determine viral shedding (Figure 5.3). Additionally, environmental samples (taken from food and water) from each group were collected daily throughout the experimental duration. On experimental day 2 (day 2 post-infection for directly infected and day 1 post-exposure for contacts), 3 birds per group (directly infected, contacts and mock) were culled and a panel of post-mortem tissues taken. Tissue sections were stored in both RNA later and snap frozen. Birds were observed twice daily by members of animal services and whilst procedures were carried out for the presence of clinical signs of infection. Mild clinical signs expected during the study included; ruffled feathers, pale comb/wattles, eye and nasal discharge, reddened eyes, snicking and depression. Additional moderate clinical signs that were expected included drooping wings, swollen heads and sporadic diarrhoea. If any signs of severe disease including laboured breathing, persistent diarrhoea,

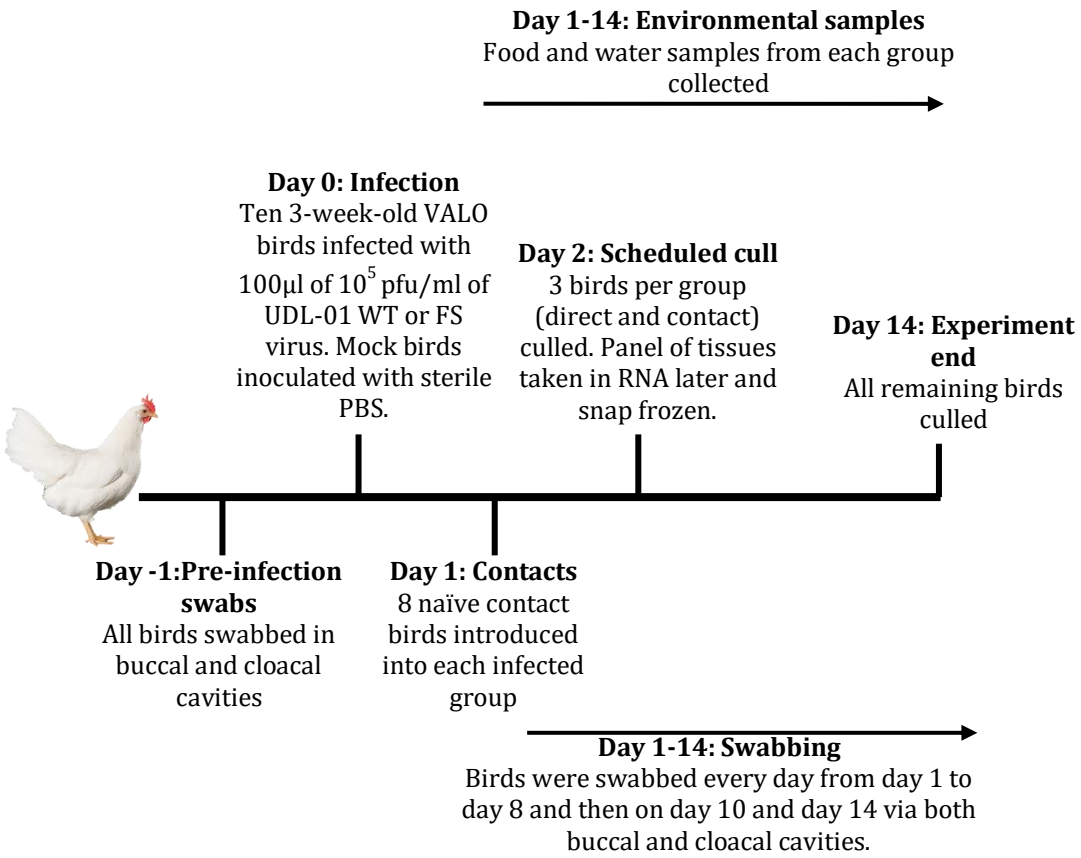

Figure 5.3: *In vivo* experimental design summary. Ten 3-week-old white leghorn (VALO) chickens housed within 2 isolators were infected with 10^5 pfu of either UDL-01 WT or UDL-01 FS virus. A 3rd mock-infected group was kept in a pen and inoculated with sterile PBS. One day post-infection, 8 naïve contact birds were introduced into each infected group. Birds were swabbed in their buccal and cloacal cavities daily between day 1 and day 8 and then on days 10 and 14 post-infection. 3 birds per group (directly infected, contacts and mock) were culled on day 2 post-infection and a panel of tissues collected in RNA later and snap frozen. Throughout the study duration environmental samples (food and water) were collected daily. All remaining birds were culled on day 14 post-infection.

sitting alone and showing no signs to evade capture and in the most extreme instances paralysis and unconsciousness were observed birds were euthanised via a schedule one method. The experiment was terminated on day 14 post initial inoculation, and all birds were humanely culled.

5.2.2.1: Viral shedding analyses from directly infected and contact birds

To study the effect of PA-X on viral pathogenicity throughout the study duration birds were monitored for clinical signs and anything of note was recorded. However, clinical signs throughout the study were minimal for the most part; too minimal to draw any conclusions. The majority of birds showed only minor signs such as mild diarrhoea and depression as expected from previous reports of H9N2 infection (Sun et al., 2010). This was in contrast to the previous study within this thesis (chapter 3), where some mortality was seen with the same UDL-01 WT virus. This difference was most likely linked to the difference in breed of chicken used for each study, with the RIR known to be more susceptible to infection than the White Leghorns (Sironi et al., 2008; Matsuu et al., 2016; Rasool et al., 2014).

In order to assess the ability of the H9N2 viruses which differ in expression of PA-X to replicate within the natural host, birds infected with UDL-01 WT or UDL-01 FS were swabbed via both the buccal and cloacal cavities throughout a two week period post-infection and virus titre determined by plaque assay. Mock-infected birds were also swabbed periodically during the infection period. Throughout the study duration, all mock infected samples were below the limit of detection via plaque assay (2.5 pfu/ml) in both buccal and

cloacal swabs (data not shown). Neither was any live virus detected in any of the cloacal swabs collected during the experiment. These latter data were consistent with Ruiz-Hernandez et al. (2016), who previously found that Line 0 (white leghorn) chickens showed a lack of detectable cloacal shedding. Similarly, although environmental samples were taken from food and water in each isolator daily throughout the experiment, no virus was detected via plaque assay. In contrast, directly infected birds showed readily detectable buccal shedding from days 1-6, peaking at titres of over 10^4 pfu/ml (Figure 5.4A). However, those birds infected with UDL-01 FS (lacking normal PA-X expression) showed a delayed shedding profile compared to birds infected with UDL-01 WT virus. On day 1 and 2 post-infection (Figure 5.4B) UDL-01 FS infected birds shed a significantly less virus than WT-infected animals. By day 3 post infection, shedding levels had evened out between groups (Figure 5.4C). However at day 6, an increased number of animals infected with UDL-01 FS were shedding than infected with UDL-01 WT (Figure 5.4D). Within both groups viral shedding was cleared by day 7 post-infection. To estimate the total amount of virus shed by each group, the area under the shedding curves (AUC) were calculated, giving values of 81,674 for WT UDL-01 versus 241,229 for the FS mutant. This suggested that UDL-01 FS infected birds shed more virus overall than the UDL-01 WT infected birds.

The same trend of delayed shedding kinetics of birds infected with the UDL-01 FS virus was observed within the buccal shedding of contact birds (Figure 5.4E). This difference in shedding with respect to the WT virus was significant on 2 post-infection (Figure 5.4F). Again by day 3 post introduction the amounts of virus shed by each group was similar (Figure 5.4G). UDL-01 FS

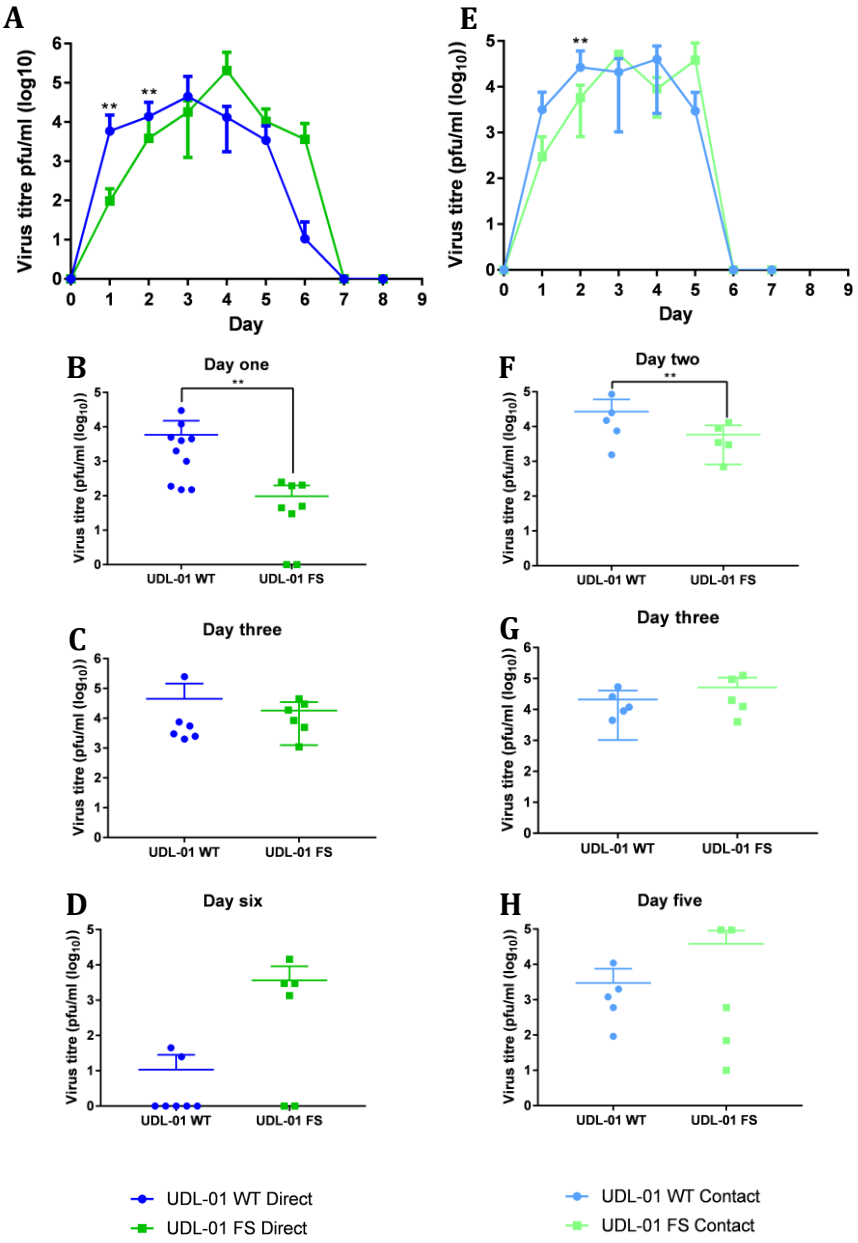

Figure 5.4: Buccal shedding profiles of White Leghorn birds infected with H9N2 AIVs. Birds were infected with either UDL-01 WT virus or a UDL-01 virus lacking expression of PA-X (UDL-01 FS) or introduced one day post inoculation. Swabs were taken from the buccal cavity throughout the study duration and virus titrated via plaque assay to calculate plaque forming units (PFU)/ml. The average +/- SD buccal shedding profile of at least 4 birds per group are shown for (A) directly infected birds and (E) contact birds. (B-D) buccal shedding on separate days post infection for directly infected birds with each bird represented via a single point. (F-I) buccal shedding on separate days for contact birds with each bird represented via a single point. Unpaired T test (Contact Day 2 (F), 3 (G) and 4) or Mann Whitney Test (Direct all days (A, B C and D), Contact Day 1 and 5 (H)) ; P values = **:<0.0063.

infected birds also displayed increased shedding on day 5 post-introduction compared to UDL-01 WT infected birds, although this was not significant (Figure 5.4H). Within both contact groups viral shedding was cleared from day 6 post-introduction. When AUC values were calculated for the contact bird populations, the UDL-01 WT AUC was 94,171 whereas the UDL-01 FS AUC was 104,655 indicating only a marginal difference in shedding. All contact birds became infected within both groups; therefore removal of PA-X from UDL-01 did not alter the transmissibility of the virus in this model. Overall, the shedding profiles of the infected birds suggested that presence of PA-X (within the WT virus) accelerated the buccal shedding of virus compared to a virus which lacked PA-X expression.

5.2.2.2: Stability of mutations to remove PA-X during replication in infected chickens

To determine if the effects on buccal shedding observed within these studies were the result of the removal of PA-X or due to other compensatory mutations within PA or other viral gene segments, RNA was extracted from swab supernatants and prepared for NGS to allow for high quality sequencing reads to be prepared. Within the input virus, the PA-X slippage site mutation were the only differences seen between UDL-01 WT and FS viruses as expected. The NGS data showed that the frameshift site mutations introduced to remove PA-X expression from the UDL-01 FS virus remained in the output viruses from samples isolated from buccal swabs. A further single Q193K amino acid change in the PA gene of a sample that was shed via the buccal cavity of an UDL-01 WT infected bird was seen at consensus sequence level. This lies with one of the PA NLSs and Llompart

et al. (2014), noted that a Q193H change in the PA gene of PR8 was present within a strain which did not have RNA polymerase II degradation ability. However, this phenotype was ascribed to other mutations within the PA and PB2 genes. No further mutations were seen in the consensus amino acid sequences of output viruses from UDL-01 WT or UDL-01 FS infected birds within either the PA gene, the accessory protein PA-X or the remainder of the viral gene sequences. Consistent with the genetic stability of the viruses, no differences were observed within the plaque phenotypes of the input viruses versus output viruses (data not shown).

5.2.2.3: Viral dissemination in tissue and organs of directly inoculated and contact birds

A panel of tissues were taken during post-mortem examination on experimental day 2 from the directly infected, contact, and mock birds and stored either in RNA later or snap frozen. This allowed for viral dissemination throughout the visceral organs to be investigated and compared between UDL-01 WT viruses and those lacking PA-X.

5.2.2.3.1: Presence of M segment RNA within tissues

Tissue samples stored in RNA later were homogenised and RNA extracted, quantified and 100ng of RNA/ sample used in triplicate within qRT-PCR for the viral M gene as a marker for presence of virus within tissues. As before an M gene RNA standard allowed for the copies of segment 7 to be calculated. Tissues from mock infected birds were also processed but all fell below the limit of detection (data not shown), further confirming no infection within this cohort.

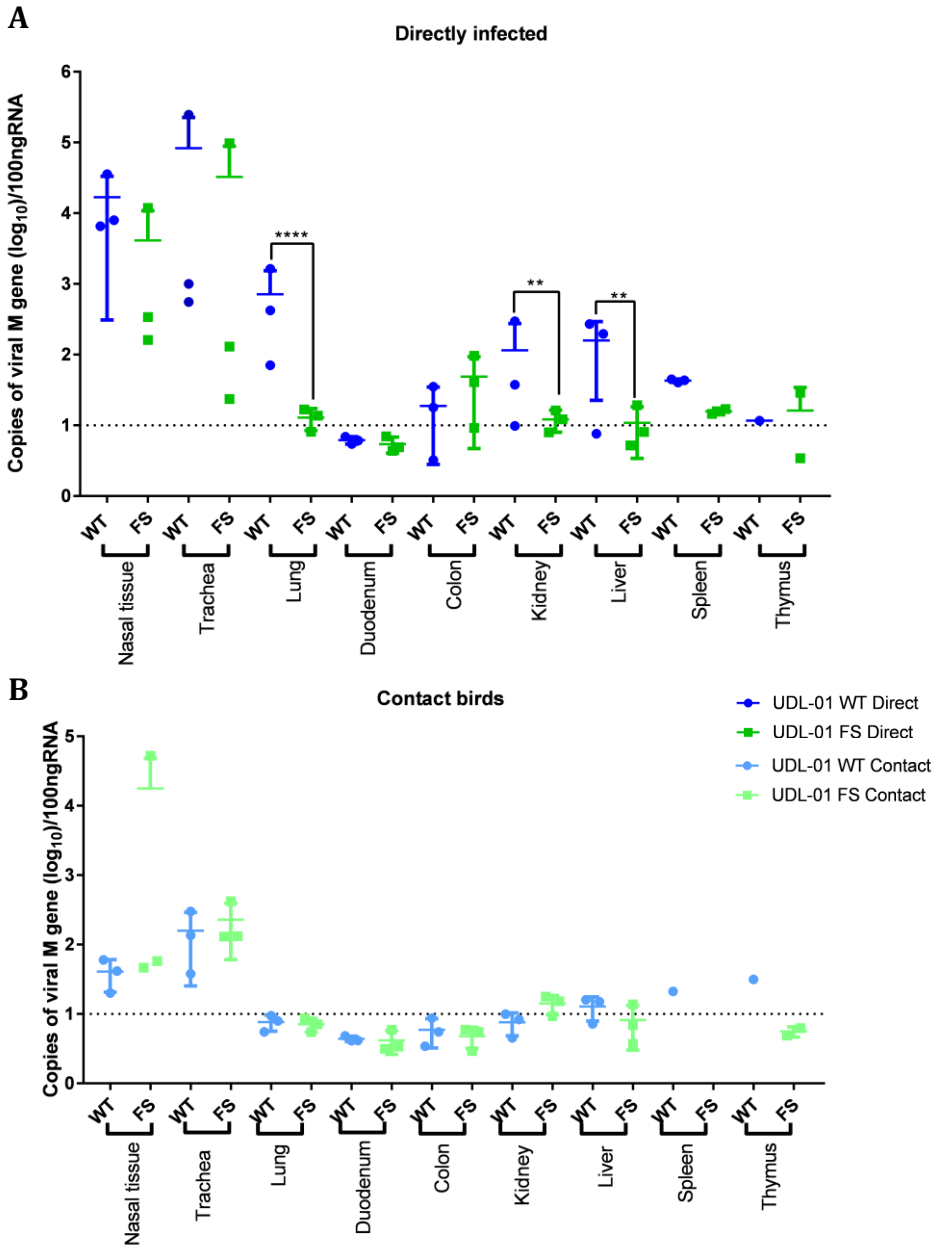

Figure 5.5: Detection of viral M gene within tissues of infected birds. On day 2 post-infection 3 birds per group were culled, a panel of tissues taken and following RNA extraction qRT-PCR for viral M gene carried out. CT values were compared to a M gene standard curve to determine copy number. Graphs show mean +/- SD viral RNA copy number detected within tissues from (A) directly infected birds and (B) contact birds. Unpaired T-test (Direct; Lung, Duodenum, Colon, Kidney, Liver, Spleen, Contact; Lung, Duodenum, Colon, Kidney and Liver) or Mann Whitney test (Direct; Nasal, Trachea and Thymus, Contact; Nasal and Trachea) P values = ****: <0.0001, **: <0.006.

Within tissues isolated from directly infected birds, viral replication was primarily observed within the upper respiratory tract in both UDL-01 WT and UDL-01 FS infected birds (Figure 5.5A). There were no significant differences in M gene copy number within the nasal tissue and trachea. However, significantly more viral RNA was detected lower down the respiratory tract from lung tissues of UDL-01 WT infected birds. Within other visceral organs, little M gene RNA was amplified, particularly in tissues collected from UDL-01 FS infected birds. Both the liver and kidneys of UDL-01 WT infected birds had significantly more viral M gene compared to tissues from UDL-01 FS infected birds. Therefore, UDL-01 WT virus showed increased viral dissemination compared to UDL-01 FS at day 2 post-inoculation. Tissues taken from the contact birds at day 2 of the experiment, and therefore day 1 post their introduction, again showed the highest level of M gene RNA detection from respiratory tissues, most notably the nasal tissue and trachea (Figure 5.5B). Viral loads were not significantly different between UDL-01 WT and FS infected birds at this point and little M gene was amplified within any other tissues tested. Overall, these data show that removal of PA-X from UDL-01 AIV (FS) led to reduced viral dissemination at day 2 post-infection for directly inoculated birds.

5.2.2.3.2: Detection of virus in the tissues from wildtype or mutant virus-infected birds

In order to determine whether the isolation of viral RNA from tissues corresponded to isolation of live virus, snap frozen tissues were processed. 30 mg of tissue was homogenised in serum free DMEM, clarified, and the supernatants

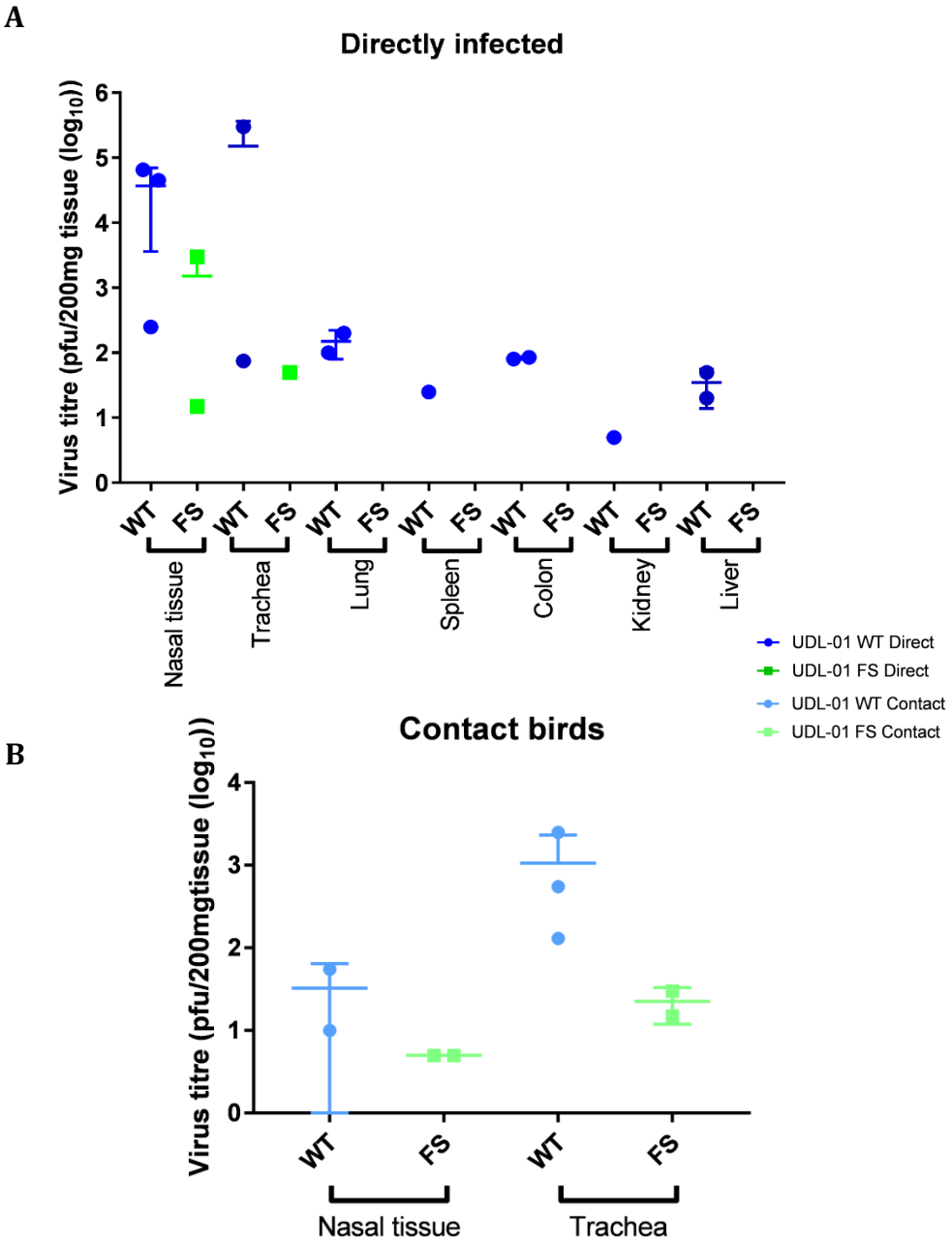

Figure 5.6: Detection of virus from tissues from infected birds. Snap frozen tissue samples were homogenised with serum free DMEM. Supernatants were clarified and titrated via plaque assay. (A) viral isolation from directly infected birds (B) viral isolation from contact birds. Data represents viral titres present in each birds tissues. Error bars +/- SD. UDL-01 WT represented in blue, UDL-01 FS represented in green.

used to titrate presence of virus via plaque assay. No infectivity was detected from any tissues collected from mock infected birds (data not shown). Tissues collected from birds directly infected with UDL-01 WT virus had variable but sometimes high titres of virus in tissues from the upper respiratory tract (Figure 5.6A). However, not all birds gave positive results using this assay, in contrast to the qRT-PCR results seen previously. Only three samples from birds directly infected with the FS mutant were positive for infectious virus; two from the nasal tissue and one from the trachea, all at lower average titres than the WT counterparts. Some of the lung, spleen, colon, kidney and liver samples collected from UDL-01 WT infected birds were also positive by plaque assay, whereas none of the same tissues were positive from the UDL-01 FS infected birds at day 2 post-infection.

In contact birds, live virus was only isolated from the nasal tissue and trachea of birds infected with either UDL-01 WT or FS viruses, again with lower average titres of the mutant virus (Figure 5.6B). All other tissues were negative for virus by plaque assay (data not shown). Unfortunately, statistical analysis could not be carried out due to the only two of the three UDL-01 FS infected birds showing positive results via this assay. Nevertheless, overall, these data support that previously seen via detection of viral M gene RNA and indicate that UDL-01 WT virus was better able to disseminate throughout the chicken visceral organs compared to UDL-01 FS virus. This suggested that the PA-X protein plays a role in viral spread throughout the host, at least within this viral pair and this model of infection.

5.2.2.4: Cytokine expression in infected tissues

Next the immune responses of the chickens to infection with the viruses were assessed. PA-X is known to alter host responses by downregulating protein synthesis (Jagger et al., 2012). Within different host species, modulation of PA-X expression has been shown to alter host expression of cytokines and chemokines; for example an H9N2 AIV unable to express PA-X has been shown have decreased expression of IL-6, IL-1β, CCL3, IFN-γ and TNF-α within a mouse model compared to a virus with PA-X expression (Gao et al., 2015c). Therefore within the experiments reported here, the aim was to determine if alteration of PA-X expression in UDL-01 led to differential cytokine and chemokine responses within the chicken host. In the first instance the tissues of the respiratory tract (trachea and nasal tissue) were selected as the most viral RNA and live virus was isolated from these tissues. As before, RNA extracted from homogenised tissues was then used to complete qRT-PCR for a range of chicken cytokines and markers of the interferon response. Three reference host genes (RPLPO-1, RPL13 and 28S rRNA) were selected for normalisation and the most stable gene across the samples chosen for normalisation.

Nasal tissue at day 2 post-infection from birds directly infected with UDL-01 WT or UDL-01 FS viruses displayed little differences in immune response (Figure 5.7A). Some minor differences were seen with expression of IFN-β, IFN-γ and IL-18 with UDL-01 WT infected birds generally expressing higher levels of cytokines. Although this only reached significance with the expression of IL-1β

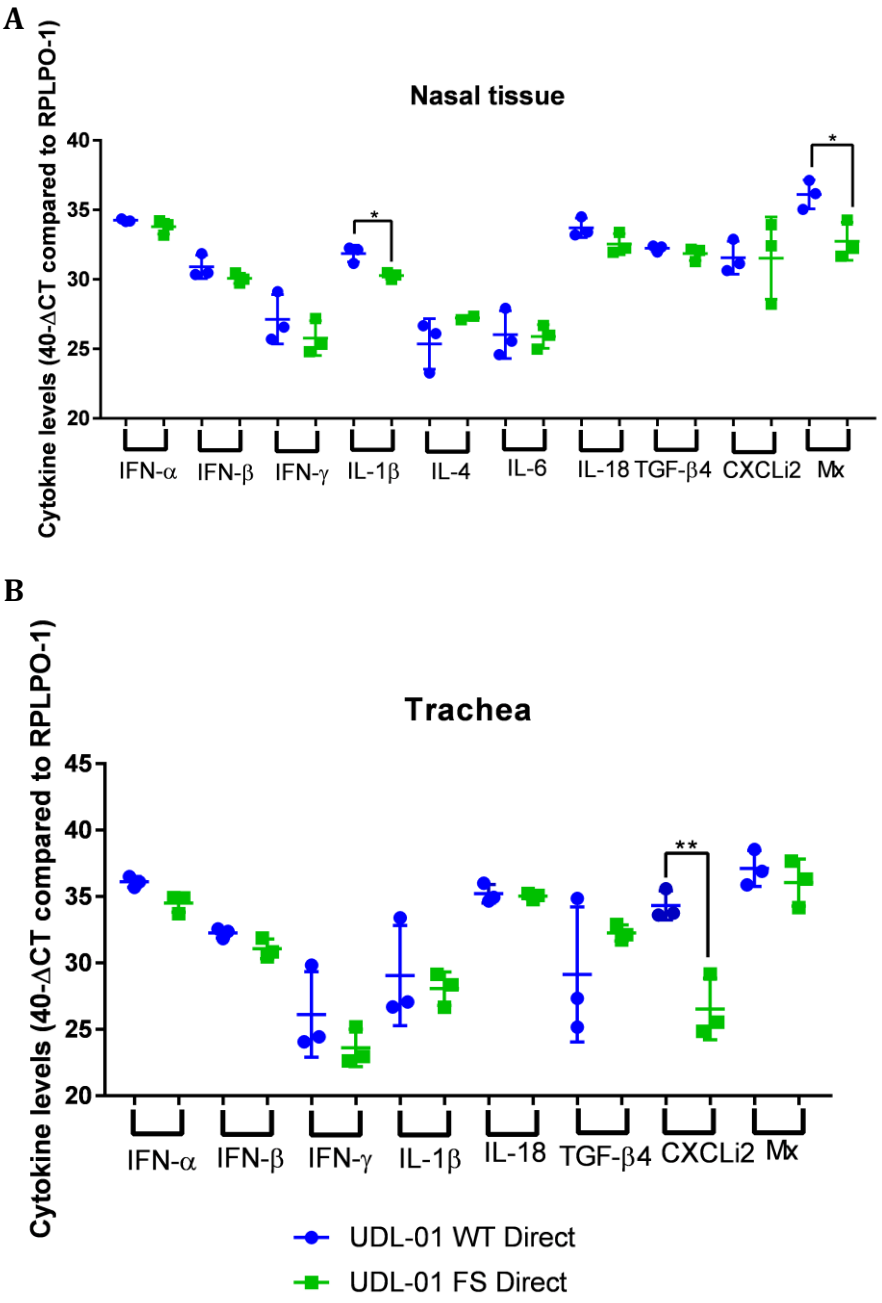

Figure 5.7: Cytokine expression compared to reference gene in directly infected birds. RNA was extracted from nasal tissue (A) or trachea (B) of WT UDL-01 and UDL-01 FS infected chickens. qRT-PCR was performed for a panel of cytokines and levels compared to RPLPO-1 reference gene were calculated. Cytokine expression for each bird is represented in a single dot, with error bars displaying mean +/- SD of tissues from n=3 chickens. Unpaired T-test (All Nasal tissue (A) Trachea- IFN-β, IFN-γ, IL-1β, IL-18, TGF-β4, CXCLi2 and Mx) or Mann-Whitney Test (Trachea IFN-α) P values = **= 0.0062, *= <0.03

and Mx, with UDL-01 WT infected birds expressing higher levels of these immune markers.

Immune responses in the tracheas of directly infected birds showed a similar trend to those in the nasal tissue (Figure 5.7B). Few differences in cytokine expression were seen between UDL-01 WT and UDL-01 FS infected animals. UDL-01 WT infected animals again tended to have an increased expression of IFN-β, IFN-γ and IL-1β although this only reached significantly different levels with CXCLi2. There was more variation in the responses within the trachea samples compared to the nasal tissue, particularly within the UDL-01 WT infected birds.

Tissues taken from contact birds on day 1 post-exposure, were also assessed for their immune responses. Within the nasal tissues of these birds, there were no significant differences in expression of any of the tested cytokines between the UDL-01 WT and UDL-01 FS infected birds (Figure 5,8A). There were some minor fluctuations with UDL-01 FS infected birds tending to show a slightly increased expression for example, IL-6, IFN-β, IL-1β and Mx. This is the opposite trend to that seen on day 2 with the directly infected birds (Figure 5.7A).

Within the trachea samples taken from contact birds on day 1 post exposure, again no significant differences were seen in cytokine expression between UDL-01 WT and UDL-01 FS infected birds (Figure 5.8B). Although as with the nasal tissue samples UDL-01 FS infected animals tended to exhibit a slightly increased response particularly with IFN-α and CXCLi-2. However, the opposite was seen with TFG-β4 where expression was higher within UDL-01 WT

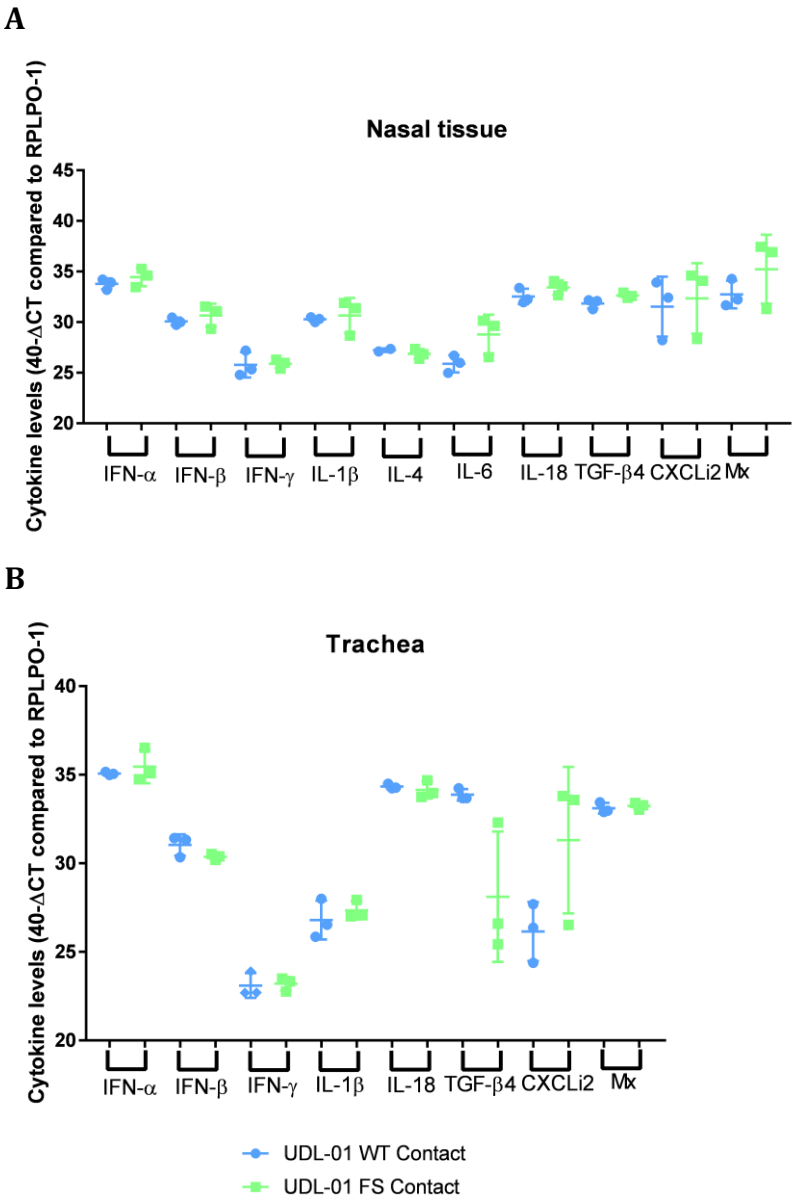

Figure 5.8: Cytokine expression compared to reference gene in contact birds. RNA was extracted from nasal tissue (A) or trachea (B) of WT UDL-01 and UDL-01 FS infected chickens. qRT-PCR was performed for a panel of cytokines and levels compared to RPLPO-1 reference gene were calculated. Cytokine expression for each bird is represented in a single dot, with error bars displaying mean +/- SD of tissues from n=3 chickens. Unpaired T-test (all contact Nasal, Contact Trachea- IFN-α, IFN-β, IL-1β, IL-18, CXCli2 and Mx) or Mann-Whitney Test (contact Trachea – IFN-γ and TGF-β4) used, no significant differences seen.

infected tracheas. Overall, there were few differences in cytokine expression between UDL-01 WT and UDL-01 FS infected birds and the differences seen appeared to be tissue dependant.

5.3: Discussion

In this chapter, the role of the accessory protein PA-X within H9N2 AIV was investigated within avian *in vivo* models; first using fertilised hens' eggs and then 3-week-old chickens. Within *in ovo* studies, UDL-01 infected embryos showed differences in their dose response to mortality, with UDL-01 WT having the expected effect, where higher viral dose leads to increased mortality, whereas UDL-01 FS had no dose response to mortality. This could suggest that removing PA-X from UDL-01 viruses does alter virus pathogenicity to some extent although repeat experiments would be required to confirm this. On the other hand, there was no difference between the WF10 virus pair in terms of dose response to mortality, this could be expected due to the lack of functionality previously seen with the WF10 PA-X protein. However, when the gross pathology of the embryos was assessed, embryos infected with UDL-01 viruses with or without PA-X expression did not differ in their gross pathology, whereas, removal of PA-X from WF10 viruses appeared to increase pathogenicity (Figures 5.3 and 5.4). This could suggest that although WF10 PA-X is not functional in terms of host cell shut off, it could have an additional, as yet unknown, function which is affected when the protein is removed from WF10. This in turn could affect gross pathology caused by the virus. Interestingly, the results seen here with non-functional WF10 PA-X differ to those seen by Hussain et al., (2019), where PR8 (H1N1)

lacking PA-X exhibits a reduced gross pathology of chicken embryos and reduced embryo size. PR8 has also been shown to have a non-functional PA-X in terms of host cell shut off. This difference is likely due to strain variations but could act via a common mechanism. This was not investigated any further during this thesis although repeat studies and additional research into the mechanism of action would be beneficial to increase the confidence in these findings.

The effect of PA-X expression *in vivo* was then assessed using chickens as an avian model for infection. In these studies, loss of PA-X from the UDL-01 background led to delayed viral shedding, with virus being shed through the buccal cavity at later time points than with the WT virus with normal PA-X expression (Figure 5.6). This is understandable as, if PA-X functions to enable the virus to escape from the host immune response by dampening host production of cytokines, it is likely the virus is able to more rapidly replicate within the host. Whereas if the virus is unable to control the host antiviral response via PA-X, it might take longer to overcome this mechanism. It may be beneficial for viruses to contain PA-X as the enhanced shedding could be enhance transmission and environmental deposition. This would provide the virus an advantage within a chicken shed, as is this situation, birds are densely packed and viruses have little need to remain in the environment for long periods of time. The replicative advantage that expression of PA-X gives the H9N2 virus within the chicken host could be enough to ensure that this virus is first transmitted to the other birds within the flock. It would be interesting to complete some competition studies to confirm any transmission advantages over the UDL-01 FS virus which were not seen within these studies. Other studies have shown the influenza PA-X also

enhances the shedding window, with FS viruses being cleared more quickly in Cal09 (H1N1) infected mice (Lee et al., 2017). An enhanced shedding period has previously been shown to be beneficial for virus transmission within chickens (James et al., 2016), with the authors hypothesising that expression of full length PB1-F2 within AIV increases the period when transmission to naïve hosts can occur, giving benefit within backyard poultry production, when contact between animals less frequent than in large poultry houses. It appears that again the role of the accessory protein PA-X in shedding and transmission may be very much strain dependant and if this links to the virus host remains to be seen. In this instance it appears that UDL-01 PA-X enhances the initial shedding period to populate other animals and the environment rapidly. This would give advantages in initial transmission in a busy poultry shed compared to viruses lacking PA-X. The reduced shedding at early time points by UDL-01 FS could of course also be related to the lack of host shut off ability of the virus, whereby the host immune response is better able to control the virus within its initial replication period compared to UDL-01 WT. This restriction appears to subside by day 2 post infection, where other viral mechanisms such as the action of NS-1 could dampen the host response to allow the virus to replicate efficiently.

Any correlation of this altered shedding with the pathogenicity of these viruses could not be determined as the clinical signs observed within the VALO chickens were minimal and no distinction could be seen between the groups. There was also a lack of cloacal shedding and environmental deposition in the VALO breed of birds, however this was expected from previous reports (Sironi et al., 2008; Matsuu et al., 2016; Rasool et al., 2014). This made it difficult to draw

firm conclusions on the impact of shedding by PA-X. As if the UDL-01 WT had for example, also had enhanced environmental deposition and cloacal shedding we could conclude that PA-X within H9N2 acts to enhance the shedding window to increase contact time between host and virus and therefore enhance shedding. Therefore, in future studies it would be more beneficial to use RIR birds to see if these conclusions can be drawn.

Viral dissemination to the chicken visceral organs of the UDL-01 WT virus compared to the FS virus was enhanced at day 2 post-infection in the directly infected birds. This is expected as if the virus is unable to control the host response as efficiently, the innate immune system is able to more rapidly clear virus infection. Samples were only collected at one time point post-infection, so in future studies it would be interesting to collect samples at later time points to determine if the FS virus can still spread systemically, but more slowly as with the shedding where overall, amounts of virus shed were similar the response was just delayed within the UDL-01 FS virus.

Immune responses within birds infected with UDL-01 FS virus were largely similar to those responses within birds infected with the WT virus. However, subtle differences were observed, although perhaps not in an expected fashion. Within the upper respiratory tract of birds directly infected with UDL-01 FS a reduction in expression of IL-1β, Mx and CXCLi-2 was seen. It would be expected that increases in expression of cytokines would be seen as with previous studies (Jagger et al., 2012; Gao et al., 2015a; Hu et al., 2015).However, our data does support that from Gao et al., (2015c), where H9N2 AIV within a

mouse model also showed a downregulation of cytokines compared to H9N2 virus containing PA-X. This could suggest that H9N2 PA-X has an alternative mechanism of action compared to other strains although further work needs to be completed to support this. The reduction in immune response at day 2 post infection seen with the UDl-01 FS virus could be linked to the reduced virus present at this time point within the tissues selected. If the ratios of M gene: cytokine expression are calculated there is a generally increase within the UDL-01 FS infected birds (data not shown). Therefore, if the same levels of replication were seen it is possible that the UDL-01 FS birds would have increased levels of cytokines as we would expected from the known functions of PA-X. To confirm this it would be useful to conduct some *in vitro* studies with equal amounts of virus to see how cytokine responses are altered. On the other hand, within contact birds at day 1 post infection, UDL-01 FS infected birds had slightly increased expression of cytokines such as the Type-1 IFNs, IL-6, IL-18, Mx and CXCLi2, however, none of these differences were significant. It appears that UDL-01 PA-X can impact upon expression of pro-inflammatory cytokines and chemotaxis. This suggests that the dynamics of cytokine expression across the infection period may differ with PA-X expression. It would be interesting to take samples at later time points post infection to determine if the immune response dynamics are altered.

The VALO breed of bird used for these studies was not the ideal choice, due to the limited clinical signs seen and the lack of cloacal shedding of the virus. This meant that viral pathogenicity was not able to be fully assessed. Unfortunately, circumstances (outside my control) with ordering of animals

meant that using White Leghorns was the only way the study could go ahead, but it would have been preferable to use RIR (as in chapter 3) to better assess pathogenicity. It would have also been interesting to assess the function of WF10 PA-X on replication, pathogenicity and transmission within chicken models due to the differences seen in embryo gross pathology with these viruses. However, due to the space limitations of our animal facility and time scales for this project only one virus pair could be assessed.

Overall, within this chapter, the effect of PA-X expression on H9N2 viral fitness, transmission, host dissemination and cytokine response was assessed. Expression of PA-X from an H9N2 AIV in a chicken model of infection enhanced viral shedding through the buccal cavity and increased the ability of the virus to disseminate throughout the host.

Chapter 6: Final Discussion

6.1: Conclusions

The aim of this study was to elucidate the mechanisms by which H9N2 AIVs have evolved increased fitness, transmission and pathogenicity within poultry populations by comparison of an early H9N2 isolate (A/guineafowl/Hong Kong/WF10/99-WF10) and a later reassortant H9N2 isolate containing PB2, PB1, PA and NS segments derived from HPAIV H7N3 (A/chicken/Pakistan/UDL-01/08). By identifying the molecular basis of the enhanced fitness of these novel reassortant viruses, innovative control mechanisms could potentially be revealed or improvements could be made to vaccine design, as well as increasing our fundamental understanding of influenza virus biology.

The data represented within this thesis provide evidence that a single amino acid change within the PA gene is able to swap several phenotypes between the two viral strains. Introduction of PA E26K within UDL-01 reduced viral plaque size and viral replication *in vitro* as well as decreasing viral shedding and pathogenicity *in vivo*. It was found that this amino acid change exerts its function at least in part by its action within the accessory protein PA-X. UDL-01 and WF10 PA-Xs exhibited differing effects on the virus's ability to induce host cell shut off; UDL-01 PA-X had high shut off activity and WF10 PA-X had no measurable shut off activity. When the amino acid change at position 26 was introduced, this host cell shut off phenotype was switched between the two viruses. However, the exact mechanism of action remains undetermined. The polymorphism is in the endonuclease domain shared by PA and PA-X and

although its location on the surface adjacent to the enzyme active site plausibly suggests an effect on RNA substrate binding, this might also predict an effect on viral mRNA synthesis through decreased cap-snatching; something that was not seen. One possibility is that other substrate-binding activities within the polymerase trimer (*e.g.* cap-binding by PB2) compensate for any defect. Detailed biochemical analyses using purified polymerase might permit this hypothesis to be tested. Another possible mechanism of action for the E26K mutation could be its ability to affect the stability of the polymerase. If having 26K within the PA protein makes the virus more unstable, it may be producing an increased number of DI particles or RNAs. This could also link with the increased detection of UDL-01 26E virus within water samples, although further work would need to be completed *in vitro* to confirm the effect on stability in the water in a more controlled manner.

The small plaque morphology of the WF10 H9N2 AIV links with its inability to control host cell shut off. This is because if the virus is unable to control the host innate immune response, the host can prevent the spread of virus to neighbouring cells. This therefore restricts the virus spread so the 'hole' within the cell sheet caused by viral CPE is smaller. The opposite can be said for UDL-01 where the virus can control the host immune response, thus can spread further between cells and cause larger areas of CPE and therefore a larger plaque. The mechanism of action of the difference in control of the host immune response between the two viruses was not fully determined within this thesis however, it was the result of an E26K change within PA. These two phenomenon were however, determined to be the result of two separate functions; the plaque

phenotype was the result of E26K's position in the PA protein, whereas the effect on host cell shut off was the result of E26K's position in the accessory protein PA-X.

Further studies also investigated the role of the PA-X protein within H9N2 AIV using chickens as an *in vivo* model. Results from this were in support of those found by Gao et al. (2015c) in some part, who looked at the role of H9N2 PA-X in a mouse model and found that it was a pro-virulence factor, whose expression led to higher expression levels of cytokine and chemokines within the animals' lungs. Within this thesis, it was demonstrated that a H9N2 virus able to express PA-X did induce higher cytokine production within the chicken respiratory tract than the mutant counterpart lacking PA-X but the role of PA-X in virulence could not be determined as no clinical signs were observed. The presence of PA-X did enhance viral replication and dissemination within chickens. These differences could be due to the different H9N2 strains used for the studies, or the limited pathogenicity seen in the precise model system used here. Plausibly, it could also be due to our using the virus's natural host as a laboratory model. These findings increase our understanding of the effect of the PA gene within H9N2 AIV biology and also increase knowledge on the accessory protein PA-X. The ability of UDL-01 WT virus to shed virus more rapidly than when PA-X was removed, shows that it is important for H9N2 AIVs to deposit in the environment quickly after infection. It may be beneficial for viruses to contain PA-X as the enhanced shedding could be beneficial for transmission and environmental deposition. This would provide the virus an advantage within a chicken shed as in this situation, birds are densely packed and viruses have little need to remain in the

environment for long periods of time. The replicative advantage that expression of PA-X gives the H9N2 virus within the chicken host could be enough to ensure that this virus is first transmitted to the other birds within the flock.

6.2: Future work and directions

There are still a number of key areas that would increase our understanding of the enhancement in viral fitness seen in H9N2 AIVs following internal gene reassortment as well as furthering the reach of these studies to look at more specific mechanisms of action. This thesis only characterised the effect of E26K on viral fitness whereas other polymorphisms are seen at this site in the natural influenza virus population, including 26G, 26D and 26Q. So to further characterise the significant amino acid variation at this position, the effect of these other polymorphisms could be investigated in a similar manner. Such studies would further our understanding of the minor variants at this position within the influenza virus population.

Another area where further study would be advised would be to look further at understanding the molecular basis for the effects of the E26K amino acid change on PA-X activity, as little was done to elucidate the exact molecular mechanism of action. Potentially the subcellular localisation of GFP tagged PA-Xs could elucidate to this. Initial studies, were completed although no differences could be seen in localisation between the mutants. However, these studies were not taken further. It was planned to complete GFP-TRAP pulldown studies following transfection of cells with GFP-PA-X in order to determine any differences in host cell interacting proteins between UDL-01 and WF10 PA-Xs

with or without the E26K mutations. However, technical difficulties with the experimental technique did not allow for this to be completed within the time constraints of the study. This would have potentially further elucidated mechanisms of action of both influenza PA-X in general and the E26K mutation. One factor which was not investigated within this thesis, was the endonuclease activity of the PA-Xs and whether UDL-01 and WF10 PA-Xs have different endonuclease activities which could explain their differences in host cell shut off ability. This would build upon data from Bavagnoli et al. (2015), who show that the truncated form of PA-X has a reduced endonuclease activity compared to full length PA-X.

Another potential mechanism of action of the PA 26 mutation could be examined by looking at the number of defective interfering (DI) RNAs produced by the viruses used in these studies. DI RNAs are incomplete RNAs with, usually, large internal deletions. They can be replicated and transcribed by the RNA polymerase and packaged into the virion. However, this allows for the production of defective viral particles (Nayak et al., 1985). The production of DIs has been suggested to be generated as the result of a "jumping" polymerase (Jennings et al., 1983). A single amino acid change within PA (R638A) has been shown to produce an increased number of DI RNAs and consequently the virus produced pin head plaques (Fodor et al., 2002). Work by Bean et al. (1985) may also support this hypothesis as they showed that viruses with increased DI production were avirulent while those without DI production had increased virulence. DI formation was not examined in this thesis. However, these previous studies could suggest the hypothesis that the presence of 26K within the PA gene leads to a

destabilised polymerase which allows for the "jumping" of the viral polymerase to produce incomplete RNAs which are then packaged into the virions. This could then lead to the production of a virus with a smaller plaque phenotype (as seen with WF10) and a reduced virulence.

The *in vivo* studies described in chapter 3 and 5 only used UDL-01 viruses due to the time and space limitations of the animal facilities at the Pirbright Institute. It would have been beneficial to investigate the effects of K26E and removal of PA-X (FS) within a WF10 viral background in order to investigate if the reciprocal effect is seen compared to UDL-01 viruses. This would further cement the importance of amino acid 26 within the phenotypes of UDL-01 and WF10 H9N2 AIVs. Investigation of WF10 viruses with altered PA-X expression could elucidate any additional mechanisms of action of PA-X, as WF10 PA-X was shown not to induce active host cell shut off *in vitro* (chapter 4). It was also planned to look at the histopathological effects of the viruses in a number of tissues and samples were collected within 10% NBF to do so. However, time constraints of the project did not allow for this to happen. Analysis and processing of these samples would allow for investigation into immune cell proliferation into different tissues to further cement the ideas that E26K and PA-X play a role within the host immune response and to identify which tissues viral antigen is present within.

One factor within the *in vivo* studies that would have been interesting to continue further was the increased detection of UDL-01 E26K virus within the isolator water samples than the UDL-01 K26E virus. This could suggest a

mechanism behind the innate immune activation differences seen between the two virus caused by viral stability differences. In order to test the stability of the two viruses in water, *in vitro* studies could be conducted whereby the two viruses were left in water samples for numerous time points and temperatures, at controlled conditions, and then after the required time had passed the quantity of virus within the sample determined via plaque assay. This would give an indication of the virus stability in the environment, which could have implications for transmission within different water systems. For example, an unstable virus would not last for long periods in water so would not have as much opportunity to successful transmit to other hosts. This would cause problems within systems where hosts are spread out and don't come into contact as frequently as in commercial chicken sheds such as backyard production.

Although the E26K amino acid change within the PA gene altered viral phenotypes between these two viral strains, it is unlikely that this polymorphism is the sole reason behind the increased replication and pathogenicity of H9N2 AIVs within the field. Of particular note, is the lack of representation of 26K sequences within IAV genomes seen in chapter 2 and the prototype early G1-like H9N2 (A/quail/Hong Kong/ G1/97) possesses PA 26E. This suggests that another factor could be important for the enhanced viral fitness. Potentially it could be one of the other genes also donated to the reassortant H9N2 viruses: PB2, PB1, NS1 or NS2. Within initial screens the NS segment was also shown to alter the viral plaque phenotypes between WF10 and UDL-01 H9N2 AIVs (unpublished data from the Iqbal lab), so this could be a good place to start. It is possible that differences in the host cell shut off activity between WF10 and UDL-01 H9N2s

could act via NS1 as well as PA-X (as seen in chapter 4). NS1 acts by binding to and inhibiting CPSF30 to prevent nuclear export of host transcripts so they can be accessed via the viral polymerase for cap snatching (Nemeroff et al., 1998). If alterations occur in the interplay between NS1 and PA-X host cell shut off, the viruses' ability to replicate within cells could be severely diminished. To first test this theory, the interaction of WF10 and UDL-01 NS1s with CPSF30 could be investigated. This could be completed via GFP-TRAP pulldown studies to assess protein-protein interactions. Plasmid-based reporter assays could also be used to look at the shut-off activities of the NS1 protein. Another function of NS1 is its blocking of PKR-mediated sensing of viral dsRNA therefore blocking the induction of the host innate immune response (Lu et al,. 1995; Tan et al., 1998). This could be investigated using transfection based reporter assays with the NS1 proteins and an IFN-β reporter plasmid or by looking at the levels of type one IFN secreted during infection of cells in the first instance.

Another limitation of the studies described within this thesis is that only one influenza virus strain was used to represent the early or reassortant H9N2 AIVs. To gain a broader understanding of the sequence differences between G1-like and novel reassortant H9N2s it would be beneficial to use a large scale bioinformatics screen with multiple sequences for each group. This would allow for trends and polymorphisms within each group to be more thoroughly investigated and would increase the impact of such studies within the future. This would require large scale bioinformatics analysis and could pose a challenging task particularly if taking into consideration the potential effect of the NS1 gene as well as PA.

Chapter 7: Materials and methods

7.1: Materials

7.1.1: General reagents

Agarose for gel electrophoresis	Eurogentec (18037G)
Agarose for plaque assay	Oxoid (LP0028)
Avicel	FMC Health and Nutrition (CL-611)
DNA molecular markers	Bioline
DNA plasmid miniprep kit	Qiagen
DNA plasmid midiprep kit	Qiagen
Lipofectamine 2000	Invitrogen
Neutral buffered formalin	Sigma
Nitrocellulose membranes	BioRad
PCR purification kit	Qiagen
Protein molecular weight markers	BioRad
Tetramethylethylenediamine (TEMED)	BioRad (161-0800)
Trizol reagent	Ambion
Superscript III platinum One-step qRT-PCR kit	Life Technologies
One-step RT-PCR kit	Invitrogen

QuikChange site directed mutagenesis kit	Agilent
Vectashield	Vector Laboratories
Polyester tip swab in tube	Technical service consultant Ltd
Puromycin	Sigma (P8833)
Chloroform	Sigma
RNA extraction kit	Qiagen
X-ray film	Thermo Fisher
Luciferase Assay kit	Promega
B-galactosidase assay kit	Promega
In Vitro Translation kit	Promega

7.1.2: Enzymes

The following enzymes were supplied by the provided suppliers and used according to the manufacturer's instructions unless otherwise stated.

DNA restriction enzymes	New England Biolabs
Taq DNA polymerase	Invitrogen
Pfu Ultra II fusion HS DNA Polymerase	Agilent
T4 DNA ligase	New England Biolabs

7.1.3: Antibodies

Table 7.1: Primary antibodies

Antibody	Application	Source
Rabbit polyclonal anti-PR8 PA (V23)	WB (1:500)	Digard group
Mouse monoclonal anti-GFP (JL8)	WB (1:5000)	Clontech (632380)
Mouse monoclonal anti-influenza NP	WB (1:1000) IF (1:500)	Iqbal group
Rabbit monoclonal anti-alpha- tubulin	WB (1:1000)	Abcam (ab15246)
Monoclonal anti-puromycin	WB (1:1000)	Millipore (MABE343)
Monoclonal anti-G3BP	IF (1:500)	BD Biosciences (611126)

Table 7.2: Secondary antibodies

Antibody	Application	Source
IRDye 680RD Goat-anti-mouse antibody	WB (1:10000)	Licor
IRDye 800RD Goat anti-rabbit antibody	WB (1:10000)	Licor
Donkey anti-Mouse IgG (H+L) Secondary Antibody, Alexa Fluor® 488 conjugate	IF (1:1000)	Thermo Fisher (A-21202).
Goat anti-Mouse IgG (H+L) Secondary Antibody, Alexa Fluor® 568 conjugate	IF (1:1000)	Life Technologies (A11004)

Table 7.3: Fluorescent dyes

Dye	Application	Source
DAPI	IF (1:10000)	Thermo Fisher

7.1.4: Eukaryotic cell culture medium

7.1.4.1: Cell lines

Madin-Darby Canine Kidney Cells (MDCK)	Sigma/ECACC
Human Embryonic Kidney 293T Cells (293T)	Sigma/ECACC
Human Adenocarcinomic Alveolar Basal Epithelial Cells (A549)	ECACC
Chicken Fibroblast Cells (DF-1s)	ATCC
Japanese Quail Fibrosarcoma cell line (QT-35)	Houghton
Primary Chicken Kidney Cells (CKC)	Pirbright Institute cell culture services
Primary chicken embryo fibroblasts (CEF)	Mariya Goncheva, The Roslin Institute

7.1.4.2: Cell culture reagents

Dulbecco's Modified Eagle Medium (DMEM)	Sigma (D6429)
Eagles Dulbecco's Modified Eagle medium (EMEM)	Sigma (M4655)
Fetal bovine serum (FBS)	Sigma (F0926)
L-Glutamine	Life Technologies (A29168-01)
Penicillin/Streptomycin (Pen/Strep)	Gibco (15140-122)
2.5% Trypsin-EDTA	Gibco (15090-046)
Opti-MEM	Gibco (31985-047)
Methionine- and Cysteine-free D-MEM	Gibco
Medium 199	Gibco (21180-02)

10x MEM	Sigma (M02075)
Bovine serum albumin (BSA)	Sigma (A7906)
Polymyxin B	Sigma
Gentamicin	Sigma
Nystatin	Sigma
Ofloxacin HCl	Sigma
Sulfamthoxazole	Sigma
Tryptose phosphate broth	Pirbright CSU
N-tosyl-L-phenylalanyl chloromethyl ketone (TPCK) treated trypsin	Sigma
Hepes	Sigma
Sodium bicarbonate	Sigma
Dextran hydrochloride	Sigma
Versene	Gibco

7.1.4.3: Cell culture media composition

Plaque assay overlay media	10x Minimum Essential Medium, 0.2% w/v BSA, 2mM L-glutamine, 0.15% w/v sodium hydrocarbonate, 10mM Hepes, 0.0005% dextran hydrochloride, 100U/ml Pen/Strep, 2µg/ml TPCK trypsin

Complete media	DMEM, 10% (v/v) FCS, 100U/ml Pen/Strep
Virus growth media	DMEM, 2µg/ml TPCK trypsin
Virus transport media	Medium 199, 0.5% (v/v BSA), Penicillin G $2x10^6$U/L, Streptomycin 200mg/L, Polymyxin B $2x10^6$ U/L, Gentamicin 250mg/L, Nystatin $5x10^5$ U/L, Ofloxacin HCl 60mg/L, Sulfamthoxazole 0.2g/L. adjusted to pH 7.4.
CKC media	EMEM, 0.6% (w/v) BSA, 10% (v/v) tryptose phosphate broth, 300U/ml Pen/Strep
CEF media	M199, 4% FCS, 100U/ml Pen/Strep
Reverse genetics media	DMEM + 2mM glutamine, 100U/ml penicillin, 100U/ml streptomycin, 0.14% (w/v) BSA, 5µg/ml TPCK-treated trypsin

7.1.5: Bacterial culture

Luria Broth (LB), LB agar and SOC media were made and provided by the Roslin Institute or Pirbright Institute cell culture services.

Luria Broth	1% (w/v) tryptone, 0.5% (v/v) yeast extract, 0.5% (w/v) sodium chloride (pH 7.0)
LB agar	1.5% (w/v) agar, 1% (w/v) tryptone, 0.5% (v/v) yeast extract, 0.5% (w/v) sodium chloride (pH7.0)

Super optimal broth with catabolite repression (SOC)

2% (w/v) tryptone, 0.5% (v/v) yeast extract, 10mM sodium chloride, 2.5mM potassium chloride, 10mM magnesium chloride, 10mM magnesium sulphate, 20mM glucose

7.1.6: Protein buffers and solutions

Protein loading buffer	8M urea, 2% (w/v) SDS, 10mM Tris HCl pH 6.8, 0.01% (v/v) bromophenol blue, 2% (v/v) β-mercaptoethanol
SDS running buffer	0.025M Tris, 0.192M glycine, 0.1% (w/v) SDS, adjusted to pH 8.5
4x resolving buffer (Protogel)	1.5M Tris-HCl, 0.4% (w/v) SDS, pH 8.8
4x stacking buffer (Protogel)	0.5M Tris-HCl, 0.4% (w/v) SDS, pH 6.8
10% resolving polyacrylamide gel	3.33ml 30% acrylamide: bisacrylamide (37.5:1) (Bio-Rad), 2.5ml 4x resolving buffer, 4.06ml water, 100µl 10% (w/v) APS, 10µl TEMED.
4% stacking polyacrylamide gel	1.3ml 30% acrylamide: bisacrylamide (37.5:1) (BioRad), 2.5ml 4x stacking buffer, 6.1ml water, 50µl 10% (w/v) APS, 10µl TEMED

Polyacrylamide gel fix solution	50% (v/v) methanol, 10% (v/v) acetic acid
Protein transfer buffer	25mM Tris, 192mM glycine, 20% (v/v) methanol
Blocking solution	PBS/0.1% (v/v) Tween20, 5% (w/v) skimmed milk
Wash buffer	PBS/0.1% (v/v) Tween20

7.1.7: Other buffers and solutions

TBE buffer	89mM Tris-borate, 2mM EDTA, adjusted to pH 8.3.
Crystal violet solution	0.1% crystal violet (Sigma), 20% Methanol

7.1.8: Plasmids

Table 7.4: Plasmids

Name	Description	Source
pHW2000	Reverse genetics plasmid. Bidirectional pol I and pol II promoters either side of insert lead to mRNA and vRNA-like RNA synthesis.	The Pirbright Institute
pDUAL	Reverse genetics plasmid. Bidirectional pol I and pol II promoters either side of insert lead to mRNA and vRNA-like RNA synthesis.	Gift from Prof. Ron Fouchier [a]
pCAGGs	Pol II expression plasmid. Contains a CMV Immediate Early promotor	The Pirbright Institute
pPol 1	Reverse genetics plasmid. Plasmid containing RNA polymerase I promoter and terminator, leading to the expression of vRNA	The Pirbright Institute
pEGFP-N1	Constitutively expresses eGFP under control of CMV promoter. MCS upstream allows opportunity to clone C-terminally tagged proteins	Clontech
pPol I Luc	Reporter for RNP reconstitution assays. Contains firefly luciferase reporter gene in the reverse orientation and flanked by the UTRs of PR8 segment 8, under the control of a pol I promoter (human or avian)	Gift from Prof. Laurence Tiley[b]
β-gal	B-galactosidase reporter plasmid, β-gal under constitutive expression of an RNA polymerase II promoter	Jagger et al., 2012

[a] Erasmus University Medical Centre, Rotterdam, Netherlands.
[b] Department of Veterinary Medicine, The University of Cambridge, Cambridge, UK.

7.1.8.1: Reverse genetics systems

i) A/Puerto/Rico/8/1934 (H1N1)

The PR8 eight-plasmid reverse genetic system was a kind gift from Prof. Ron Fouchier (Erasmus University Medical Centre, Rotterdam, Netherlands) (de Wit et al., 2004).

Table 7.5: PR8 reverse genetics system

Plasmid backbone	Segment	Accession number	Reference
pDUAL	PB2	EF467818	(de Wit et al., 2004)
	PB1	EF467819	
	PA	EF467820	
	HA	EF467821	

	NP	EF467822	
	NA	EF467823	
	M	EF467824	
	NS	EF467817	

ii) A/Chicken/Pakistan/UDL-01/08 (H9N2)

The UDL-01 reverse genetics systems was produced in house by Dr Joe James (The Pirbright Institute, UK). A helper expression plasmid encoding A/Victoria/3/75 PB1 was co-transfected with the 8 UDL-01 plasmids to provide an initial boost of a high activity PB1 protein (Neumann et al., 1999; Elleman and Barclay, 2004).

Table 7.6: UDL-01 reverse genetics system

Plasmid backbone	Segment	Accession number	Reference
pHW2000	PB2	CY038455	Long et al., 2016; Iqbal et al., 2013
polI	PB1	CY038456	
pHW2000	PA	CY038457	
	HA	CY038458	
	NP	CY038459	
	NA	CY038460	
	M	CY038461	
	NS	CY038462	

iii) A/GuineaFowl/Hong Kong/WF10/99 (H9N2)

The eight-plasmid reverse genetics system for WF10 was kindly provided to the Iqbal lab by Dr. Daniel Perez.

Table 7.7: WF10 reverse genetics system

Plasmid backbone	Segment	Accession number	Reference
pHW2000	PB2	AOT22419	Perez et al., 2003
	PB1	AOT22413	
	PA	AOT22417	
	HA	AOT22363	
	NP	AOT22392	
	NA	AOT22367	
	M	AOT22377	

	NS	AOT22410	

7.1.9: Oligonucleotides

Table 7.8: Sequencing primers

Name	Sequence	Description
pDUAL FP	ATGTCGTAACAACTCCGCCC	For sequencing from the 5' end of insert in pDUAL plasmid
pDUAL RP	TTTTTGGGGACAGGTGTCCG	For sequencing from the 3' end of insert in pDUAL plasmid
Uni12	AGCAAAAGCAGG	Complementary to the 3' end of all IAV vRNA segments.
T7F	TAA TAC GAC TCA CTA TAG GG	Sequencing PHW2000 from T7F site
pHW2000 RP	CAGGTGTCCGTGTCGCGCGTC	Sequencing PHW2000, reverse primer
eGFPN1 FP	GGCGGTAGGCGTGTA	For sequencing insert from 5' end in pEGFPN1.
PA seq FP 755-775	GGCAAGCTTTCTCAAATGTCG	For forward sequencing from bp 755-775 of H9 PA
PA seq RP 2200	TAGCAAATAGTAGCATTGCCACA	For reverse sequencing from by 2200 of H9 PA
PA seq FP 9-31	CAGGTACTGATCCAAAATGGAAG	For forward sequencing from bp 9-31 of H9 PA
PA seg RP 798-778	CTCAATTCTGGCGTTCACTTC	For reverse sequencing from bp 798-778 of H9 PA
Uni-12FA primer,	ACGCGTGATCAGCAAAAGCAGG	Primers for isolation of all influenza segments for next generation sequencing
Uni-12FG primer	ACGCGTGATCAGCGAAAGCAGG	
Uni-13R primer	ACGCGTGATCAGTAGAAACAAGG	

Table 7.9: Cloning primers

Name	Sequence	Description
UDL-01 PA pCAGGs cloning FP	TTATTTATAAGCGGCCGCATGGAAAAC TTTGTGCGACAGTGC	UDL-01 PA gene start codon with an NotI enzyme site forward primer

UDL-01PA pCAGGS cloning RP	TTATATATTAGTCGACCTATCTCAGTG CATGTGTGAGG	UDL-01 PA gene stop codon with a SalI enzyme site reverse primer
WF10 PA pCAGGS cloning FP	TTATTTATAAGCGGCCGCATGGAAGAC TTTGTGCGACAGTGC	UDL-01 PA gene start codon with an NotI enzyme site forward primer
WF10 PA pCAGGs cloning RP	TTATATATTACTCGAGCTATTTTAGTG CATGTGTGAGGAAGGAGTTGAACC	WF10 PA gene stop codon with a XhoI enzyme site reverse primer

Table 7.10: reverse transcription primers

Name	Sequence	Description
Uni12	AGCAAAAGCAGG	Complementary to the 5' end of vRNA of all IAV segments
FluG	TATTCGTCTCACCCAGCGAAAGCA GG	Complementary to the 5' end of vRNA with a biased toward polymerase segments

Table 7.11: qRT-PCR primers

Name	Sequence	Description
Influenza M FP	AGATGAGTCTTCTAACCGAGGTCG	Designed to amplify influenza M segment
Influenza M RP	TGCAAAAACATCTTCAAGTCTCTG	
Influenza M probe	FAM-TCAGGCCCCCTCAAAGCCGA-TAMRA	
IFNα FP	GACAGCCAACGCCAAAGC	Designed to amplify chicken IFNα
IFNα RP	GTCGCTGCTGTCCAAGCATT	
IFNα probe	FAM-CTCAACCGGATCCACCGCTACACC-TAMRA	
IFNβ FP	CCTCCAACACCTCTTCAACATG	Designed to amplify chicken IFNβ
IFNβ RP	TGGCGTGTGCGGTCAAT	
IFNβ Probe	FAM-TTAGCAGCCCACACACTCCAAAACACTG-TAMRA	
IFNγ FP	GTGAAGAAGGTGAAAGATATCATGGA	Designed to amplify chicken IFNγ
IFNγ RP	GCTTTGCGCTGGATTCTCA	
IFNγ probe	FAM-TGGCCAAGCTCCCGATGAACGA-TAMRA	
IL-1β FP	GCTCTACATGTCGTGTGTGATGAG	Designed to amplify chicken IL-1β
IL-1β RP	TGTCGATGTCCCGCATGA	
IL-1β probe	FAM-CCACACTGCAGCTGGAGGAAGCC-TAMRA	
IL-4 FP	AACATGCGTCAGCTCCTGAAT	Designed to amplify chicken IL-4
IL-4 RP	TCTGCTAGGAACTTCTCCATTGAA	
IL-4 probe	FAM-AGCAGCACCTCCCTCAAGGCACC-TAMRA	
IL-6 FP	GCTCGCCGGCTTCGA	Designed to amplify chicken IL-6
IL-6 RP	GGTAGGTCTGAAAGGCGAACAG	

IL-6 probe	FAM-AGGAGAAATGCCTGACGAAGCTCTCCA-TAMRA	
IL-18 FP	AGGTGAAATCTGGCAGTGGAAT	Designed to amplify chicken IL-18
IL-18 RP	ACCTGGACGCTGAATGCAA	
IL-18 probe	FAM-CCGCGCCTTCAGCACGGATG-TAMRA	
TGF-β4 FP	AGGATCTGCAGTGGAAGTGGAT	Designed to amplify chicken TGF-β4
TGF-β4 RP	CCCCGGGTTGTGTTGGT	
TGF-β4 probe	FAM-ACCCAAAGGTTATATGGCCAACTTCTGCAT-TAMRA	
CXCLi2 FP	GCCCTCCTCCTGGTTTCAG	Designed to amplify chicken CXCLi2
CXCLi2 RP	TGGCACCGCAGCTCATT	
CXCLi2 probe	FAM-TCTTTACCAGCGTCCTACCTTGCGACA-TAMRA	
Mx FP	CACTGCAACAAGCAAAGAAGGA	Designed to amplify chicken Mx
Mx RP	TGATCAACCCCACAAGGAAAA	
Mx probe	FAM-ACAAAGCACACACCCAACTGTCAGCG-TAMRA	
28S FP	GGCGAAGCCAGAGGAAACT	Designed to amplify chicken ribosomal protein 28S
28S RP	GACGACCGATTTGCACGTC	
28S probe	FAM-AGGACCGCTACGGACCTCCACCA-TAMRA	
RPLPO-1 FP	TTGGGCATCACCACAAAGATT	Designed to amplify chicken Ribosomal phosphoprotein PO
RPLPO-1 RP	CCCACTTGTCTCCGGTCTTAA	
RPLPO-1 probe	FAM-CATCACTCAGAATTTCAATGGTCCCTCGGG-TAMRA	
RPL13 FP	TCGTGCTGGCAGGATTC	Designed to amplify chicken Ribosomal protein L13
RPL13 RP	TCGTCCGAGCAAACCTTTTG	
RPL13 probe	FAM-TAATGCCCGCCAGTTTAAGCTCTTCTAGGC-TAMRA	

Table 7.12: Mutagenesis primers

Name	**Sequence**	**Description**
A20T FP	GTCGAGCTTGCGGAAAAGACAATGAAAGAATATGGGG	Introduction of A20T change in UDL-01 PA
A20T RP	CCCCATATTCTTTCATTGTCTTTTCCGCAAGCTCGAC	
T20A FP	CCCATACTCCTTCATTGCCTTTTCCGCAAGCTCGA	Introduction of T20A change in WF10 PA
T20A RP	TCGAGCTTGCGGAAAAGGCAATGAAGGAGTATGGG	
E26K FP	GTTTGTTTCGATTTTCGGATCTTTCCCATATTCTTTCATTGCCTTTT	Introduction of E26K change in UDL-01 PA
E26K RP	AAAAGGCAATGAAAGAATATGGGAAAGATCCGAAAATCGAAACAAAC	

K26E FP	ATTTGTTTCAATTTTCGGATCTTCCCCATACTCCTTCATTGTCTTTT	Introduction of K26E change in WF10 PA
K26E RP	AAAAGACAATGAAGGAGTATGGGGAAGATCCGAAAATTGAAACAAAT	
T85I FP	CCAGGCCATCGCTCGGTCTCTCCCTTCAATT	Introduction of 85I change in UDL-01 PA
T85I RP	AATTGAAGGGAGAGACCGAGCGATGGCCTGG	
I85T FP	CTGTCCAGGCCATTGTTCGGTCTCTTCCTTC	Introduction of I85T change in WF10 PA
I85T RP	GAAGGAAGAGACCGAACAATGGCCTGGACAG	
I100V_E101D FP	GGGAGAAATTTAGGCTTATCGACTCCTGTGGTGTTGCAGA	Introduction of I100V_E101Dchange in UDL-01 PA
I100V_E101D RP	TCTGCAACACCACAGGAGTCGATAAGCCTAAATTTCTCCC	
V100I_D101E FP	CCGGAAGAAATTTGGGTTTCTCGATTCCTGTTGTGTTGCAGATG	Introduction of V100I_D101Echange in WF10 PA
V100I_D101E FP	CATCTGCAACACAACAGGAATCGAGAAACCCAAATTTCTTCCGG	
I118T FP	CGTGTTACTCCAATTTCAGTGAATCTGTTCTCCTTGTAGTCAT	Introduction of I118T change in UDL-01 PA
I118T RP	ATGACTACAAGGAGAACAGATTCACTGAAATTGGAGTAACACG	
T118I FP	GTGTCACACCAATTTCAATGAATCGGTTTTCCTTGTAGTCG	Introduction of T118I change in WF10 PA
T118I RP	CGACTACAAGGAAAACCGATTCATTGAAATTGGTGTGACAC	
E237K FP	AATGCAGCCGTTCGGTTTGAATCCATCCACATAGG	Introduction of E237K change in UDL-01 PA
E237K RP	CCTATGTGGATGGATTCAAACCGAACGGCTGCATT	
K237E FP	AATGCAGCCGTTCGGTTCGAATCCATCCACATAGG	Introduction of K237E change in WF10 PA
K237E RP	CCTATGTGGATGGATTCGAACCGAACGGCTGCATT	
G316D FP	TTACAATGTTGGGATCTTTCCAGTCAAAAAATGTCTTCATGCATTTG	Introduction of G316D change in UDL-01 PA
G316D RP	CAAATGCATGAAGACATTTTTTGACTGGAAAGATCCCAACATTGTAA	
D316G FP	TGTTGGGCTCTCTCCAGCCAAAGAATGTTTTCATGC	Introduction of D316G change in WF10 PA
D316G RP	GCATGAAAACATTCTTTGGCTGGAGAGAGCCCAACA	
K327E FP	GGGGTTTATTCCCTTCTCATGTGGTTTTACAATGTTGGGATC	Introduction of K327E change in UDL-01 PA
K327E RP	GATCCCAACATTGTAAAACCACATGAGAAGGGAATAAACCCC	
E327K FP	ATTGGGATTTATACCTTTCTTGTGTGGCTTGATGATGTTGG	Introduction of E327K change in WF10 PA
E327K RP	CCAACATCATCAAGCCACACAAGAAAGGTATAAATCCCAAT	
K367M FP	TCTCACCTAGTGCCCACATCAACTGGCTAGTTTTT	Introduction of K367M change in UDL-01 PA

K367M RP	AAAAACTAGCCAGTTGATGTGGGCACTAGGTGAG A	
M367K FP	CCCGAGTGCCCACTTTAATTGGCTTGTTTTCTTC ATGT	Introduction of M367K change in WF10 PA
M367K RP	ACATGAAGAAAACAAGCCAATTAAAGTGGGCAC TCGGG	
S400L FP	GATCCAACTTGCTAACGATCTAAGCTCTGGTTCA TCACTATCATAC	Introduction of S400L change in UDL-01 PA
S400L RP	GTATGATAGTGATGAACCAGAGCTTAGATCGTTA GCAAGTTGGATC	
L400S FP	CAAAGTGATGAGCCAGAGTCCAGATCGCTAGCAA GCTG	Introduction of L400S change in WF10 PA
L400S RP	CAGCTTGCTAGCGATCTGGACTCTGGCTCATCAC TTTG	
G684E FP	TCAATTGCCTCATATAACCCTTCAAGATCGAAAG TTCCAGGTTC	Introduction of G684E change in UDL-01 PA
G684E RP	GAACCTGGAACTTTCGATCTTGAAGGGTTATATG AGGCAATTGA	
E684G FP	CAATTGCTCCATATAGCCCCCCAAGATCAAAGGT TCCAGGTT	Introduction of E684G change in WF10 PA
E684G RP	AACCTGGAACCTTTGATCTTGGGGGGCTATATGG AGCAATTG	
E688G FP	TCAGGCACTCCTCAATTGCTCCATATAACCCCCC AAGATC	Introduction of E688G change in UDL-01 PA
E688G RP	GATCTTGGGGGGTTATATGGAGCAATTGAGGAG TGCCTGA	
G688E FP	TCAGGCACTCCTCAATTGCCTCATATAGCCCTTC AAGATC	Introduction of G688E change in WF10 PA
G688E RP	GATCTTGAAGGGCTATATGAGGCAATTGAGGAG TGCCTGA	
R221L FP	TCAAGGCTGGAGAAGTTAGGTGGTAGACTTTGGT C	Introduction of R221L change in UDL-01 PA-X
R221L RP	GACCAAAGTCTACCACCTAACTTCTCCAGCCTTG A	
L221R FP	CAAGGCTGGAGAAGTTCGGTGGGAGACTTTGGT	Introduction of L221R change in WF10 PA-X
L221R RP	ACCAAAGTCTCCCACCGAACTTCTCCAGCCTTG	
Q250R FP	GCAAGCTTTCTCAAATGTCGAAAGAAGTGAACGC CAGAA	Introduction of Q250R change in UDL-01 PA-X
Q250R RP	TTCTGGCGTTCACTTCTTTCGACATTTGAGAAAG CTTGC	
R250Q FP	TTCTGGCGTTCACTTCTTTTGACATTTGAGAAAG CTTGC	Introduction of R250Q change in WF10 PA-X
R250Q RP	GCAAGCTTTCTCAAATGTCAAAAGAAGTGAACGC CAGAA	
UDL-01 PTC1 FP	TTTGAAATTACAGGGACAATGCGCAAGCTTGCCG A	Introduction of premature termination codon 1 into UDL-01 PA-X
UDL-01 PTC1 RP	TCGGCAAGCTTGCGCATTGTCCCTGTAATTTCAA A	
WF10 PTC1 FP	CGCATGGTCCCTGTTATTTCAAATCTTTCTTCAA TTGTCTCT	Introduction of premature

WF10 PTC1 RP	AGAGACAATTGAAGAAAGATTTGAAATAACAGG GACCATGCG	termination codon 1 into WF10 PA-X
UDL-01 PTC2 FP	TGGTAGACTTTGGTCGGCTAGCTTCCTCATGGTC CCTGTAATTTC	Introduction of premature termination codon 2 into UDL-01 PA-X
UDL-01 PTC2 RP	GAAATTACAGGGACCATGAGGAAGCTAGCCGACC AAAGTCTACCA	
WF10 PTC2 FP	GGAGACTTTGGTCGGCTAGCCTCCTCATGGTCCC TGTGATT	Introduction of premature termination codon 2 into WF10 PA-X
WF10 PTC2 FP	AATCACAGGGACCATGAGGAGGCTAGCCGACCAA AGTCTCC	
UDL-01 PTC3 FP	CCGAACTTCTCCAGCCTAGAAAACTTTAGAGCCT A	Introduction of premature termination codon 3 into UDL-01 PA-X
UDL-01 PTC3 RP	TAGGCTCTAAAGTTTTCTAGGCTGGAGAAGTTCG G	
WF10 PTC3 FP	CATAGGCTCTAAAGTTTTCTAGGCTGGAGAAGTT AGGTG	Introduction of premature termination codon 3 into WF10 PA-X
WF10 PTC3 FP	CACCTAACTTCTCCAGCCTAGAAAACTTTAGAGC CTATG	
UDL-01 PTC4 FP	AAAACTTTAGAGCCTATGTAGATGGATTCGAACC GAACG	Introduction of premature termination codon 4 into UDL-01 PA-X
UDL-01 PTC4 RP	CGTTCGGTTCGAATCCATCTACATAGGCTCTAAA GTTTT	
WF10 PTC4 FP	GAAAACTTTAGAGCCTATGTAGATGGATTCAAAC CGAACGG	Introduction of premature termination codon 4 into WF10 PA-X
WF10 PTC4 RP	CCGTTCGGTTTGAATCCATCTACATAGGCTCTAA AGTTTTC	
UDL-01 FS FP	GCCAACAGGGGTCTGTGGGATAGCTTCAGACAAT CCGAAAGAGGCGAAGAG	Introduction of mutation to frameshift site to remove PA-X expression in UDL-01
UDL-01 FS RP	CTCTTCGCCTCTTTCGGATTGTCTGAAGCTATCC CACAGACCCCTGTTGGC	
WF10 FS FP	CTTCGCCTCTCTCGGACTGTCTGAAGCTATCCCA TAGACCCCTGCTTG	Introduction of mutation to frameshift site to remove PA-X expression in WF10
WF10 FS RP	CAAGCAGGGGTCTATGGGATAGCTTCAGACAGTC CGAGAGAGGCGAAG	
UDL-01 delC FP	GGTCTGTGGGATTCCTTTGTCAATCCGAAAGAGG C	Removal of C in frameshift site to drive expression towards +1 ORF of PA-X
UDL-01 delC RP	GCCTCTTTCGGATTGACAAAGGAATCCCACAGAC C	
WF10 delC FP	GTCTATGGGATTCCTTTGTCAGTCCGAGAGAGG	Removal of C in frameshift site to drive expression towards +1 ORF of PA-X
WF10 delC RP	CCTCTCTCGGACTGACAAAGGAATCCCATAGAC	
UDL-01 d108a FP	CTCCTTGTAGTCATACAAAGCTGGGAGAAATTTG GGCTT	Introduce d108a into UDL-01 PA to inactivate endonuclease activity
UDL-01 d108a RP	AAGCCCAAATTTCTCCCAGCTTTGTATGACTACA AGGAG	
WF10 d108a FP	CCTTGTAGTCGTATAGGGCCGGAAGAATTTGGGT	Introduce d108a into WF10 PA to inactivate endonuclease activity
WF10 d108a RP	ACCCAAATTTCTTCCGGCCCTATACGACTACAAG G	

7.1.10: Radiolabels

[^{35}S]-L-methionine and [^{35}S]-L-cysteine protein labelling mix	Perkin-Elmer.
[^{14}C] Protein Molecular Weight Marker	Perkin-Elmer.

7.2: Methods

7.2.1: DNA preparation, cloning and analysis

7.2.1.1: Site directed mutagenesis

Primers for site directed mutagenesis were designed using Agilent QuikChange primer design programme (www.genomics.agilent.com/primerDesignProgram.jsp). This allowed for the generation of primers where the intended mutation was positioned in the middle of the sequence and had a T_m of 65-70°C. The primers had a GC content of approximately 40% and terminated on one or more C or G bases.

Site directed mutagenesis was performed on the H9 PA gene containing pHW2000 plasmids using the QuikChange Lightning Site-Directed Mutagenesis system (Agilent - #210519), as per the manufacturer's instruction except using half volumes of each reagent. Briefly, within a 25 µl reaction mix: 5µl 10x reaction buffer, 50ng of dsDNA template, 125ng forward primer, 125ng reverse primer, 1µl dNTP mix, 1.5µl QuikSolution reagent, 1µl QuikChange Lightning Enzyme, made up to 25µl with ddH_20. Thermocycling conditions as follows: i) 2 min denaturing step at 95°C, ii) 2 sec denaturing step at 95°C, iii) 10 sec primer annealing step at 60°C, iv) 2 min 30 sec elongation step at 68°C, with steps ii) to iv) performed for 18 cycles, and v) final 5 min elongation step at 68°C. PCR

products were digested using *Dpn* 1 enzyme to remove parental methylated and hemimethylated DNA, 1µl of enzyme added per reaction and incubated for 30 min at 37°C. *Dpn* 1 digested product was visualised via gel electrophoresis (section 7.2.1.5) before transformation into competent *E.coli* (section 7.2.1.2).

7.2.1.2: Transformation of competent bacteria with plasmid DNA

Commercial competent cells (DH5α, XL10-Gold ultracompetent cells) or home-made cells derived from One Shot® TOP10 Chemically Competent *E.coli* (Life Tech) were used for transformation with plasmid DNA. Briefly, 250ng of plasmid DNA (or 2µl of site-directed mutagenesis product) was added to 25µl of competent cells (thawed on ice), mixed gently and incubated for 30 min on ice. Cells were transformed by a 45 sec heat shock at 42°C followed by immediate placement on ice for a further 2 min. 250µl of pre-warmed SOC medium was added to the cells, which were allowed to recover for 1h at 37°C, shaking. Cells were spread onto appropriate antibiotic selection plates using a sterile spreader and Bunsen burner to reduce contamination. Plates were incubated at 37°C overnight. Single colonies were selected and grown in LB broth (5ml for mini-prep, 100ml for midi-prep) containing the appropriate antibiotic (37°C, 16h, shaking). Bacterial cells were pelleted via centrifugation (1,600xg, 20 min, 4°C), and supernatants removed. Cells were used immediately or stored at -20°C for processing at a later date via plasmid DNA purification (section 7.2.1.3).

7.2.1.3: Plasmid DNA purification

Plasmid DNA mini-preps were performed using QIAGEN's Plasmid DNA Mini Prep kit according to the manufacturer's instructions. Plasmid DNA midi-

preps were performed using QIAGEN's Plasmid Plus DNA Midi Prep kit according to manufacturer's instructions. DNA was eluted in water and the quality and concentration of purified plasmid DNA assessed via a NanoDrop ND-1000 spectrophotometer (Thermo Scientific).

7.2.1.4: Plasmid sequencing

After cloning or site-directed mutagenesis, sequencing of the DNA plasmid was completed to ensure presence of the correct insert or mutation. Sanger sequencing was performed by GATC or Source Biosciences. Each plasmid was sequenced with primers designed for the vector backbone (see Table 7.8 for details).

7.2.1.5: DNA gel electrophoresis

Gel electrophoresis was used to separate DNA. Agarose was boiled in 1x TBE buffer at typically 1.0% (w/v) and 1x GelRed nucleic acid stain (Biotium) was added to cooled molten agarose and mixed. DNA samples were mixed with 1x DNA loading dye (final concentration) and loaded onto the set agarose gel alongside a Promega 1kb DNA ladder marker or Hyperladder™ 1kb (Bioline) to estimate DNA band sizes. Gels were run at between 50-100V for the desired length of time. DNA was visualised using a Gel Doc™ EZ Imager (BioRad) using the 'GelRed' setting.

7.2.1.6: Cloning PA segments in pCAGGs

The ORFs of both UDL-01 and WF10 PAs were cloned out of the pHW2000 plasmids using primers designed to insert a 5' *NotI* site and a 3' *SalI* site (UDL-01

PA) or a 5' *NotI* site and a 3' *XhoI* site (WF10 PA). 10ng of DNA template was amplified in a 50µl PCR reaction using Pfu Ultra II fusion HS DNA Polymerase (Agilent) using the reaction set up as per manufacturers' instructions. Thermocycling conditions were as follows: i) a 2 min denaturation step at 95°C, ii) a 20 sec denaturation step at 95°C, iii) a 20 sec primer annealing step at 60°C, iv) a 15 sec elongation step at 72°C, with steps ii) – iv) performed for 30 cycles, and v) a final 3 min elongation step at 72°C. PCR product was analysed via gel electrophoresis and purified using Qiagen's QIAquick PCR purification kit as per manufacturers instruction eluting in 30µl of water. The whole reaction plus 5µg of pCAGGs vector was digested with *NotI, SalI* or *XhoI*- HF DNA endonuclease (New England Biolabs) using conditions recommended by manufacturer and again purified as above. 50ng of cut pCAGGs vector was used in a ligation reaction at a molecular ratio of 5:1 (vector: insert) using T4 DNA ligase (New England Biolabs), following recommendations from manufacturer. 2µl of ligation product was transformed into competent *E.coli* as described in section 7.2.1.2. Plasmid DNA was extracted from individual colony suspensions by mini-prep purification (section 7.2.1.3).

7.2.2: Cell culture

7.2.2.1: Passaging of continuous cell lines

MDCK cells, 293T cells, DF-1 cells and QT-35 cells were maintained in DMEM supplemented with 10% (v/v) FBS and 100U/ml Penicillin-Streptomycin (complete DMEM). All cells were grown at 37°C, 5% CO_2. Cells were typically passaged every 3-4 days: cells were washed twice (once for 293T cells) with PBS

and removed using 0.25% (v/v) trypsin/versene. Cells were resuspended in a 1 in10 dilution in complete DMEM.

7.2.2.2: Preparation of primary chicken cells

Primary chicken kidney cells (CKCs) were generated as previously described by the cell culture team at the Pirbright Institute (Hennion et al., 2015). Briefly, kidneys from 3 week old SPF Rhode Island Red birds were removed, shredded, washed in PBS and then trypsinised and filtered. Cells were resuspended in CKC growth media (EMEM + 0.6% w/v BSA, 10% v/v tryptose phosphate broth, 300U/ml penicillin/streptomycin), plated and grown at 37°C, 5% CO_2.

Primary chicken embryo fibroblast cells (CEF) were generated by Mariya Goncheva at the Roslin Institute. Briefly, 9-11-day old chicken embryos were removed from their egg, the head and viscera removed and the embryos washed three times in PBS. Embryos were chopped up and passed through a 20ml syringe and added to a 50ml falcon topped up with PBS. Chopped embryos were centrifuged (500xg, 5 min), supernatants discarded and then passed through 10ml syringe into a 50ml falcon topped up with PBS. This was repeated 5 times. To each mashed embryo 5ml of trypsin/EDTA was added and stirred for 30min at 37°C, 5% CO_2. Supernatant was passed through a metal mesh filter, a further 5ml of trypsin/EDTA was added to the solid phase and the process repeated. Supernatants were centrifuged (500xg, 10 min) and the resulting supernatant passed through a 100µm nylon filter unit and centrifuged once more. Cell pellet

resuspended in CEF media (M199, 4% (v/v) FBS and 100U/ml Pen/Strep), plated and grown at 37°C, 5% CO_2.

7.2.3: Virus rescue, growth and titration

7.2.3.1: Virus rescue via reverse genetics

7.2.3.1.1: PR8 7:1 H9N2 reassortant viruses

Reverse genetics plasmid sets (7 segments derived from PR8 and the UDL-01 or WF10 segment 3) were transfected into 293T cells in 6 well plates using Lipofectamine2000 transfection reagent. 250ng of each reverse genetics plasmid was diluted into 100µl of Opti-MEM. 4µl (4µg) of Lipofectamine2000 was mixed with 100µl of Opti-MEM for 5 min at room temperature. The Lipofectamine2000 and diluted DNA were then mixed and left for a further 30 min at room temperature. Meanwhile, 293T cells were washed once with PBS and overlaid with Opti-MEM. After the 30 min incubation, the transfection mix was added dropwise over the 293T cells. 16h post transfection, media was changed to reverse genetics media (DMEM + 2mM glutamine, 100U/ml penicillin, 100U/ml streptomycin, 0.14% (w/v) BSA, 5µg/ml TPCK-treated trypsin). Following a 48h incubation at 37°C, 5%CO_2 supernatants were collected and stored at -80°C. These were termed P_0 stocks.

7.2.3.1.2: H9N2 avian influenza viruses

Reverse genetics plasmid sets for UDL-01 (9-plasmids) and WF10 (8 plasmids) were transfected into 293T cells using Lipofectamine2000 transfection reagent. The transfection protocol was as described above except 1µg of each

reverse genetics plasmid was included in the DNA mix along with 10µl (10µg) of Lipofectamine2000. 24h post transfection, 293T cells were co-cultured with MDCK cells in a T25 flask, once cells had adhered (8-16h post transfection), media was changed to DMEM + 2µg/ml TPCK trypsin. Cells were assessed for presence of cytopathic effect (CPE) and 2-7 days post co-culture, once CPE was visible, supernatants were harvested, clarified (1000xg, 5 min) and stored at -80°C in 0.5ml or 1ml aliquots. These were termed P_0 stocks.

7.2.3.2: Virus propagation

7.2.3.2.1: PR8 7:1 H9N2 reassortant viruses

P_1 virus stocks were generated on MDCK cells seeded in T150 flasks or within embryonated hens' eggs. MDCK stocks were produced as follows; 100µl of P_0 stock was diluted in 1ml of reverse genetics media. A confluent T150 flask of MDCK cells was washed twice with PBS before the P_0 stock dilution added. Cells were incubated for 1h at 37°C before 20ml of reverse genetics medium added. Supernatants were clarified via centrifugation (1000xg, 5 min) and stored at -80°C in 0.5ml or 1ml aliquots. Virus titration was performed after one round of freeze-thaw to account for any losses in infectivity.

Egg grown P_1 virus stocks were produced as follows; 100µl of P_0 stock was diluted in 1ml of serum-free DMEM. Embryonated hens' eggs (Henry Stewart & Co.) were incubated at 37°C, 40-50% humidity, for 10 days and candled to ensure viability prior to inoculation. A small hole was introduced into the egg shell just below the line of the air sac. The shell was sterilised with 70% (v/v) ethanol. 100µl of the P_0 stock was introduced into the allantoic cavity using a 1ml syringe

and 25G needle. The hole was sealed with Scotch tape and eggs were incubated for 48-72h. Eggs were culled via refrigeration at 4°C for a minimum of 6h. The top of the shell removed using forceps and the air sac punctured using a P1000 Gilson pipette tip. Allantoic fluid was collected using a P1000 Gilson pipette, pooled and clarified (1400xg, 10 min), then stored in 0.5 or 1ml aliquots at -80°C. Virus titration was performed after one round of freeze-thaw to account for any losses in infectivity arising from the freeze thaw step.

7.2.3.2.2: H9N2 avian influenza viruses

To produce P_1 stocks of H9N2 AIVs, embryonated hens' eggs were utilised. The protocol was as described above, except the embryonated hens' eggs were supplied by VALO.

7.2.3.3: Virus titration

7.2.3.3.1: PR8 7:1 H9N2 reassortant viruses

Plaque assays within MDCK cells were used to titrate viral stocks or supernatants (Huprikar, 1980). Briefly, the day prior to assay, MDCK cells were seeded in 6-well plates to achieve 100% confluency (typically seeding 0.3 $x10^6$ cells per well). Virus samples were serially diluted 10-fold in serum-free DMEM. Cells were washed once in PBS before 400µl of virus dilution applied to each well. Cells were incubated for 1h at 37°C, after which virus was removed and 2ml of overlay added per well. Avicel overlay: virus growth media supplemented with 1.2% (w/v) Avicel. Plates were incubated at 37°C for 48h. Cells were fixed with 2ml/well of 10% neutral buffered formalin (NBF) for 20 min-24h. Formalin was

removed and cells were stained with 0.1% (w/v) toluidine blue for 20 min-6h. Stain was removed and plates washed with water prior to plaque counting and titre calculations or plaque imaging.

7.2.3.3.2: H9N2 AIVs

Plaque assays within MDCK cells were also used to titrate H9N2 viral stocks or supernatants though the protocol differed slightly. The day prior to plaque assay, MDCK cells were seeded in 12-well plates to achieve 100% confluency (typically seeding 0.1 x 10^6 cells per well). Virus samples were serially diluted 10-fold in serum-free DMEM. Cells were washed once with PBS before 200µl of virus dilution applied to each well. Cells were incubated for 1h at 37°C, after which virus was removed and 1ml of 0.6% agarose overlay was added to each well. For the agarose overlay, 2% (w/v) agar was boiled and incubated at 55°C, 15ml was mixed with 35ml of plaque assay overlay media incubated at 37°C. After agarose had set, plates were inverted and incubated at 37°C for 72h. Plaque assays were fixed and stained via one of two methods. First, the agarose plugs were removed and cells fixed and stained with 1ml of 0.1% (v/v) crystal violet solution (+20% methanol). Second, agarose plugs were removed and cells were fixed with 1ml of 10% NBF per well for 30 min. NBF was removed and cells washed twice with PBS. Cells were permeabilised with 1ml PBS/0.2 %(v/v) Triton X-100 per well. Cells were washed twice with PBS and incubated with 250µl/well of mouse monoclonal α-NP (in house) which was diluted 1:2000 in PBS/2 %(w/v) BSA for 1h at room temperature on a rocker. Cells were washed twice in PBS and then incubated with 250µl/ well of goat anti-mouse IgG 568

conjugated secondary antibody (LICOR) diluted 1:10000 in PBS/2% (w/v) BSA for 1h at room temperature on a rocker. Cells were washed with water and plates imaged on the Odyssey to visualise immunofluorescence.

7.2.3.4: Measurement of plaque diameter

Post plaque assay the diameter of 20 plaques per virus was measured (unless otherwise stated) to calculate average plaque diameters within MDCK cells. Stained plates were photographed/scanned and ImageJ analysis software (Abramoff et al., 2004) was used to estimate plaque diameter based on the known diameter of the well using the 'set scale' function.

7.2.3.5: Virus infections of cells

Cells were plated the day prior to infection to achieve around 90% confluency. Cells were washed in serum-free DMEM to remove residual FCS. Virus stocks were diluted in serum-free DMEM to achieve the desired multiplicity of infection (MOI) and applied to cells in a low volume (e.g. 100µl in a 24 well plate format) for 1h at 37°C. Cells were then overlaid with virus growth media (CKC growth media for CK cells) to achieve multicycle replication. Supernatants were collected at the desired time points post infection, clarified (1000xg, 5 min) and stored at -80°C for downstream analysis.

7.2.3.6: Virus detection via immunofluorescence "in-cell westerns"

Cells infected with virus were stained for presence of viral NP to assess infection rates. At 8h post infection, cells in 24 well plates were washed twice with PBS and fixed using 250µl PBS/4% (v/v) formaldehyde for 20 min. Fixed

cells were again washed with PBS before permeablisation with 250µl PBS/0.2% (v/v) Triton X-100 for 5 min. Cells were washed with 1ml PBS/1% (v/v) FCS and stained with α-NP (1:2000) for 1h at room temperature. Cells were washed with 1ml PBS/1% (v/v) FCS and incubated with the appropriate secondary antibody diluted 1:10000 in PBS/1% (v/v) FCS for 1h at room temperature protected from light by foil. The presence of NP was detected via imaging on the Odyssey imager or via an epi-fluorescence microscope.

7.2.3.7: Extraction of RNA from cell supernatants/allantoic fluid

Viral RNA extraction from cell culture media or egg allantoic fluid was completed using the QIAamp Viral RNA mini kit (Qiagen) following the manufacturer's instructions. Briefly, 140µl of sample was added to 560µl of prepared AVL buffer containing carrier RNA and was incubated at room temperature for 10 min to ensure sufficient lysis. 560µl (96-100%) ethanol was added to precipitate RNA and the mix added to the QIAamp Mini column. Columns were centrifuged (5800xg, 1 min) and flow through removed. The columns were then washed twice with the provided buffers and RNA eluted into a final volume of 60µl of Buffer AVE.

7.2.3.8: Virus sequencing

Viral RNA was extracted from P_1 stocks as described above. cDNA synthesis from the viral RNA was completed using the Verso cDNA synthesis kit (Thermo Scientific; #AB-1453) as per the manufacturer's instructions using the FluG (H9N2) or Uni12 (PR8 7:1) primers. Briefly, reverse transcription reactions were set up as follows: RT mix; vRNA- 200ng, Primer- 120ng (each), H_2O- made

up to 10µl, then heated at 65°C for 10 min. Afterwards, RT mix (10µl-from above), dNTPs- 5mM each, RT enzyme- 1µl, 5x cDNA synthesis buffer- 4µl and H_2O- made up to 20µl were added and the mix proceeded to RT programme (42°C for 60 min) followed by an inactivation step of 95°C for 2 min.

The cDNA product was amplified using PCR prior to sequencing. 2.5U Taq DNA polymerase was used within a 25µl reaction volume containing 1.5mM magnesium chloride, 1x Taq PCR buffer (Invitrogen), 200nM forward primer, 200nM reverse primer and 250µM (each) dNTPs. Thermocycling conditions depended on the amplicon targeted. Typically an annealing temperature of Tm-5°C (primer with lowest Tm) was adopted. For example, the following conditions were used for amplification of UDL-01 PA segment cDNA: i) a 2 min denaturation step at 94°C, ii) a 1 min denaturation step at 94°C, iii) a 1 min primer annealing step at 55°C, iv) a 3 min elongation step at 72°C, with steps ii) – iv) performed for 30 cycles, and v) a final 10 min elongation step at 72°C.

Prior to sequencing, PCR product was purified using QIAGEN's QIAquick PCR purification kit as per the manufacturer's protocol. The PCR product was eluted in 30µl of water and run on a 1% agarose gel (section 7.2.1.5). Sanger sequencing of cDNA was performed by GATC (PR8 7:1 viruses) or Source Biosciences (H9N2 viruses).

7.2.4: Transfection based assays

7.2.4.1: Minireplicon assays

293T cells were seeded into 24 well plates to achieve 70-80% confluency for transfection the following day (0.05 x 10^6 cells per well seeded). Protein expression plasmids for each of the components of a vRNP (PB2, PB1, PA and NP) along with a firefly luciferase reporter construct (pPol I Luc) at the following concentrations: PB2- 80ng, PB1- 80ng, PA- 20ng, NP- 160ng, pPol I Luc- 80ng, were added to 50µl of Opti-MEM. 2.5µl (2.5µg) of Lipofectamine2000 transfection reagent was mixed with another 50µl of Opti-MEM and incubated for 5 min at room temperature. The DNA and Lipofectamine2000 samples were mixed and incubated at room temperature for a further 30 min. 293T cell media was removed and replaced with 0.5ml of Opti-MEM per well. 100µl of transfection mixes was added dropwise to each well, with each sample repeated in triplicate. Cells were incubated at 37°C for 48h, after 8h media was removed and complete DMEM added for the remaining time. After 48h, media was gently removed and cells lysed in 100µl of 1x Passive Lysis Buffer (Promega). Plates were freeze-thawed once to ensure efficient cell lysis. Cells were scraped and mixed with a P200 Gilson pipette tip. 10µl of cell lysate was added to a white bottomed 96-well plate. A Promega GloMax Multi Detection unit was employed to inject 25µl of Luciferase Assay Reagent II (Promega) per well and to measure the luciferase activity (injection speed 200µl/sec, 0.5 sec gap, 5 sec integration time) following the manufacturer's instructions.

For RNP reconstitution assays within DF-1 cells, the protocol was as described above except twice the concentration of DNA was included within each reaction and the firefly luciferase reporter construct was driven by a chicken promotor (CKpPol I Luc).

7.2.4.2: Plasmid based host cell shut off assays

293T cells were seeded as above into 24 well plates to achieve 70-80% confluency for transfection the following day (0.05 x 10^6 cells per well seeded). 5ng/µl of protein expression plasmids of the influenza segment 3 (PA) and 1ng/µl of a β-galactosidase (β-gal) reporter construct were added to 50µl of Opti-MEM. In a separate tube 50µl of Opti-MEM, 2.5µl (0.05µg/µl) of Lipofectamine2000 were added. Mixes were incubated for 5 min at room temperature after which they were mixed and incubated for a further 30 min. Meanwhile, 293T cell media was removed and replaced with 0.5ml of Opti-MEM per well. 100µl of transfection mixes were added dropwise to each well, with each sample repeated in triplicate. Cells were incubated at 37°C for 48h, after 8h media was removed and complete DMEM added for the remaining time. After 48h, cells were lysed with 100µl of 1x Reporter lysis buffer (RLB; Promega). β-gal expression was measured using the β-galactosidase enzyme assay system (Promega). Briefly, 20µl of cell lysate was diluted in 30µl of 1xRLB in a clear bottomed 96-well plate. 50µl of 2x Assay buffer was added to each well and the samples mixed by pipetting. The plate was incubated at 37°C for 30 min until the development of a yellow colour within the wells. Reaction progression was stopped via the addition

of 150µl of 1M sodium carbonate. A Promega GloMax Multi Detection unit was employed to read absorbance at 420nm.

For β-gal assays within DF-1 cells, the protocol was as described above, except the concentrations of DNA were doubled within the transfection mix and the cell lysates were read neat and not diluted further in 1xRLB.

7.2.5: Protein Analyses

7.2.5.1: Protein Electrophoresis

Proteins were separated by molecular weight by sodium dodecyl sulphate polyacrylamide gel electrophoresis (SDS-PAGE) using a discontinuous polyacrylamide gel system. SDS-PAGE equipment was supplied by Bio-Rad (Mini-PROTEAN tetra system). Polyacrylamide gels were cast using buffers and solutions supplied by Protogel according to manufacturers' instructions, altering the concentration of acrylamide: bisacrylamide (37.5:1) solution to produce the required resolving gel percentage. Stacking gels were cast at 4%. Examples of resolving and stacking gel recipes are seen within section 7.1.6. 0.75mm spacer plates were used with appropriate short plates. *In Vitro* Translations (IVTs) were run on large gels with equipment supplied by BioRad.

To generate cell lysates, typically cells seeded in 24-well plates were lysed in 200µl of protein loading buffer. Samples were boiled for 5 min at 95°C, vortexed and the briefly centrifuged. 10-20µl (25µl for IVTs) were loaded per lane of each gel. Gels were run vertically at a constant voltage of 100-120V for the

desired length of time, using a pre-stained molecular weight marker (Promega) as a guide for protein migration.

7.2.5.2: Western Blotting

Proteins separated via SDS-PAGE were blotted onto nitrocellulose membranes (BioRad) using a semi-dry blotting system (Trans-Blot Turbo Transfer System (Bio-Rad). The nitrocellulose membrane was placed onto the polyacrylamide gel supported by stacks of filter paper, this was then placed into the Trans-Blot system with the membrane on the negative cathode side. Protein transfers were run for 10min at 25V, 2.5A. Nitrocellulose membranes were blocked in PBS/0.1% (v/v) Tween20 with 5% (w/v) skimmed milk (Marvel) for at least 1h at room temperature on a rocker. Blocked membranes were probed with primary antibody, diluted in PBS/0.1% (v/v) Tween20 with 2% (w/v) skimmed milk (Marvel), typically, overnight at 4°C with rocking. Membranes were washed 3x 5 min in PBS/0.1% (v/v) Tween20, and then incubated with secondary antibody, diluted in PBS/0.1% (v/v) Tween20, for 1h at room temperature, rocking and covered from light by foil. Membranes were washed 3x 5 min in PBS/0.1% (v/v) Tween20 before imaging on the Odyssey CLX (LI-COR Biosciences).

7.2.5.3: ^{35}S-methionine/cysteine-labelling protein studies

CEF cells were seeded in 24-well plates and infected with virus at an MOI of 3 using standard protocols (section 7.2.3.5). Cells were seeded in duplicate to allow for generation of cell lysates and assessment of successful infection via IF.

At 6h post-infection, cells were washed twice in warmed PBS before overlay with 1ml of methionine-and cysteine- free DMEM supplemented with 5% (v/v) dialysed FCS and 2mM L-Glutamine to starve the cells of methionine and cysteine. At 8h post infection, cells were washed twice with warm PBS and overlaid with 0.5ml of methionine- and cysteine- free DMEM (supplemented as above) including ^{35}-S-methionine/cysteine protein labelling mix (Perkin/Elmer) at 0.8mBq/ml. Cells were incubated at 37°C in a vented box containing activated charcoal (Fisher) for 1h. Cells were washed once with ice-cold PBS and then cells lysed in protein loading buffer for SDS-PAGE as above and processed via autoradiography (section 7.2.5.1 + 7.2.5.6).

7.2.5.4: Puromycin labelling protein studies

MDCK cells were seeded into 12 well plates and infected with virus at an MOI of 5 using the standard protocol (section 7.2.3.5). At 7.5h post infection cells were washed with PBS and the medium changed to 1ml of complete DMEM containing 10µg/ml of Puromycin dihydrochloride from *Streptomyces alboniger* for 30 min. Cells were washed with ice cold PBS and lysed in 100µl of protein loading buffer for SDS-PAGE and western blotting for puromycin as above. Puromycylated protein synthesis was quantified in the region of the gel between 45kDa and 80kDa.

7.2.5.5: *In Vitro* translations

To perform *in vitro* translations to visualise radiolabelled proteins the TnT® Coupled Reticulocyte Lysate system (Promega; #L4610) was adopted. Briefly, TnT reaction were set up as follows: 8µl TnT mix, 4µCi ^{35}S-Methinone,

made up to 15µl with H_2O, 200ng plasmid DNA. Mixes were prepared on ice using sawn off pipette tips to aliquot the TnT mix before reactions were incubated at 37°C for 90 min. The reactions were denatured in 50µl protein loading buffer and analysed via SDS-PAGE and autoradiography (section 7.2.5.1 and 7.2.5.6)

7.2.5.6: Autoradiography of dried polyacrylamide gels

SDS-PAGE was run as described previously. Gels were fixed by rocking in gel fix solution (50% methanol (v/v), 10% acetic acid (v/v)) for 5-15 min depending on the size of the gel. The fix solution was replaced for 2 more rounds of fixing. Gels were laid on 3MM Whatman filter paper and covered with Clingfilm then dried in a gel dryer (Bio-Rad) by heating up to 80°C for 2-4h under vacuum pressure. Dried gels were placed in a sealed cassette with an X-ray film (Thermo Fisher) overnight, at a minimum or until the desired signal strength was achieved. X-ray films were developed using a Konica SRX-101A X-ograph film processor using manufacturers' instructions.

7.2.5.7: Densitometry

Protein quantification following autoradiography was determined by densitometry using ImageJ analysis software. The gel analyser tool was used on scans of exposed films to measure the area under the peak generated by each 'band' on the autoradiograph. The larger the peak, the brighter the band, the higher the amount of protein present.

7.2.6: Modelling, sequence analysis and bioinformatics

7.2.6.1: Modelling and mapping of PA structures

Structural prediction of UDL-01 and WF10 endonuclease domains after mutation were completed using the I-TASSER server for protein structure prediction accessed online at https://zhanglab.ccmb.med.umich.edu/I-TASSER/. This platform has been developed as an integrated system for automated protein structure analysis. The amino acid sequence of the protein is used to generate 3-D atomic models from multiple threading alignments and iterative structural assembly situations (Roy et al., 2010). Known PA structures were downloaded from the Protein Data Bank (PDB) for annotation with mutations identified during the study. All structural images were generated and annotated using PyMol v1.5.0 (www.pymol.org; Schrodinger, 2010).

7.2.6.2: Analysis of sequencing data

Sanger sequencing was outsourced to GATC and Source Biosciences (Lifesciences). Alignment of sequencing reads to plasmids or influenza gene segments were performed using CLUSTAL multiple alignment or optimal GLOBAL alignment functions (BioEdit).

7.2.6.3: Bioinformatics of PA sequences

To perform analysis of the diversity and distribution of amino acids across the PA gene bioinformatics analysis was carried out by Dr Samantha Lycett at the Roslin Institute. Full length sequences, with coding regions marked as complete or nearly complete, were downloaded from the NCBI influenza virus resource

(23th June 2015). Files were split into 1000 base pair regions and aligned using MUSCLE (MEGA6) and then re-joined. Incomplete sequences or sequences with runs of non-identified amino acids were excluded from the analysis (totalling 88 avian, 14 swine, 55 human and 1 canine-derived virus sequences). This left 12,248 avian, 3082 swine, 12,148 human, 77 canine and 177 equine virus sequences for further analysis. The data sets were analysed by host and the consensus amino acid as well as the further 3 most common amino acids identified for each position. The fraction of sequences with each of the amino acids was also calculated.

7.2.7: *In ovo* characterisation of H9N2 AIVs

7.2.7.1: Inoculation of embryonated eggs

To characterise H9N2 AIVs *in ovo*, embryonated hens' eggs (VALO breed) were used. The eggs were incubated at 37°C, 40-50% humidity, for 10 days and candled to ensure viability prior to inoculation. Virus stocks were diluted to the required pfu in 1ml of PBS. A small hole was introduced into the egg shell just below the line of the air sac. The shell was sterilised with 70% (v/v) ethanol. 100µl of the diluted virus was introduced into the allantoic cavity using a 1ml syringe and 25 gauge needle. The hole was sealed with Scotch tape and eggs were incubated for 4-72h. Eggs were culled via refrigeration at 4°C for a minimum of 6h. The top of the shell was removed using forceps and the air sac punctured using a P1000 Gilson pipette tip. Allantoic fluid from each egg was collected using a P1000 Gilson pipette and clarified by centrifugation (1400xg, 10 min). Viral

replication within the eggs was assessed via plaque assay or via immunostaining for NP (Sections 7.2.3.3.2 and 7.2.3.6).

Viral passage in eggs was completed as above, except the allantoic fluid samples were titrated via plaque assay (section 7.2.3.3.2) after each passage and 100 pfu inoculated into one egg per passage.

7.2.7.2: Assessment of embryo gross pathology

Six eggs per group were inoculated with 100 pfu of each virus, or sterile PBS as described above (section 7.2.7.1). Embryos were candled twice daily to check for embryo viability. Eggs were assessed for experimental end points including lack of movement of the embryo, disruption of blood vessels and/or signs of haemorrhage. If any end point signs were observed, embryos were chilled immediately. At 48h post infection, all remaining embryos were refrigerated for a minimum of 6h. Each embryo was removed from the shell, washed twice with PBS and photographed to document the gross pathology. Samples of allantoic fluid were collected and viral titres within each egg assessed via plaque assay (section 7.2.3.3.2). Images of embryos which were positive for detection of virus and had not died early within the experiment (prior to the final candling) were selected for further analysis.

The gross pathology of the embryos was then blindly scored by three group members. The scoring criteria were as follows: 0- no obvious bleeding, 1- subtle bleeding, 2- considerable bleeding, 3- very obvious bleeding and/or embryo not intact. Each scorer independently examined the embryo images and assigned a score between 0 and 3 with no half scores being given. This enabled a

quantifiable measure to be allocated to each infected group. Embryo size was assessed using ImageJ analysis software. Estimates of embryo length were calculated from the images using the known diameter of the petri dishes the embryos were imaged in. The 'set scale' analysis tool was used to estimate length.

7.2.7.3: Calculation of Egg infectious Dose 50 (EID_{50})

A 10-fold serial dilution of the relevant virus (10000 pfu to 0.001 pfu) was made as used to infect 5 embryonated eggs per virus per dilution (as described in section 7.2.7.1). Samples of allantoic fluid were collected and presence of virus detected via immunofluorescence for viral NP protein (Section 7.2.3.6). To calculate the Egg Infectious Dose 50 (EID_{50}), the Reed-Muench method was adopted (Reed and Muench, 1938):

$$Proportionate\ distance = \frac{50\% - (\%infection\ at\ dilution\ below)}{(\%infection\ at\ dilution\ above) - (\%infection\ at\ dilution\ below)}$$

$$Log10\ EID50 = log10\ of\ dilution\ showing\ infection\ above\ 50\% - PD * logarithm\ of\ dilution\ factor$$

This allowed for the dilution of virus in which 50% of the inoculated eggs showed viable infection to be calculated.

7.2.7.4: Assessment of embryo survival

A 10-fold serial dilution of the relevant virus (10000 pfu to 0.001 pfu) was made as used to infect 5 embryonated eggs per virus per dilution (as described

in section 7.2.7.1). Embryos were candled twice daily throughout the study period to check for embryo viability (up to 84 hours post infection). If eggs reached a predetermined end point at candling they were deemed to be dead and the eggs chilled to ensure death before disposal. The markers of the end point included; lack of movement of the embryo, disruption of blood vessels within the egg and/or signs of haemorrhage. If the embryos survived until the experiment end (84 hours post infection) they were culled via a schedule one method (chilling). Samples of allantoic fluid were collected and presence of virus detected via immunostaining for viral NP protein (section 7.2.3.6). Any eggs without positive detection of viral NP were removed from the study.

7.2.8: *In vivo* characterisation of H9N2 AIVs

7.2.8.1: Ethics statement

All animal experiments were carried out in strict accordance with the European and United Kingdom Home Office Regulations and the Animal (Scientific Procedures) Act 1986 Amendment regulation 2012, under the authority of a United Kingdom Home Office Licence (Project Licence Numbers: P68D44CF4 X and PPL3002952).

7.2.8.2: Influenza infectivity, transmission and pathogenicity experiment set up

Rhode Island Red (RIR) or White Leghorn fertilised embryos were purchased from the National Avian Research Facility (NARF) or VALO respectively and housed within the Pirbright Institute BSU. Embryonated eggs

were incubated for 21 days and hatched at the Pirbright Institute by members of the animal services team after which point they were housed in floor pens within the Pirbright Institute BSU until 3 weeks old. Prior to the commencement of the study, all birds were swabbed (in both oropharyngeal and cloacal cavities) and bled via wing prick to determine any pre-study infection. The relevant number of birds were transferred into self-contained BioFlex B50 Rigid Body Poultry isolators (Bell Isolation Systems) so that they could remain at negative pressure. The remaining birds were kept housed in floor pens within the same room. Infection of RIR or VALO chickens was conducted by Prof. Munir Iqbal, Dr Holly Shelton and Dr Jean-Remy Sadeyen (The Pirbright Institute, UK). 10-20 birds per group were directly inoculated with 100µl of a 10^5 pfu/ml virus stock diluted in PBS via the nares (50µl in each nostril). Mock infected birds were inoculated with sterile PBS as an alternative. One day post infection 8 naïve contact birds were introduced into each isolator to determine viral transmissibility.

Throughout the experiment, birds were swabbed in the buccal and cloacal cavities (on day 1-8, 10 and 14 post infection) by a trained member of staff who held a personal licence (Prof. Munir Iqbal, Dr. Holly Shelton, Dr. Jean-Remy Sadeyen, Dr. Pengxiang Chang, Dr. Sushant Bhat, Joshua Sealy, Anabel Clements). Swabs were collected into 1ml of virus transport media (WHO standard). Swabs were soaked in media and vortexed for 10 sec before centrifuging (2300xg, 10 min) and aliquoting supernatant. Viral titres in swabs were determined via plaque assay (described in section 7.2.3.3.2). Environmental samples (at least 1g of food and 1ml of water) were collected on a daily basis from each isolator and the pen. 1g of food sample was weighed, mixed with 1ml of serum-free DMEM,

vortexed until homogenised and the clarified (5800xg, 15 min). Food and water samples were stored at -80°C before virus titrated via plaque assay.

At various time points post infection; day 2 in both studies and day 1 and 3 within the RIR study, birds housed within isolators were euthanised via overdose of pentobarbital (at least 1ml) injected into the wing vein or jugular (Prof. Munir Iqbal or Dr. Holly Shelton). Mock infected birds were culled via cervical dislocation (Rachel New, Billy Matthews). A panel of tissues were collected with the help of Dr. Jean-Remy Sadeyen during post-mortem examination. Tissues were split into 2 sections and stored in RNA later or snap frozen in dry ice. The RNA later and snap frozen tissues were stored at -80°C until further processing. On day 14 post infection, all remaining birds were culled via overdose of pentobarbital or cervical dislocation.

7.2.8.3: Clinical scoring system

Birds were observed twice daily by members of animal services and whilst procedures were carried out. Birds were monitored for the presence of clinical signs of infection. Mild clinical signs expected during the study included, ruffled feathers, pale comb/wattles, eye and nasal discharge, reddened eyes, snicking and depression. Additional moderate clinical signs that may be expected included drooping wings, swollen heads and sporadic diarrhoea. If any signs of severe disease including laboured breathing, persistent diarrhoea, sitting alone and showing no signs to evade capture and in the most extreme instances paralysis and unconsciousness were observed birds were euthanised via a schedule one method and post mortem examination carried out.

7.2.8.4: Isolation of virus from tissues

50mg of snap frozen tissues (collected during post mortem examination) were weighed and added to 250µl of sterile PBS + 100U/ml penicillin/streptomycin to make 20% (w/v) in a safe-lock Eppendorf tube. One sterile 5mm stainless steel bead was added per tube and tissues homogenised using the Retsch MM 300 Bead Mill system (20Hz, 4min). After one round of homogenisation, tissue disruption was checked and repeated if necessary until tissue was fully homogenised. Samples were centrifuged (16,000xg, 5 min, 4°C) and kept on ice. Supernatants were titrated via plaque assay (section 7.2.3.3.2) to determine presence of infectious virus.

7.2.8.5: Trizol extraction of RNA from tissues

30mg of tissue collected in RNA later were weighed and placed in a safe-lock Eppendorf tube with 750µl of Trizol. One sterile 5mm stainless steel bead was added per tube and tissues homogenised using the Retsch MM 300 Bead Mill system (20Hz, 4 min). After one round of homogenisation, tissue disruption was checked and repeated if necessary until tissue fully homogenised. 200µl of chloroform was added per tube. Tubes were shaken vigorously and incubated for 5 min at room temperature. Samples were centrifuged (9,200xg, 30 min, 4°C). The top aqueous phase containing total RNA was added to a new microcentrifuge tube and the remaining fluid discarded. RNA extraction was then carried out using the QIAGEN RNeasy mini kit following manufacturers' instructions.

7.2.8.6: qRT-PCR

100ng of RNA extracted from tissue samples (section 7.2.8.5) was used for qRT-PCR. All qRT-PCR was completed using the Superscript III platinum One step qRT-PCR kit (Life Technologies) following manufacturer's instructions for reaction set up. Primer probe sets outlined in Table 7.11. qRT-PCR was run in a 7500 FAST ABI RT-PCR thermocycler (Applied Biosystems). Cycling conditions as follows: i) 5 min hold step at 50°C, ii) a 2 min hold step at 95°C, and 40 cycles of iii) 3 sec at 95 °C and iv) 30 sec annealing and extension at 60 °C. Cycle threshold (CT) values were obtained using 7500 softwarev2.3 and exported to Microsoft excel for further analysis. Mean CT values were calculated from triplicate data. Negative controls were included within each plate to determine any unspecific amplification or contamination.

Within viral M segment qRT-PCR an M segment RNA standard curve was completed alongside the samples to quantify the amount of M gene RNA within the sample from the CT value. T7 RNA polymerase-derived transcripts from UDL-01 segment 7 were used for the preparation of the standard curve (provided by Dr. Joe James).

Within the cytokine qRT-PCRs, three housekeeping genes were included per sample (RPLPO-1, RPL13 and 28S rRNA). These had previously determined to be the most stable housekeeping genes within the broadest range of tissues (Tom Whitehead, personal communication). Briefly, the geNorm algorithm (Vandesompele et al., 2002) was adopted to calculate the stability for each reference gene and the optimal reference gene number from raw Cq values of

candidate reference genes using qbase+ real-time qPCR software version 3.0 (Biogazelle).

7.2.8.7: Next Generation Sequencing

RNA was extracted from swab supernatants (Section 7.2.3.7) and RT-PCR for next generation sequencing was conducted using the Invitrogen one-step RT-PCR kit (CAT#12574-035) and universal influenza primers (see table 7.10 for details). 30µl RT-PCR mixes were set up as follows: 15.0µl 2x RTPCR buffer, 2µM Uni-12FA primer, 6µM Uni-12FG primer, 6µM Uni-13R primer, 0.5µl enzyme mix, 5µl of required RNA, made up to 30µl with H_20. Reaction mixes were placed in a pre-warmed thermocycler paused at 42°C. Cycling conditions were as follows: i) 42°C for 50 min, ii) 50°C for 10 min, iii) 94°C for 2 min, 5 cycles of iv) 94°C for 2 min, v) 43°C for 30 sec, vi) 68°C for 4 min, followed by a further 31 cycles of vii) 94°C for 30 sec viii) 57°C for 30 sec ix)68°C for 4 min, then 68°C for 10 min. PCR products were analysed via gel electrophoresis to visualise the banding pattern spanning the influenza gene sizes (section 7.2.1.5). Products were then purified using the Qiagen PCR purification kit following manufacturers' instruction. Samples were sent to the Francis Crick Institute (London) for NGS on the Illumina MiSeq using Illumina Nextera XT for library preparation. NGS reads were analysed for consensus sequences by Joshua Sealy. Consensus sequences were aligned as described in section 7.2.6.2.

7.2.9: Statistical analyses

All statistical analysis was carried out using GraphPad Prism 6/7 software. Distribution of data was assessed prior to deciding on the statistical test to use.

Chapter 8: References

Aamir, U. B., Wernery, U., Ilyushina, N. and Webster, R. G. (2007) 'Characterization of avian H9N2 influenza viruses from United Arab Emirates 2000 to 2003', Virology, 361(1), pp. 45-55.

Abramoff M, Magalhaes P, Ram S. (2004) 'Image processing with ImageJ'.Biophotonics International. LAURIN Publishing.

Acland, H. M., Silverman Bachin, L. A. and Eckroade, R. J. (1984) 'Lesions in broiler and layer chickens in an outbreak of highly pathogenic avian influenza virus infection', Vet Pathol, 21(6), pp. 564-9.

Akarsu, H., Burmeister, W. P., Petosa, C., Petit, I., Müller, C. W., Ruigrok, R. W. and Baudin, F. (2003) 'Crystal structure of the M1 protein-binding domain of the influenza A virus nuclear export protein (NEP/NS2)', EMBO J, 22(18), pp. 4646-55.

Alexander, D. J. (2000) 'A review of avian influenza in different bird species', Vet Microbiol, 74(1-2), pp. 3-13.

Amorim, M. J., Bruce, E. A., Read, E. K., Foeglein, A., Mahen, R., Stuart, A. D. and Digard, P. (2011) 'A Rab11- and microtubule-dependent mechanism for cytoplasmic transport of influenza A virus viral RNA', J Virol, 85(9), pp. 4143-56.

Amorim, M. J., Read, E. K., Dalton, R. M., Medcalf, L. and Digard, P. (2007) 'Nuclear export of influenza A virus mRNAs requires ongoing RNA polymerase II activity', Traffic, 8(1), pp. 1-11.

Aranda, M. and Maule, A. (1998) 'Virus-induced host gene shutoff in animals and plants', Virology, 243(2), pp. 261-7.

Arranz, R., Coloma, R., Chichón, F. J., Conesa, J. J., Carrascosa, J. L., Valpuesta, J. M., Ortín, J. and Martín-Benito, J. (2012) 'The structure of native influenza virion ribonucleoproteins', Science, 338(6114), pp. 1634-7.

Arzey, G. G., Kirkland, P. D., Arzey, K. E., Frost, M., Maywood, P., Conaty, S., Hurt, A. C., Deng, Y. M., Iannello, P., Barr, I., Dwyer, D. E., Ratnamohan, M., McPhie, K. and Selleck, P. (2012) 'Influenza virus A (H10N7) in chickens and poultry abattoir workers, Australia', Emerg Infect Dis, 18(5), pp. 814-6.

Ayllon, J., Domingues, P., Rajsbaum, R., Miorin, L., Schmolke, M., Hale, B. G. and García-Sastre, A. (2014) 'A single amino acid substitution in the novel H7N9 influenza A virus NS1 protein increases CPSF30 binding and virulence', J Virol, 88(20), pp. 12146-51.

Bahari, P., Pourbakhsh, S. A., Shoushtari, H. and Bahmaninejad, M. A. (2015) 'Molecular characterization of H9N2 avian influenza viruses isolated from vaccinated broiler chickens in northeast Iran', Trop Anim Health Prod, 47(6), pp. 1195-201.

Baer, A., & Kehn-Hall, K. (2014). Viral concentration determination through plaque assays: using traditional and novel overlay systems. *Journal of visualized experiments : JoVE*, (93), e52065. doi:10.3791/5206

Bano, S., Naeem, K. and Malik, S. A. (2003) 'Evaluation of pathogenic potential of avian influenza virus serotype H9N2 in chickens', Avian Dis, 47(3 Suppl), pp. 817-22.

Barker, K. A., Hampe, A., Stoeckle, M. Y. and Hanafusa, H. (1993) 'Transformation-associated cytokine 9E3/CEF4 is chemotactic for chicken peripheral blood mononuclear cells', J Virol, 67(6), pp. 3528-33.

Baskin C.R., Bielefeldt-Ohmann H., Tumpey T.M., Sabourin P.J., Long J.P., García-Sastre A., Tolnay A-E., Albrecht R., Pyles J.A., Olson P.H., Aicher L.D., Rosenzweig E.R., Murali-Krishna K., Clark E.A., Kotur M.S., Fornek J.L., Proll S., Palermo R.E., Sabourin C.L., Katze M.G. (2009) 'Early and sustained innate immune response defines pathology and death in nonhuman primates infected by highly

pathogenic influenza virus' Proceedings of the National Academy of Sciences, 106 (9) 3455-3460; DOI: 10.1073/pnas.0813234106
Baudin, F., Bach, C., Cusack, S. and Ruigrok, R. W. (1994) 'Structure of influenza virus RNP. I. Influenza virus nucleoprotein melts secondary structure in panhandle RNA and exposes the bases to the solvent', EMBO J, 13(13), pp. 3158-65.
Bavagnoli, L., Cucuzza, S., Campanini, G., Rovida, F., Paolucci, S., Baldanti, F. and Maga, G. (2015) 'The novel influenza A virus protein PA-X and its naturally deleted variant show different enzymatic properties in comparison to the viral endonuclease PA', Nucleic Acids Res, 43(19), pp. 9405-17.
Bean, W. J., Kawaoka, Y., Wood, J. M., Pearson, J. E. and Webster, R. G. (1985) 'Characterization of virulent and avirulent A/chicken/Pennsylvania/83 influenza A viruses: potential role of defective interfering RNAs in nature', J Virol, 54(1), pp. 151-60.
Betts MJ., and Russell RB. (2003) 'Amino acid properties and consequences of substitutions'. Bioinformatics for geneticists: John Wiley & Sons, Ltd. Available at: http://www.ksrbiotech.com/uploads/Aminoacid%20Substitutions.pdf.
Bier, K., York, A. and Fodor, E. (2011) 'Cellular cap-binding proteins associate with influenza virus mRNAs', J Gen Virol, 92(Pt 7), pp. 1627-34.
Bingham J., Green DJ., Lowther S.,Klippel J., Burggraaf S., Anderson DE., Wibawa H., Hoa DM., Long NT., Vu PP., Middleton DJ., and Daniels PW. (2009) 'Infection studies with two highly pathogenic avian influenza virus strains (Veitnamese and Indonesian) in Pekin Ducks (Anas platyrhynchos), with particular reference to clinical disease, tissue tropism and viral shedding.'. Avian Pathol (38), pp. 267-278.
Bizebard, T., Gigant, B., Rigolet, P., Rasmussen, B., Diat, O., Bösecke, P., Wharton, S. A., Skehel, J. J. and Knossow, M. (1995) 'Structure of influenza virus haemagglutinin complexed with a neutralizing antibody', Nature, 376(6535), pp. 92-4.
Blaas, D., Patzelt, E. and Kuechler, E. (1982) 'Identification of the cap binding protein of influenza virus', Nucleic Acids Res, 10(15), pp. 4803-12.
Bourmakina, S. V. and García-Sastre, A. (2003) 'Reverse genetics studies on the filamentous morphology of influenza A virus', *J Gen Virol*, 84(Pt 3), pp. 517-27.
Braam, J., Ulmanen, I. and Krug, R. M. (1983) 'Molecular model of a eukaryotic transcription complex: functions and movements of influenza P proteins during capped RNA-primed transcription', Cell, 34(2), pp. 609-18.
Bradel-Tretheway, B. G., Mattiacio, J. L., Krasnoselsky, A., Stevenson, C., Purdy, D., Dewhurst, S. and Katze, M. G. (2011) 'Comprehensive proteomic analysis of influenza virus polymerase complex reveals a novel association with mitochondrial proteins and RNA polymerase accessory factors', J Virol, 85(17), pp. 8569-81.
Brown, D. A. and London, E. (1998) 'Functions of lipid rafts in biological membranes', Annu Rev Cell Dev Biol, 14, pp. 111-36.
Brown, J. D., Swayne, D. E., Cooper, R. J., Burns, R. E. and Stallknecht, D. E. (2007) 'Persistence of H5 and H7 avian influenza viruses in water', Avian Dis, 51(1 Suppl), pp. 285-9.
Bruce, E. A., Digard, P. and Stuart, A. D. (2010) 'The Rab11 pathway is required for influenza A virus budding and filament formation', *J Virol*, 84(12), pp. 5848-59.
Bruce, E. A., Stuart, A., McCaffrey, M. W. and Digard, P. (2012) 'Role of the Rab11 pathway in negative-strand virus assembly', Biochem Soc Trans, 40(6), pp. 1409-15.
Bui, M., Whittaker, G. and Helenius, A. (1996) 'Effect of M1 protein and low pH on nuclear transport of influenza virus ribonucleoproteins', J Virol, 70(12), pp. 8391-401.
Burnet, F. M. and Stone, J. D. (1949) 'The genetic character of O-D change in influenza A', Br J Exp Pathol, 30(5), pp. 419-25.

Cameron, K. R., Gregory, V., Banks, J., Brown, I. H., Alexander, D. J., Hay, A. J. and Lin, Y. P. (2000) 'H9N2 subtype influenza A viruses in poultry in pakistan are closely related to the H9N2 viruses responsible for human infection in Hong Kong', Virology, 278(1), pp. 36-41.

Capua, I. and Alexander, D. J. (2004) 'Avian influenza: recent developments', Avian Pathol, 33(4), pp. 393-404.

Capua, I. and Marangon, S. (2004) 'Vaccination for avian influenza in Asia', Vaccine, 22(31-32), pp. 4137-8.

Centers for Disease C, Prevention. Update: influenza activity--United States and worldwide, 2003-04 season, and composition of the 2004-05 influenza vaccine. MMWR Morbidity and mortality weekly report. 2004 Jul 2;53(25):547-52. PubMed PMID: 15229411.

Centers for Disease C, Prevention. Notes from the field: Highly pathogenic avian influenza A (H7N3) virus infection in two poultry workers--Jalisco, Mexico, July 2012. MMWR Morbidity and mortality weekly report. 2012 Sep 14;61(36):726-7. PubMed PMID: 22971746.

Chase, G. P., Rameix-Welti, M. A., Zvirbliene, A., Zvirblis, G., Götz, V., Wolff, T., Naffakh, N. and Schwemmle, M. (2011) 'Influenza virus ribonucleoprotein complexes gain preferential access to cellular export machinery through chromatin targeting', PLoS Pathog, 7(9), p. e1002187.

Chen, W., Calvo, P. A., Malide, D., Gibbs, J., Schubert, U., Bacik, I., Basta, S., O'Neill, R., Schickli, J., Palese, P., Henklein, P., Bennink, J. R. and Yewdell, J. W. (2001) 'A novel influenza A virus mitochondrial protein that induces cell death', *Nat Med*, 7(12), pp. 1306-12.

Chen, B. J., Leser, G. P., Morita, E. and Lamb, R. A. (2007) 'Influenza virus hemagglutinin and neuraminidase, but not the matrix protein, are required for assembly and budding of plasmid-derived virus-like particles', J Virol, 81(13), pp. 7111-23.

Chen, B.L, Zhang, Z, and Chen WB.(1994) 'The study of avian influenza: I. The isolation and preliminary serological identification of avian influenza virus in chicken'. China J Vet Med (20), pp. 3-5.

Chen, G. W., Chang, S. C., Mok, C. K., Lo, Y. L., Kung, Y. N., Huang, J. H., Shih, Y. H., Wang, J. Y., Chiang, C., Chen, C. J. and Shih, S. R. (2006) 'Genomic signatures of human versus avian influenza A viruses', Emerg Infect Dis, 12(9), pp. 1353-60.

Chen, H., Yuan, H., Gao, R., Zhang, J., Wang, D., Xiong, Y., Fan, G., Yang, F., Li, X., Zhou, J., Zou, S., Yang, L., Chen, T., Dong, L., Bo, H., Zhao, X., Zhang, Y., Lan, Y., Bai, T., Dong, J., Li, Q., Wang, S., Li, H., Gong, T., Shi, Y., Ni, X., Li, J., Fan, J., Wu, J., Zhou, X., Hu, M., Wan, J., Yang, W., Li, D., Wu, G., Feng, Z., Gao, G. F., Wang, Y., Jin, Q., Liu, M. and Shu, Y. (2014) 'Clinical and epidemiological characteristics of a fatal case of avian influenza A H10N8 virus infection: a descriptive study', Lancet, 383(9918), pp. 714-21.

Chen, J., Lee, K. H., Steinhauer, D. A., Stevens, D. J., Skehel, J. J. and Wiley, D. C. (1998a) 'Structure of the hemagglutinin precursor cleavage site, a determinant of influenza pathogenicity and the origin of the labile conformation', Cell, 95(3), pp. 409-17.

Chen, J., Skehel, J. J. and Wiley, D. C. (1998b) 'A polar octapeptide fused to the N-terminal fusion peptide solubilizes the influenza virus HA2 subunit ectodomain', Biochemistry, 37(39), pp. 13643-9.

Chen, Y., Meng, X., Liu, Q., Huang, X., Huang, S., Liu, C., Shi, K., Guo, J., Chen, F. and Hu, L. (2008) '[Phylogenetic analysis of human/swine/avian gene reassortant H1N2 influenza A virus isolated from a pig in China]', Wei Sheng Wu Xue Bao, 48(4), pp. 466-72.

Choi, Y. K., Ozaki, H., Webby, R. J., Webster, R. G., Peiris, J. S., Poon, L., Butt, C., Leung, Y. H. and Guan, Y. (2004) 'Continuing evolution of H9N2 influenza viruses in Southeastern China', J Virol, 78(16), pp. 8609-14.

Chou, Y. Y., Vafabakhsh, R., Doğanay, S., Gao, Q., Ha, T. and Palese, P. (2012) 'One influenza virus particle packages eight unique viral RNAs as shown by FISH analysis', Proc Natl Acad Sci U S A, 109(23), pp. 9101-6.

Chrzastek, K., Lee, D. H., Gharaibeh, S., Zsak, A. and Kapczynski, D. R. (2018) 'Characterization of H9N2 avian influenza viruses from the Middle East demonstrates heterogeneity at amino acid position 226 in the hemagglutinin and potential for transmission to mammals', Virology, 518, pp. 195-201.

Ciampor, F., Thompson, C. A., Grambas, S. and Hay, A. J. (1992) 'Regulation of pH by the M2 protein of influenza A viruses', *Virus Res*, 22(3), pp. 247-58.

Cingolani, G., Bednenko, J., Gillespie, M. T. and Gerace, L. (2002) 'Molecular basis for the recognition of a nonclassical nuclear localization signal by importin beta', Mol Cell, 10(6), pp. 1345-53.

Claes, G., Welby, S., Van Den Berg, T., Van Der Stede, Y., Dewulf, J., Lambrecht, B. and Marché, S. (2013) 'The impact of viral tropism and housing conditions on the transmission of three H5/H7 low pathogenic avian influenza viruses in chickens', Epidemiol Infect, 141(11), pp. 2428-43.

Clifford, M., Twigg, J. and Upton, C. (2009) 'Evidence for a novel gene associated with human influenza A viruses', *Virol J*, 6, p. 198.

Coloma, R., Valpuesta, J. M., Arranz, R., Carrascosa, J. L., Ortín, J. and Martín-Benito, J. (2009) 'The structure of a biologically active influenza virus ribonucleoprotein complex', PLoS Pathog, 5(6), p. e1000491.

Compans, R. W., Content, J. and Duesberg, P. H. (1972) 'Structure of the ribonucleoprotein of influenza virus', J Virol, 10(4), pp. 795-800.

Cong, Y. L., Pu, J., Liu, Q. F., Wang, S., Zhang, G. Z., Zhang, X. L., Fan, W. X., Brown, E. G. and Liu, J. H. (2007) 'Antigenic and genetic characterization of H9N2 swine influenza viruses in China', J Gen Virol, 88(Pt 7), pp. 2035-41.

Cong, Y. L., Wang, C. F., Yan, C. M., Peng, J. S., Jiang, Z. L. and Liu, J. H. (2008) 'Swine infection with H9N2 influenza viruses in China in 2004', Virus Genes, 36(3), pp. 461-9.

Connor, R. J., Kawaoka, Y., Webster, R. G. and Paulson, J. C. (1994) 'Receptor specificity in human, avian, and equine H2 and H3 influenza virus isolates', Virology, 205(1), pp. 17-23.

Costa, T., Chaves, A. J., Valle, R., Darji, A., van Riel, D., Kuiken, T., Majó, N. and Ramis, A. (2012) 'Distribution patterns of influenza virus receptors and viral attachment patterns in the respiratory and intestinal tracts of seven avian species', Vet Res, 43, p. 28.

Costello, D. A., Whittaker, G. R. and Daniel, S. (2015) 'Variations in pH sensitivity, acid stability, and fusogenicity of three influenza virus H3 subtypes', J Virol, 89(1), pp. 350-60.

Cox, J. C., Hampson, A. W. and Hamilton, R. C. (1980) 'An immunofluorescence study of influenza virus filament formation', Arch Virol, 63(3-4), pp. 275-84.

Dadonaite, B., Vijayakrishnan, S., Fodor, E., Bhella, D. and Hutchinson, E. C. (2016) 'Filamentous influenza viruses', J Gen Virol, 97(8), pp. 1755-64.

de Wit, E., Spronken, M. I., Bestebroer, T. M., Rimmelzwaan, G. F., Osterhaus, A. D. and Fouchier, R. A. (2004) 'Efficient generation and growth of influenza virus A/PR/8/34 from eight cDNA fragments', Virus Res, 103(1-2), pp. 155-61.

Deng, G., Bi, J., Kong, F., Li, X., Xu, Q., Dong, J., Zhang, M., Zhao, L., Luan, Z., Lv, N. and Qiao, J. (2010) 'Acute respiratory distress syndrome induced by H9N2 virus in mice', Arch Virol, 155(2), pp. 187-95.

Deng, T., Engelhardt, O. G., Thomas, B., Akoulitchev, A. V., Brownlee, G. G. and Fodor, E. (2006) 'Role of ran binding protein 5 in nuclear import and assembly of the influenza virus RNA polymerase complex', J Virol, 80(24), pp. 11911-9.
Desmet, E. A., Bussey, K. A., Stone, R. and Takimoto, T. (2013) 'Identification of the N-terminal domain of the influenza virus PA responsible for the suppression of host protein synthesis', J Virol, 87(6), pp. 3108-18.
DesRochers, B. L., Chen, R. E., Gounder, A. P., Pinto, A. K., Bricker, T., Linton, C. N., Rogers, C. D., Williams, G. D., Webby, R. J. and Boon, A. C. (2016) 'Residues in the PB2 and PA genes contribute to the pathogenicity of avian H7N3 influenza A virus in DBA/2 mice', Virology, 494, pp. 89-99.
Dias, A., Bouvier, D., Crépin, T., McCarthy, A. A., Hart, D. J., Baudin, F., Cusack, S. and Ruigrok, R. W. (2009) 'The cap-snatching endonuclease of influenza virus polymerase resides in the PA subunit', Nature, 458(7240), pp. 914-8.
Dinarello, C. A. (1999) 'IL-18: A TH1-inducing, proinflammatory cytokine and new member of the IL-1 family', J Allergy Clin Immunol, 103(1 Pt 1), pp. 11-24.
Dinarello, C. A. (2011) 'A clinical perspective of IL-1β as the gatekeeper of inflammation', Eur J Immunol, 41(5), pp. 1203-17.
Dong, G., Luo, J., Zhang, H., Wang, C., Duan, M., Deliberto, T. J., Nolte, D. L., Ji, G. and He, H. (2011a) 'Phylogenetic diversity and genotypical complexity of H9N2 influenza A viruses revealed by genomic sequence analysis', PLoS One, 6(2), p. e17212.
Dong, G., Xu, C., Wang, C., Wu, B., Luo, J., Zhang, H., Nolte, D. L., Deliberto, T. J., Duan, M., Ji, G. and He, H. (2011b) 'Reassortant H9N2 influenza viruses containing H5N1-like PB1 genes isolated from black-billed magpies in Southern China', PLoS One, 6(9), p. e25808.
Drake, J. W. (1993) 'Rates of spontaneous mutation among RNA viruses', Proc Natl Acad Sci U S A, 90(9), pp. 4171-5.
Duhaut, S. D. and McCauley, J. W. (1996) 'Defective RNAs inhibit the assembly of influenza virus genome segments in a segment-specific manner', Virology, 216(2), pp. 326-37.
Dzananovic E., McKenna S.A., and Patel T.R. (2018) 'Viral proteins targeting host protein kinase R to evade an innate immune response: a mini review', Biotechnology and Genetic Engineering Reviews, 34:1, 33-59, DOI: 10.1080/02648725.2018.1467151
Eibauer, M., Pellanda, M., Turgay, Y., Dubrovsky, A., Wild, A. and Medalia, O. (2015) 'Structure and gating of the nuclear pore complex', Nat Commun, 6, p. 7532.
Eierhoff, T., Hrincius, E. R., Rescher, U., Ludwig, S. and Ehrhardt, C. (2010) 'The epidermal growth factor receptor (EGFR) promotes uptake of influenza A viruses (IAV) into host cells', PLoS Pathog, 6(9), p. e1001099.
Eisfeld, A. J., Kawakami, E., Watanabe, T., Neumann, G. and Kawaoka, Y. (2011) 'RAB11A is essential for transport of the influenza virus genome to the plasma membrane', J Virol, 85(13), pp. 6117-26.
Eisfeld, A. J., Neumann, G. and Kawaoka, Y. (2015) 'At the centre: influenza A virus ribonucleoproteins', *Nat Rev Microbiol*, 13(1), pp. 28-41.
El Houadfi, M., Fellahi, S., Nassik, S., Guérin, J. L. and Ducatez, M. F. (2016) 'First outbreaks and phylogenetic analyses of avian influenza H9N2 viruses isolated from poultry flocks in Morocco', Virol J, 13(1), p. 140.
Elgadi, M. M. and Smiley, J. R. (1999) 'Picornavirus internal ribosome entry site elements target RNA cleavage events induced by the herpes simplex virus virion host shutoff protein', J Virol, 73(11), pp. 9222-31.
Elleman, C. J. and Barclay, W. S. (2004a) 'The M1 matrix protein controls the filamentous phenotype of influenza A virus', Virology, 321(1), pp. 144-53.

Elton, D., Simpson-Holley, M., Archer, K., Medcalf, L., Hallam, R., McCauley, J. and Digard, P. (2001) 'Interaction of the influenza virus nucleoprotein with the cellular CRM1-mediated nuclear export pathway', J Virol, 75(1), pp. 408-19.

Engelhardt, O. G., Smith, M. and Fodor, E. (2005) 'Association of the influenza A virus RNA-dependent RNA polymerase with cellular RNA polymerase II', J Virol, 79(9), pp. 5812-8.

Fan, S., Hatta, M., Kim, J. H., Le, M. Q., Neumann, G. and Kawaoka, Y. (2014) 'Amino acid changes in the influenza A virus PA protein that attenuate avian H5N1 viruses in mammals', J Virol, 88(23), pp. 13737-46.

Feng, K. H., Sun, M., Iketani, S., Holmes, E. C. and Parrish, C. R. (2016) 'Comparing the functions of equine and canine influenza H3N8 virus PA-X proteins: Suppression of reporter gene expression and modulation of global host gene expression', Virology, 496, pp. 138-146.

Firth, A. E., Jagger, B. W., Wise, H. M., Nelson, C. C., Parsawar, K., Wills, N. M., Napthine, S., Taubenberger, J. K., Digard, P. and Atkins, J. F. (2012) 'Ribosomal frameshifting used in influenza A virus expression occurs within the sequence UCC_UUU_CGU and is in the +1 direction', Open Biol, 2(10), p. 120109.

Fodor, E. (2013) 'The RNA polymerase of influenza a virus: mechanisms of viral transcription and replication', Acta Virol, 57(2), pp. 113-22.

Fodor, E., Crow, M., Mingay, L. J., Deng, T., Sharps, J., Fechter, P. and Brownlee, G. G. (2002) 'A single amino acid mutation in the PA subunit of the influenza virus RNA polymerase inhibits endonucleolytic cleavage of capped RNAs', J Virol, 76(18), pp. 8989-9001.

Fodor, E., Mingay, L. J., Crow, M., Deng, T. and Brownlee, G. G. (2003) 'A single amino acid mutation in the PA subunit of the influenza virus RNA polymerase promotes the generation of defective interfering RNAs', J Virol, 77(8), pp. 5017-20.

Fodor, E., Pritlove, D. C. and Brownlee, G. G. (1994) 'The influenza virus panhandle is involved in the initiation of transcription', J Virol, 68(6), pp. 4092-6.

Fodor, E. and Smith, M. (2004) 'The PA subunit is required for efficient nuclear accumulation of the PB1 subunit of the influenza A virus RNA polymerase complex', J Virol, 78(17), pp. 9144-53.

Foeglein, Á., Loucaides, E. M., Mura, M., Wise, H. M., Barclay, W. S. and Digard, P. (2011) 'Influence of PB2 host-range determinants on the intranuclear mobility of the influenza A virus polymerase', J Gen Virol, 92(Pt 7), pp. 1650-61.

Fouchier, R. A., Rimmelzwaan, G. F., Kuiken, T. and Osterhaus, A. D. (2005) 'Newer respiratory virus infections: human metapneumovirus, avian influenza virus, and human coronaviruses', Curr Opin Infect Dis, 18(2), pp. 141-6.

Fouchier, R. A., Schneeberger, P. M., Rozendaal, F. W., Broekman, J. M., Kemink, S. A., Munster, V., Kuiken, T., Rimmelzwaan, G. F., Schutten, M., Van Doornum, G. J., Koch, G., Bosman, A., Koopmans, M. and Osterhaus, A. D. (2004) 'Avian influenza A virus (H7N7) associated with human conjunctivitis and a fatal case of acute respiratory distress syndrome', Proc Natl Acad Sci U S A, 101(5), pp. 1356-61.

Fournier, E., Moules, V., Essere, B., Paillart, J. C., Sirbat, J. D., Isel, C., Cavalier, A., Rolland, J. P., Thomas, D., Lina, B. and Marquet, R. (2012) 'A supramolecular assembly formed by influenza A virus genomic RNA segments', Nucleic Acids Res, 40(5), pp. 2197-209.

Francis, T., Quilligan, J. J. and Miuse, E. (1950) 'Identification of another epidemic respiratory disease', Science, 112(2913), pp. 495-7.

Frolov, I. and Schlesinger, S. (1994) 'Comparison of the effects of Sindbis virus and Sindbis virus replicons on host cell protein synthesis and cytopathogenicity in BHK cells', J Virol, 68(3), pp. 1721-7.

Fujii, Y., Goto, H., Watanabe, T., Yoshida, T. and Kawaoka, Y. (2003) 'Selective incorporation of influenza virus RNA segments into virions', Proc Natl Acad Sci U S A, 100(4), pp. 2002-7.

Gabriel, G., Abram, M., Keiner, B., Wagner, R., Klenk, H. D. and Stech, J. (2007) 'Differential polymerase activity in avian and mammalian cells determines host range of influenza virus', J Virol, 81(17), pp. 9601-4.

Gabriel, G., Dauber, B., Wolff, T., Planz, O., Klenk, H. D. and Stech, J. (2005) 'The viral polymerase mediates adaptation of an avian influenza virus to a mammalian host', Proc Natl Acad Sci U S A, 102(51), pp. 18590-5.

Gabriel, G., Herwig, A. and Klenk, H. D. (2008) 'Interaction of polymerase subunit PB2 and NP with importin alpha1 is a determinant of host range of influenza A virus', PLoS Pathog, 4(2), p. e11.

Gabriel, G., Klingel, K., Otte, A., Thiele, S., Hudjetz, B., Arman-Kalcek, G., Sauter, M., Shmidt, T., Rother, F., Baumgarte, S., Keiner, B., Hartmann, E., Bader, M., Brownlee, G. G., Fodor, E. and Klenk, H. D. (2011) 'Differential use of importin-α isoforms governs cell tropism and host adaptation of influenza virus', Nat Commun, 2, p. 156.

Galloway, S. E., Reed, M. L., Russell, C. J. and Steinhauer, D. A. (2013) 'Influenza HA subtypes demonstrate divergent phenotypes for cleavage activation and pH of fusion: implications for host range and adaptation', PLoS Pathog, 9(2), p. e1003151.

Gambaryan, A. S., Tuzikov, A. B., Piskarev, V. E., Yamnikova, S. S., Lvov, D. K., Robertson, J. S., Bovin, N. V. and Matrosovich, M. N. (1997) 'Specification of receptor-binding phenotypes of influenza virus isolates from different hosts using synthetic sialylglycopolymers: non-egg-adapted human H1 and H3 influenza A and influenza B viruses share a common high binding affinity for 6'-sialyl(N-acetyllactosamine)', Virology, 232(2), pp. 345-50.

Gao, H., Sun, H., Hu, J., Qi, L., Wang, J., Xiong, X., Wang, Y., He, Q., Lin, Y., Kong, W., Seng, L. G., Pu, J., Chang, K. C., Liu, X., Liu, J. and Sun, Y. (2015a) 'Twenty amino acids at the C-terminus of PA-X are associated with increased influenza A virus replication and pathogenicity', J Gen Virol, 96(8), pp. 2036-49.

Gao, H., Sun, Y., Hu, J., Qi, L., Wang, J., Xiong, X., Wang, Y., He, Q., Lin, Y., Kong, W., Seng, L. G., Sun, H., Pu, J., Chang, K. C., Liu, X. and Liu, J. (2015b) 'The contribution of PA-X to the virulence of pandemic 2009 H1N1 and highly pathogenic H5N1 avian influenza viruses', Sci Rep, 5, p. 8262.

Gao, H., Xu, G., Sun, Y., Qi, L., Wang, J., Kong, W., Sun, H., Pu, J., Chang, K. C. and Liu, J. (2015c) 'PA-X is a virulence factor in avian H9N2 influenza virus', J Gen Virol, 96(9), pp. 2587-94.

Gao, R., Bai, T., Li, X., Xiong, Y., Huang, Y., Pan, M., Zhang, Y., Bo, H., Zou, S. and Shu, Y. (2016) 'The comparison of pathology in ferrets infected by H9N2 avian influenza viruses with different genomic features', Virology, 488, pp. 149-55.

Gao, R., Cao, B., Hu, Y., Feng, Z., Wang, D., Hu, W., Chen, J., Jie, Z., Qiu, H., Xu, K., Xu, X., Lu, H., Zhu, W., Gao, Z., Xiang, N., Shen, Y., He, Z., Gu, Y., Zhang, Z., Yang, Y., Zhao, X., Zhou, L., Li, X., Zou, S., Zhang, Y., Yang, L., Guo, J., Dong, J., Li, Q., Dong, L., Zhu, Y., Bai, T., Wang, S., Hao, P., Yang, W., Han, J., Yu, H., Li, D., Gao, G. F., Wu, G., Wang, Y., Yuan, Z. and Shu, Y. (2013) 'Human infection with a novel avian-origin influenza A (H7N9) virus', N Engl J Med, 368(20), pp. 1888-97.

Gerber, M., Isel, C., Moules, V. and Marquet, R. (2014) 'Selective packaging of the influenza A genome and consequences for genetic reassortment', Trends Microbiol, 22(8), pp. 446-55.

Ghanem, A., Mayer, D., Chase, G., Tegge, W., Frank, R., Kochs, G., García-Sastre, A. and Schwemmle, M. (2007) 'Peptide-mediated interference with influenza A virus polymerase', J Virol, 81(14), pp. 7801-4.

Gog, J. R., Afonso, E. o. S., Dalton, R. M., Leclercq, I., Tiley, L., Elton, D., von Kirchbach, J. C., Naffakh, N., Escriou, N. and Digard, P. (2007) 'Codon conservation in the influenza A virus genome defines RNA packaging signals', Nucleic Acids Res, 35(6), pp. 1897-907.

Gong, X. Q., Sun, Y. F., Ruan, B. Y., Liu, X. M., Wang, Q., Yang, H. M., Wang, S. Y., Zhang, P., Wang, X. H., Shan, T. L., Tong, W., Zhou, Y. J., Li, G. X., Zheng, H., Tong, G. Z. and Yu, H. (2017) 'PA-X protein decreases replication and pathogenicity of swine influenza virus in cultured cells and mouse models', Vet Microbiol, 205, pp. 66-70.

Gong, Y. N., Chen, G. W., Chen, C. J., Kuo, R. L. and Shih, S. R. (2014) 'Computational analysis and mapping of novel open reading frames in influenza A viruses', PLoS One, 9(12), p. e115016.

González, S., Zürcher, T. and Ortín, J. (1996) 'Identification of two separate domains in the influenza virus PB1 protein involved in the interaction with the PB2 and PA subunits: a model for the viral RNA polymerase structure', Nucleic Acids Res, 24(22), pp. 4456-63.

Goodman, C. A. and Hornberger, T. A. (2013) 'Measuring protein synthesis with SUnSET: a valid alternative to traditional techniques?', Exerc Sport Sci Rev, 41(2), pp. 107-15.

Gorai, T., Goto, H., Noda, T., Watanabe, T., Kozuka-Hata, H., Oyama, M., Takano, R., Neumann, G., Watanabe, S. and Kawaoka, Y. (2012) 'F1Fo-ATPase, F-type proton-translocating ATPase, at the plasma membrane is critical for efficient influenza virus budding', Proc Natl Acad Sci U S A, 109(12), pp. 4615-20.

Gu, M., Chen, H., Li, Q., Huang, J., Zhao, M., Gu, X., Jiang, K., Wang, X., Peng, D. and Liu, X. (2014) 'Enzootic genotype S of H9N2 avian influenza viruses donates internal genes to emerging zoonotic influenza viruses in China', Vet Microbiol, 174(3-4), pp. 309-315.

Gu, M., Liu, W. B., Cao, J. P., Cao, Y. Z., Zhang, X. R., Peng, D. X. and Liu, X. F. (2010) '[Genome sequencing and genetic analysis of a natural reassortant H5N1 subtype avian influenza virus possessing H9N2 internal genes]', Bing Du Xue Bao, 26(4), pp. 298-304.

Gu, W., Gallagher, G. R., Dai, W., Liu, P., Li, R., Trombly, M. I., Gammon, D. B., Mello, C. C., Wang, J. P. and Finberg, R. W. (2015) 'Influenza A virus preferentially snatches noncoding RNA caps', RNA, 21(12), pp. 2067-75.

Guan, Y., Shortridge, K. F., Krauss, S., Chin, P. S., Dyrting, K. C., Ellis, T. M., Webster, R. G. and Peiris, M. (2000) 'H9N2 influenza viruses possessing H5N1-like internal genomes continue to circulate in poultry in southeastern China', J Virol, 74(20), pp. 9372-80.

Guan, Y., Shortridge, K. F., Krauss, S. and Webster, R. G. (1999) 'Molecular characterization of H9N2 influenza viruses: were they the donors of the "internal" genes of H5N1 viruses in Hong Kong?', Proc Natl Acad Sci U S A, 96(16), pp. 9363-7.

Guo, Y. J., Krauss, S., Senne, D. A., Mo, I. P., Lo, K. S., Xiong, X. P., Norwood, M., Shortridge, K. F., Webster, R. G. and Guan, Y. (2000) 'Characterization of the pathogenicity of members of the newly established H9N2 influenza virus lineages in Asia', Virology, 267(2), pp. 279-88.

Guu, T. S., Dong, L., Wittung-Stafshede, P. and Tao, Y. J. (2008) 'Mapping the domain structure of the influenza A virus polymerase acidic protein (PA) and its interaction with the basic protein 1 (PB1) subunit', Virology, 379(1), pp. 135-42.

Gómez-Puertas, P., Albo, C., Pérez-Pastrana, E., Vivo, A. and Portela, A. (2000) 'Influenza virus matrix protein is the major driving force in virus budding', J Virol, 74(24), pp. 11538-47.

Hale BG., Jackson D., Chen YH., Lamb RA., and Randall RE. (2006) 'Influenza A virus NS1 protein binds p58b and activates phosphatidylinositol-3-kinase signalling'. PNAS (103), pp. 14194-14199 38. Available at: http://www.pnas.org/content/pnas/103/38/14194.full.pdf.

Hale, B. G., Randall, R. E., Ortín, J. and Jackson, D. (2008) 'The multifunctional NS1 protein of influenza A viruses', J Gen Virol, 89(Pt 10), pp. 2359-76.

Hao, L., Sakurai, A., Watanabe, T., Sorensen, E., Nidom, C. A., Newton, M. A., Ahlquist, P. and Kawaoka, Y. (2008) 'Drosophila RNAi screen identifies host genes important for influenza virus replication', Nature, 454(7206), pp. 890-3.

Hara, K., Nakazono, Y., Kashiwagi, T., Hamada, N. and Watanabe, H. (2013) 'Co-incorporation of the PB2 and PA polymerase subunits from human H3N2 influenza virus is a critical determinant of the replication of reassortant ribonucleoprotein complexes', J Gen Virol, 94(Pt 11), pp. 2406-16.

Hara, K., Schmidt, F. I., Crow, M. and Brownlee, G. G. (2006) 'Amino acid residues in the N-terminal region of the PA subunit of influenza A virus RNA polymerase play a critical role in protein stability, endonuclease activity, cap binding, and virion RNA promoter binding', J Virol, 80(16), pp. 7789-98.

Harris, A., Cardone, G., Winkler, D. C., Heymann, J. B., Brecher, M., White, J. M. and Steven, A. C. (2006) 'Influenza virus pleiomorphy characterized by cryoelectron tomography', Proc Natl Acad Sci U S A, 103(50), pp. 19123-7.

Hatta, M., Hatta, Y., Kim, J. H., Watanabe, S., Shinya, K., Nguyen, T., Lien, P. S., Le, Q. M. and Kawaoka, Y. (2007) 'Growth of H5N1 influenza A viruses in the upper respiratory tracts of mice', PLoS Pathog, 3(10), pp. 1374-9.

Hause, B. M., Collin, E. A., Liu, R., Huang, B., Sheng, Z., Lu, W., Wang, D., Nelson, E. A. and Li, F. (2014) 'Characterization of a novel influenza virus in cattle and Swine: proposal for a new genus in the Orthomyxoviridae family', MBio, 5(2), pp. e00031-14.

Hay, A. J., Skehel, J. J. and McCauley, J. (1982) 'Characterization of influenza virus RNA complete transcripts', Virology, 116(2), pp. 517-22.

Hayashi T., Watanabe C., Suzuki Y., Tanikawa T., Uchida Y. and Saito T., (2014) 'Chicken MDA5 senses short double-stranded RNA with implication for antiviral response against avian influenza viruses in chicken. Journal of Innate Immunity 6: 58-71.

Hayashi, T., Chaimayo, C., McGuinness, J. and Takimoto, T. (2016) 'Critical Role of the PA-X C-Terminal Domain of Influenza A Virus in Its Subcellular Localization and Shutoff Activity', J Virol, 90(16), pp. 7131-7141.

Hayashi, T., MacDonald, L. A. and Takimoto, T. (2015) 'Influenza A Virus Protein PA-X Contributes to Viral Growth and Suppression of the Host Antiviral and Immune Responses', J Virol, 89(12), pp. 6442-52.

He, Q. (2012) 'Isolation and Whole Genome sequencing Analysis of Equine H9N2 influenza virus in Guang Xi'. Master Dissertation: Guangxi University, Nanning, China.

He, X., Zhou, J., Bartlam, M., Zhang, R., Ma, J., Lou, Z., Li, X., Li, J., Joachimiak, A., Zeng, Z., Ge, R., Rao, Z. and Liu, Y. (2008) 'Crystal structure of the polymerase PA(C)-PB1(N) complex from an avian influenza H5N1 virus', Nature, 454(7208), pp. 1123-6.

Heinrich, P. C., Behrmann, I., Haan, S., Hermanns, H. M., Müller-Newen, G. and Schaper, F. (2003) 'Principles of interleukin (IL)-6-type cytokine signalling and its regulation', Biochem J, 374(Pt 1), pp. 1-20.

Hennion, R. M. and Hill, G. (2015) 'The preparation of chicken kidney cell cultures for virus propagation', Methods Mol Biol, 1282, pp. 57-62.

Herfst, S., Imai, M., Kawaoka, Y. and Fouchier, R. A. (2014) 'Avian influenza virus transmission to mammals', Curr Top Microbiol Immunol, 385, pp. 137-55.

Hinshaw, V. S., Webster, R. G. and Turner, B. (1979) 'Water-bone transmission of influenza A viruses?', Intervirology, 11(1), pp. 66-8.
Hirst, G. K. (1941) 'The agglutination of red cells by allantoic fluid of chick embryos infected with influenza virus', Science, 94(2427), pp. 22-3.
Homme, P. J. and Easterday, B. C. (1970) 'Avian influenza virus infections. I. Characteristics of influenza A-turkey-Wisconsin-1966 virus', Avian Dis, 14(1), pp. 66-74.
Horibe, T., Torisawa, A., Akiyoshi, R., Hatta-Ohashi, Y., Suzuki, H. and Kawakami, K. (2014) 'Transfection efficiency of normal and cancer cell lines and monitoring of promoter activity by single-cell bioluminescence imaging', Luminescence, 29(1), pp. 96-100.
Horimoto, T. and Kawaoka, Y. (2005) 'Influenza: lessons from past pandemics, warnings from current incidents', Nat Rev Microbiol, 3(8), pp. 591-600.
Horwood, P. F., Horm, S. V., Suttie, A., Thet, S., Y, P., Rith, S., Sorn, S., Holl, D., Tum, S., Ly, S., Karlsson, E. A., Tarantola, A. and Dussart, P. (2018) 'Co-circulation of Influenza A H5, H7, and H9 Viruses and Co-infected Poultry in Live Bird Markets, Cambodia', Emerg Infect Dis, 24(2), pp. 352-355.
Hsu, M. T., Parvin, J. D., Gupta, S., Krystal, M. and Palese, P. (1987) 'Genomic RNAs of influenza viruses are held in a circular conformation in virions and in infected cells by a terminal panhandle', Proc Natl Acad Sci U S A, 84(22), pp. 8140-4.
Hu, J., Hu, Z., Mo, Y., Wu, Q., Cui, Z., Duan, Z., Huang, J., Chen, H., Chen, Y., Gu, M., Wang, X., Hu, S., Liu, H., Liu, W. and Liu, X. (2013a) 'The PA and HA gene-mediated high viral load and intense innate immune response in the brain contribute to the high pathogenicity of H5N1 avian influenza virus in mallard ducks', J Virol, 87(20), pp. 11063-75.
Hu, J., Hu, Z., Song, Q., Gu, M., Liu, X., Wang, X., Hu, S., Chen, C., Liu, H., Liu, W., Chen, S. and Peng, D. (2013b) 'The PA-gene-mediated lethal dissemination and excessive innate immune response contribute to the high virulence of H5N1 avian influenza virus in mice', J Virol, 87(5), pp. 2660-72.
Hu, J., Mo, Y., Gao, Z., Wang, X., Gu, M., Liang, Y., Cheng, X., Hu, S., Liu, W., Liu, H., Chen, S., Liu, X. and Peng, D. (2016) 'PA-X-associated early alleviation of the acute lung injury contributes to the attenuation of a highly pathogenic H5N1 avian influenza virus in mice', Med Microbiol Immunol, 205(4), pp. 381-95.
Hu, J., Mo, Y., Wang, X., Gu, M., Hu, Z., Zhong, L., Wu, Q., Hao, X., Hu, S., Liu, W., Liu, H. and Liu, X. (2015) 'PA-X decreases the pathogenicity of highly pathogenic H5N1 influenza A virus in avian species by inhibiting virus replication and host response', J Virol, 89(8), pp. 4126-42.
Hu J., Ma C., and Liu X., (2018) ' PA-X: A key regulator of influenza A virus pathogenicity and host immune responses.' Medical Microbiology and Immunology 207 (5-6) pp 255-269.
Huang, R. T., Rott, R. and Klenk, H. D. (1981) 'Influenza viruses cause hemolysis and fusion of cells', Virology, 110(1), pp. 243-7.
Huang, T. S., Palese, P. and Krystal, M. (1990) 'Determination of influenza virus proteins required for genome replication', J Virol, 64(11), pp. 5669-73.
Huarte, M., Falcón, A., Nakaya, Y., Ortín, J., García-Sastre, A. and Nieto, A. (2003) 'Threonine 157 of influenza virus PA polymerase subunit modulates RNA replication in infectious viruses', J Virol, 77(10), pp. 6007-13.
Huarte, M., Sanz-Ezquerro, J. J., Roncal, F., Ortín, J. and Nieto, A. (2001) 'PA subunit from influenza virus polymerase complex interacts with a cellular protein with homology to a family of transcriptional activators', J Virol, 75(18), pp. 8597-604.
Huprikar, J. and Rabinowitz, S. (1980) 'A simplified plaque assay for influenza viruses in Madin-Darby kidney (MDCK) cells', J Virol Methods, 1(2), pp. 117-20.

Hussain S., Turnbull M.L., Wise H.M., Jagger B.W., Beard P.M., Kovacikova K., Taubenberger J.K., Vervelde L., Engelhardt O.G., Digard P. (2019) 'Mutation of Influenza A Virus PA-X Decreases Pathogenicity in Chicken Embryos and Can Increase the Yield of Reassortant Candidate Vaccine Viruses' Journal of Virology, 93 (2) e01551-18; DOI: 10.1128/JVI.01551-18

Hutchinson, E. C., Charles, P. D., Hester, S. S., Thomas, B., Trudgian, D., Martínez-Alonso, M. and Fodor, E. (2014) 'Conserved and host-specific features of influenza virion architecture', Nat Commun, 5, p. 4816.

Hutchinson, E. C., von Kirchbach, J. C., Gog, J. R. and Digard, P. (2010) 'Genome packaging in influenza A virus', J Gen Virol, 91(Pt 2), pp. 313-28.

Ilyushina, N. A., Ducatez, M. F., Rehg, J. E., Marathe, B. M., Marjuki, H., Bovin, N. V., Webster, R. G. and Webby, R. J. (2010) 'Does pandemic A/H1N1 virus have the potential to become more pathogenic?', MBio, 1(5).

Imai, M. and Kawaoka, Y. (2012) 'The role of receptor binding specificity in interspecies transmission of influenza viruses', Curr Opin Virol, 2(2), pp. 160-7.

Inagaki, A., Goto, H., Kakugawa, S., Ozawa, M. and Kawaoka, Y. (2012) 'Competitive incorporation of homologous gene segments of influenza A virus into virions', J Virol, 86(18), pp. 10200-2.

Inglis, S. C., Gething, M. J. and Brown, C. M. (1980) 'Relationship between the messenger RNAs transcribed from two overlapping genes of influenza virus', *Nucleic Acids Res*, 8(16), pp. 3575-89.

International Centre for Diarrhoeal Disease Research (ICDDRB). Outbreak of mild respiratory disease caused by H5N1 and H9N2 infections among young children in Dhaka, Bangladesh. Health and Science Bulletin: 2011.

Iqbal, M., Yaqub, T., Mukhtar, N., Shabbir, M. Z. and McCauley, J. W. (2013) 'Infectivity and transmissibility of H9N2 avian influenza virus in chickens and wild terrestrial birds', Vet Res, 44, p. 100.

Iqbal, M., Yaqub, T., Reddy, K. and McCauley, J. W. (2009) 'Novel genotypes of H9N2 influenza A viruses isolated from poultry in Pakistan containing NS genes similar to highly pathogenic H7N3 and H5N1 viruses', PLoS One, 4(6), p. e5788.

Ito, T., Couceiro, J. N., Kelm, S., Baum, L. G., Krauss, S., Castrucci, M. R., Donatelli, I., Kida, H., Paulson, J. C., Webster, R. G. and Kawaoka, Y. (1998) 'Molecular basis for the generation in pigs of influenza A viruses with pandemic potential', J Virol, 72(9), pp. 7367-73.

Jackson D., Hossain J.M., Hickman D., Perez D.R. and Lamb R.A. (2007) 'A new influenza virus virulence deterimant: The NS1 protein four C-terminal residues modulate pathogenicity'. PNAS 105, pp. 4381-4386. Available at: http://www.pnas.org/content/pnas/105/11/4381.full.pdf.

Jagger, B. W., Wise, H. M., Kash, J. C., Walters, K. A., Wills, N. M., Xiao, Y. L., Dunfee, R. L., Schwartzman, L. M., Ozinsky, A., Bell, G. L., Dalton, R. M., Lo, A., Efstathiou, S., Atkins, J. F., Firth, A. E., Taubenberger, J. K. and Digard, P. (2012) 'An overlapping protein-coding region in influenza A virus segment 3 modulates the host response', Science, 337(6091), pp. 199-204.

Jagger B.W. (2012) 'The influenza A polymerase in viral pathogenesis'.

http://ethos.bl.uk/OrderDetails.do?uin=uk.bl.ethos.610897. PhD Thesis: University of Cambridge.

James, J., Howard, W., Iqbal, M., Nair, V. K., Barclay, W. S. and Shelton, H. (2016) 'Influenza A virus PB1-F2 protein prolongs viral shedding in chickens lengthening the transmission window', J Gen Virol, 97(10), pp. 2516-2527.

Jardetzky, T. S. and Lamb, R. A. (2004) 'Virology: a class act', Nature, 427(6972), pp. 307-8.

Jennings, P. A., Finch, J. T., Winter, G. and Robertson, J. S. (1983) 'Does the higher order structure of the influenza virus ribonucleoprotein guide sequence rearrangements in influenza viral RNA?', Cell, 34(2), pp. 619-27.
Johnson, C. A., Pekas, D. J. and Winzler, R. J. (1964) 'Neuraminidases and influenza virus infection in embryonated eggs', Science, 143(3610), pp. 1051-2.
Johnson, N. P. and Mueller, J. (2002) 'Updating the accounts: global mortality of the 1918-1920 "Spanish" influenza pandemic', Bull Hist Med, 76(1), pp. 105-15.
Juarez D., Long K.C., Aguilar P., Kochel T.J. and Halsey E.S. (2013) 'Assessment of plaque assay methods for alphaviruses'. Journal of virological methods 187 (1) pp 185-189.
Kageyama, T., Fujisaki, S., Takashita, E., Xu, H., Yamada, S., Uchida, Y., Neumann, G., Saito, T., Kawaoka, Y. and Tashiro, M. (2013) 'Genetic analysis of novel avian A(H7N9) influenza viruses isolated from patients in China, February to April 2013', Euro Surveill, 18(15), p. 20453.
Kainulainen, M., Lau, S., Samuel, C. E., Hornung, V. and Weber, F. (2016) 'NSs Virulence Factor of Rift Valley Fever Virus Engages the F-Box Proteins FBXW11 and β-TRCP1 To Degrade the Antiviral Protein Kinase PKR', J Virol, 90(13), pp. 6140-7.
Kajihara, M., Sakoda, Y., Soda, K., Minari, K., Okamatsu, M., Takada, A. and Kida, H. (2013) 'The PB2, PA, HA, NP, and NS genes of a highly pathogenic avian influenza virus A/whooper swan/Mongolia/3/2005 (H5N1) are responsible for pathogenicity in ducks', Virol J, 10, p. 45.
Kalthoff, D., Bogs, J., Grund, C., Tauscher, K., Teifke, J. P., Starick, E., Harder, T. and Beer, M. (2014) 'Avian influenza H7N9/13 and H7N7/13: a comparative virulence study in chickens, pigeons, and ferrets', J Virol, 88(16), pp. 9153-65.
Karpala A.J., Stewart C., McKay J., Lowenthal J.W., Bean A.G.D. (2011) 'Characterisation of Chicken MDA-5 activity: regulation of IFN-β in the absence of RIG-I functionality.' The journal of Immunology. 186 (9) 5397-5405.
Kashiwahi T., Leung B.W., Deng T., Chen H, Brownlee G.C. (2009) ' The N-terminal region of the PA subunit of the RNA polymerase of influenza A/HongKong/156/97 (H5N1) influences promotor binding.' PLos One 4(5): e5473. https://doi.org/10.1371/journal.pone.0005473.
Kawaguchi, A., Matsumoto, K. and Nagata, K. (2012) 'YB-1 functions as a porter to lead influenza virus ribonucleoprotein complexes to microtubules', J Virol, 86(20), pp. 11086-95.
Kawaguchi, A. and Nagata, K. (2007) 'De novo replication of the influenza virus RNA genome is regulated by DNA replicative helicase, MCM', EMBO J, 26(21), pp. 4566-75.
Kawaoka, Y., Krauss, S. and Webster, R. G. (1989) 'Avian-to-human transmission of the PB1 gene of influenza A viruses in the 1957 and 1968 pandemics', J Virol, 63(11), pp. 4603-8.
Khaperskyy, D. A. and McCormick, C. (2015) 'Timing Is Everything: Coordinated Control of Host Shutoff by Influenza A Virus NS1 and PA-X Proteins', J Virol, 89(13), pp. 6528-31.
Khaperskyy, D. A., Schmaling, S., Larkins-Ford, J., McCormick, C. and Gaglia, M. M. (2016) 'Selective Degradation of Host RNA Polymerase II Transcripts by Influenza A Virus PA-X Host Shutoff Protein', PLoS Pathog, 12(2), p. e1005427.
Kilany, W. H., Ali, A., Bazid, A. H., El-Deeb, A. H., El-Abideen, M. A., Sayed, M. E. and El-Kady, M. F. (2016) 'A Dose-Response Study of Inactivated Low Pathogenic Avian Influenza H9N2 Virus in Specific-Pathogen-Free and Commercial Broiler Chickens', Avian Dis, 60(1 Suppl), pp. 256-61.

Kim, J. H., Hatta, M., Watanabe, S., Neumann, G., Watanabe, T. and Kawaoka, Y. (2010) 'Role of host-specific amino acids in the pathogenicity of avian H5N1 influenza viruses in mice', J Gen Virol, 91(Pt 5), pp. 1284-9.

Kishida, N., Sakoda, Y., Eto, M., Sunaga, Y. and Kida, H. (2004) 'Co-infection of Staphylococcus aureus or Haemophilus paragallinarum exacerbates H9N2 influenza A virus infection in chickens', Arch Virol, 149(11), pp. 2095-104.

Kishida N., Sakoda Y., Isoda N., Matsuda K., Eto M., Sunaga Y., Umemura T., and Kida H. (2005) 'Pathogenicity of H5 influenza viruses for ducks'. Arch Virol (150), pp. 1383-1392.

Klumpp, K., Ruigrok, R. W. and Baudin, F. (1997) 'Roles of the influenza virus polymerase and nucleoprotein in forming a functional RNP structure', EMBO J, 16(6), pp. 1248-57.

Kobasa, D., Kodihalli, S., Luo, M., Castrucci, M. R., Donatelli, I., Suzuki, Y., Suzuki, T. and Kawaoka, Y. (1999) 'Amino acid residues contributing to the substrate specificity of the influenza A virus neuraminidase', J Virol, 73(8), pp. 6743-51.

Kobasa D., Jones S.M., Shinya K., Kash J.C., Copps J., Ebihara H., Hatta Y., Kim J.H., Halfmann P., Hatta M., Feldmann F., Alimonti J.B., Fernando L., Li Y., Katze M.G., Feldman H.and Kawaoka Y. (2007) 'Abberant innate immune response in lethal infection of macques with the 1918 infleunza virus. Nature 445 (319-323).

Kong, W., Liu, L., Wang, Y., He, Q., Wu, S., Qin, Z., Wang, J., Sun, H., Sun, Y., Zhang, R., Pu, J. and Liu, J. (2015) 'C-terminal elongation of NS1 of H9N2 influenza virus induces a high level of inflammatory cytokines and increases transmission', J Gen Virol, 96(Pt 2), pp. 259-68.

Krenn, B. M., Egorov, A., Romanovskaya-Romanko, E., Wolschek, M., Nakowitsch, S., Ruthsatz, T., Kiefmann, B., Morokutti, A., Humer, J., Geiler, J., Cinatl, J., Michaelis, M., Wressnigg, N., Sturlan, S., Ferko, B., Batishchev, O. V., Indenbom, A. V., Zhu, R., Kastner, M., Hinterdorfer, P., Kiselev, O., Muster, T. and Romanova, J. (2011) 'Single HA2 mutation increases the infectivity and immunogenicity of a live attenuated H5N1 intranasal influenza vaccine candidate lacking NS1', PLoS One, 6(4), p. e18577.

Kuyumcu-Martinez, N. M., Joachims, M. and Lloyd, R. E. (2002) 'Efficient cleavage of ribosome-associated poly(A)-binding protein by enterovirus 3C protease', J Virol, 76(5), pp. 2062-74.

Lai, J. C., Chan, W. W., Kien, F., Nicholls, J. M., Peiris, J. S. and Garcia, J. M. (2010) 'Formation of virus-like particles from human cell lines exclusively expressing influenza neuraminidase', J Gen Virol, 91(Pt 9), pp. 2322-30.

Lam, T. T., Wang, J., Shen, Y., Zhou, B., Duan, L., Cheung, C. L., Ma, C., Lycett, S. J., Leung, C. Y., Chen, X., Li, L., Hong, W., Chai, Y., Zhou, L., Liang, H., Ou, Z., Liu, Y., Farooqui, A., Kelvin, D. J., Poon, L. L., Smith, D. K., Pybus, O. G., Leung, G. M., Shu, Y., Webster, R. G., Webby, R. J., Peiris, J. S., Rambaut, A., Zhu, H. and Guan, Y. (2013) 'The genesis and source of the H7N9 influenza viruses causing human infections in China', Nature, 502(7470), pp. 241-4.

Lamb, R. A. and Choppin, P. W. (1981) 'Identification of a second protein (M2) encoded by RNA segment 7 of influenza virus', *Virology*, 112(2), pp. 729-37.

Lauring, A. S. and Andino, R. (2010) 'Quasispecies theory and the behavior of RNA viruses', PLoS Pathog, 6(7), p. e1001005.

Laver, W. G. and Valentine, R. C. (1969) 'Morphology of the isolated hemagglutinin and neuraminidase subunits of influenza virus', Virology, 38(1), pp. 105-19.

Lebel-Binay S., Berger A., Zinzindohoue F., Cugnenc P-H., Thiounn N., Fridman W.H., and Pages F. (2000) ' Interleukin-18: biological properties and clinical implications.' European Cytokine Network 11 (1) 15-26.

Lee, C. Y., An, S. H., Kim, I., Choi, J. G., Lee, Y. J., Kim, J. H. and Kwon, H. J. (2018) 'Novel mutations in avian PA in combination with an adaptive mutation in PR8 NP exacerbate the virulence of PR8-derived recombinant influenza A viruses in mice', Vet Microbiol, 221, pp. 114-121.

Lee, J., Yu, H., Li, Y., Ma, J., Lang, Y., Duff, M., Henningson, J., Liu, Q., Nagy, A., Bawa, B., Li, Z., Tong, G., Richt, J. A. and Ma, W. (2017) 'Impacts of different expressions of PA-X protein on 2009 pandemic H1N1 virus replication, pathogenicity and host immune responses', Virology, 504, pp. 25-35.

Leser, G. P. and Lamb, R. A. (2005) 'Influenza virus assembly and budding in raft-derived microdomains: a quantitative analysis of the surface distribution of HA, NA and M2 proteins', Virology, 342(2), pp. 215-27.

Li Xuyong , L. B., Ma Shujie, Cui Pengfe i , Liu W enqiang, Li Yubao, Guo Jing , Chen Hualan 222 (2018) 'High frequency of reassortment after co-infection of chickens with the H4N6 and H9N2 influenza A viruses and the biological characteristics of the reassortants'. Veterinary Microbiology, pp. 11-17. Available at: https://www.sciencedirect.com/science/article/pii/S0378113517314669.

Li, C., Yu, K., Tian, G., Yu, D., Liu, L., Jing, B., Ping, J. and Chen, H. (2005) 'Evolution of H9N2 influenza viruses from domestic poultry in Mainland China', Virology, 340(1), pp. 70-83.

Li M.O. and Flavell R.A. (2008) 'TGF-β4: A master of all T cell trades'. Cell 134(3) pp 392-404.

Li, Q., Yuan, X., Wang, Q., Chang, G., Wang, F., Liu, R., Zheng, M., Chen, G., Wen, J. and Zhao, G. (2016) 'Interactomic landscape of PA-X-chicken protein complexes of H5N1 influenza A virus', J Proteomics, 148, pp. 20-5.

Li, X., Shi, J., Guo, J., Deng, G., Zhang, Q., Wang, J., He, X., Wang, K., Chen, J., Li, Y., Fan, J., Kong, H., Gu, C., Guan, Y., Suzuki, Y., Kawaoka, Y., Liu, L., Jiang, Y., Tian, G., Bu, Z. and Chen, H. (2014) 'Genetics, receptor binding property, and transmissibility in mammals of naturally isolated H9N2 Avian Influenza viruses', PLoS Pathog, 10(11), p. e1004508.

Liao, Y., Gu, F., Mao, X., Niu, Q., Wang, H., Sun, Y., Song, C., Qiu, X., Tan, L. and Ding, C. (2016) 'Regulation of de novo translation of host cells by manipulation of PERK/PKR and GADD34-PP1 activity during Newcastle disease virus infection', J Gen Virol, 97(4), pp. 867-79.

Linster, M., van Boheemen, S., de Graaf, M., Schrauwen, E. J. A., Lexmond, P., Mänz, B., Bestebroer, T. M., Baumann, J., van Riel, D., Rimmelzwaan, G. F., Osterhaus, A. D. M. E., Matrosovich, M., Fouchier, R. A. M. and Herfst, S. (2014) 'Identification, characterization, and natural selection of mutations driving airborne transmission of A/H5N1 virus', Cell, 157(2), pp. 329-339.

Liu, D., Shi, W., Shi, Y., Wang, D., Xiao, H., Li, W., Bi, Y., Wu, Y., Li, X., Yan, J., Liu, W., Zhao, G., Yang, W., Wang, Y., Ma, J., Shu, Y., Lei, F. and Gao, G. F. (2013) 'Origin and diversity of novel avian influenza A H7N9 viruses causing human infection: phylogenetic, structural, and coalescent analyses', Lancet, 381(9881), pp. 1926-32.

Liu, K. 33:116 (2012) 'Epidemiology and control of H9N2 subtype avian infleunza virus'. Anim. Husb. Feed Sci.

Liu, Y., Lou, Z., Bartlam, M. and Rao, Z. (2009) 'Structure-function studies of the influenza virus RNA polymerase PA subunit', Sci China C Life Sci, 52(5), pp. 450-8.

Liu, Y. F., Lai, H. Z., Li, L., Liu, Y. P., Zhang, W. Y., Gao, R., Huang, W. K., Luo, Q. F., Gao, Y., Luo, Q., Xie, X. Y., Xu, J. H. and Chen, R. A. (2016) 'Endemic Variation of H9N2 Avian Influenza Virus in China', Avian Dis, 60(4), pp. 817-825.

Llompart, C. M., Nieto, A. and Rodriguez-Frandsen, A. (2014) 'Specific residues of PB2 and PA influenza virus polymerase subunits confer the ability for RNA

polymerase II degradation and virus pathogenicity in mice', J Virol, 88(6), pp. 3455-63.
Londt, BZ., Nunez A., Banks J., Nili H., Johnson LK., and Alexander DJ. (2008) 'Pathogenesis of highly pathogenic avian influenza A/turkey/Turkey/1/2005 H5N1 in Pekin ducks (Anas platyrhynchos) infected experimentally'. Avian Pathol (37), pp. 619-627.
Long, J. S., Giotis, E. S., Moncorgé, O., Frise, R., Mistry, B., James, J., Morisson, M., Iqbal, M., Vignal, A., Skinner, M. A. and Barclay, W. S. (2016) 'Species difference in ANP32A underlies influenza A virus polymerase host restriction', Nature, 529(7584), pp. 101-4.
Long, J. S., Howard, W. A., Núñez, A., Moncorgé, O., Lycett, S., Banks, J. and Barclay, W. S. (2013) 'The effect of the PB2 mutation 627K on highly pathogenic H5N1 avian influenza virus is dependent on the virus lineage', J Virol, 87(18), pp. 9983-96.
Lu, J. H., Liu, X. F., Shao, W. X., Liu, Y. L., Wei, D. P. and Liu, H. Q. (2005) 'Phylogenetic analysis of eight genes of H9N2 subtype influenza virus: a mainland China strain possessing early isolates' genes that have been circulating', Virus Genes, 31(2), pp. 163-9.
Lu, Y., Wambach, M., Katze, M. G. and Krug, R. M. (1995) 'Binding of the influenza virus NS1 protein to double-stranded RNA inhibits the activation of the protein kinase that phosphorylates the elF-2 translation initiation factor', Virology, 214(1), pp. 222-8.
Ludwig S., Pleschka S., and Wolff T. (1999) 'A Fatal Relationship- Influenza virus interaction with the host cell'. Viral Immunology, 12.3.
Lutz, A., Dyall, J., Olivo, P. D. and Pekosz, A. (2005) 'Virus-inducible reporter genes as a tool for detecting and quantifying influenza A virus replication', J Virol Methods, 126(1-2), pp. 13-20.
Luytjes, W., Krystal, M., Enami, M., Parvin, J. D. and Palese, P. (1989) 'Amplification, expression, and packaging of foreign gene by influenza virus', Cell, 59(6), pp. 1107-13.
Lv, J., Wei, L., Yang, Y., Wang, B., Liang, W., Gao, Y., Xia, X., Gao, L., Cai, Y., Hou, P., Yang, H., Wang, A., Huang, R., Gao, J. and Chai, T. (2015) 'Amino acid substitutions in the neuraminidase protein of an H9N2 avian influenza virus affect its airborne transmission in chickens', Vet Res, 46, p. 44.
Ma, M. J., Zhao, T., Chen, S. H., Xia, X., Yang, X. X., Wang, G. L., Fang, L. Q., Ma, G. Y., Wu, M. N., Qian, Y. H., Dean, N. E., Yang, Y., Lu, B. and Cao, W. C. (2018) 'Avian Influenza A Virus Infection among Workers at Live Poultry Markets, China, 2013-2016', Emerg Infect Dis, 24(7), pp. 1246-1256.
Maeda, T. and Ohnishi, S. (1980) 'Activation of influenza virus by acidic media causes hemolysis and fusion of erythrocytes', FEBS Lett, 122(2), pp. 283-7.
Maier, H. J., Kashiwagi, T., Hara, K. and Brownlee, G. G. (2008) 'Differential role of the influenza A virus polymerase PA subunit for vRNA and cRNA promoter binding', Virology, 370(1), pp. 194-204.
Massin, P., van der Werf, S. and Naffakh, N. (2001) 'Residue 627 of PB2 is a determinant of cold sensitivity in RNA replication of avian influenza viruses', J Virol, 75(11), pp. 5398-404.
Matrosovich, M., Tuzikov, A., Bovin, N., Gambaryan, A., Klimov, A., Castrucci, M. R., Donatelli, I. and Kawaoka, Y. (2000) 'Early alterations of the receptor-binding properties of H1, H2, and H3 avian influenza virus hemagglutinins after their introduction into mammals', J Virol, 74(18), pp. 8502-12.
Matrosovich, M. N., Krauss, S. and Webster, R. G. (2001) 'H9N2 influenza A viruses from poultry in Asia have human virus-like receptor specificity', Virology, 281(2), pp. 156-62.

Matrosovich, M. N., Matrosovich, T. Y., Gray, T., Roberts, N. A. and Klenk, H. D. (2004) 'Neuraminidase is important for the initiation of influenza virus infection in human airway epithelium', J Virol, 78(22), pp. 12665-7.
Matsuoka, Y., Swayne, D. E., Thomas, C., Rameix-Welti, M. A., Naffakh, N., Warnes, C., Altholtz, M., Donis, R. and Subbarao, K. (2009) 'Neuraminidase stalk length and additional glycosylation of the hemagglutinin influence the virulence of influenza H5N1 viruses for mice', J Virol, 83(9), pp. 4704-8.
Matsuu, A., Kobayashi, T., Patchimasiri, T., Shiina, T., Suzuki, S., Chaichoune, K., Ratanakorn, P., Hiromoto, Y., Abe, H., Parchariyanon, S. and Saito, T. (2016) 'Pathogenicity of Genetically Similar, H5N1 Highly Pathogenic Avian Influenza Virus Strains in Chicken and the Differences in Sensitivity among Different Chicken Breeds', PLoS One, 11(4), p. e0153649.
McAuley, J. L., Zhang, K. and McCullers, J. A. (2010) 'The effects of influenza A virus PB1-F2 protein on polymerase activity are strain specific and do not impact pathogenesis', J Virol, 84(1), pp. 558-64.
McGeoch, D., Fellner, P. and Newton, C. (1976) 'Influenza virus genome consists of eight distinct RNA species', Proc Natl Acad Sci U S A, 73(9), pp. 3045-9.
Mehle, A., Dugan, V. G., Taubenberger, J. K. and Doudna, J. A. (2012) 'Reassortment and mutation of the avian influenza virus polymerase PA subunit overcome species barriers', J Virol, 86(3), pp. 1750-7.
Mellacheruvu, D., Wright, Z., Couzens, A. L., Lambert, J. P., St-Denis, N. A., Li, T., Miteva, Y. V., Hauri, S., Sardiu, M. E., Low, T. Y., Halim, V. A., Bagshaw, R. D., Hubner, N. C., Al-Hakim, A., Bouchard, A., Faubert, D., Fermin, D., Dunham, W. H., Goudreault, M., Lin, Z. Y., Badillo, B. G., Pawson, T., Durocher, D., Coulombe, B., Aebersold, R., Superti-Furga, G., Colinge, J., Heck, A. J., Choi, H., Gstaiger, M., Mohammed, S., Cristea, I. M., Bennett, K. L., Washburn, M. P., Raught, B., Ewing, R. M., Gingras, A. C. and Nesvizhskii, A. I. (2013) 'The CRAPome: a contaminant repository for affinity purification-mass spectrometry data', *Nat Methods*, 10(8), pp. 730-6.
Moeller, A., Kirchdoerfer, R. N., Potter, C. S., Carragher, B. and Wilson, I. A. (2012) 'Organization of the influenza virus replication machinery', Science, 338(6114), pp. 1631-4.
Momose, F., Kikuchi, Y., Komase, K. and Morikawa, Y. (2007) 'Visualization of microtubule-mediated transport of influenza viral progeny ribonucleoprotein', Microbes Infect, 9(12-13), pp. 1422-33.
Monne, I., Fusaro, A., Nelson, M. I., Bonfanti, L., Mulatti, P., Hughes, J., Murcia, P. R., Schivo, A., Valastro, V., Moreno, A., Holmes, E. C. and Cattoli, G. (2014) 'Emergence of a highly pathogenic avian influenza virus from a low-pathogenic progenitor', J Virol, 88(8), pp. 4375-88.
Monne, I., Hussein, H. A., Fusaro, A., Valastro, V., Hamoud, M. M., Khalefa, R. A., Dardir, S. N., Radwan, M. I., Capua, I. and Cattoli, G. (2013) 'H9N2 influenza A virus circulates in H5N1 endemically infected poultry population in Egypt', Influenza Other Respir Viruses, 7(3), pp. 240-3.
Mor, A., White, A., Zhang, K., Thompson, M., Esparza, M., Muñoz-Moreno, R., Koide, K., Lynch, K. W., García-Sastre, A. and Fontoura, B. M. (2016) 'Influenza virus mRNA trafficking through host nuclear speckles', Nat Microbiol, 1(7), p. 16069.
Morens, D. M., Taubenberger, J. K. and Fauci, A. S. (2008) 'Predominant role of bacterial pneumonia as a cause of death in pandemic influenza: implications for pandemic influenza preparedness', J Infect Dis, 198(7), pp. 962-70.
Mosley, V. M. and Wyckoff, R. W. (1946) 'Electron micrography of the virus of influenza', Nature, 157, p. 263.

Muramoto, Y., Noda, T., Kawakami, E., Akkina, R. and Kawaoka, Y. (2013) 'Identification of novel influenza A virus proteins translated from PA mRNA', J Virol, 87(5), pp. 2455-62.

Muratore, G., Goracci, L., Mercorelli, B., Foeglein, Á., Digard, P., Cruciani, G., Palù, G. and Loregian, A. (2012) 'Small molecule inhibitors of influenza A and B viruses that act by disrupting subunit interactions of the viral polymerase', *Proc Natl Acad Sci U S A*, 109(16), pp. 6247-52.

Mänz, B., Brunotte, L., Reuther, P. and Schwemmle, M. (2012) 'Adaptive mutations in NEP compensate for defective H5N1 RNA replication in cultured human cells', Nat Commun, 3, p. 802.

Mänz, B., Dornfeld, D., Götz, V., Zell, R., Zimmermann, P., Haller, O., Kochs, G. and Schwemmle, M. (2013a) 'Pandemic influenza A viruses escape from restriction by human MxA through adaptive mutations in the nucleoprotein', PLoS Pathog, 9(3), p. e1003279.

Mänz, B., Schwemmle, M. and Brunotte, L. (2013b) 'Adaptation of avian influenza A virus polymerase in mammals to overcome the host species barrier', J Virol, 87(13), pp. 7200-9.

Naeem, K. and Siddique, N. (2006) 'Use of strategic vaccination for the control of avian influenza in Pakistan', Dev Biol (Basel), 124, pp. 145-50.

Naffakh, N., Massin, P. and van der Werf, S. (2001) 'The transcription/replication activity of the polymerase of influenza A viruses is not correlated with the level of proteolysis induced by the PA subunit', Virology, 285(2), pp. 244-52.

Naguib, M. M., Arafa, A. S., El-Kady, M. F., Selim, A. A., Gunalan, V., Maurer-Stroh, S., Goller, K. V., Hassan, M. K., Beer, M., Abdelwhab, E. M. and Harder, T. C. (2015) 'Evolutionary trajectories and diagnostic challenges of potentially zoonotic avian influenza viruses H5N1 and H9N2 co-circulating in Egypt', Infect Genet Evol, 34, pp. 278-91.

Nakatsu, S., Sagara, H., Sakai-Tagawa, Y., Sugaya, N., Noda, T. and Kawaoka, Y. (2016) 'Complete and Incomplete Genome Packaging of Influenza A and B Viruses', MBio, 7(5).

Nayak, D. P., Chambers, T. M. and Akkina, R. K. (1985) 'Defective-interfering (DI) RNAs of influenza viruses: origin, structure, expression, and interference', Curr Top Microbiol Immunol, 114, pp. 103-51.

Nemeroff, M. E., Barabino, S. M., Li, Y., Keller, W. and Krug, R. M. (1998) 'Influenza virus NS1 protein interacts with the cellular 30 kDa subunit of CPSF and inhibits 3'end formation of cellular pre-mRNAs', Mol Cell, 1(7), pp. 991-1000.

Neumann, G., Watanabe, T., Ito, H., Watanabe, S., Goto, H., Gao, P., Hughes, M., Perez, D. R., Donis, R., Hoffmann, E., Hobom, G. and Kawaoka, Y. (1999) 'Generation of influenza A viruses entirely from cloned cDNAs', Proc Natl Acad Sci U S A, 96(16), pp. 9345-50.

Neumann, G., Hughes, M. T. and Kawaoka, Y. (2000) 'Influenza A virus NS2 protein mediates vRNP nuclear export through NES-independent interaction with hCRM1', *EMBO J*, 19(24), pp. 6751-8.

Newby C.M., Sabin L., Pekosz A. (2007) 'The RNA Binding Domain of Influenza A Virus NS1 Protein Affects Secretion of Tumor Necrosis Factor Alpha, Interleukin-6, and Interferon in Primary Murine Tracheal Epithelial Cells' Journal of Virology, 81 (17) 9469-9480; DOI: 10.1128/JVI.00989-07

Noda, T., Murakami, S., Nakatsu, S., Imai, H., Muramoto, Y., Shindo, K., Sagara, H. and Kawaoka, Y. (2018) 'Importance of the 1+7 configuration of ribonucleoprotein complexes for influenza A virus genome packaging', Nat Commun, 9(1), p. 54.

Noda, T., Sagara, H., Yen, A., Takada, A., Kida, H., Cheng, R. H. and Kawaoka, Y. (2006) 'Architecture of ribonucleoprotein complexes in influenza A virus particles', Nature, 439(7075), pp. 490-2.
Noda, T., Sugita, Y., Aoyama, K., Hirase, A., Kawakami, E., Miyazawa, A., Sagara, H. and Kawaoka, Y. (2012) 'Three-dimensional analysis of ribonucleoprotein complexes in influenza A virus', Nat Commun, 3, p. 639.
Noton, S. L., Medcalf, E., Fisher, D., Mullin, A. E., Elton, D. and Digard, P. (2007) 'Identification of the domains of the influenza A virus M1 matrix protein required for NP binding, oligomerization and incorporation into virions', J Gen Virol, 88(Pt 8), pp. 2280-90.
Noton, S. L., Simpson-Holley, M., Medcalf, E., Wise, H. M., Hutchinson, E. C., McCauley, J. W. and Digard, P. (2009) 'Studies of an influenza A virus temperature-sensitive mutant identify a late role for NP in the formation of infectious virions', J Virol, 83(2), pp. 562-71.
OIE (2017) Infection with avian influenza viruses, Chapter 10.4.Terrestrial Animal Health Code. http://www.oie.int/
O'Neill, R. E., Jaskunas, R., Blobel, G., Palese, P. and Moroianu, J. (1995) 'Nuclear import of influenza virus RNA can be mediated by viral nucleoprotein and transport factors required for protein import', J Biol Chem, 270(39), pp. 22701-4.
O'Neill, R. E., Talon, J. and Palese, P. (1998) 'The influenza virus NEP (NS2 protein) mediates the nuclear export of viral ribonucleoproteins', EMBO J, 17(1), pp. 288-96.
Obadan, A. O., Kimble, B. J., Rajao, D., Lager, K., Santos, J. J., Vincent, A. and Perez, D. R. (2015) 'Replication and transmission of mammalian-adapted H9 subtype influenza virus in pigs and quail', J Gen Virol, 96(9), pp. 2511-21.
Obayashi, E., Yoshida, H., Kawai, F., Shibayama, N., Kawaguchi, A., Nagata, K., Tame, J. R. and Park, S. Y. (2008) 'The structural basis for an essential subunit interaction in influenza virus RNA polymerase', Nature, 454(7208), pp. 1127-31.
Oishi, K., Yamayoshi, S. and Kawaoka, Y. (2015) 'Mapping of a Region of the PA-X Protein of Influenza A Virus That Is Important for Its Shutoff Activity', J Virol, 89(16), pp. 8661-5.
Oishi, K., Yamayoshi, S. and Kawaoka, Y. (2018) 'Identification of novel amino acid residues of influenza virus PA-X that are important for PA-X shutoff activity by using yeast', Virology, 516, pp. 71-75.
Ortega, J., Martín-Benito, J., Zürcher, T., Valpuesta, J. M., Carrascosa, J. L. and Ortín, J. (2000) 'Ultrastructural and functional analyses of recombinant influenza virus ribonucleoproteins suggest dimerization of nucleoprotein during virus amplification', J Virol, 74(1), pp. 156-63.
Palese, P., Tobita, K., Ueda, M. and Compans, R. W. (1974) 'Characterization of temperature sensitive influenza virus mutants defective in neuraminidase', Virology, 61(2), pp. 397-410.
Pan, Q., Liu, A., Zhang, F., Ling, Y., Ou, C., Hou, N. and He, C. (2012) 'Co-infection of broilers with Ornithobacterium rhinotracheale and H9N2 avian influenza virus', BMC Vet Res, 8, p. 104.
Pantin-Jackwood, M., Swayne, D. E., Smith, D. and Shepherd, E. (2013) 'Effect of species, breed and route of virus inoculation on the pathogenicity of H5N1 highly pathogenic influenza (HPAI) viruses in domestic ducks', Vet Res, 44, p. 62.
Pappas C., Aguilar P.V., Basler C.F., Solórzano A., Zeng H., Perrone L.A., Palese P., García-Sastre A., Katz J.M. and Tumpey T.M. (2008) 'Single gene reassortants identify a critical role for PB1, HA, and NA in the high virulence of the 1918 pandemic influenza virus' Proceedings of the National Academy of Sciences, 105 (8) 3064-3069; DOI: 10.1073/pnas.0711815105

Parvin, R., Heenemann, K., Halami, M. Y., Chowdhury, E. H., Islam, M. R. and Vahlenkamp, T. W. (2014) 'Full-genome analysis of avian influenza virus H9N2 from Bangladesh reveals internal gene reassortments with two distinct highly pathogenic avian influenza viruses', Arch Virol, 159(7), pp. 1651-61.

Paterson, D. and Fodor, E. (2012) 'Emerging roles for the influenza A virus nuclear export protein (NEP)', PLoS Pathog, 8(12), p. e1003019.

Pawar, S. D., Tandale, B. V., Raut, C. G., Parkhi, S. S., Barde, T. D., Gurav, Y. K., Kode, S. S. and Mishra, A. C. (2012) 'Avian influenza H9N2 seroprevalence among poultry workers in Pune, India, 2010', PLoS One, 7(5), p. e36374.

Peiris, M., Yuen, K. Y., Leung, C. W., Chan, K. H., Ip, P. L., Lai, R. W., Orr, W. K. and Shortridge, K. F. (1999) 'Human infection with influenza H9N2', Lancet, 354(9182), pp. 916-7.

Peng, X., Liu, F., Wu, H., Xu, Y., Wang, L., Chen, B., Sun, T., Yang, F., Ji, S. and Wu, N. (2018) 'Amino Acid Substitutions HA A150V, PA A343T, and PB2 E627K Increase the Virulence of H5N6 Influenza Virus in Mice', Front Microbiol, 9, p. 453.

Perales, B., Sanz-Ezquerro, J. J., Gastaminza, P., Ortega, J., Santarén, J. F., Ortín, J. and Nieto, A. (2000) 'The replication activity of influenza virus polymerase is linked to the capacity of the PA subunit to induce proteolysis', J Virol, 74(3), pp. 1307-12.

Perdue, M. L., García, M., Senne, D. and Fraire, M. (1997) 'Virulence-associated sequence duplication at the hemagglutinin cleavage site of avian influenza viruses', Virus Res, 49(2), pp. 173-86.

Perez, D. R. and Donis, R. O. (2001) 'Functional analysis of PA binding by influenza a virus PB1: effects on polymerase activity and viral infectivity', J Virol, 75(17), pp. 8127-36.

Perez, D. R., Lim, W., Seiler, J. P., Yi, G., Peiris, M., Shortridge, K. F. and Webster, R. G. (2003) 'Role of quail in the interspecies transmission of H9 influenza A viruses: molecular changes on HA that correspond to adaptation from ducks to chickens', J Virol, 77(5), pp. 3148-56.

Perez, J. T., Varble, A., Sachidanandam, R., Zlatev, I., Manoharan, M., García-Sastre, A. and tenOever, B. R. (2010) 'Influenza A virus-generated small RNAs regulate the switch from transcription to replication', Proc Natl Acad Sci U S A, 107(25), pp. 11525-30.

Perrone, L. A., Plowden, J. K., García-Sastre, A., Katz, J. M. and Tumpey, T. M. (2008) 'H5N1 and 1918 pandemic influenza virus infection results in early and excessive infiltration of macrophages and neutrophils in the lungs of mice', PLoS Pathog, 4(8), p. e1000115.

Pflug, A., Guilligay, D., Reich, S. and Cusack, S. (2014) 'Structure of influenza A polymerase bound to the viral RNA promoter', Nature, 516(7531), pp. 355-60.

Pinto, L. H., Holsinger, L. J. and Lamb, R. A. (1992) 'Influenza virus M2 protein has ion channel activity', *Cell*, 69(3), pp. 517-28.

Platanias L.C. (2005) 'Mechanisms of type-I and Type-II- interferon-mediated signalling. Nature Rev. Imm 5, 375-386.

Plotch, S. J., Bouloy, M., Ulmanen, I. and Krug, R. M. (1981) 'A unique cap(m7GpppXm)-dependent influenza virion endonuclease cleaves capped RNAs to generate the primers that initiate viral RNA transcription', Cell, 23(3), pp. 847-58.

Poon, L. L., Pritlove, D. C., Sharps, J. and Brownlee, G. G. (1998) 'The RNA polymerase of influenza virus, bound to the 5' end of virion RNA, acts in cis to polyadenylate mRNA', J Virol, 72(10), pp. 8214-9.

Pu, J., Wang, S., Yin, Y., Zhang, G., Carter, R. A., Wang, J., Xu, G., Sun, H., Wang, M., Wen, C., Wei, Y., Wang, D., Zhu, B., Lemmon, G., Jiao, Y., Duan, S., Wang, Q., Du, Q., Sun, M., Bao, J., Sun, Y., Zhao, J., Zhang, H., Wu, G., Liu, J. and Webster, R. G. (2015)

'Evolution of the H9N2 influenza genotype that facilitated the genesis of the novel H7N9 virus', Proc Natl Acad Sci U S A, 112(2), pp. 548-53.
Pérez-González, A., Rodriguez, A., Huarte, M., Salanueva, I. J. and Nieto, A. (2006) 'hCLE/CGI-99, a human protein that interacts with the influenza virus polymerase, is a mRNA transcription modulator', J Mol Biol, 362(5), pp. 887-900.
Rahn, J., Hoffmann, D., Harder, T. C. and Beer, M. (2015) 'Vaccines against influenza A viruses in poultry and swine: Status and future developments', Vaccine, 33(21), pp. 2414-24.
Rasool F., Nizamani Z.A., Soomro N.M., Afzal F., Parvenn F., and Rahman S. (2014) 'Susceptibility of Desi and Commercial Layer breeds to low pathogenicity avian influenza virus infection'. The Journal of Animal and Plant Sciences (24), pp. 1643-1648 6.
Read, E. K. and Digard, P. (2010) 'Individual influenza A virus mRNAs show differential dependence on cellular NXF1/TAP for their nuclear export', J Gen Virol, 91(Pt 5), pp. 1290-301.
Read, G. S., Karr, B. M. and Knight, K. (1993) 'Isolation of a herpes simplex virus type 1 mutant with a deletion in the virion host shutoff gene and identification of multiple forms of the vhs (UL41) polypeptide', J Virol, 67(12), pp. 7149-60.
Reed, M. L., Bridges, O. A., Seiler, P., Kim, J. K., Yen, H. L., Salomon, R., Govorkova, E. A., Webster, R. G. and Russell, C. J. (2010) 'The pH of activation of the hemagglutinin protein regulates H5N1 influenza virus pathogenicity and transmissibility in ducks', J Virol, 84(3), pp. 1527-35.
Reed L.J., and Muench H. (1938) 'A simple method of estimating fifty percent endpoints'. The American Journal of Hygiene (27), pp. 493–497.
Regan, J. F., Liang, Y. and Parslow, T. G. (2006) 'Defective assembly of influenza A virus due to a mutation in the polymerase subunit PA', J Virol, 80(1), pp. 252-61.
Reich, S., Guilligay, D., Pflug, A., Malet, H., Berger, I., Crépin, T., Hart, D., Lunardi, T., Nanao, M., Ruigrok, R. W. and Cusack, S. (2014) 'Structural insight into cap-snatching and RNA synthesis by influenza polymerase', Nature, 516(7531), pp. 361-6.
Richardson, J. C. and Akkina, R. K. (1991) 'NS2 protein of influenza virus is found in purified virus and phosphorylated in infected cells', Arch Virol, 116(1-4), pp. 69-80.
Robb, N. C. and Fodor, E. (2012) 'The accumulation of influenza A virus segment 7 spliced mRNAs is regulated by the NS1 protein', J Gen Virol, 93(Pt 1), pp. 113-8.
Robb, N. C., Smith, M., Vreede, F. T. and Fodor, E. (2009) 'NS2/NEP protein regulates transcription and replication of the influenza virus RNA genome', J Gen Virol, 90(Pt 6), pp. 1398-407.
Roberts, P. C. and Compans, R. W. (1998) 'Host cell dependence of viral morphology', Proc Natl Acad Sci U S A, 95(10), pp. 5746-51.
Robertson, J. S., Schubert, M. and Lazzarini, R. A. (1981) 'Polyadenylation sites for influenza virus mRNA', J Virol, 38(1), pp. 157-63.
Rogers, G. N., Paulson, J. C., Daniels, R. S., Skehel, J. J., Wilson, I. A. and Wiley, D. C. (1983) 'Single amino acid substitutions in influenza haemagglutinin change receptor binding specificity', Nature, 304(5921), pp. 76-8.
Rossman, J. S., Jing, X., Leser, G. P. and Lamb, R. A. (2010) 'Influenza virus M2 protein mediates ESCRT-independent membrane scission', Cell, 142(6), pp. 902-13.
Rossman, J. S., Leser, G. P. and Lamb, R. A. (2012) 'Filamentous influenza virus enters cells via macropinocytosis', J Virol, 86(20), pp. 10950-60.
Rota, P. A., Wallis, T. R., Harmon, M. W., Rota, J. S., Kendal, A. P. and Nerome, K. (1990) 'Cocirculation of two distinct evolutionary lineages of influenza type B virus since 1983', Virology, 175(1), pp. 59-68.

Rowe, M., Glaunsinger, B., van Leeuwen, D., Zuo, J., Sweetman, D., Ganem, D., Middeldorp, J., Wiertz, E. J. H. J. and Ressing, M. E. (2007) 'Host shutoff during productive Epstein–Barr virus infection is mediated by BGLF5 and may contribute to immune evasion', Proceedings of the National Academy of Sciences, 104(9), pp. 3366-3371.

Roy, A., Kucukural, A. and Zhang, Y. (2010) 'I-TASSER: a unified platform for automated protein structure and function prediction', Nat Protoc, 5(4), pp. 725-38.

Ruigrok, R. W., Barge, A., Durrer, P., Brunner, J., Ma, K. and Whittaker, G. R. (2000) 'Membrane interaction of influenza virus M1 protein', Virology, 267(2), pp. 289-98.

Ruiz-Hernandez, R., Mwangi, W., Peroval, M., Sadeyen, J. R., Ascough, S., Balkissoon, D., Staines, K., Boyd, A., McCauley, J., Smith, A. and Butter, C. (2016) 'Host genetics determine susceptibility to avian influenza infection and transmission dynamics', Sci Rep, 6, p. 26787.

Russier, M., Yang, G., Rehg, J. E., Wong, S. S., Mostafa, H. H., Fabrizio, T. P., Barman, S., Krauss, S., Webster, R. G., Webby, R. J. and Russell, C. J. (2016) 'Molecular requirements for a pandemic influenza virus: An acid-stable hemagglutinin protein', Proc Natl Acad Sci U S A, 113(6), pp. 1636-41.

Sakabe, S., Ozawa, M., Takano, R., Iwastuki-Horimoto, K. and Kawaoka, Y. (2011) 'Mutations in PA, NP, and HA of a pandemic (H1N1) 2009 influenza virus contribute to its adaptation to mice', Virus Res, 158(1-2), pp. 124-9.

Salvatore, M., Basler, C. F., Parisien, J. P., Horvath, C. M., Bourmakina, S., Zheng, H., Muster, T., Palese, P. and García-Sastre, A. (2002) 'Effects of influenza A virus NS1 protein on protein expression: the NS1 protein enhances translation and is not required for shutoff of host protein synthesis', J Virol, 76(3), pp. 1206-12.

Santhakumar D., Rubbenstroth D., Martinez-Sobribo and Munir M. (2017) 'Avian Interferons and their antiviral effectors'. Front. Immunol https://doi.org/10.3389/fimmu.2017.00049

Sanz-Ezquerro, J. J., Zürcher, T., de la Luna, S., Ortín, J. and Nieto, A. (1996) 'The amino-terminal one-third of the influenza virus PA protein is responsible for the induction of proteolysis', J Virol, 70(3), pp. 1905-11.

Sauter, N. K., Bednarski, M. D., Wurzburg, B. A., Hanson, J. E., Whitesides, G. M., Skehel, J. J. and Wiley, D. C. (1989) 'Hemagglutinins from two influenza virus variants bind to sialic acid derivatives with millimolar dissociation constants: a 500-MHz proton nuclear magnetic resonance study', Biochemistry, 28(21), pp. 8388-96.

Schmidt, E. K., Clavarino, G., Ceppi, M. and Pierre, P. (2009) 'SUnSET, a nonradioactive method to monitor protein synthesis', Nat Methods, 6(4), pp. 275-7.

Schmitt, A. P. and Lamb, R. A. (2005) 'Influenza virus assembly and budding at the viral budozone', Adv Virus Res, 64, pp. 383-416.

Scholtissek, C. (1995) 'Molecular evolution of influenza viruses', Virus Genes, 11(2-3), pp. 209-15.

Scholtissek, C., Rohde, W., Von Hoyningen, V. and Rott, R. (1978) 'On the origin of the human influenza virus subtypes H2N2 and H3N2', Virology, 87(1), pp. 13-20.

Schrauwen, E. J. and Fouchier, R. A. (2014) 'Host adaptation and transmission of influenza A viruses in mammals', Emerg Microbes Infect, 3(2), p. e9.

Schrauwen, E. J., Richard, M., Burke, D. F., Rimmelzwaan, G. F., Herfst, S. and Fouchier, R. A. (2016) 'Amino Acid Substitutions That Affect Receptor Binding and Stability of the Hemagglutinin of Influenza A/H7N9 Virus', J Virol, 90(7), pp. 3794-9.

Schröder M., Meisel C., Buhl K., Profanter N., Sievert N.,Volk H-D. and Grütz G. (2003) 'Different Modes of IL-10 and TGF-β to Inhibit Cytokine-Dependent IFN-γ Production: Consequences for Reversal of Lipopolysaccharide Desensitization' The journal of immunology 170 (10) 5260-5267.

Schrodinger LLC. (2010) 'The PyMOL molecular graphics system, version 1.3r1'.
Sealy J.E., Yaqub T., Peacock T.P., Chang P., Ermetal B., Clements A., Sadeyen J-R., Mehboob A., Shelton H., Bryant J.E., Daniels R.S., McCauley J.W. and Iqbal M. (2019). ' Association of increased receptor-binding avidity of influenza A(H9N2) viruses with escape from Antibody-based immunity and enhanced zoonotic potential. Emerg Infect Dis. 25 (1) 63-72.
Seifi S., 80 (2010) 'Natural co-infection caused by avian influenza H9 subtypes and infectious bronchitis virus in broiler chicken farms' Asasi K., M. A. Veterinarski Archiv, pp. 269-281 2.
Seiler, P., Kercher, L., Feeroz, M. M., Shanmuganatham, K., Jones-Engel, L., Turner, J., Walker, D., Alam, S. M. R., Hasan, M. K., Akhtar, S., McKenzie, P., Franks, J., Krauss, S., Webby, R. J. and Webster, R. G. (2018) 'H9N2 influenza viruses from Bangladesh: transmission in chicken and New World quail', Influenza Other Respir Viruses.
Selman, M., Dankar, S. K., Forbes, N. E., Jia, J. J. and Brown, E. G. (2012) 'Adaptive mutation in influenza A virus non-structural gene is linked to host switching and induces a novel protein by alternative splicing', *Emerg Microbes Infect*, 1(11), p. e42.
Senne, D. A., Panigrahy, B., Kawaoka, Y., Pearson, J. E., Süss, J., Lipkind, M., Kida, H. and Webster, R. G. (1996) 'Survey of the hemagglutinin (HA) cleavage site sequence of H5 and H7 avian influenza viruses: amino acid sequence at the HA cleavage site as a marker of pathogenicity potential', Avian Dis, 40(2), pp. 425-37.
Seyer, R., Hrincius, E. R., Ritzel, D., Abt, M., Mellmann, A., Marjuki, H., Kühn, J., Wolff, T., Ludwig, S. and Ehrhardt, C. (2012) 'Synergistic adaptive mutations in the hemagglutinin and polymerase acidic protein lead to increased virulence of pandemic 2009 H1N1 influenza A virus in mice', J Infect Dis, 205(2), pp. 262-71.
Shanmuganatham, K., Feeroz, M. M., Jones-Engel, L., Walker, D., Alam, S., Hasan, M., McKenzie, P., Krauss, S., Webby, R. J. and Webster, R. G. (2014) 'Genesis of avian influenza H9N2 in Bangladesh', Emerg Microbes Infect, 3(12), p. e88.
Shapiro, G. I., Gurney, T. and Krug, R. M. (1987) 'Influenza virus gene expression: control mechanisms at early and late times of infection and nuclear-cytoplasmic transport of virus-specific RNAs', J Virol, 61(3), pp. 764-73.
Shaw, M. L., Stone, K. L., Colangelo, C. M., Gulcicek, E. E. and Palese, P. (2008) 'Cellular proteins in influenza virus particles', PLoS Pathog, 4(6), p. e1000085.
Shen, Y., Lu, H., Qi, T., Gu, Y., Xiang, M., Lu, S., Qu, H., Zhang, W., He, J., Cao, H., Ye, J., Fang, X., Wu, X. and Zhang, Z. (2015) 'Fatal cases of human infection with avian influenza A (H7N9) virus in Shanghai, China in 2013', Biosci Trends, 9(1), pp. 73-8.
Shen, Y. Y., Ke, C. W., Li, Q., Yuan, R. Y., Xiang, D., Jia, W. X., Yu, Y. D., Liu, L., Huang, C., Qi, W. B., Sikkema, R., Wu, J., Koopmans, M. and Liao, M. (2016) 'Novel Reassortant Avian Influenza A(H5N6) Viruses in Humans, Guangdong, China, 2015', Emerg Infect Dis, 22(8), pp. 1507-9.
Shi, M., Jagger, B. W., Wise, H. M., Digard, P., Holmes, E. C. and Taubenberger, J. K. (2012) 'Evolutionary conservation of the PA-X open reading frame in segment 3 of influenza A virus', J Virol, 86(22), pp. 12411-3.
Shi, W., Shi, Y., Wu, Y., Liu, D. and Gao, G. F. (2013) 'Origin and molecular characterization of the human-infecting H6N1 influenza virus in Taiwan', Protein Cell, 4(11), pp. 846-53.
Shi, Y., Wu, Y., Zhang, W., Qi, J. and Gao, G. F. (2014) 'Enabling the 'host jump': structural determinants of receptor-binding specificity in influenza A viruses', Nat Rev Microbiol, 12(12), pp. 822-31.
Shih, S. R., Suen, P. C., Chen, Y. S. and Chang, S. C. (1998) 'A novel spliced transcript of influenza A/WSN/33 virus', *Virus Genes*, 17(2), pp. 179-83.

Shortridge, K. F., Zhou, N. N., Guan, Y., Gao, P., Ito, T., Kawaoka, Y., Kodihalli, S., Krauss, S., Markwell, D., Murti, K. G., Norwood, M., Senne, D., Sims, L., Takada, A. and Webster, R. G. (1998) 'Characterization of avian H5N1 influenza viruses from poultry in Hong Kong', Virology, 252(2), pp. 331-42.

Simpson, R. W. and Hirst, G. K. (1961) 'Genetic recombination among influenza viruses. I. Cross reactivation of plaque-forming capacity as a method for selecting recombinants from the progeny of crosses between influenza A strains', Virology, 15, pp. 436-51.

Sironi, L., Williams, J. L., Moreno-Martin, A. M., Ramelli, P., Stella, A., Jianlin, H., Weigend, S., Lombardi, G., Cordioli, P. and Mariani, P. (2008) 'Susceptibility of different chicken lines to H7N1 highly pathogenic avian influenza virus and the role of Mx gene polymorphism coding amino acid position 631', Virology, 380(1), pp. 152-6.

Skehel, J. J., Bayley, P. M., Brown, E. B., Martin, S. R., Waterfield, M. D., White, J. M., Wilson, I. A. and Wiley, D. C. (1982) 'Changes in the conformation of influenza virus hemagglutinin at the pH optimum of virus-mediated membrane fusion', Proc Natl Acad Sci U S A, 79(4), pp. 968-72.

Skehel, J. J. and Wiley, D. C. (2000) 'Receptor binding and membrane fusion in virus entry: the influenza hemagglutinin', Annu Rev Biochem, 69, pp. 531-69.

Solórzano A., Webby R.J., Lager K.M., Janke B.H., García-Sastre A., and Richt J.A.(2005) 'Mutations in the NS1 Protein of Swine Influenza Virus Impair Anti-Interferon Activity and Confer Attenuation in Pigs' Journal of Virology May 79 (12) 7535-7543; DOI: 10.1128/JVI.79.12.7535-7543.2005

Song, J., Feng, H., Xu, J., Zhao, D., Shi, J., Li, Y., Deng, G., Jiang, Y., Li, X., Zhu, P., Guan, Y., Bu, Z., Kawaoka, Y. and Chen, H. (2011a) 'The PA protein directly contributes to the virulence of H5N1 avian influenza viruses in domestic ducks', J Virol, 85(5), pp. 2180-8.

Spekreijse, D., Bouma, A., Koch, G. and Stegeman, J. A. (2011) 'Airborne transmission of a highly pathogenic avian influenza virus strain H5N1 between groups of chickens quantified in an experimental setting', Vet Microbiol, 152(1-2), pp. 88-95.

Spickler, A. R., Trampel, D. W. and Roth, J. A. (2008) 'The onset of virus shedding and clinical signs in chickens infected with high-pathogenicity and low-pathogenicity avian influenza viruses', Avian Pathol, 37(6), pp. 555-77.

Steel, J. and Lowen, A. C. (2014) 'Influenza A virus reassortment', Curr Top Microbiol Immunol, 385, pp. 377-401.

Steel, J., Lowen, A. C., Mubareka, S. and Palese, P. (2009) 'Transmission of influenza virus in a mammalian host is increased by PB2 amino acids 627K or 627E/701N', PLoS Pathog, 5(1), p. e1000252.

Su, S., Bi, Y., Wong, G., Gray, G. C., Gao, G. F. and Li, S. (2015) 'Epidemiology, Evolution, and Recent Outbreaks of Avian Influenza Virus in China', J Virol, 89(17), pp. 8671-6.

Su, S., Zhou, P., Fu, X., Wang, L., Hong, M., Lu, G., Sun, L., Qi, W., Ning, Z., Jia, K., Yuan, Z., Wang, H., Ke, C., Wu, J., Zhang, G., Gray, G. C. and Li, S. (2014) 'Virological and epidemiological evidence of avian influenza virus infections among feral dogs in live poultry markets, china: a threat to human health?', Clin Infect Dis, 58(11), pp. 1644-6.

Subbarao, E. K., London, W. and Murphy, B. R. (1993) 'A single amino acid in the PB2 gene of influenza A virus is a determinant of host range', J Virol, 67(4), pp. 1761-4.

Sun, X., Xu, X., Liu, Q., Liang, D., Li, C., He, Q., Jiang, J., Cui, Y., Li, J., Zheng, L., Guo, J., Xiong, Y. and Yan, J. (2013a) 'Evidence of avian-like H9N2 influenza A virus among dogs in Guangxi, China', Infect Genet Evol, 20, pp. 471-5.

Sun, Y., Pu, J., Jiang, Z., Guan, T., Xia, Y., Xu, Q., Liu, L., Ma, B., Tian, F., Brown, E. G. and Liu, J. (2010) 'Genotypic evolution and antigenic drift of H9N2 influenza viruses in China from 1994 to 2008', Vet Microbiol, 146(3-4), pp. 215-25.
Sun, Y., Qin, K., Wang, J., Pu, J., Tang, Q., Hu, Y., Bi, Y., Zhao, X., Yang, H., Shu, Y. and Liu, J. (2011) 'High genetic compatibility and increased pathogenicity of reassortants derived from avian H9N2 and pandemic H1N1/2009 influenza viruses', Proc Natl Acad Sci U S A, 108(10), pp. 4164-9.
Sun, Y., Tan, Y., Wei, K., Sun, H., Shi, Y., Pu, J., Yang, H., Gao, G. F., Yin, Y., Feng, W., Perez, D. R. and Liu, J. (2013b) 'Amino acid 316 of hemagglutinin and the neuraminidase stalk length influence virulence of H9N2 influenza virus in chickens and mice', J Virol, 87(5), pp. 2963-8.
Sun, Y., Xu, Q., Shen, Y., Liu, L., Wei, K., Sun, H., Pu, J., Chang, K. C. and Liu, J. (2014) 'Naturally occurring mutations in the PA gene are key contributors to increased virulence of pandemic H1N1/09 influenza virus in mice', J Virol, 88(8), pp. 4600-4.
Suzuki, Y., Uchida, Y., Tanikawa, T., Maeda, N., Takemae, N. and Saito, T. (2014) 'Amino acid substitutions in PB1 of avian influenza viruses influence pathogenicity and transmissibility in chickens', J Virol, 88(19), pp. 11130-9.
Swayne, D. E. (2012) 'Impact of vaccines and vaccination on global control of avian influenza', Avian Dis, 56(4 Suppl), pp. 818-28.
Swayne, D. E. and Beck, J. R. (2005) 'Experimental study to determine if low-pathogenicity and high-pathogenicity avian influenza viruses can be present in chicken breast and thigh meat following intranasal virus inoculation', Avian Dis, 49(1), pp. 81-5.
Swayne, D. E. and Pantin-Jackwood, M. (2006) 'Pathogenicity of avian influenza viruses in poultry', Dev Biol (Basel), 124, pp. 61-7.
Takeda, M., Leser, G. P., Russell, C. J. and Lamb, R. A. (2003) 'Influenza virus hemagglutinin concentrates in lipid raft microdomains for efficient viral fusion', Proc Natl Acad Sci U S A, 100(25), pp. 14610-7.
Tan, S. L. and Katze, M. G. (1998) 'Biochemical and genetic evidence for complex formation between the influenza A virus NS1 protein and the interferon-induced PKR protein kinase', J Interferon Cytokine Res, 18(9), pp. 757-66.
Tarendeau, F., Boudet, J., Guilligay, D., Mas, P. J., Bougault, C. M., Boulo, S., Baudin, F., Ruigrok, R. W., Daigle, N., Ellenberg, J., Cusack, S., Simorre, J. P. and Hart, D. J. (2007) 'Structure and nuclear import function of the C-terminal domain of influenza virus polymerase PB2 subunit', Nat Struct Mol Biol, 14(3), pp. 229-33.
Taubenberger, J. K., Baltimore, D., Doherty, P. C., Markel, H., Morens, D. M., Webster, R. G. and Wilson, I. A. (2012) 'Reconstruction of the 1918 influenza virus: unexpected rewards from the past', MBio, 3(5).
Taubenberger, J. K. and Kash, J. C. (2010) 'Influenza virus evolution, host adaptation, and pandemic formation', Cell Host Microbe, 7(6), pp. 440-51.
Taubenberger, J. K. and Morens, D. M. (2006) '1918 Influenza: the mother of all pandemics', Emerg Infect Dis, 12(1), pp. 15-22.
Tchatalbachev, S., Flick, R. and Hobom, G. (2001) 'The packaging signal of influenza viral RNA molecules', RNA, 7(7), pp. 979-89.
Te Velthuis, A. J. and Fodor, E. (2016) 'Influenza virus RNA polymerase: insights into the mechanisms of viral RNA synthesis', Nat Rev Microbiol, 14(8), pp. 479-93.
Teng, Q., Xu, D., Shen, W., Liu, Q., Rong, G., Li, X., Yan, L., Yang, J., Chen, H., Yu, H., Ma, W. and Li, Z. (2016) 'A Single Mutation at Position 190 in Hemagglutinin Enhances Binding Affinity for Human Type Sialic Acid Receptor and Replication of H9N2 Avian Influenza Virus in Mice', J Virol, 90(21), pp. 9806-9825.

Tiley, L. S., Hagen, M., Matthews, J. T. and Krystal, M. (1994) 'Sequence-specific binding of the influenza virus RNA polymerase to sequences located at the 5' ends of the viral RNAs', *J Virol*, 68(8), pp. 5108-16.

Tong, S., Li, Y., Rivailler, P., Conrardy, C., Castillo, D. A., Chen, L. M., Recuenco, S., Ellison, J. A., Davis, C. T., York, I. A., Turmelle, A. S., Moran, D., Rogers, S., Shi, M., Tao, Y., Weil, M. R., Tang, K., Rowe, L. A., Sammons, S., Xu, X., Frace, M., Lindblade, K. A., Cox, N. J., Anderson, L. J., Rupprecht, C. E. and Donis, R. O. (2012) 'A distinct lineage of influenza A virus from bats', Proc Natl Acad Sci U S A, 109(11), pp. 4269-74.

Tong, S., Zhu, X., Li, Y., Shi, M., Zhang, J., Bourgeois, M., Yang, H., Chen, X., Recuenco, S., Gomez, J., Chen, L. M., Johnson, A., Tao, Y., Dreyfus, C., Yu, W., McBride, R., Carney, P. J., Gilbert, A. T., Chang, J., Guo, Z., Davis, C. T., Paulson, J. C., Stevens, J., Rupprecht, C. E., Holmes, E. C., Wilson, I. A. and Donis, R. O. (2013) 'New world bats harbor diverse influenza A viruses', PLoS Pathog, 9(10), p. e1003657.

Tong, X. C., Weng, S. S., Xue, F., Wu, X., Xu, T. M. and Zhang, W. H. (2018) 'First human infection by a novel avian influenza A(H7N4) virus', J Infect.

Uchikawa E. Lethier M.,Malet H., Brunel J., Gerlier D., and Cusack S., (2016) 'Structural analysis of dsRNA binding to anti-viral pattern recognition receptor LGP2 and MDA5.' Molecualr Cell. 62 (4) pp 568-602.

Ul-Haq Z., Naz S., and Mesaik A.M. (2016) 'Interleukin-4 receptor signalling and its binding mechanism: A therapeutic insight from inhibitors tool box. Cytokine and growth factor reviews 32 pp 3-15.

Uyeki, T. M., Chong, Y. H., Katz, J. M., Lim, W., Ho, Y. Y., Wang, S. S., Tsang, T. H., Au, W. W., Chan, S. C., Rowe, T., Hu-Primmer, J., Bell, J. C., Thompson, W. W., Bridges, C. B., Cox, N. J., Mak, K. H. and Fukuda, K. (2002) 'Lack of evidence for human-to-human transmission of avian influenza A (H9N2) viruses in Hong Kong, China 1999', Emerg Infect Dis, 8(2), pp. 154-9.

van der Goot, J. A., de Jong, M. C., Koch, G. and Van Boven, M. (2003) 'Comparison of the transmission characteristics of low and high pathogenicity avian influenza A virus (H5N2)', Epidemiol Infect, 131(2), pp. 1003-13.

Vandesompele, J., De Preter, K., Pattyn, F., Poppe, B., Van Roy, N., De Paepe, A. and Speleman, F. (2002) 'Accurate normalization of real-time quantitative RT-PCR data by geometric averaging of multiple internal control genes', Genome Biol, 3(7), p. RESEARCH0034.

Vasin, A. V., Temkina, O. A., Egorov, V. V., Klotchenko, S. A., Plotnikova, M. A. and Kiselev, O. I. (2014) 'Molecular mechanisms enhancing the proteome of influenza A viruses: an overview of recently discovered proteins', Virus Res, 185, pp. 53-63.

Ventoso, I., Barco, A. and Carrasco, L. (1998) 'Mutational analysis of poliovirus 2Apro. Distinct inhibitory functions of 2apro on translation and transcription', J Biol Chem, 273(43), pp. 27960-7.

Vey, M., Orlich, M., Adler, S., Klenk, H. D., Rott, R. and Garten, W. (1992) 'Hemagglutinin activation of pathogenic avian influenza viruses of serotype H7 requires the protease recognition motif R-X-K/R-R', Virology, 188(1), pp. 408-13.

Villa, M. and Lässig, M. (2017) 'Fitness cost of reassortment in human influenza', PLoS Pathog, 13(11), p. e1006685.

von Itzstein, M. (2007) 'The war against influenza: discovery and development of sialidase inhibitors', Nat Rev Drug Discov, 6(12), pp. 967-74.

Vreede, F. T., Gifford, H. and Brownlee, G. G. (2008) 'Role of initiating nucleoside triphosphate concentrations in the regulation of influenza virus replication and transcription', J Virol, 82(14), pp. 6902-10.

Wakefield, L. and Brownlee, G. G. (1989) 'RNA-binding properties of influenza A virus matrix protein M1', Nucleic Acids Res, 17(21), pp. 8569-80.

Wan, H. and Perez, D. R. (2006) 'Quail carry sialic acid receptors compatible with binding of avian and human influenza viruses', Virology, 346(2), pp. 278-86.
Wan, H. and Perez, D. R. (2007) 'Amino acid 226 in the hemagglutinin of H9N2 influenza viruses determines cell tropism and replication in human airway epithelial cells', J Virol, 81(10), pp. 5181-91.
Wan, H., Sorrell, E. M., Song, H., Hossain, M. J., Ramirez-Nieto, G., Monne, I., Stevens, J., Cattoli, G., Capua, I., Chen, L. M., Donis, R. O., Busch, J., Paulson, J. C., Brockwell, C., Webby, R., Blanco, J., Al-Natour, M. Q. and Perez, D. R. (2008) 'Replication and transmission of H9N2 influenza viruses in ferrets: evaluation of pandemic potential', PLoS One, 3(8), p. e2923.
Wang, G., Zhang, T., Li, X., Jiang, Z., Jiang, Q., Chen, Q., Tu, X., Chen, Z., Chang, J., Li, L. and Xu, B. (2014) 'Serological evidence of H7, H5 and H9 avian influenza virus co-infection among herons in a city park in Jiangxi, China', Sci Rep, 4, p. 6345.
Wang, J., Wu, M., Hong, W., Fan, X., Chen, R., Zheng, Z., Zeng, Y., Huang, R., Zhang, Y., Lam, T. T., Smith, D. K., Zhu, H. and Guan, Y. (2016a) 'Infectivity and Transmissibility of Avian H9N2 Influenza Viruses in Pigs', J Virol, 90(7), pp. 3506-14.
Wang, M., Fu, C. X. and Zheng, B. J. (2009) 'Antibodies against H5 and H9 avian influenza among poultry workers in China', N Engl J Med, 360(24), pp. 2583-4.
Wang, Q., Li, Q., Liu, T., Chang, G., Sun, Z., Gao, Z., Wang, F., Zhou, H., Liu, R., Zheng, M., Cui, H., Chen, G., Li, H., Yuan, X., Wen, J., Peng, D. and Zhao, G. (2018) 'Host Interaction Analysis of PA-N155 and PA-N182 in Chicken Cells Reveals an Essential Role of UBA52 for Replication of H5N1 Avian Influenza Virus', Front Microbiol, 9, p. 936.
Wang, W., Cui, Z. Q., Han, H., Zhang, Z. P., Wei, H. P., Zhou, Y. F., Chen, Z. and Zhang, X. E. (2008) 'Imaging and characterizing influenza A virus mRNA transport in living cells', Nucleic Acids Res, 36(15), pp. 4913-28.
Wang, Y., Yuan, X., Qi, L., Zhang, Y., Xu, H., Yang, J., Ai, W., Qi, W., Liao, M., Wang, D., Song, M. and Li, F. (2016b) 'H9N2 avian influenza virus-derived natural reassortant H5N2 virus in swan containing the hemagglutinin segment from Eurasian H5 avian influenza virus with an in-frame deletion of four basic residues in the polybasic hemagglutinin cleavage site', Infect Genet Evol, 40, pp. 17-20.
Wang, P., Palese, P. and O'Neill, R. E. (1997) 'The NPI-1/NPI-3 (karyopherin alpha) binding site on the influenza a virus nucleoprotein NP is a nonconventional nuclear localization signal', *J Virol*, 71(3), pp. 1850-6.
Washington, N., Steele, R. J., Jackson, S. J., Bush, D., Mason, J., Gill, D. A., Pitt, K. and Rawlins, D. A. (2000) 'Determination of baseline human nasal pH and the effect of intranasally administered buffers', Int J Pharm, 198(2), pp. 139-46.
Watanabe, K., Ishikawa, T., Otaki, H., Mizuta, S., Hamada, T., Nakagaki, T., Ishibashi, D., Urata, S., Yasuda, J., Tanaka, Y. and Nishida, N. (2017) 'Structure-based drug discovery for combating influenza virus by targeting the PA-PB1 interaction', Sci Rep, 7(1), p. 9500.
Watanabe, K., Takizawa, N., Katoh, M., Hoshida, K., Kobayashi, N. and Nagata, K. (2001) 'Inhibition of nuclear export of ribonucleoprotein complexes of influenza virus by leptomycin B', Virus Res, 77(1), pp. 31-42.
Watanabe, T., Watanabe, S., Maher, E. A., Neumann, G. and Kawaoka, Y. (2014) 'Pandemic potential of avian influenza A (H7N9) viruses', Trends Microbiol, 22(11), pp. 623-31.
Weber, F. and Haller, O. (2007) 'Viral suppression of the interferon system', Biochimie, 89(6-7), pp. 836-42.
Webster, R. G. (1968) 'The immune response to influenza virus. 3. Changes in the avidity and specificity of early IgM and IgG antibodies', Immunology, 14(1), pp. 39-52.
Webster, R. G., Bean, W. J., Gorman, O. T., Chambers, T. M. and Kawaoka, Y. (1992) 'Evolution and ecology of influenza A viruses', Microbiol Rev, 56(1), pp. 152-79.

Webster, R. G., Yakhno, M., Hinshaw, V. S., Bean, W. J. and Murti, K. G. (1978) 'Intestinal influenza: replication and characterization of influenza viruses in ducks', Virology, 84(2), pp. 268-78.
White, J., Matlin, K. and Helenius, A. (1981) 'Cell fusion by Semliki Forest, influenza, and vesicular stomatitis viruses', J Cell Biol, 89(3), pp. 674-9.
White, L. K., Sali, T., Alvarado, D., Gatti, E., Pierre, P., Streblow, D. and Defilippis, V. R. (2011) 'Chikungunya virus induces IPS-1-dependent innate immune activation and protein kinase R-independent translational shutoff', J Virol, 85(1), pp. 606-20.
Wise, H. M., Foeglein, A., Sun, J., Dalton, R. M., Patel, S., Howard, W., Anderson, E. C., Barclay, W. S. and Digard, P. (2009) 'A complicated message: Identification of a novel PB1-related protein translated from influenza A virus segment 2 mRNA', J Virol, 83(16), pp. 8021-31.
Wise, H. M., Hutchinson, E. C., Jagger, B. W., Stuart, A. D., Kang, Z. H., Robb, N., Schwartzman, L. M., Kash, J. C., Fodor, E., Firth, A. E., Gog, J. R., Taubenberger, J. K. and Digard, P. (2012) 'Identification of a novel splice variant form of the influenza A virus M2 ion channel with an antigenically distinct ectodomain', PLoS Pathog, 8(11), p. e1002998.
Wong, S. S., Yoon, S. W., Zanin, M., Song, M. S., Oshansky, C., Zaraket, H., Sonnberg, S., Rubrum, A., Seiler, P., Ferguson, A., Krauss, S., Cardona, C., Webby, R. J. and Crossley, B. (2014) 'Characterization of an H4N2 influenza virus from Quails with a multibasic motif in the hemagglutinin cleavage site', Virology, 468-470, pp. 72-80.
Wood, G. W., Banks, J., Strong, I., Parsons, G. and Alexander, D. J. (1996) 'An avian influenza virus of H10 subtype that is highly pathogenic for chickens, but lacks multiple basic amino acids at the haemagglutinin cleavage site', Avian Pathol, 25(4), pp. 799-806.
Wood, G. W., McCauley, J. W., Bashiruddin, J. B. and Alexander, D. J. (1993) 'Deduced amino acid sequences at the haemagglutinin cleavage site of avian influenza A viruses of H5 and H7 subtypes', Arch Virol, 130(1-2), pp. 209-17.
World Health Organisation. Influenza at the human-animal interface, Summary and assessment, 20 June to 3 October 2016. www.who.int: World Health Organisation, 2016.
World Health Organisation. Cumulative number of confirmed human cases of avian influenza A(H5N1) reported to WHO, 2003-2018. www.who.int: World Health Organisation, 2018a.
World Health Organisation. Influenza at the human-animal interface, Summary and assessment, 26th January to 2nd March 2018. www.who.int: World Health Organisation, 2018b.
Wright F., Neumann G., and Kawaoka Y., (2007) 'Orthomyxoviruses' 5. Fields Virology: Lippincott Williams & Wilkins, Philadelphia, pp. 1692-1740.
Wu, H., Peng, X., Cheng, L., Lu, X., Jin, C., Xie, T., Yao, H. and Wu, N. (2015) 'Genetic and molecular characterization of H9N2 and H5 avian influenza viruses from live poultry markets in Zhejiang Province, eastern China', Sci Rep, 5, p. 17508.
Xu, C., Fan, W., Wei, R. and Zhao, H. (2004) 'Isolation and identification of swine influenza recombinant A/Swine/Shandong/1/2003(H9N2) virus', Microbes Infect, 6(10), pp. 919-25.
Xu, G., Zhang, X., Gao, W., Wang, C., Wang, J., Sun, H., Sun, Y., Guo, L., Zhang, R., Chang, K. C., Liu, J. and Pu, J. (2016a) 'Prevailing PA Mutation K356R in Avian Influenza H9N2 Virus Increases Mammalian Replication and Pathogenicity', J Virol, 90(18), pp. 8105-14.

Xu, G., Zhang, X., Liu, Q., Bing, G., Hu, Z., Sun, H., Xiong, X., Jiang, M., He, Q., Wang, Y., Pu, J., Guo, X., Yang, H., Liu, J. and Sun, Y. (2017) 'PA-X protein contributes to virulence of triple-reassortant H1N2 influenza virus by suppressing early immune responses in swine', Virology, 508, pp. 45-53.

Xu, G., Zhang, X., Sun, Y., Liu, Q., Sun, H., Xiong, X., Jiang, M., He, Q., Wang, Y., Pu, J., Guo, X., Yang, H. and Liu, J. (2016b) 'Truncation of C-terminal 20 amino acids in PA-X contributes to adaptation of swine influenza virus in pigs', Sci Rep, 6, p. 21845.

Xu, K. M., Li, K. S., Smith, G. J., Li, J. W., Tai, H., Zhang, J. X., Webster, R. G., Peiris, J. S., Chen, H. and Guan, Y. (2007a) 'Evolution and molecular epidemiology of H9N2 influenza A viruses from quail in southern China, 2000 to 2005', J Virol, 81(6), pp. 2635-45.

Xu, K. M., Smith, G. J., Bahl, J., Duan, L., Tai, H., Vijaykrishna, D., Wang, J., Zhang, J. X., Li, K. S., Fan, X. H., Webster, R. G., Chen, H., Peiris, J. S. and Guan, Y. (2007b) 'The genesis and evolution of H9N2 influenza viruses in poultry from southern China, 2000 to 2005', J Virol, 81(19), pp. 10389-401.

Yamaji, R., Yamada, S., Le, M. Q., Ito, M., Sakai-Tagawa, Y. and Kawaoka, Y. (2015) 'Mammalian adaptive mutations of the PA protein of highly pathogenic avian H5N1 influenza virus', J Virol, 89(8), pp. 4117-25.

Yamayoshi, S., Watanabe, M., Goto, H. and Kawaoka, Y. (2016) 'Identification of a Novel Viral Protein Expressed from the PB2 Segment of Influenza A Virus', J Virol, 90(1), pp. 444-56.

Yamayoshi, S., Yamada, S., Fukuyama, S., Murakami, S., Zhao, D., Uraki, R., Watanabe, T., Tomita, Y., Macken, C., Neumann, G. and Kawaoka, Y. (2014) 'Virulence-affecting amino acid changes in the PA protein of H7N9 influenza A viruses', J Virol, 88(6), pp. 3127-34.

Yang, J. R. and Liu, M. T. (2017) 'Human infection caused by an avian influenza A (H7N9) virus with a polybasic cleavage site in Taiwan, 2017', J Formos Med Assoc, 116(3), pp. 210-212.

Yasuda J., Bucher D.J., and Ishihama A. (1994) 'Growth control of influenza A virus by M1 protein: analysis of transfectant viruses carrying the chimeric M gene.' Journal of Virology, 68 (12) 8141-8146

Yewdell, J. W. and Ince, W. L. (2012) 'Virology. Frameshifting to PA-X influenza', Science, 337(6091), pp. 164-5.

Yoon, S. W., Webby, R. J. and Webster, R. G. (2014) 'Evolution and ecology of influenza A viruses', Curr Top Microbiol Immunol, 385, pp. 359-75.

York, A. and Fodor, E. (2013) 'Biogenesis, assembly, and export of viral messenger ribonucleoproteins in the influenza A virus infected cell', RNA Biol, 10(8), pp. 1274-82.

Yu, H., Hua, R. H., Wei, T. C., Zhou, Y. J., Tian, Z. J., Li, G. X., Liu, T. Q. and Tong, G. Z. (2008) 'Isolation and genetic characterization of avian origin H9N2 influenza viruses from pigs in China', Vet Microbiol, 131(1-2), pp. 82-92.

Yu, X., Jin, T., Cui, Y., Pu, X., Li, J., Xu, J., Liu, G., Jia, H., Liu, D., Song, S., Yu, Y., Xie, L., Huang, R., Ding, H., Kou, Y., Zhou, Y., Wang, Y., Xu, X., Yin, Y., Wang, J., Guo, C., Yang, X., Hu, L., Wu, X., Wang, H., Liu, J., Zhao, G., Zhou, J., Pan, J., Gao, G. F. and Yang, R. (2014) 'Influenza H7N9 and H9N2 viruses: coexistence in poultry linked to human H7N9 infection and genome characteristics', J Virol, 88(6), pp. 3423-31.

Yuan, J., Xu, L., Bao, L., Yao, Y., Deng, W., Li, F., Lv, Q., Gu, S., Wei, Q. and Qin, C. (2015) 'Characterization of an H9N2 avian influenza virus from a Fringilla montifringilla brambling in northern China', Virology, 476, pp. 289-297.

Yuan, P., Bartlam, M., Lou, Z., Chen, S., Zhou, J., He, X., Lv, Z., Ge, R., Li, X., Deng, T., Fodor, E., Rao, Z. and Liu, Y. (2009) 'Crystal structure of an avian influenza polymerase PA(N) reveals an endonuclease active site', Nature, 458(7240), pp. 909-13.

Yuen, K. Y., Chan, P. K., Peiris, M., Tsang, D. N., Que, T. L., Shortridge, K. F., Cheung, P. T., To, W. K., Ho, E. T., Sung, R. and Cheng, A. F. (1998) 'Clinical features and rapid viral diagnosis of human disease associated with avian influenza A H5N1 virus', Lancet, 351(9101), pp. 467-71.

Yángüez, E. and Nieto, A. (2011) 'So similar, yet so different: selective translation of capped and polyadenylated viral mRNAs in the influenza virus infected cell', Virus Res, 156(1-2), pp. 1-12.

Zaraket, H., Bridges, O. A. and Russell, C. J. (2013) 'The pH of activation of the hemagglutinin protein regulates H5N1 influenza virus replication and pathogenesis in mice', J Virol, 87(9), pp. 4826-34.

Zebedee, S. L. and Lamb, R. A. (1988) 'Influenza A virus M2 protein: monoclonal antibody restriction of virus growth and detection of M2 in virions', J Virol, 62(8), pp. 2762-72.

Zeng, H., Belser, J. A., Goldsmith, C. S., Gustin, K. M., Veguilla, V., Katz, J. M. and Tumpey, T. M. (2015) 'A(H7N9) virus results in early induction of proinflammatory cytokine responses in both human lung epithelial and endothelial cells and shows increased human adaptation compared with avian H5N1 virus', J Virol, 89(8), pp. 4655-67.

Zepeda, C. and Salman, M. D. (2007) 'Assessing the probability of the presence of low pathogenicity avian influenza virus in exported chicken meat', Avian Dis, 51(1 Suppl), pp. 344-51.

Zhang, H., Li, X., Guo, J., Li, L., Chang, C., Li, Y., Bian, C., Xu, K., Chen, H. and Sun, B. (2014a) 'The PB2 E627K mutation contributes to the high polymerase activity and enhanced replication of H7N9 influenza virus', J Gen Virol, 95(Pt 4), pp. 779-86.

Zhang, J. and Lamb, R. A. (1996) 'Characterization of the membrane association of the influenza virus matrix protein in living cells', Virology, 225(2), pp. 255-66.

Zhang, P., Tang, Y., Liu, X., Liu, W., Zhang, X., Liu, H., Peng, D., Gao, S., Wu, Y., Zhang, L. and Lu, S. (2009) 'A novel genotype H9N2 influenza virus possessing human H5N1 internal genomes has been circulating in poultry in eastern China since 1998', J Virol, 83(17), pp. 8428-38.

Zhang, P., Tang, Y., Liu, X., Peng, D., Liu, W., Liu, H. and Lu, S. (2008) 'Characterization of H9N2 influenza viruses isolated from vaccinated flocks in an integrated broiler chicken operation in eastern China during a 5 year period (1998-2002)', J Gen Virol, 89(Pt 12), pp. 3102-12.

Zhang, Q., Shi, J., Deng, G., Guo, J., Zeng, X., He, X., Kong, H., Gu, C., Li, X., Liu, J., Wang, G., Chen, Y., Liu, L., Liang, L., Li, Y., Fan, J., Wang, J., Li, W., Guan, L., Li, Q., Yang, H., Chen, P., Jiang, L., Guan, Y., Xin, X., Jiang, Y., Tian, G., Wang, X., Qiao, C., Li, C., Bu, Z. and Chen, H. (2013) 'H7N9 influenza viruses are transmissible in ferrets by respiratory droplet', Science, 341(6144), pp. 410-4.

Zhang, X. (2016) 'Much Higher Case-fatality Rates of Index Cases. Commentary: Differences in the Epidemiology of Human Cases of Avian Influenza A(H7N9) and A(H5N1) Viruses Infection', Front Public Health, 4, p. 116.

Zhang, Y., Guo, X., Qi, J., Liu, L., Wang, J., Xu, S. and Yin, Y. (2014b) 'Complete Genome Sequence of an H9N2 Influenza Virus Lethal to Chickens', Genome Announc, 2(6).

Zhang, Z., Chen, B. and Chen, W. 20 (1994) 'The study of avian influenza:II. The incidence and serological survey of avian infleunza'. China J Vet Med, pp. 6-7.

Zhao, G., Gu, X., Lu, X., Pan, J., Duan, Z., Zhao, K., Gu, M., Liu, Q., He, L., Chen, J., Ge, S., Wang, Y., Chen, S., Wang, X., Peng, D., Wan, H. and Liu, X. (2012) 'Novel reassortant highly pathogenic H5N2 avian influenza viruses in poultry in China', PLoS One, 7(9), p. e46183.

Zhao, H., Chu, H., Zhao, X., Shuai, H., Wong, B. H., Wen, L., Yuan, S., Zheng, B. J., Zhou, J. and Yuen, K. Y. (2016) 'Novel residues in the PA protein of avian influenza H7N7 virus affect virulence in mammalian hosts', Virology, 498, pp. 1-8.

Zhong, L., Wang, X., Li, Q., Liu, D., Chen, H., Zhao, M., Gu, X., He, L., Liu, X., Gu, M. and Peng, D. (2014) 'Molecular mechanism of the airborne transmissibility of H9N2 avian influenza A viruses in chickens', J Virol, 88(17), pp. 9568-78.

Zhou, H., He, S. Y., Sun, L., He, H., Ji, F., Sun, Y., Jia, K., Ning, Z., Wang, H., Yuan, L., Zhou, P., Zhang, G. and Li, S. (2015) 'Serological evidence of avian influenza virus and canine influenza virus infections among stray cats in live poultry markets, China', Vet Microbiol, 175(2-4), pp. 369-73.

Zhou, J., Wu, J., Zeng, X., Huang, G., Zou, L., Song, Y., Gopinath, D., Zhang, X., Kang, M., Lin, J., Cowling, B. J., Lindsley, W. G., Ke, C., Peiris, J. S. and Yen, H. L. (2016) 'Isolation of H5N6, H7N9 and H9N2 avian influenza A viruses from air sampled at live poultry markets in China, 2014 and 2015', Euro Surveill, 21(35).

Zhu, W., Zhu, Y., Qin, K., Yu, Z., Gao, R., Yu, H., Zhou, J. and Shu, Y. (2012) 'Mutations in polymerase genes enhanced the virulence of 2009 pandemic H1N1 influenza virus in mice', PLoS One, 7(3), p. e33383.